Expanding the complexity and functional diversity of *bis*-amino acid building blocks

by

Sharad Gupta

M.Sc.(Int.), Indian Institute of Technology Kanpur, India, 2003

Submitted to the Graduate Faculty of

Arts and Sciences in partial fulfillment

of the requirements for the degree of

Doctor of Philosophy

University of Pittsburgh

2009

UNIVERSITY OF PITTSBURGH

FACULTY OF ARTS AND SCIENCES

This dissertation was presented

by

Sharad Gupta

It was defended on

July 13, 2009

and approved by

Toby Chapman, Professor, Department of Chemistry, Faculty of Arts and Sciences

Craig S. Wilcox, Professor, Department of Chemistry, Faculty of Arts and Sciences

Subha R. Das, Assistant Professor, Department of Chemistry, Carnegie Melon University

Dissertation Advisor: Christian E. Schafmeister, Associate Professor, Department of

Chemistry, Temple University

Expanding the complexity and functional diversity of *bis*-amino acid building blocks

Sharad Gupta, PhD

University of Pittsburgh, 2009

We are developing a unique approach to the synthesis of macromolecules with programmable shape. These scaffolds are assembled from stereochemically pure orthogonally protected bis-amino acids that are interconnected by two amide bonds. This ladder-like arrangement restricts the conformational flexibility of bis-amino acids to a large extent which in turn drastically reduces the number of allowed conformations for an oligomer. As a result, significantly lesser computing power is needed for the final three-dimensional structure prediction. Several stereochemically pure bis-amino acid monomers have been synthesized by our research group and incorporated into a number of homo- and hetero-oligomers.

In this dissertation we present the synthesis of a new pipecolic acid based bis-amino acid building block pip5(2S5S). Assembly of this monomer into a short spiroladder oligomer utilizing solid-phase synthesis followed by in situ activation by dicyclohexylcarbodiimide and N-hydroxysuccinimide has been demonstrated. The structure of the oligomer was determined in aqueous solution using two-dimensional NMR.

We report improved conditions for rapidly and simultaneously closing multiple diketopiperazines on solid support. These new conditions involve either heating of a suspension of solid supported amino-tetrafluoropropyl esters in acetic acid/triethylamine catalyst solution in a microwave oven or continuous flow of catalyst solution through the resin, heated in a special flow cell apparatus.

Finally, the synthesis of the first functionalized bis-amino acid monomer proAc(2S3S4R) that carries an acetyl side chain is presented. This monomer was incorporated into a short oligomer and the solution phase structure was determined using two-dimensional nuclear magnetic resonance. The solution structure confirmed the intended connectivity and stereochemistry of the oligomer. This first functionalized bis-amino acid represents a milestone towards functionalized bis-peptide nanostructures for catalytic, molecular recognition and nanotechnology applications.

TABLE OF CONTENTS

LIST OF TABLES

LIST OF FIGURES

LIST OF SCHEMES

ACKNOWLEDGEMENTS

1.0   INTRODUCTION

Most of the biological functions such as transportation, molecular recognition, catalysis, storage and self replication are carried out by large macromolecules. These macromolecules are essentially oligomers, made of only a few monomers. For example DNAs and RNAs are polymers of nucleotides, while monosaccharides serve as monomer units for carbohydrates. However, the most complex of these oligomers are proteins that are made of 22 natural amino acids. Proteins consist of long peptide chains that fold into well defined secondary structures such as α-helices. These secondary structural elements organize themselves into tertiary and quaternary structures that are held together in a functional form by weak non-covalent interactions.

The versatility and the variety of tasks that these "Nanomachines of Nature" perform is astonishing. Scientists have longed to develop tools that allow an access to artificial macromolecules that could rival natural proteins in their function.[1-3] However, it is extremely difficult to emulate nature and design proteins that could perform a desired task. The biggest hurdle being 'The Folding Problem':[4-6] For a protein to attain its native state, the linear peptide chain must fold into a specific 3-D shape. In a natural environment, proteins fold on microsecond timescales but it takes years of CPU time to simulate those few 'microseconds'.

1

In recent years, researchers have developed an understanding of molecular basis for folding and function. There is a growing consensus that protein folding and its assembly into a functional form is largely regulated by noncovalent interaction and this hypothesis has been tested by the successful design of proteins from scratch by computational methods. [7-9]

Chemists have adopted another powerful approach toward protein mimicry that focuses on oligomers and polymers that adopt defined conformations. These molecules have come to be known collectively as "foldamers"[10-12] that adopt a secondary structure stabilized by non-covalent interactions (which are essentially similar to those found in natural peptides). These foldamers mimic the ability of proteins, nucleic acids or polysaccharides to form well-defined secondary structures, such as helices and ß-sheets.[10-12]

Foldamers are chemically assembled from a myriad of non-natural monomers. These monomers come in a variety of sizes, shapes and arrangements and can lead to the efficient designs of molecular scaffolds. A number of functional foldamers have been synthesized that display a number of interesting biological properties. They mediate cell penetration[13, 14] and bind to proteins,[15-20] RNAs,[21, 22] and membranes.[23-25] Recently, there has been a renewed interest in peptidomimetic oligomer that has been fuelled by an increase in efforts toward new peptide based drugs development.[26-30] In this chapter we present a few highlights from this emerging field of foldamers. Later part of this chapter discusses our contribution to this growing field of research.

1.1   FOLDAMERS RESEARCH

Advent of foldamer research can be dated back to 1975 when Karle, Handa and Hassall first studied the conformation of a 14-membered cyclic peptide that contained β-amino acids.[31] This field came to limelight only in 1993 when Zuckerman[32] examined peptoids in detail. Since then foldamers research has come of age and great progress has been made by scientists.

Foldamers can be broadly divided into two categories based on the types of monomers used. The first category contains foldamers made of aliphatic monomers such as β peptides[33-35] and γ peptides,[36] azapeptides,[37, 38] oligoureas,[39-41] peptoids[42, 43] and α-aminoxy peptides.[44] The second category includes aryl based foldamers. Some examples are phenylene ethynylenes,[45-48] anthranilamides[49, 50] and substituted pyridines.[51, 52] Structures of a few represenative monomers are shown in Figure 1.
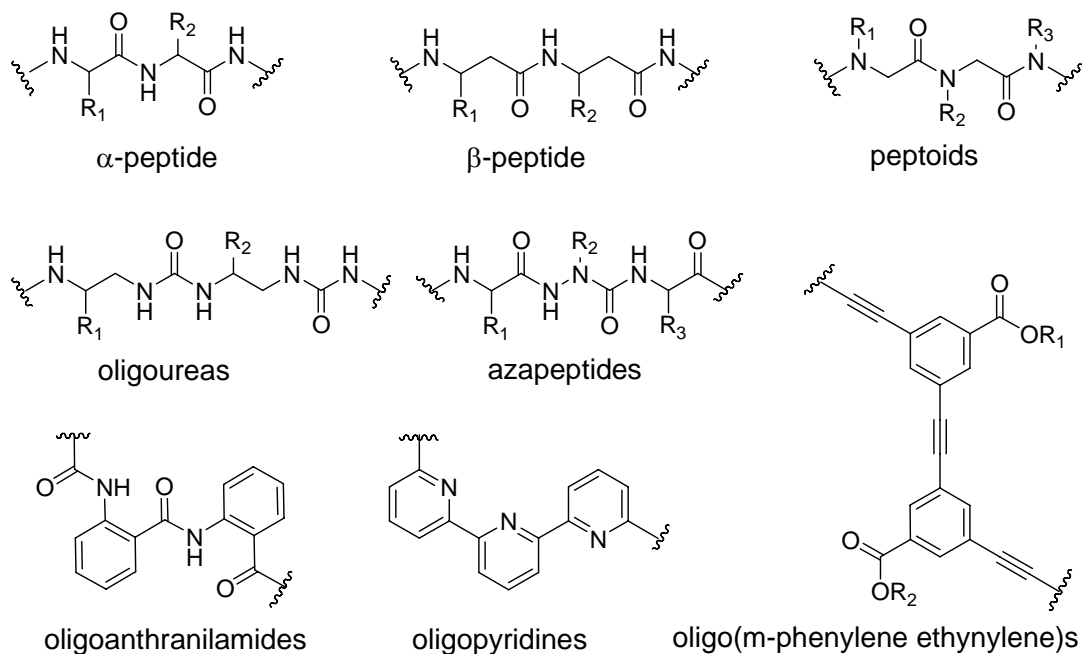
Figure 1: Structures of some foldamer backbones

3

β-Peptides were first prepared and investigated by Seebach and coworkers in 1996.[53, 54] Their approach was based on the conformationally rigidified residues that limit the degrees of freedom about the C_α-C_β bond.[55-58] These β-peptides and α/β hybrid peptides have been shown to bind to a variety of protein targets. Some of the targets include major histocompatibility complex (MHC) proteins,[59] the oncoprotein RDM2[60] and G-protein coupled somatostatin hsst receptors.[61-63]

Gellman and coworkers in 1999 reported the synthesis of a hexameric β-peptide and showed that it exists as short stable helices in aqueous solution.[64] Apart from forming helices these oligomers also form β-sheet and hairpin turns.[65-67] They have recently developed one such helical foldamer made of α/β-amino acids that binds to anti-apoptotic protein BCL-X_L with nanomolar affinity.[18, 68-70]

α-Aminoxy acids were first studied by Yang and coworkers in 1996 when they reported a novel turn structure in the peptides that contain these analogs of β-amino acids.[71] Homochiral oligomers form an extended helical structure (1.8$_8$ helix).[72, 73] A bent reverse turn structure is formed if the chirality is reversed.[73, 74] These α-aminoxy acids have good affinities toward anions and this property has been exploited to create cyclic and acyclic anion receptors for Cl^- [75, 76] and chiral carboxylate[77] anions.

Recently, Barron and coworkers have reported the development of poly-N-substituted glycine (peptoid) analogs of surfactant protein C (SP-C33).[78] By utilizing peptoid scaffold they were able to mimic helical structure and hydrophobic patterning of SP-C33 and slowed down the enzymatic degradation that was a big concern with natural α-amino acid based mimics.[79-82]

In 1999, Moore and coworkers[45, 83] observed that oligo(phenylene ethynylene)s fold into a helix in solution and later on continued to demonstrate that these foldamers can be used for molecular recognition.[84-86] The helical conformation formed by these foldamers has an internal cavity lined with non-polar surfaces and forms complexes with hydrophobic molecules of appropriate size.[87-90] These oligomers have led to the discovery of new polymeric materials such as self healing polymers and elastomers that change color as they are stretched.[91-93]

Hamilton and coworkers in 1996 reported an arylamide oligomer made from anthranillic monomers that fold into a helical strand.[49] The helical conformation of these oligomers is stabilized by hydrophobic interactions.[49, 50] A variety of scaffolds has been prepared that bind and recognize surfaces of proteins,[94, 95] disrupt protein-protein interaction,[96-98] influence cellular processes in vivo by binding selectively to biological targets.[99-102]

Other examples of these aryl-based foldamers include cationic arylamides that bind to heparin,[79-82] fluorescent oligoindole foldamers that bind anions,[103] and meta/para linked benzene backbone based foldamers that form hollow crescents, helices and macrocycles.[104-106]

1.2   OUR BIS-PEPTIDE APPROACH

Foldamers are being used to study various types of biomolecular interactions such as protein-protein, protein-oligosaccharides and peptide-membrane interaction. They are good candidates for these applications as the synthesis of foldamers is highly modular that enables rapid assembly of desired oligomers. A fewer number of monomeric units are required to attain a desired well

defined secondary structure. Usually, the reactions required for coupling two monomers are very efficient. They are generally more stable to enzymatic degradation than natural peptides.[107]

Despite these advantages they suffer from a serious drawback: Foldamers need to fold into well defined secondary structures to attain their functional form. This is similar to the natural proteins. The substitution of proteins with foldamers reduces the problem from predicting the folding in a large protein to a small macromolecule but an enormous computational effort is still required. In the light of this problem, bis-peptide oligomers assembled from the stereochemically pure bis-amino acid monomers synthesized in our lab could be an effective alternative.

A generic bis-amino acid monomer (e.g. pro4(2S4S) as shown in Figure 2) carries two α-amino acid moieties installed on a cyclic framework. These functionalities are orthogonally protected to enable solid phase peptide assembly. One of these two amino acid functionalities is consumed in assembling a head to tail peptide like oligomer while the second functionality is utilized to rigidify this flexible oligomer. A judicious choice of orthogonal protecting groups is required for a successful synthesis of a desired oligomer.
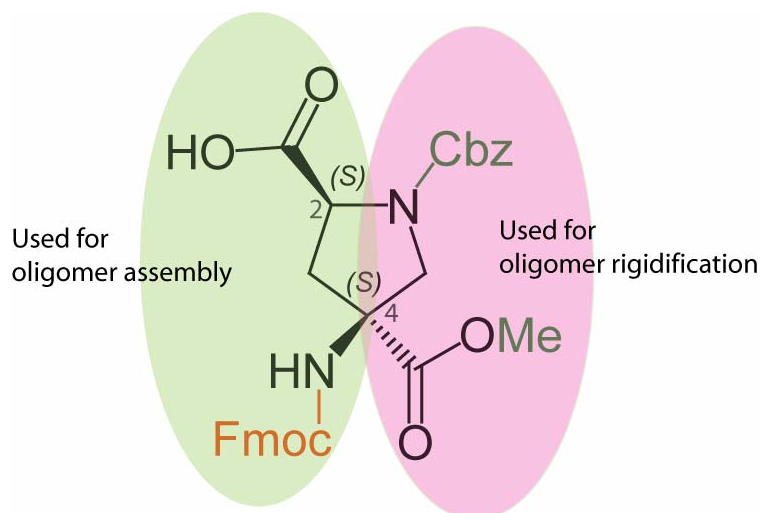
Figure 2: Structural features of pro4(2S4S) bis-amino acid monomer

The overall synthesis of a rigidified oligomer is conveniently carried out in two phases. The first phase, termed as "elongation", involves assembly of the desired oligomeric sequence from its constituent bis-amino acid monomers. We employ standard Fmoc based solid phase peptide synthesis techniques for this elongation process. A schematic representation is shown in Figure 3.
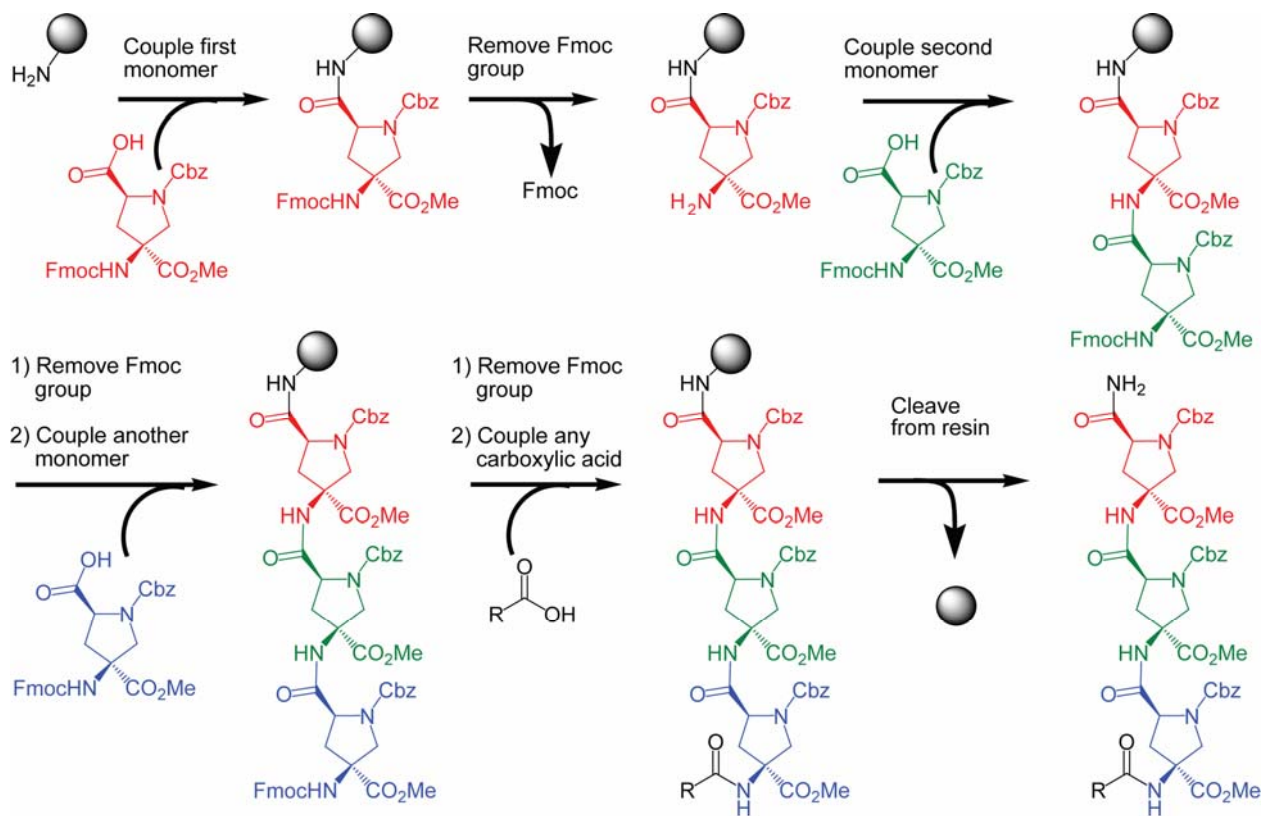
Figure 3: A schematic representation of the elongation phase in oligomer synthesis

In second "rigidification" phase these flexible oligomer sequences are subjected to appropriate reaction conditions that are conducive for the aminolysis of an ester by a secondary amine. A second amide bond between two adjacent monomers is formed and the net result is a rigidified oligomer. This rigidification results in the formation of the 1,4-diketopiperazine framework and eliminates any possibility of free rotation of the amide bonds. This simultaneous formation of multiple 1,4-diketopiperazines is depicted in Figure 4. The resulting bis-peptides are mostly water soluble (unless decorated with hydrophobic groups) and, in purified form, are stable under neutral or acidic aqueous conditions for weeks.
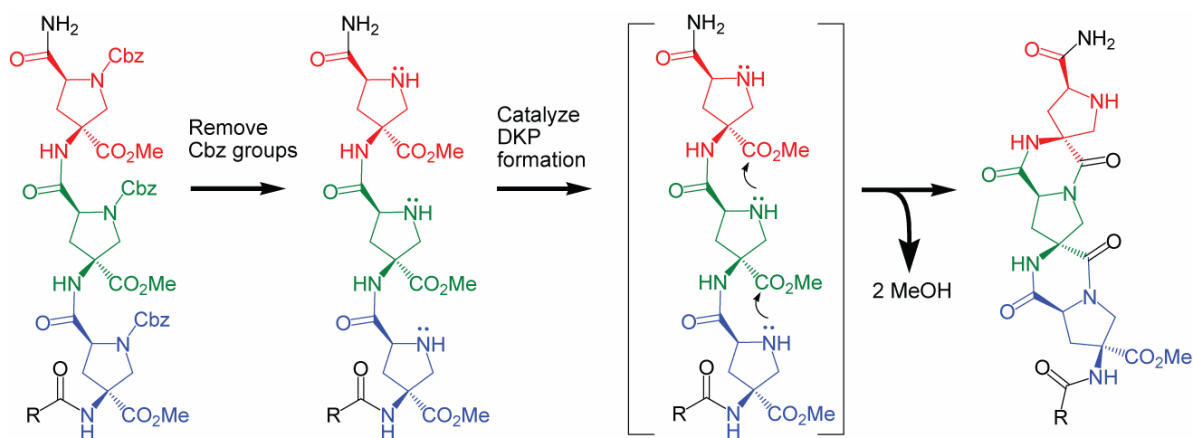
Figure 4: A schematic representation of the rigidification phase

These rigidified oligomers are conformationally restricted and have access to only a limited number of conformations. The oligomers need not go through a complex folding process that is required in the case of natural peptides and the functional forms are held together by covalent bonds. The overall structure of a rigidified oligomer depends on the stereochemistry and the conformational preferences of the monomers involved. This ability to rigidify a peptide like backbone that greatly simplifies the prediction of structure of large functional macromolecules could be a milestone towards reducing the folding problem.

We aim to study the conformational preferences for different monomers by determining the structure of small oligomers by NMR and X-ray crystallography and comparing them with those predicted by computational methods. By applying the knowledge gained from these initial experiments, we expect to perfect our computational models so that we can predict structures of large sequences *in silico* and design macromolecules with the desired shapes and functions for various applications related to peptidomimetics and nanotechnology.

Towards this goal, our lab has previously synthesized bis-amino acid monomers pro4(2S4S),[108] pro4 (2S4R),[109, 110] pro4(2R4R),[109, 110] pro4(2R4S),[109, 110] and hin(2S4R7R9R).[111] These monomers are easily coupled to each other to form rods and turns. To access a larger universe of structures we needed more building blocks.
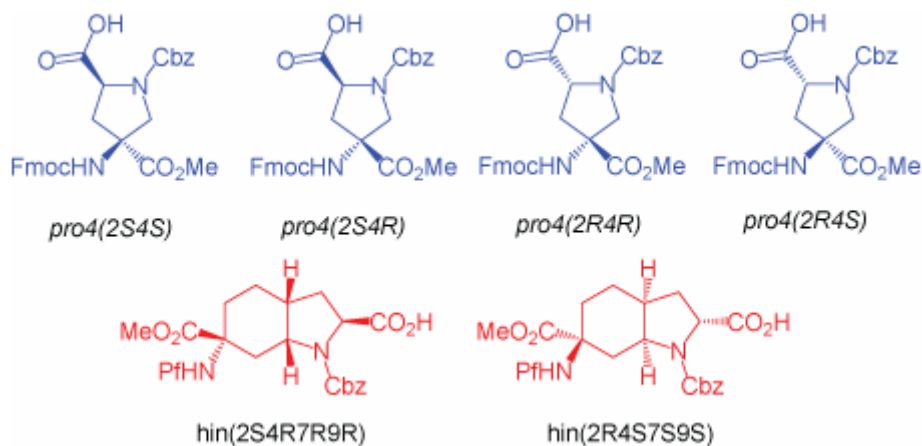
Figure 5: Bis-amino acid building blocks previously developed by Schafmeister group

This inspired us to undertake the synthesis of pipecolinic acid based monomers that are described in Chapter 2.[112] We report a new approach for the formation of DKP between two adjacent pip5(2S5S) monomers that was successfully used to synthesize a three-mer. We also present the solution phase NMR structure of this oligomer.

Chapter 3[113] primarily details our efforts toward the development and optimization of various catalysts and reaction conditions for DKP formation. We report synthesis of 2,2,3,3-tetrafluoropropyl ester versions of bis-amino acid monomers that in combination with AcOH/Et$_3$N solution in a non-polar solvent such as xylene and heat could form multiple DKPs in less than an hour.

In Chapter 4,[114] we describe the synthesis of a functionalized bis-amino acid monomer proAc(2S3S4R) that carries an acetyl side chain. The synthesis presented for this monomer is highly reproducible and easily applicable for the introduction of other functionalities as well. We also report the synthesis of a short oligomer that contains this monomer. The solution phase structure of this monomer was determined by NMR and compared with the molecular mechanics predicted structure.

Chapter 5 details progress made towards the synthesis of other stereochemical isomers of proAc(2S3S4R) monomer and preliminary results for the synthesis of a functionalized monomer that carries a methylimidazole side chain.

2.0   PIPECOLIC ACID BASED MONOMERS AND OLIGOMER ASSEMBLY

Our long-term goal is to design, synthesize, and study macromolecules that have well defined three-dimensional structures displaying various functional groups in desired orientations. This shall enable us to develop functional molecules for various applications such as binding protein surfaces, stereoselective catalysts and molecular sensors. Earlier, the synthetic access to bis-amino acid monomers (pro4[108, 109] and hin[111] class of monomers) had been developed in the Schafmeister research group. A combination of pro4 (4 monomers) and hin (2 monomers) building blocks in sequence M monomers long gives access to a total of 6^M possible structures. However, more building blocks with diverse structural features were needed to access an even larger universe of structures; thus enhancing the probability of synthesizing a predesigned molecule for a specific application that has all the required functional groups in optimum orientation. This inspired us to undertake the synthesis of pipecolic acid based monomers, later named as pip5[112] and pip4. In this chapter the synthesis of pip5 monomers and their successful assembly into a short rigidified oligomer will be discussed.

L-Pipecolic acid (Figure 6), a natural α-amino acid and a homologue of L-proline is a constituent of immunosuppressants[115] such as rapamycin[116] and several antibiotics.[117-119] Similar to proline, introduction of a pipecolic acid in a peptide induces a β-turn and this property has been exploited in various β-turn mimics.[120, 121] Pipecolic acid has been successfully utilized as proline substitute in a number of peptidomimetic drug candidates to enhance their biological

activity and/or specificity.[122-124] When incorporated into a peptide, pipecolic acid residue adopts a chair conformation as revealed by X-ray crystallography.[125, 126] Empirical calculation show that chair conformations are preferred over boat conformations by 3-5 kcal/mol.[125] Recently this has been substantiated by quantum mechanical calculations.[127] The synthesis of pipecolic acid based monomers was further inspired by the fact that the chair conformation of six-membered rings are easier to assign by NMR than envelop and twisted conformations of their five-membered ring counterpart.

Figure 6: Proline and pipecolic acid.

2.1   SYNTHESIS OF PIP5(2S5S) MONOMER

In principle, the pip5 series of monomers e.g. pip5(2S5S) **3** can be obtained from the ketone **4** via a methodology similar to the one developed for pro4 monomers (Figure 7). The ketone **4** is a homologue of ketone **5** and several one carbon insertion methods based on diazomethane derivatives have been reported in literature to affect this type of transformation.[128-133] The ketone **5** was easily available from *trans*-4-hydroxy-L-proline **6** via a three step process[108] which had previously been optimized for large scale synthesis in our lab. Since the proposed protecting group scheme was the same as for the pro4 monomers[108], we expected the solid phase assembly and the subsequent rigidification to be straightforward.
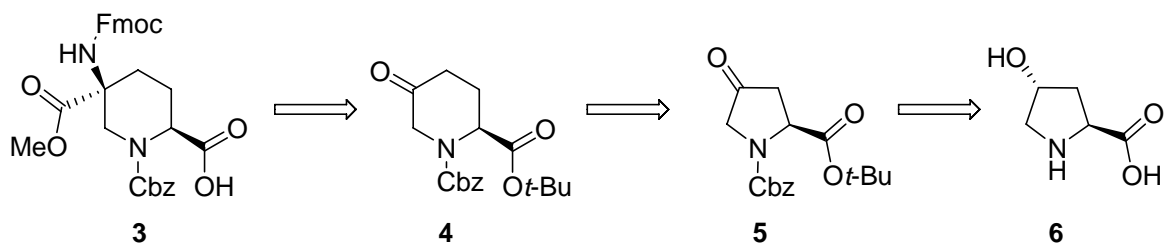
Figure 7: Retrosynthetic analysis of pip5(2S5S) monomer.

2.1.1 Synthesis of hydantoins

The ketone **5** was synthesized from inexpensive *trans*-4-hydroxy-L-proline **6** in three steps in good yield. The synthetic sequence started with Cbz protection of **6** with benzylchloroformate.[134] This was followed by Jones oxidation[135] and subsequent *t*-butyl esterification with isobutylene and catalytic sulfuric acid as reported in a previous study.[136] The crude ketone **5** was then subjected to a ketone homologation reaction that yielded a mixture of the regioisomeric ketones **4** and **8** as reported in literature.[137] This homologation was a two step reaction, the first step being ring expansion by reaction with ethyl diazoacetate in the presence of $BF_3.Et_2O$ at 0 °C in anhydrous ether (Scheme 1, Figure 8).[138-140]

This was followed by a Krepcho decarboethoxylation[141] which removed the residual carboethoxy group from the previous step. We observed that the insertion of a purification step prior to decarboethoxylation (mixture of **7a** and **7b**) enhanced the yield and simplified the chromatographic separation of the mixture of regioisomeric ketones (**4** and **8**) following the decarboethoxylation reaction.
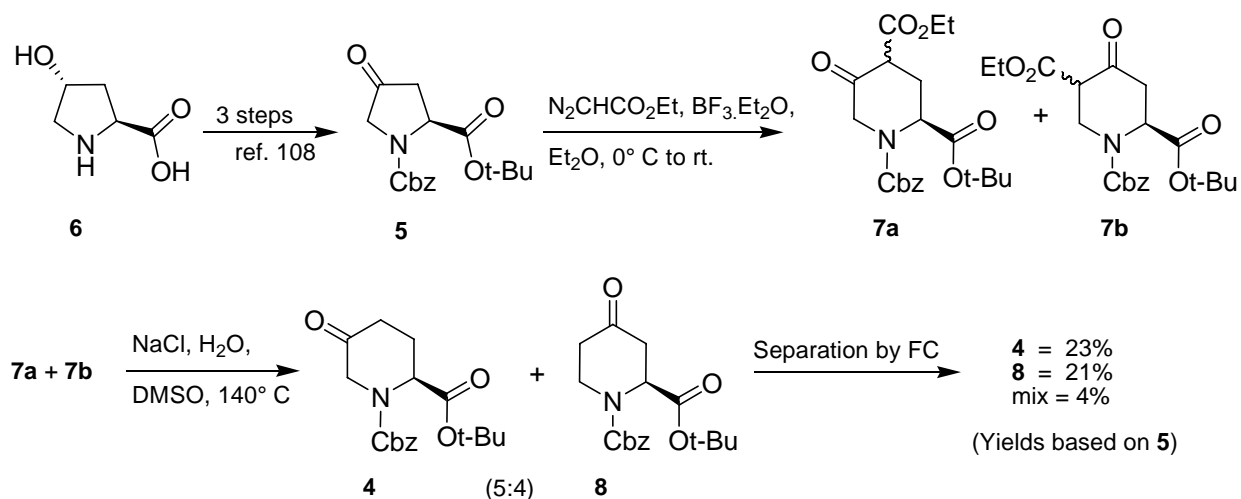
Scheme 1: Synthesis of homologous ketone **4**
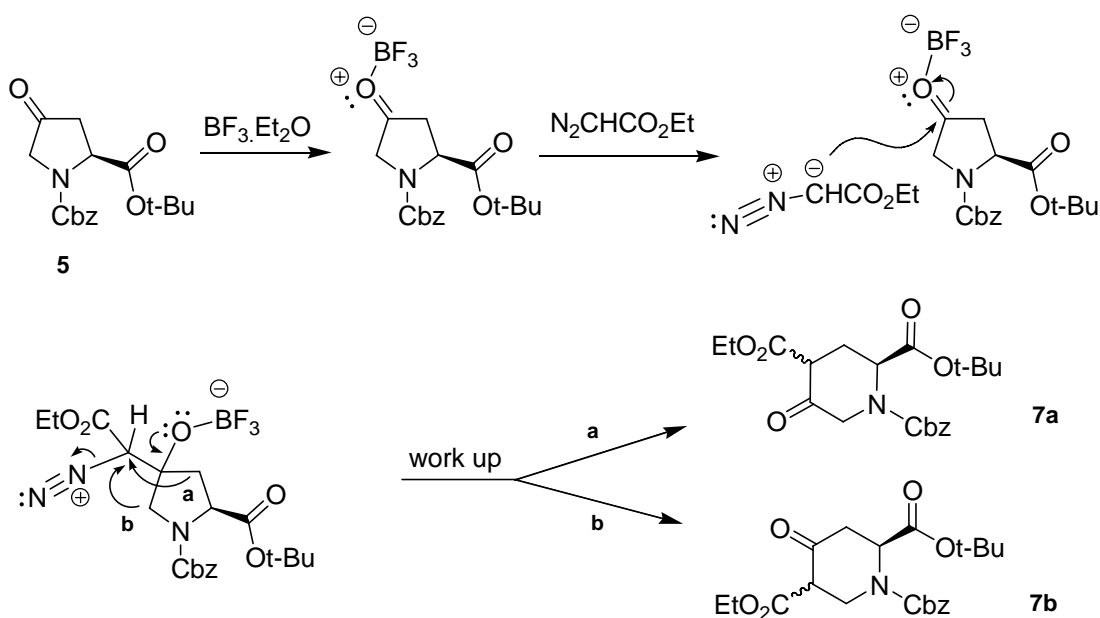
Figure 8: Mechanism of ring expansion reaction

We found that the optimum conditions for the decarboethoxylation reaction were to heat at 140-150 °C for 4-5 hours. A further increase in temperature reduced the reaction time, but raised the amount of byproducts formed due to thermal decomposition and this complicated the separation step. Ketones **4** and **8** were separated by flash chromatography on SiO_2 gel using a

5%-25% EtOAc in hexanes gradient. A typical chromatographic run yielded about 40-50% recovery of purified ketones from the mixture and a total of three sequential chromatographic runs were required to affect > 90% recovery of purified ketones. (Scheme 1)

After purification, ketone **4** was subjected to a Bucherer-Bergs reaction,[142, 143] thereby installing a quarternary stereocenter with a diasterselectivity of 5:2 as determined by NMR of the crude mixture of hydantoins **9a** and **9b**. The best yields were obtained by using 1.1 equivalents of KCN and DMF/H$_2$O (1:1) as the solvent. We observed that heating at 60 °C for 4 hours in a sealed pressure vessel was sufficient to complete the desired transformation. (Scheme 2)
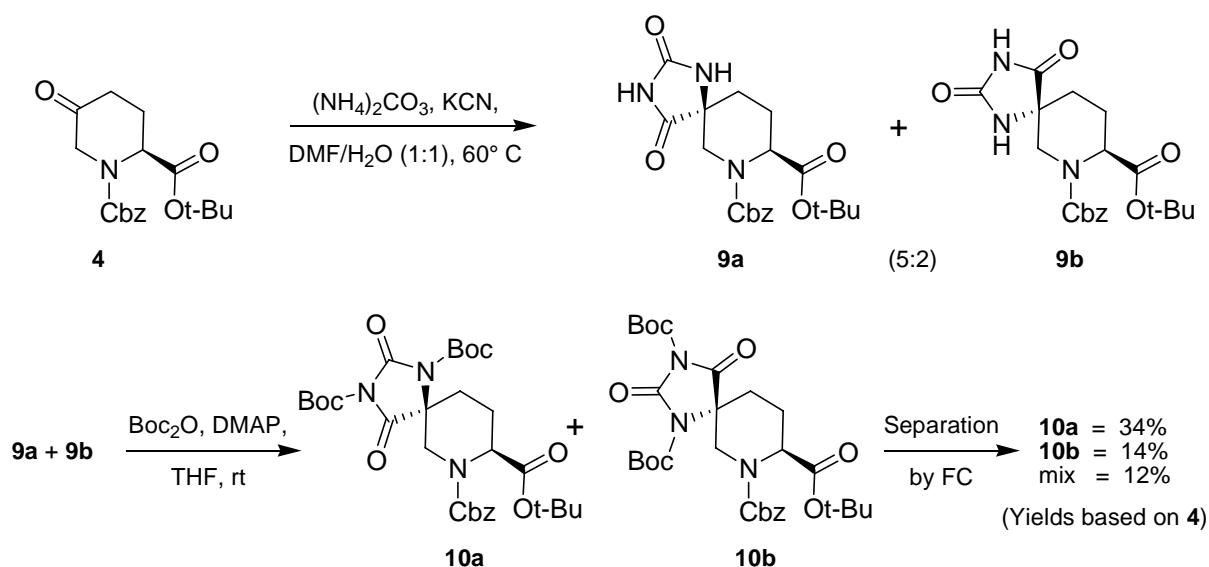
Scheme 2: Synthesis and separation of bis-Boc protected hydantoins

This mixture of diastereomeric hydantoins (**9a** and **9b**) thus obtained was found to be inseparable by silica gel chromatography. However, after protection with Boc groups the hydantoins became easily separable. These bis-Boc protected hydantoins **10a** and **10b** were separated by flash chromatography on SiO$_2$ gel using a 10%-30% EtOAc in hexanes gradient

16

(Scheme 2). We avoided prolonged contact with silica gel during the chromatographic separation and high temperature, while concentrating, as the Boc groups were found to be moderately labile under these conditions. We also observed that in the event of a partial removal of Boc groups, residual mono protected hydantoins can be easily re-protected with Boc anhydride and purified to recover additional quantities of bis-Boc protected hydantoins **10a** and **10b**. This extra effort ensured a near quantitative recovery of the purified products **10a** and **10b**.

2.1.2   Determination of stereochemistry

Previously, for pro4 series of monomers, the stereochemistry of the diastereometric hydantoins had been determined by taking advantage of the difference in the proximities of the amide –NH of the hydantoin to α, β and δ protons of the pyrrolidine ring which is detectable by ROESY or NOESY spectra.[108] We decided to use a similar approach to determine the relative stereochemistry for pip5 series of monomers. Because of the unavailibilty of pure hydantoins **9a** and **9b**, bis-Boc protected hydantoins **10a** and **10b**, available in pure form were deprotected to unmask the amide –NH. This was achieved by stirring **10a** or **10b** in a 3:7 mixture of TFA/DCM for 3 hours. This removed the two Boc groups and the *t*-Bu group to yield deprotected hydantoin-acids **11a** and **11b** (Figure 9a). 2D NOESY spectra were recorded for **11a** and **11b** in DMSO-d_6 at ambient temperature on a 600MHZ NMR instrument. Spectral analysis showed a correlation of amide hydrogen 7NH with 4Hα and 6Hα for hydantoin **11a**. However, for **11b** the amide hydrogen 7NH shows a correlation only with 3Hβ. These correlations are justified only if **11a** and **11b** are assigned S and R stereochemistry respectively at quarternary centre 5C. To further support this assignment, a stochastic conformational search[144] of the hydantoins **11a** and **11b** was carried out *in vacuo* using the AMBER94[145] force field within molecular mechanics

17

package MOE.[146] The modeled structures at the global energy minimum confirmed the experimentally observed correlations and suggested that both **11a** and **11b** existed in chair form (Figure 9b).
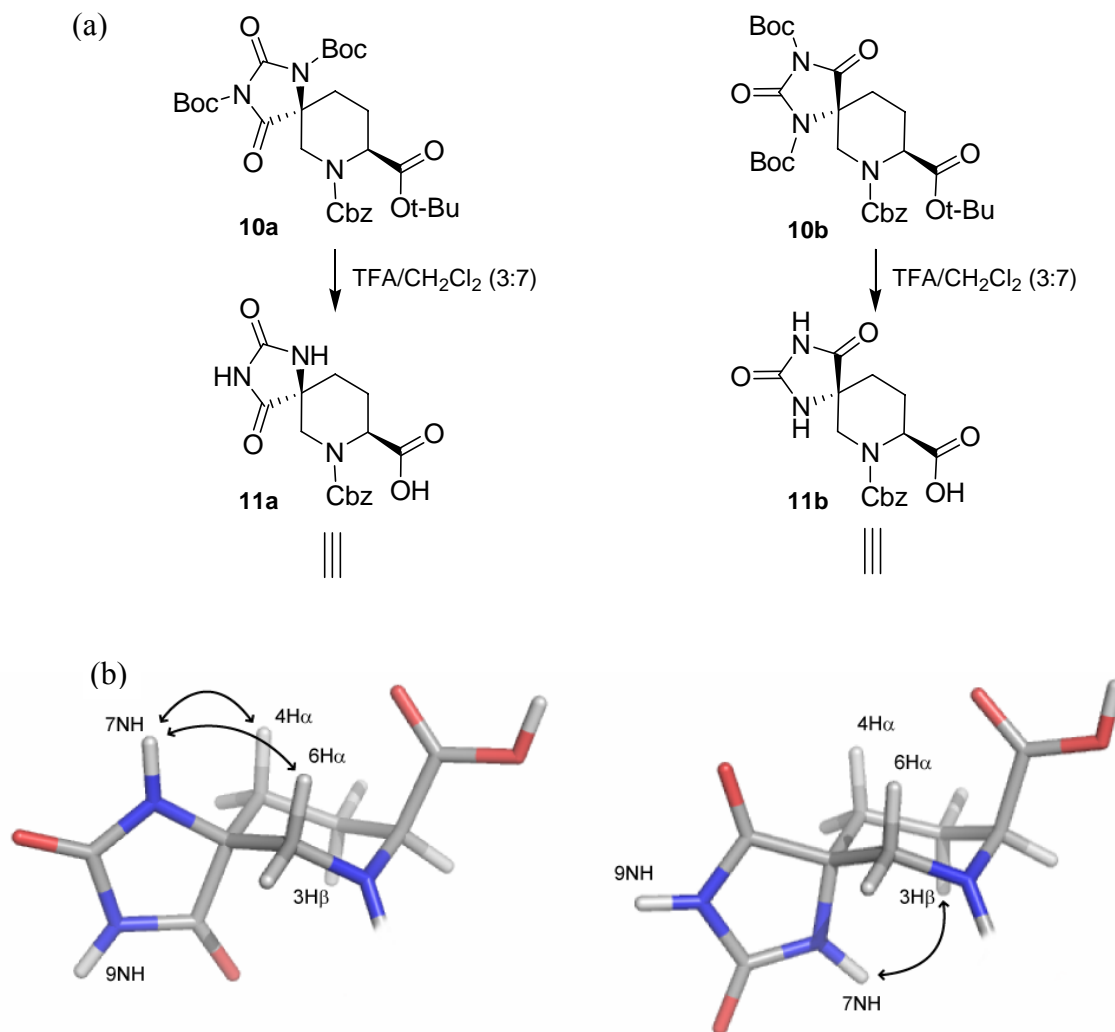
Figure 9: Stereochemistry of hydantoins: (a) Synthesis of hydantoin-acids and (b) NOESY correlation projected upon corresponding lowest energy conformations as determined by MOE.

2.1.3 Methyl ester version of pip5(2S5S) monomer

The major diasteromer **10a** was hydrolyzed using 1:1 2M-KOH/THF to give the corresponding amino acid **12**.[147] This amino acid was suspended in dichloromethane with DIPEA and TMS-Cl and refluxed to yield *N,O-bis*-TMS intermediate (not isolated).[134] After cooling, Fmoc-Cl was added to the reaction mixture and stirred until the reaction is complete. After an acidic workup, Fmoc protected amino acid **13** was obtained. We observed that the amino acid must be well dried for this reaction. Such a level of dryness can be obtained by storing the amino acid in a vacuum oven at 60-80 °C for a couple of days. This intermediate **13** was than esterified by treatment with trimethylsilyldiazomethane to give the fully protected ester **14**. Subsequent removal of the *t*-Bu group by treatment with 3:7 TFA/DCM exposed the carboxyl functionality to give the orthogonally protected building block **3**, that was suitable for sequential solid phase coupling. (Scheme 3)
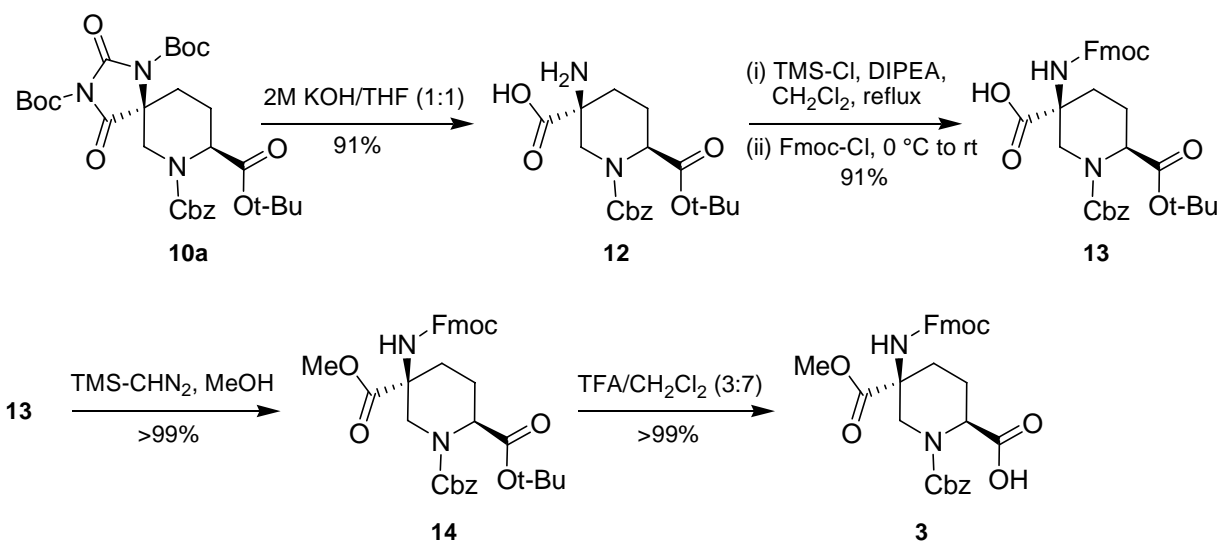
Scheme 3: Synthesis of methyl ester version of pip5(2S5S) monomer.

2.2   TRIAL ASSEMBLY OF A HOMO-OLIGOMER

In order to test the ability of monomer **3** to form spiro ladder oligomers, a dimer was synthesized

on 6.3 μmole scale on rink amide resin[148] using Fmoc solid phase peptide synthesis methods

(Scheme 4). Two methyl ester monomer units **3** were sequentially attached to the resin followed

by an Fmoc-L-tyrosine residue. The role of tyrosine was to provide a UV active group. Each

residue was activated as the HOAt ester[149] and near quantitative coupling to the previous

monomer was achieved through double coupling of 2 equivalents of activated monomer with

respect to the resin loading. We observed that longer coupling times were needed (90-120

minutes) as compared to the pro4 monomers (20-30 minutes) to affect quantitative couplings.

After removal of the terminal Fmoc group the oligomer **15** was cleaved from the resin by

treatment with 95:2.5:2.5 TFA/water/triisopropylsilane[150] for 2 hours. Hydrogenolysis gave the

completely deprotected oligomer **16**, which was used for subsequent studies on DKP closure.

(Scheme 4)
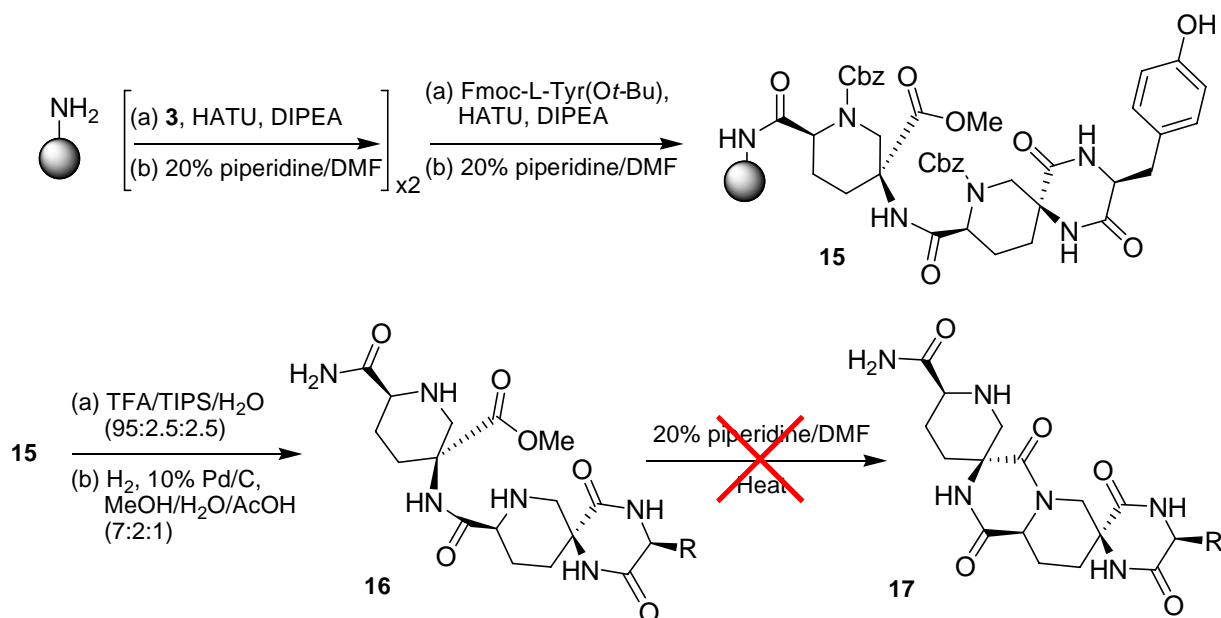
Scheme 4: An attempt to form DKP between two pip5(2S5S)(OMe) monomers

Oligomer **16** was incubated in a solution of 20% piperidine in DMF, first at room temperature and then at higher temperature (Scheme 4). These conditions for aminolysis were used effectively for the oligomers containing pro4 (at ambient temperature) and hin (at elevated temperature) monomers. To our surprise oligomer **16** did not undergo aminolysis even under forcing conditions (4 days and temperatures up to 100 °C). No trace of expected product **17** was detected and after a few days oligomer **16** decomposed.

These observations led us to conclude that secondary amines on the pip5 (2S4S) monomer were not as reactive as those in the pro4 and hin monomers. This relatively poor nucleophilicity of secondary amines in piperidine derivatives than those in pryrolidine derivatives has been widely observed. The coupling of a DCC activated acid to methyl prolinate has been found to be much faster than to a methyl pipecolinate.[151] Piperidine reacts much slower than pyrrolidine towards aromatic nucleophilic substitution and the difference in rates varies with reaction conditions.[152] The reaction of an amine with a ketone to give enamine is slower for piperidine than pyrrolidine.[153] This lower nucleophilicity of piperidine has been attributed to stereoelctronic effects in the transition states leading to the products.[154] Similiarly, piperazic acids that contain a six-membered piperidazine ring and their derivatives are very resistant to acylation at the α-nitrogen.[155]

In light of these precedents, we concluded that the rate enhancement provided by prolonged heating at high temperatures in 20% piperidine/DMF was unable to compensate for the deceleration caused by the 6-membered piperidine ring of the pip5(2S5S) monomer and a different approach for DKP closure was needed.

2.3   ALTERNATIVE STRATEGY: BENZYL ESTER VERSION OF PIP5(2S5S) MONOMER

The most widespread method to form an amide bond in peptide chemistry is through *in-situ* activation of carboxylic acids by reaction with activating reagents.[156-158] A wide range of peptide coupling reagents such as uronium reagents (e.g. HBTU,[159] TBTU[158]), carbodiimide reagents (e.g. DCC,[160] DIC[161]), or acid halogenating reagents (e.g. cyanuric fluoride[162]) are commercially available and each can be screened to find appropriate reaction conditions. However, some modification of the monomer **3** was required before applying this approach. A benzyl ester was chosen to replace the methyl ester, as the hydrogenolysis conditions employed for Cbz deprotection also remove benzyl groups to unmask the carboxylic acids in a single step. A retrosynthetic approach is shown in Figure 10.
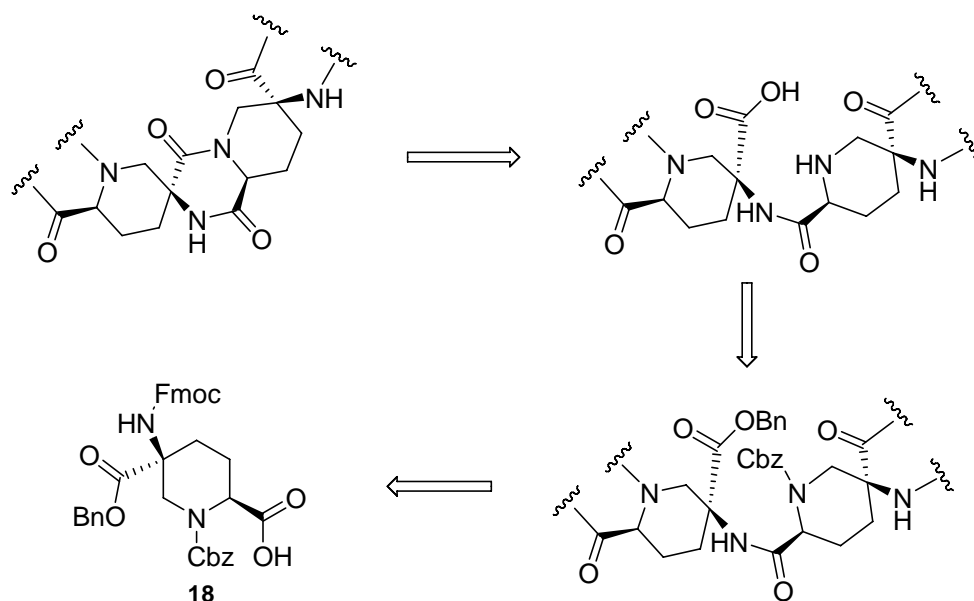
Figure 10: A retrosynthetic approach for *in situ* DKP formation

Pip5(2S5S)(OBn) **18**, a benzyl ester version of the monomer was synthesized from the intermediate **13** as shown in Scheme 5. A simple esterification with benzyl alcohol via DMAP catalyzed DCC activation yielded fully protected ester intermediate **19**. The *t*-Bu group was quantitatively removed by treating with 30% TFA in DCM to yield the monomer **18** with a free carboxylic acid for peptide synthesis.
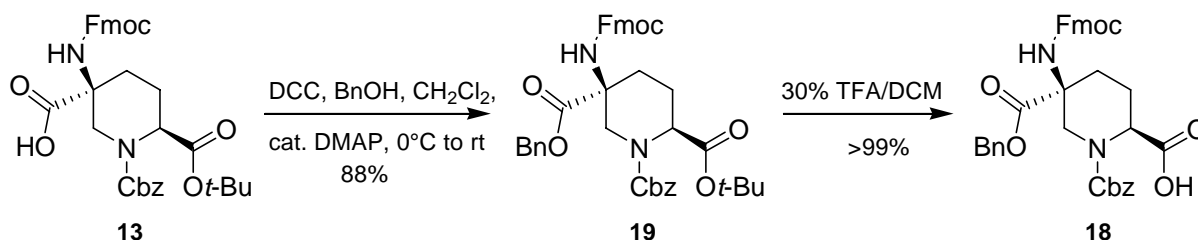
Scheme 5: Synthesis of benzyl ester version of pip5(2S5S) monomer

2.4   ASSEMBLY AND STRUCTURAL ANALYSIS OF PIP5(2S5S) OLIGOMER

2.4.1   Solid phase assembly of a trimer

A homo-oligomer consisting of three pip5(2S5S) monomer units **18** was synthesized on a 16.5 µmol scale on Rink acid resin[148] using Fmoc solid-phase peptide synthesis techniques (Scheme 6). The mild deprotection conditions (10% TFA/DCM) used for Rink acid resin ensured a clean product with near quantitative yield. The sequence consisted of *gly*-pip5(2S5S)-pip5(2S5S)-pip5(2S5S)-*(L)-tyrosine*. A glycine residue was first attached to the resin followed by two benzyl ester monomers **18** and a methyl ester monomer **3**. Each residue was activated as an HOAt ester and near quantitative coupling to the previous monomer was achieved through double-coupling

of 2 equivalents of activated monomer with respect to the resin loading. Finally, an Fmoc-L-tyrosine residue was added, and the amine of the tyrosine was capped with a trimethyl acetyl group to stop the terminal DKP formation, thus reducing the hydrophilic character of the the oligomer. The oligomer was then cleaved from the Rink acid resin using 10% TFA/DCM. The carboxybenzoyl (Cbz) and benzyl groups were removed simultaneously by hydrogenolysis under hydrogen atmosphere using 10% Pd/C to yield oligomer **21** that has a free amine and a free carboxylic acid between each adjacent pair of monomers.

2.4.2 Rigidification of homo-oligomer

The carboxylic acids on oligomer **21** were then activated *in situ* using 1,3-dicyclohexylcarbodiimide (DCC) and N-hydroxysuccinimide[163-165] (HOSu) in the presence of base (DIPEA), in NMP. These conditions were found to be the most efficient with cleanest product after screening a few commercially available coupling reagents in a separate set of experiments with a dimer. We qualitatively observed that the anhydride based reagents were more effective than the activated-ester based reagents. Also, DCC by itself in the absence of NHS was mildly active and gave poor yield.

Intramolecular amide formation took place between each adjacent pair of monomers to yield the rigidified scaffold **22** (Scheme 6). This *in situ* coupling reaction simultaneously forms three diketopiperazine rings and produces a single pure product as determined by C_{18} RP-HPLC and NMR. This indicates that the diketopiperazine rings form faster than any other macrocycles that would result from one of the three amines N8, N18, or N27 attacking one of the other activated carbonyl groups at C9, C19, or C28.

24
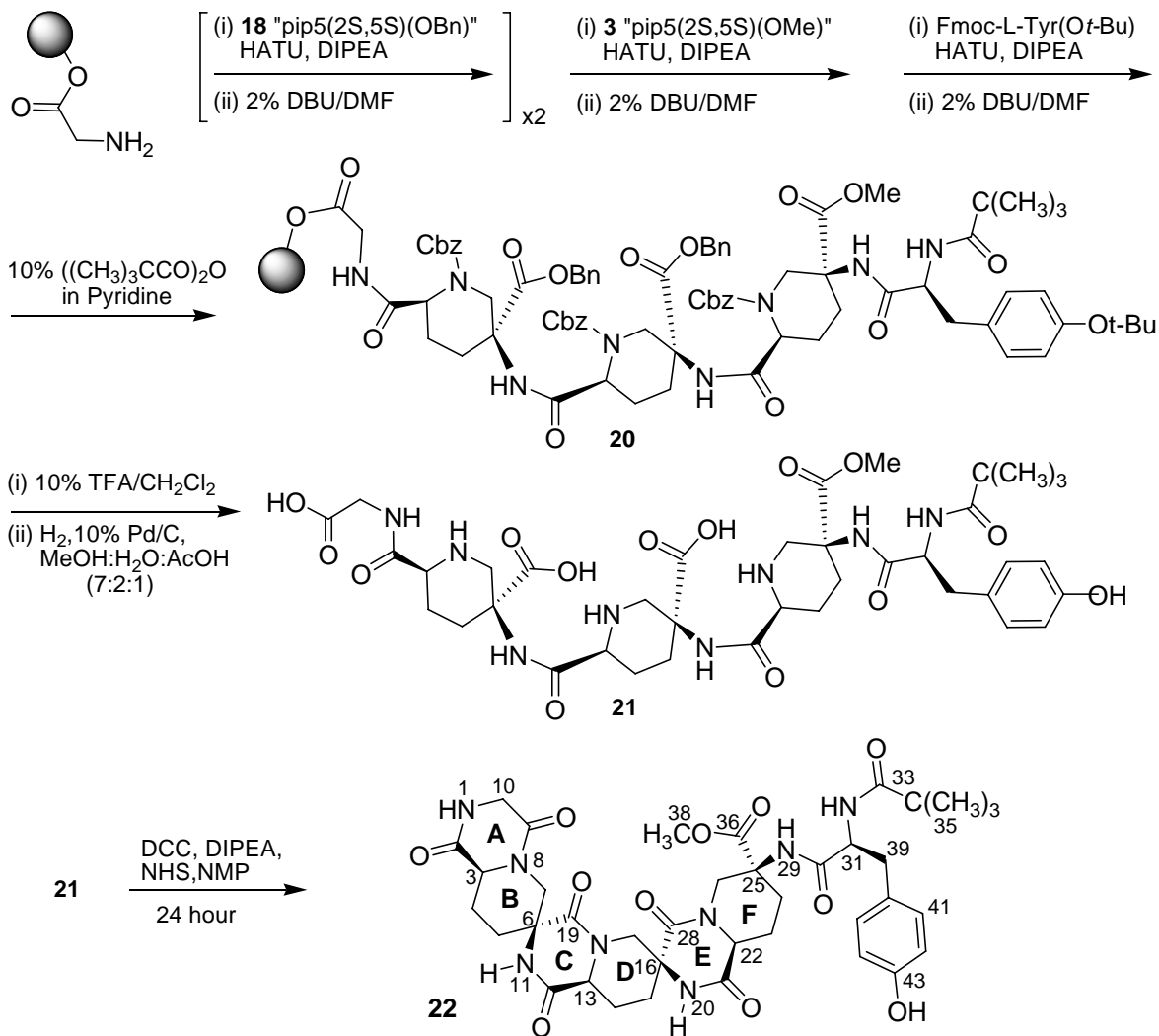
Scheme 6: Assembly of a pip5(2S5S) oligomer and DKP closure

2.4.3 Solution phase NMR structure and conformational analysis

The molecular mechanics package MOE was used to carry out a stochastic conformational search of the three-mer sequence *gly*-pip5(2S5S)-pip5(2S5S)-pip5(2S5S) in order to locate the lowest energy minima *in vacuo* using the AMBER94 force field. The modeled structure at the global energy minimum suggests that the sequence forms a helical rod and each pipecolic acid ring adopts a chair like conformation, placing the amide nitrogens N11, N20, and N29 in the

axial positions. A superposition of next several lowest energy predicted conformations revealed that a change in any of the chair conformations to the boat conformation raised the energy by at least 6.3 Kcal/mol. This suggested that the preference of pip5(2S5S) monomers to adopt this chair like conformation, when incorporated into a bis-peptide oligomer is very strong and that should translate into a high degree of rigidity and thus high predictability for the overall oligomer structure.

We determined the conformational preferences of the component rings of the oligomer **22** using two-dimensional NMR in $H_2O:D_2O$ 90:10 at 25°C. The ^{1}H and ^{13}C resonances were assigned through the interpretation of a collection of 2D spectra including a DQF-COSY, a TOCSY, an HMQC, an HMBC and a ROESY. The assignment was carried out using the software package SPARKY.[166] Diastereotopic hydrogens are labeled "α" if they go into the page and "β" if they come out of the page. For protons that were correlated to several other protons in the ROESY spectrum, the relative intensity of the cross-peaks were assigned as strong, medium or weak based on integrated intensity.

The overall conformation of **22** is that of a left handed helix. The chair conformation of each pipecolic acid ring was indicated by the correlation of three axial protons syn to each other on each ring. On the **B** ring of **22**, correlations are seen between H3, H5α and H7α and the axial orientation of the amine substituent N11 is indicated by the correlation between H11 and H4β. On the the **D** ring of **22**, protons H13, H15α, H17α are correlated and the axial orientation of N20 is seen in the correlation between H20 and H14β. In the **F** ring of **22** correlations are seen between H22, H24α and H26α. The amine substituent N29 is not the part of a diketopiperazine ring and can rotate freely. However, we observe a correlation between H29 and H23β,

suggesting that N29 is axial to ring **F**. These observations are consistent with rings **B**, **D** and **F** each being in a chair conformation.

The conformation of the diketopiperazine ring **C** is not clear because the only correlation seen across this ring is a very weak correlation between H11 and H13. A correlation is seen between H17β and H23β suggesting that the diketopiperazine ring **E** is in a boat conformation that places C23 and C17 in a pseudoaxial orientation. Combining these conformational preferences allowed us to validate a three-dimensional model of the spiro-fused ring structure of **22** at the global energy minimum shown in (Figure 11).
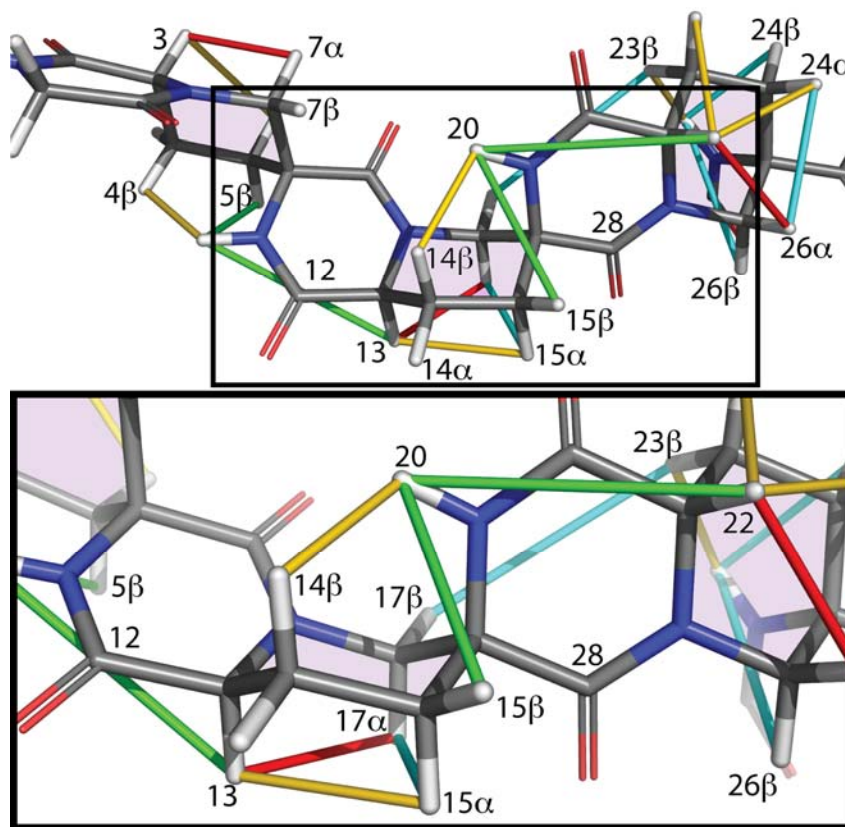
Figure 11: The global minimum energy structure of compound **22** with the ROESY correlations superimposed. The piperazine rings are shaded purple. The ROESY correlations were most consistent with the minimum energy structure using the Amber94 force field. The colors of the ROESY correlation lines are related to the intensity of the ROESY correlation peak (red=strong, yellow=medium, green=weak).

2.5   EXTENSION TO LONGER SEQUENCES

After successfully demonstrating that three DKP rings in a pip5(2S5S) homooligomer can be closed simultaneously we focused on developing pip5(2S5R) monomer and extend this methodology to longer sequences comprising different combinations of monomers. Bis Boc protected minor hydantoin **10b** was hydrolyzed and the resulting amino acid **23** was protected with an Fmoc group to yield **24.** This intermediate **24** was than esterified with benzyl alcohol using DCC in the presence of catalytic DMAP to yield fully protected ester **25**. Subsequent *t*-Bu deprotection gave **26**, the orthogonally protected benzyl ester version of the pip5(2S5R) monomer.
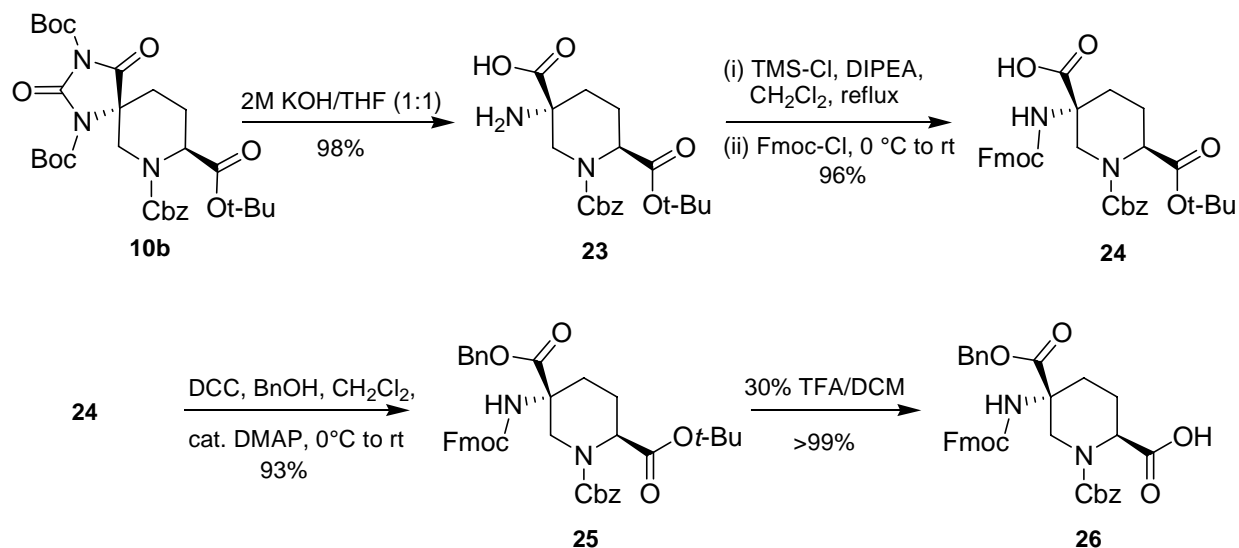
Scheme 7: Synthesis of pip5(2S5R)(OBn) monomer

We assembled a heterooligomer sequence *tyr*-pip5*(2S5R)*-pip5*(2S5R)*-pip5(2S5S)-pip5(2S5S) on trityl chloride resin using the Fmoc solid phase methodology as described earlier. Each residue was activated as HOAt ester and terminal amino group was protected by acyl

group. After the cleavage from the resin and hydrogenolysis, a fully deprotected oligomer **27** was recovered in moderate yields only. The hydrogenolysis reaction was very sluggish and low yielding. The oligomer **27** had 5 pairs of free carboxylic acids and free amines on adjacent monomers and was sparingly soluble in NMP, DMF and other polar aprotic solvents. A suspension of **27** in NMP was activated with DCC and NHS in the presence of DIPEA. Even though the suspension was sonicated repeatedly and the stirring was continued for days, we could obtain only a trace amount of fully rigidified oligomer **28**.
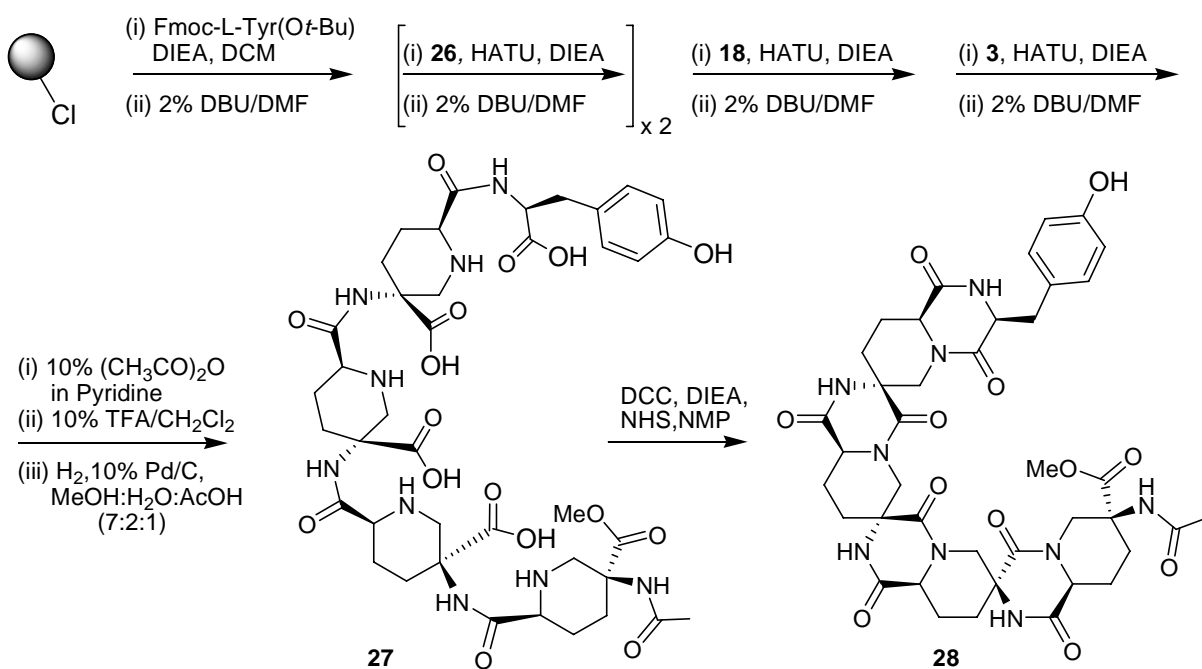
Scheme 8: Extension of the *in situ* DKP closure methodology to longer sequences

These observations, supported by the other experiments on similar sequences led us to hypothesize that as the sequence grows, the number of pairs of free amines and free carboxylic acids on adjacent monomers also increases. Consequently, the oligomers increasingly adopt

polar zwitterionic structure and their solubility in organic solvents decreases. This in turn slows down rigidification process resulting in low yield.

The oligomer **27** was readily soluble in water. This prompted us to test water soluble coupling reagents such as EDC[167] and DMT-MM[168] in buffered as well as in biphasic medium but no product was observed.

2.6   SUMMARY

In this chapter we demonstrated a successful synthesis of pipecolic acid based bis-amino acid monomers, namely pip5(2S5S) and pip5(2S5R). By incorporating these monomers in short oligomers, we confirmed that these monomers are amenable to solid phase synthesis. A new approach for DKP closure in oligomers containing pip5(2S5S) monomers was developed that utilized *in situ* activation of carboxylic acid by DCC and NHS. We determined the conformational preferences of the monomers within the oligomer, and together they suggested that the oligomer forms a left-handed helix.

Our attempts to extend this approach for DKP formation to longer sequences for DKP closure were unsuccessful and we concluded that *in situ* activation approach for DKP ring closure, though very powerful and high yielding was limited to small sequences only and a universal methodology that works for all types of monomers and sequences of all lengths required further development.

2.7   EXPERIMENTAL METHODS

2.7.1   General methods

THF was distilled from Na/benzophenone under N_2. CH_2Cl_2 was distilled from CaH_2. All other reagents were used as received unless otherwise noted. All reactions were carried out in flame-dried or oven-dried glassware under N_2 atmosphere unless otherwise noted. Column chromatography was performed either manually using ICN Silitech 32-63 D (60 Å) grade silica gel or using Redisep normal phase flash chromatography silica columns on CombiFlash companion purification system from ISCO Inc. TLC analysis was performed on EM Science Silica Gel 60 F_{254} plates (250 μm thickness). NMR experiments were performed on Bruker Avance 300 MHz, Bruker Avance DRX 500 MHz or Bruker Avance DRX 600 MHz spectrometers. Chemical shifts (δ) are reported relative to $CDCl_3$ or DMSO-d_6 residual solvent peaks, unless otherwise noted. If possible, rotational isomers were resolved by obtaining spectra at 77 °C in DMSO-d_6. IR spectra were obtained on a Nicolet Avatar E.S.P. 360 FT-IR. Optical rotations were obtained on a Perkin-Elmer 241 polarimeter at the indicated temperatures. High resolution ESI-MS was performed on a Waters LC/Q-TOF instrument. HPLC analysis was performed on a Hewlett-Packard Series1050 instrument with diode array detector, using a Varian Chrompack Microsorb 100 C_{18} column (5 μm packing, 2.6 mm x 250 mm). HPLC-MS analysis was performed on a Hewlett-Packard Series 1100 instrument with diode array detector, HP 1100 MS detector (ESI), using a Waters Xterra MS C_{18} column (3.5 μm packing, 4.6 mm x 100 mm). Purification by preparative HPLC was performed on a Varian ProStar 500 HPLC system with a

Varian Chrompack Micrsorb 100-C$_{18}$ column (8 μm packing; 21.5mm x 50mm; designated "prep Varian C$_{18}$).

2.7.2 Monomer synthesis

(5S,8S)-2,4-Dioxo-1,3,7-triazaspiro[4.5]decane-7,8-dicarboxylic acid 7-benzyl ester 8-*tert*-butyl ester (9a) and (5R,8S)-2,4-Dioxo-1,3,7-triazaspiro[4.5]decane-7,8-dicarboxylic acid 7-benzyl ester 8-*tert*-butyl ester (9b)

A solution of ammonium carbonate (6.0 g, 62 mmol), and potassium cyanide (0.9 g, 14 mmol) in deionized water (63 mL) was transferred to a 350 mL pressure vessel. To this vessel a solution of **(2S)-5-Oxopiperidine-1,2-dicarboxylic acid 1-benzyl ester 2-*tert*-butyl ester (4)** (4.1 g, 12.5 mmol) in DMF (63 mL) was added. The pressure vessel was sealed and the reaction mixture was heated at 60 °C for 4 hours with vigorous stirring. After cooling to 0 °C, the pressure vessel was opened cautiously and the reaction mixture was poured into a 500 mL beaker. Reaction mixture was neutralized by addition of 1N HCl and pH was reduced to ~2. The resulting solution including any oily residue (soluble in EtOAc) was transferred to a separatory funnel and extracted with EtOAc (500mL). The aqueous layer was extracted back with EtOAc (3 x 200mL). All the organic Layers were combined and washed with brine (200 mL) and dried over anhydrous Na$_2$SO$_4$. The solvent was removed *in vacuo* by rotary evaporation to yield a crude mixture of products **9a** and **9b** in a ratio of ~ 5:2 (as determined by ^{1}H NMR of crude). This mixture was found to be inseparable by flash chromatography and taken to the next step without further purification.

(5S,8S)-2,4-Dioxo-1,3,7-triazaspiro[4.5]decane-1,3,7,8-tetracarboxylic acid 7-benzyl ester 1,3,8-tri-*tert*-butyl ester (10a) and (5R,8S)-2,4-Dioxo-1,3,7-triazaspiro[4.5] decane-1,3,7,8-tetracarboxylic acid 7-benzyl ester 1,3,8-tri-*tert*-butyl ester (10b)

The crude mixture of hydantoins (**9a** and **9b**) from previous reaction was dissolved in dry THF (190 mL) in a 500 mL round bottom flask. Di-tert-butyl dicarbonate (8.2g, 37.5mmol) and catalytic amount of DMAP (230mg, 1.9mmol) was added to the flask under N_2 flow. The reaction mixture was stirred for 3 hours to ensure complete conversion to the desired products and was monitored by TLC. The reaction volume was reduced to ~50 mL by rotary evaporation and then adsorbed on celite. Any residual solvent was removed by drying under reduced pressure. This was immediately followed by purification and separation of the desired products **10a** and **10b** by automated flash chromatography (40 gm silica columns; Solvent A: Hexanes, Solvent B: EtOAc; Gradient elution: 0-5 CVs, solvent B 10% followed by 5-45 CVs, solvent B 10% to 30%). The fractions containing pure products **10a** or **10b** were combined separately and concentrated by rotary evaporation under reduced pressure. *In vacuo* drying of the resulting viscous oils yielded **10a** (2.6g, 34.4% yield based on **7** over two steps) and **10b** (1.1g, 14.5% yield based on **7** over two steps) as white foams, along with a mixture of **10a** and **10b** (0.9g).

Less polar **10a:**

(5S,8S)-2,4-Dioxo-1,3,7-triazaspiro[4.5]decane-1,3,7,8-tetracarboxylic acid 7-benzyl ester 1,3,8-tri-*tert*-butyl ester (10a) $[\alpha]^{23}_D$ = 4.8 (*c* 1.8, CHCl$_3$); IR (film) ν_{max} 2981, 1825, 1783, 1731, 1423, 1370, 1309, 1253, 1149, 976, 843, 757, 698 cm^{-1}; ^{1}H NMR (300 MHz, 20 °C, CDCl$_3$) (mixture of rotamers) δ 7.26-7.28 (m, 5H), 4.99-5.21 (m, 2H), 4.69-4.91 (m, 1H), 3.92-4.17 (m, 2H), 2.39-2.62 (m, 2H), 2.22-2.25 (m, 1H), 1.80-1.86 (m, 1H), 1.37-1.53 (m, 27H); ^{13}C

NMR (75.4 MHz, 20 °C, CDCl$_3$) (mixture of rotamers) δ 169.7, 169.5, 167.7, 167.6, 155.5, 155.3, 148.3, 148.2, 146.9, 146.8, 144.9, 136.2, 136.0, 128.3, 128.2, 127.9, 127.8, 127.7, 127.5, 86.5, 85.2, 82.0, 67.7, 67.4, 60.4, 60.3, 53.7, 53.3, 42.8, 42.4, 27.8, 27.5, 25.6, 22.1, 21.9; HRMS-ES (*m/z*): 626.2720 (C$_{30}$H$_{41}$N$_3$O$_{10}$ + Na$^+$ requires 626.2690).

More polar **10b:**

(5R,8S)-2,4-Dioxo-1,3,7-triazaspiro[4.5] decane-1,3,7,8-tetracarboxylic acid 7-benzyl ester 1,3,8-tri-*tert*-butyl ester (10b) [α]$^{23}_D$ = -16.6 (*c* 2.9, CHCl$_3$); IR (film) ν$_{max}$ 2980, 1826, 1785, 1740, 1422, 1369, 1317, 1254, 1143, 843, 752, 698 cm^{-1}; ^{1}H NMR (300 MHz, 20 °C, CDCl$_3$) (mixture of rotamers) δ 7.26-7.31 (m, 5H), 4.93-5.19 (m, 2H), 4.26-4.44 (m, 2H), 3.66-3.82 (m, 1H), 1.95-2.37 (m, 4H), 1.32-1.52 (m, 27H); ^{13}C NMR (75.4 MHz, 20 °C, CDCl$_3$) (mixture of rotamers) δ 170.4, 170.0, 169.2, 168.9, 154.9, 154.8, 148.0, 146.4, 144.5, 135.9, 135.7, 128.0, 127.9, 127.6, 127.4, 127.2, 86.3, 84.6, 81.0, 67.0, 66.8, 63.3, 63.1, 54.7, 54.5, 46.5, 46.2, 27.4, 27.2, 21.7, 21.0; HRMS-ES (*m/z*): 626.2709 (C$_{30}$H$_{41}$N$_3$O$_{10}$ + Na$^+$ requires 626.2690).

General procedure for the hydrolysis of *t*-Boc protected hydantoins (10a and 10b)

The bis-Boc protected hydantoin was dissolved in a mixture of 3:7 TFA/DCM (40 mL per mmol of ester) and stirred at room temperature for 3 hours. The reaction progress was monitored by TLC. After the complete deprotection, the reaction mixture was diluted with some toluene and the solvents were removed by rotary evaporation. The residual viscous oil was dissolved in DCM and evaporated *in vacuo* to yield the desired product as white foam in near quantitative yield. The products were analyzed without any further purification.

(5S,8S)-2,4-Dioxo-1,3,7-triazaspiro[4.5]decane-7,8-dicarboxylic acid 7-benzyl ester (11a):

$[\alpha]^{23}_D$ = 32.5 (*c* 1.3, MeOH); IR (film) ν_{max} 3242, 1721, 1429, 1230, 1147 cm^{-1}; ^{1}H NMR (600 MHz, 20 °C, DMSO-d_6) (mixture of rotamers) δ 13.14 (br s, 1H), 10.64-10.68 (m, 1H), 7.91-7.93 (m, 1H), 7.32-7.35 (m, 5H), 5.06-5.11 (m, 2H), 4.80 (br s, 1H), 3.99-4.02 (m, 1H), 2.98-3.13 (m, 1H), 2.31 (br s, 1H), 2.04 (br s, 1H), 1.92-1.94 (m, 1H), 1.55-1.57 (m, 1H); ^{13}C NMR (75.4 MHz, 20 °C, DMSO-d_6) δ 176.4, 172.1, 156.0, 155.0, 136.7, 128.4 (2C), 127.8 (2C), 127.3, 66.7, 57.1, 52.9 and 52.5 (rotamer), 46.3, 29.0, 21.6; HRMS-ES (*m/z*): 370.1023 (C$_{16}$H$_{17}$N$_3$O$_6$ + Na$^+$ requires 370.1015).

(5R,8S)-2,4-Dioxo-1,3,7-triazaspiro[4.5]decane-7,8-dicarboxylic acid 7-benzyl ester (11b):

$[\alpha]^{23}_D$ = 8.0 (*c* 1.1, MeOH); IR (film) ν_{max} 3240, 1717, 1422, 1254, 1146 cm^{-1}; ^{1}H NMR (600 MHz, 20 °C, DMSO-d_6) (mixture of rotamers) δ 13.20 (br s, 1H), 10.82-10.83 (m, 1H), 8.70-8.71 (m, 1H), 7.30-7.35 (m, 5H), 5.06-5.16 (m, 2H), 4.77 (br s, 1H), 3.86-3.90 (m, 1H), 3.09-3.27 (m, 1H), 1.99-2.12 (m, 2H), 1.63 (br s, 2H); ^{13}C NMR (75.4 MHz, 20 °C, DMSO-d_6) δ 175.9, 172.1, 156.3, 155.4 and 155.3 (rotamers), 136.7, 128.5 and 128.5 (rotamers, 2C), 127.9, 127.5 and 127.4 (rotamers, 2C), 66.7, 60.5, 53.2 and 52.8 (rotamers), 47.8 and 47.6 (rotamers), 28.4, 21.2; HRMS-ES (*m/z*): 370.1017 (C$_{16}$H$_{17}$N$_3$O$_6$ + Na$^+$ requires 370.1015).

(2S,5S)-5-Aminopiperidine-1,2,5-tricarboxylic acid 1-benzyl ester 2-tert-butyl ester (12)

Pure bis-Boc hydantoin **10a** (2.1g, 3.5mmol) was dissolved in THF (14 mL) in a 100 mL round bottom flask. To this solution 2M aqueous KOH solution (14 ml) was added and the resulting mixture was stirred vigorously for 30 minutes at ambient temperature. The reaction mixture was extracted with EtOAc (10 mL). The aqueous layer was saved and the organic layer was further

extracted with water (2x5 mL). All the aqueous layers were combined in a beaker and cooled to

0 °C. This cooled solution was acidified by a dropwise addition of 40% aqueous HCl under

mechanical stirring. A thick white precipitate appeared as the pH approached 4-5. The addition

of HCl solution was continued until no further precipitation was observed. The solution was

filtered through a sintered glass funnel (medium pore size) and the precipitate was washed with

ice cold deionized water (~ 50 mL). This precipitate was first air dried overnight and then *in

vacuo* over anhydrous calcium sulphate. This yielded the desired amino acid **12** (1.2 gm, 91%) as

a white powder that was used as such for the next step: $[\alpha]^{23}_D$ = -26.0 (*c* 0.5, MeOH); IR (film)

ν_{max} 3314, 2977, 1730, 1526, 1449, 1368, 1328, 1251, 1152, 758, 698 cm^{-1}; ^{1}H NMR (300 MHz,

77 °C, DMSO-d_6) δ 7.33 (br s, 5H), 5.06 (br s, 2H), 4.48 (br s, 1H), 4.32 (br s, 2H), 4.22 (d, *J* =

12.4 Hz, 1H), 2.72 (d, *J* = 12.4 Hz, 1H), 1.85-2.01 (m, 3H), 1.39 (br s, 9H), 1.13-1.17 (m, 1H);

^{13}C NMR (75.4 MHz, 20 °C, DMSO-d_6) δ 173.9, 170.4, 155.8 and 155.1 (rotamers), 136.9,

128.3 (2C), 127.6, 127.2 (2C), 80.9, 66.1, 55.5, 53.7, 48.8, 30.1, 27.6 (3C), 23.1; HRMS-ES

(*m/z*): 401.1715 ($C_{19}H_{26}N_2O_6$ + Na$^+$ requires 401.1689).

(2S,5S)-5-(9H-Fluoren-9-ylmethoxycarbonylamino)-piperidine-1,2,5-tricarboxylic acid 1-benzyl ester 2-tert-butyl ester (13)

Amino acid **12** (800 mg, 2.11 mmol) was suspended in dry DCM (21 mL) under N$_2$ atmosphere

in a 100 mL 3-neck round bottom flask fitted with a condenser. To this suspension DIPEA (1.07

mL, 8.46 mmol) was added in one portion that resulted in a clear solution. A dropwise addition

of TMS-Cl (1.47 mL, 8.46 mmol) released sufficient heat to start the reflux that was continued

for an additional 90 minutes. The reaction mixture was cooled to 0 °C and 9-fluorenylmethyl

chloroformate (870 mg, 3.36 mmol) was added in one portion. The solution was allowed to

slowly warm up to room temperature and the stirring was continued under N_2 atmosphere. The reaction progress was monitored by TLC. After the completion of reaction (approximately 2 days), the reaction mixture was directly absorbed on celite and any residual solvent was removed *in vacuo*. This was followed by automated flash chromatography (40 gm silica columns; Solvent A: $CHCl_3$ with 0.1% AcOH, Solvent B: 10% MeOH/ $CHCl_3$ with 0.1% AcOH; Gradient elution: 0-5 CVs, solvent B 20% followed by 5-45 CVs, solvent B 20% to 100%). The fractions that contain the desired product, as indicated by TLC were combined and the solvent was removed by rotary evaporation. The resulting viscous oil was dried *in vacuo* to yield the desired product **13** (1.16 gm, 91%) as a white foam: $[\alpha]^{23}_D$ = -10.6 (*c* 3.9, $CHCl_3$); IR (film) ν_{max} 3156, 2977, 1737, 1691, 1583, 1452, 1433, 1405, 1352, 1280, 1226, 1154, 1109, 1012, 697 cm^{-1}; ^{1}H NMR (300 MHz, 77 °C, DMSO-d_6) δ 12.13 (br s, 1H), 7.85 (d, *J* = 7.5 Hz, 2H), 7.68 (d, *J* = 7.4 Hz, 2H), 7.51 (s, 1H), 7.28-7.42 (m, 9H), 5.10 (br s, 2H), 4.65 (d, *J* = 13.3 Hz, 1H), 4.58-4.62 (m, 1H), 4.28-4.30 (m, 2H), 4.20 (m, 1H), 2.95 (d, *J* = 13.3 Hz, 1H), 2.18 (br d, *J* = 13.5 Hz, 1H), 1.84-2.04 (m, 2H), 1.56 (ddd, *J* = 13.1, 13.1, 3.6 Hz, 1H), 1.41 (br s, 9H); ^{13}C NMR (75.4 MHz, 20 °C, DMSO-d_6) δ 172.9, 170.1 and 169.8 (rotamers), 155.0, 155.2 and 154.8 (rotamers), 143.8 (2C), 140.7 (2C), 136.9 and 136.7 (rotamers), 128.3 (2C), 127.7 (2C), 127.2 (3C), 127.1 (2C), 125.2 (2C), 120.1 (2C), 81.3, 79.2, 66.3, 65.5, 55.9 and 55.8 (rotamers), 53.9 and 53.7(rotamers), 46.8 and 46.6 (rotamers), 28.8, 27.6 (3C), 22.5; HRMS-ES (*m/z*): 623.2373 ($C_{34}H_{36}N_2O_8$ + Na^+ requires 623.2369).

(2S,5S)-5-(9H-Fluoren-9-ylmethoxycarbonylamino)-piperidine-1,2,5-tricarboxylic acid 1-benzyl ester 2-tert-butyl ester 5-methyl ester (14)

The Fmoc protected amino acid **13** (165 mg, 0.28 mmol) was placed in a 25 mL round bottom flask and dissolved in dry MeOH (3 mL) under N_2 atomsphere To this clear solution, TMS-CHN_2 was slowly added until no further evolution of N_2 was observed and the reaction mixture turned yellow. The excess of TMS-CHN_2 was quenched by an addition of 10% AcOH/MeOH (~1 mL). The reaction mixture was concentrated by rotary evaporation and the residual solvent was removed *in vacuo* to yield **14** (169 mg, >99%) as a white foam. An analytical sample was prepared by manual flash chromatography (silica column; solvent: 30% EtOAc/Hexanes, Isocratic elution): $[\alpha]^{23}_D$ = -12.8 (*c* 4.8, CHCl$_3$); IR (film) ν_{max} 3322, 2977, 2951, 1731, 1527, 1449, 1368, 1323, 1252, 1153, 758, 698 cm^{-1}; ^{1}H NMR (300 MHz, 77 °C, DMSO-d_6) δ 7.86 (d, *J* = 7.5 Hz, 2H), 7.66-7.69 (m, 3H), 7.29-7.43 (m, 9H), 5.11-5.13 (m, 2H), 4.60-4.69 (m, 2H), 4.34 (d, *J* = 6.6 Hz, 2H), 4.20 (t, *J* = 6.6 Hz, 1H), 3.54 (br s, 3H), 2.96 (d, *J* = 13.5 Hz, 1H), 2.17 (br d, *J* = 13.5 Hz, 1H), 1.98-2.04 (m, 1H), 1.78-1.88 (m, 1H) 1.57 (ddd, *J* = 13.1, 13.1, 3.7 Hz, 1H), 1.42 (br s, 9H); ^{13}C NMR (75.4 MHz, 20 °C, DMSO-d_6) δ 171.7, 169.9 and 169.7 (rotamers), 155.0, 154.8, 143.7 and 143.6 (rotamers, 2C), 140.8 (2C), 136.8 and 136.7 (rotamers), 128.3 (2C), 127.7 (2C), 127.3 (3C), 127.0 (2C), 125.1 (2C), 120.1 (2C), 81.4, 79.2, 66.4 and 66.3 (rotamers), 65.4, 56.2 and 56.1 (rotamers), 53.8 and 53.5 (rotamers), 52.0, 46.7, 29.0 and 28.8 (rotamers), 27.5 (3C), 22.5; HRMS-ES (*m/z*): 637.2546 (C$_{35}$H$_{38}$N$_2$O$_8$ + Na$^+$ requires 637.2526).

(2S,5S)-5-(9H-Fluoren-9-ylmethoxycarbonylamino)-piperidine-1,2,5-tricarboxylic acid 1,5-dibenzyl ester 2-tert-butyl ester (19)

The Fmoc protected amino acid **13** (408 mg, 0.67 mmol) was transferred to a 25 mL round bottom flask and dissolved in dry DCM (4 mL) under N_2 atomsphere. This was followed by addition of a catalytic amount of DMAP (8 mg, 0.06 mmol) and then benzyl alcohol (1 mL). The resultant solution was cooled in an ice bath and DCC (139 mg, 0.67 mmol) was added in one portion. The reaction mixture was allowed to warm up to room temperature and the stirring was continued. The reaction progress was monitored by TLC. After the completion of reaction (about 2 days) the reaction mixture was diluted with DCM and filtered to remove the byproduct DCU precipitate. The filtrate was concentrated and absorbed on celite. Any residual solvent was removed *in vacuo* and the crude product on celite was purified by automated flash chromatography (40 gm silica columns; Solvent A: Hexanes, Solvent B: EtOAc; Gradient elution: 0-5 CVs, solvent A 100% followed by 5-45 CVs, solvent B 0% to 30%). The fractions that contain the desired product were combined and the solvent was removed by rotary evaporation. The resulting viscous oil was dried *in vacuo* to yield the desired product **19** (406 mg, 88%) as a white foam: $[\alpha]^{23}_D$ = -15.0 (*c* 1.8, CHCl$_3$); IR (film) ν_{max} 3322, 2976, 1731, 1526, 1450, 1321, 1252, 741, 697 cm^{-1}; ^{1}H NMR (300 MHz, 77 °C, DMSO-*d$_6$*) δ 7.85 (d, *J* = 7.5 Hz, 2H), 7.71 (s, 1H), 7.65 (d, *J* = 7.4 Hz, 2H), 7.26-7.42 (m, 14H), 5.04 (br s, 4H), 4.70 (d, *J* = 13.3 Hz, 1H), 4.61 (m, 1H), 4.30 (d, *J* = 6.6 Hz, 2H), 4.16 (t, *J* = 6.6 Hz, 1H), 2.97 (d, *J* = 13.3 Hz, 1H), 2.20 (br d, *J* = 13.5 Hz, 1H), 1.98-2.03 (m, 1H), 1.72-1.88 (m, 1H) 1.58 (ddd, *J* = 12.9, 12.9, 3.5 Hz, 1H), 1.41 (br s, 9H); ^{13}C NMR (75.4 MHz, 20 °C, DMSO-*d$_6$*) δ 171.1, 169.9 and 166.6 (rotamers), 155.1 (2C), 154.7, 143.7 and 143.6 (rotamers, 2C), 140.7 (2C), 136.7, 135.9, 128.3 (2C), 128.2 (2C), 127.8 (2C), 127.6 (2C), 127.3 (3C), 127.0 (2C), 125.1 (2C), 120.1 (2C),

81.4, 79.2, 66.5, 66.0, 65.6, 56.3 and 56.2 (rotamers), 53.7 and 53.5 (rotamers), 46.6, 29.1, 24.5

(3C) 22.4; HRMS-ES (*m/z*): 713.2875 ($C_{41}H_{42}N_2O_8$ + Na^+ requires 713.2839).

General procedure for the hydrolysis of *t*-butyl esters (14 and 19)

The *t*-butyl ester was dissolved in a mixture of 3:7 TFA/DCM (40 mL per mmol of ester) and was stirred at room temperature for 2-3 hours. The reaction progress was monitored by TLC. After the completion, the reaction mixture was diluted with some toluene (to protect against high concentration of TFA during evaporation) and the solvents were removed by rotary evaporation. The residual viscous oil was dissolved in DCM and evaporated *in vacuo* to yield the desired product as white foam in quantitative yield. An analytical sample was prepared by manual flash chromatography (silica column; solvent: 5% MeOH/CHCl₃, Isocratic elution).

(2S,5S)-5-(9H-Fluoren-9-ylmethoxycarbonylamino)-piperidine-1,2,5-tricarboxylic acid 1,5-dibenzyl ester (18)

$[\alpha]^{23}_D$ = -16.7 (*c* 5.1, CHCl₃); IR (film) ν_{max} 3317, 3034, 2952, 1717, 1522, 1449, 1315, 1251, 758, 741, 697 cm⁻¹; ¹H NMR (300 MHz, 77 °C, DMSO-*d₆*) δ 12.30 (br s, 1H), 7.85 (d, *J* = 7.5 Hz, 2H), 7.69 (s, 1H), 7.65 (d, *J* = 7.4 Hz, 2H), 7.23-7.42 (m, 14H), 5.03-5.06 (m, 4H), 4.67-4.73 (m, 2H), 4.28 (d, *J* = 6.6 Hz, 2H), 4.16 (t, *J* = 6.6 Hz, 1H), 3.01 (d, *J* = 13.3 Hz, 1H), 2.22 (br d, *J* = 13.5 Hz, 1H), 2.00-2.06 (m, 1H), 1.85 (m, 1H) 1.59 (ddd, *J* = 13.2, 13.2, 3.8 Hz, 1H); ¹³C NMR (75.4 MHz, 20 °C, DMSO-*d₆*) δ 172.3 and 172.1 (rotamers), 171.2, 155.1 (2C), 154.7, 143.7 (2C), 140.8 (2C), 136.7, 135.9, 128.4 (2C), 128.3 (2C), 127.9 (2C), 127.7 (2C), 127.3 (3C), 127.1 (2C), 125.1 (2C), 120.1 (2C), 79.2, 66.5, 66.1, 65.7, 56.2, 53.2 and 52.9 (rotamers), 46.6, 29.3, 22.3; HRMS-ES (*m/z*): 657.2230 ($C_{37}H_{34}N_2O_8$ + Na^+ requires 657.2213).

(2S,5S)-5-(9H-Fluoren-9-ylmethoxycarbonylamino)-piperidine-1,2,5-tricarboxylic acid 1-benzyl ester 5-methyl ester (3)

$[\alpha]^{23}_D$ = -8.0 (*c* 0.9, CHCl$_3$); IR (film) ν_{max} 3317, 3033, 2952, 1716, 1523, 1448, 1318, 1237, 758, 741, 697 cm^{-1}; ^{1}H NMR (300 MHz, 77 °C, DMSO-d_6) δ 12.30 (br s, 1H), 7.85 (d, *J* = 7.5 Hz, 2H), 7.66 (d, *J* = 7.4 Hz, 2H), 7.60 (s, 1H), 7.27-7.42 (m, 9H), 5.11 (br s, 2H), 4.67-4.70 (m, 1H), 4.62 (d, *J* = 13.3 Hz, 1H), 4.31 (d, *J* = 6.6 Hz, 2H), 4.19 (t, *J* = 6.6 Hz, 1H), 3.52 (br s, 3H), 2.99 (d, *J* = 13.3 Hz, 1H), 2.17 (br d, *J* = 13.5 Hz, 1H), 2.00-2.06 (m, 1H), 1.83-1.88 (m, 1H) 1.57 (ddd, *J* = 13.1, 13.1, 3.8 Hz, 1H); ^{13}C NMR (75.4 MHz, 20 °C, DMSO-d_6) δ 172.3 and 172.1 (rotamers), 171.7, 155.0, 154.7, 143.7 (2C), 140.8 (2C), 136.8, 128.4 (2C), 127.7 (2C), 127.3 (3C), 127.1 (2C), 125.1 (2C), 120.3 (2C), 80.3, 78.1, 65.5, 56.1, 52.9, 52.0, 46.7, 29.1, 22.4; HRMS-ES (*m/z*): 581.1892 (C$_{31}$H$_{30}$N$_2$O$_8$ + Na$^+$ requires 581.1900).

2.7.3   Solid Phase synthesis

The Solid phase chemistry was performed on a home-built manual synthesizer. Dry dichloromethane used in coupling reactions was obtained from distillation over CaH$_2$. Diisopropylethyl amine (DIPEA) was distilled under nitrogen sequentially from ninhydrin and potassium hydroxide and stored over molecular sieves (4Å). Rink Acid resin was purchased from NovaBiochem. Anhydrous DMF and O-(7-azabenzotriazol-1-yl)-N,N,N',N'-tetramethyluronium hexafluorophosphate (HATU) was obtained from Aldrich. All other reagents used were purchased either from Aldrich or Acros and used as such. All solid phase reactions were mixed by bubbling argon through the reaction mixture and kept under argon atmosphere.

General procedure A: Washing

In a typical washing sequence, the resin was washed 5 times with DCM and DMF alternately. This was followed by a final wash with DCM.

General procedure B: HATU coupling

In a 1.5 mL polypropylene micro centrifuge vial the amino acid (as given) was dissolved in a solution of 10% DCM/ DMF (as given). To this mixture was added DIPEA (as given) followed by HATU (as given). The resulting coupling mixture was mixed briefly and immediately added to the SPPS reaction vessel carrying the resin. After mixing for the given amount of time, the resin was drained and washed according to the general procedure (A).

General procedure C: Fmoc deprotection

To the SPPS reactor carrying the resin added 1000 μL of a solution of 2% DBU in DMF. After 5 minutes of mixing, a volume of 40 μL of deprotection mixture was withdrawn and diluted 50 fold with a solution of 20% piperidine in DMF. A UV-visible spectroscopic analysis of the piperidine-fluorenyl adduct was performed and the absorbance at 301 nm ($\varepsilon = 7800$ M^{-1}cm^{-1}) was recorded. This value of the absorbance was used to estimate coupling yield. Following the Fmoc deprotection, the resin was washed according to general procedure (A).

General procedure D: Capping of the residual free amine

To the SPPS reactor carrying the resin added 250 μL of a solution of 10% pivalic anhydride in pyridine. After 5 minutes of mixing, the resin was drained and washed according to the general procedure (A).

Solid phase assembly of pip5(2S5S) threemer

The coupling of Fmoc-glycine to rink acid resin was achieved via a procedure similar to the one described in Novabiochem catalogue (2006/07 section 2.17). 18 mg of resin (0.68 mmole/g loading) were transferred to a 1 mL polypropylene solid phase peptide synthesis (SPPS) reaction vessel and allowed to swell in DMF for 1 hour.

In a 1.5 mL polypropylene micro centrifuge vial N-α-Fmoc-glycine (18.2 mg, 61.2 μmol), NMM (1.7 μL, 15.2 μmol), DIPCDI (10.2 μL, 65 μmol) and DMAP (0.1 mg, 0.8 μmol) in DCE (306 μL) were mixed for a minute and added to the SPPS reaction vessel carrying the resin. After 4 hours of mixing, the solution was drained and the resin was washed according to general procedure (A). The terminal Fmoc group was deblocked by general procedure (C). The resin loading was determined as 15.1 μmoles and was used for all further calculations of reagents.

Monomer **18**, pip5(2S5S)*(OBn)* (19.2 mg, 30.2 μmol, 2 equivalent) was dissolved in 20% DCM/ DMF solution (151 μL) and coupled for 1.5 hours according to general procedure (B) by using DIPEA (10.5 μL, 60.5 μmol) and HATU (11.5 mg, 30.2 μmol). The resin was subjected to a second coupling reaction under identical conditions. Any residual free amine was capped according to general procedure (D). The terminal Fmoc group was deblocked by general procedure (C). The coupling yield was estimated as 85%.

This coupling sequence was repeated one more time with monomer **18** as above that resulted in near quantitative coupling.

Monomer **3**, pip5(2S5S)*(OMe)* (16.9 mg, 30.2 μmol, 2 equivalent) was dissolved in 20% DCM/ DMF solution (151 μL) and coupled for 1.5 hours according to general procedure (B) by using DIPEA (10.5 μL, 60.5 μmol) and HATU (11.5 mg, 30.2 μmol). The resin was subjected to a second coupling reaction under identical conditions. Any residual free amine was capped

according to general procedure (D). The terminal Fmoc group was deblocked by general procedure (C). The coupling yield was estimated as near quantitative.

N-α-Fmoc-*O-tert*-butyl-L-tyrosine (15.2 mg, 33 μmol, 2.2 equiv) was dissolved in 20% DCM/ DMF solution (165 μL) and coupled for 1 hour according to general procedure (B) by using DIPEA (11.5 μL, 66 μmol) and HATU (12.6 mg, 33 μmol). The resin was subjected to a second coupling reaction under identical conditions. The terminal Fmoc group was deblocked by general procedure (C). The coupling yield was estimated as near quantitative. The terminal amine was acylated according to general procedure (D). The acylation procedure (D) was repeated one additional time to ensure complete acylation. The resin was prepared for cleavage by washing with MeOH and DCM alternately followed by drying under reduced pressure.

The cleavage of the oligomer from resin was affected by treatment of the resin with 10% TFA/DCM (0.5 mL) for 5 minute. The cleavage solution was collected after filtration and the resin was treated again two more times with TFA solution. All filtered solutions were combined and stirred at room temperature for 90 additional minutes to ensure the complete removal of the *t*-butyl group on tyrosine. The solvent was evaporated under a stream of dry nitrogen and any residual solvent was removed *in vacuo*, yielding oligomer **29** as a white residue.
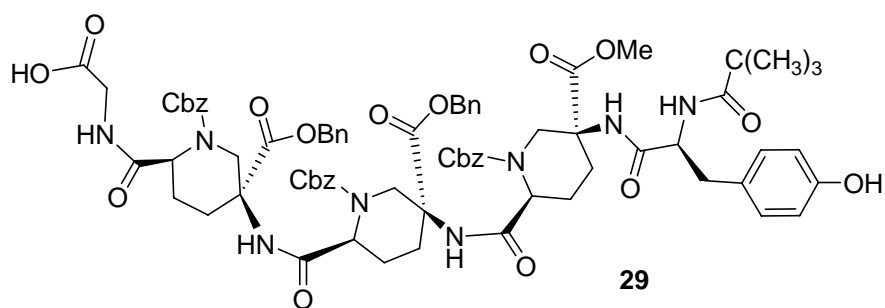
HPLC-MS: Column, Waters XTerra MS C_{18} 4.6 mm x 100 mm; mobile phase, MeCN/water (0.1% Formic acid), 5% to 95% MeCN over 30 minutes; flow rate, 0.40 mL/min; UV detection at 274 nm; t_R for **29**, 27.1 min; ES-MS: m/z (ion) 1429.3 (M+H^{+} expected 1429.6)

Removal of Cbz groups

Cbz and benzyl protected oligomer **29** was dissolved in a mixture of 7:2:1 methanol/water/acetic acid (2 mL) in a 10 mL round bottom flask. 10 wt.% Pd on activated carbon (~ 5 mg) was added to this solution and after degassing under reduced pressure the reaction flask was backfilled with H_2 gas several times. The process of degassing and backfilling with H_2 gas was repeated and the stirring was continued overnight. The reaction mixture was filtered through a Spin-X centrifuge filter (0.2 micron nylon frit). The residue was washed with methanol (2 x 100 µL) and all filtrates were combined. A small volume (10 µL) was set aside for HPLC-MS analysis and rest of the solution was dried *in vacuo* to yield **21** as a white solid.

HPLC-MS: column, Waters XTerra MS C_{18} 4.6 mm x 100 mm; mobile phase, MeCN/water (0.1% Formic acid), 5% to 95% MeCN over 30 minutes; flow rate, 0.40 mL/min; UV detection at 274 nm; t_R for **21**, 10.3 min; ES-MS m/z (ion) 847.3 (M+H$^+$ expected 847.4).

DKP closure via *in situ* activation methodology

Oligomer **21** was dissolved in 1.5 mL of dry NMP in a 10 mL round bottom flask and a small volume (10 µL) was set aside for HPLC-MS analysis. To the rest of the solution, DIPEA (40 µL, 230 µmol, 6 equiv per amide bond) was added. This was followed by addition of DCC (25 mg, 126 µmol, 3 equiv per amide bond, predissolved in 250 µL of NMP) and N-hydroxysuccinimide (25mg, 220 µmol, 6 equiv per amide bond, predissolved in 250 µL of NMP). The reaction mixture was stirred at room temperature. In order to monitor the reaction progress, a volume of 5 µL was withdrawn from the reaction mixture and injected into HPLC-MS for analysis. After 24 hours of stirring the reaction was complete as indicated by HPLC-MS.

HPLC-MS: column, Waters XTerra MS C_{18} column 4.6 mm x 100 mm; mobile phase, MeCN/water (0.1% Formic acid), 5% to 95% MeCN over 30 minutes; flow rate, 0.40 mL/min; UV detection at 274 nm; t_R for **22**, 13.9 min; ES-MS m/z (ion) 793.3 (M+H$^+$ expected 793.4).

The reaction mixture was filtered through a Spin-X centrifuge filter and purified by preparative HPLC on a Varian ProStar 500 HPLC system with a Varian Chrompack Micrsorb 100-C_{18} column (8 μm packing; 21.5mm x 50mm): mobile phase, MeCN (0.1%TFA)/water (0.05% TFA), 5% to 95% MeCN over 30 minutes; flow rate, 15 mL/min; UV detection at 274 nm). The product containing fractions were lyophilized to yield the desired rigidified oligomer **22** as a fluffy white powder (2.5 mg). HRMS-ES (*m/z*): 793.3606 ($C_{38}H_{48}N_8O_{11}$ + H$^+$ requires 793.3521).

NMR Sample Preparation

Approximately 2.5 mg of purified oligomer **22** was dissolved in 400 μL of 9:1 H_2O/D_2O and transferred to an advanced microtube matched with D_2O purchased from Shigemi, Inc. All 1-D and 2-D spectra at room temperature were recorded either on Bruker 500MHz or 600MHz instrument. NMR spectra (1D and 2D) and other relevant data are supplied in appendix.

3.0 IMPROVED METHODOLOGY FOR DIKETOPIPERAZINE FORMATION AND APPLICATION TO THE ASSEMBLY OF HETEROOLIGOMERS

As described in Chapter 2, we successfully utilized *in-situ* activation of carboxylic acid for the formation of amide bonds for the rigidification of small oligomers, however it was not extendable to long sequences. This prompted us to reconsider ester aminolysis for DKP formation.

Diketopiperazine formation has been the subject of several reviews and numerous catalysts have been reported for aminolysis.[169, 170] A particularly facile reagent and the one that we initially used to catalyze an intramolecular aminolysis reaction between an amine and an ester, was a 20% (v/v) solution of piperidine in dimethylformamide (Scheme 9).[108, 111] We found these conditions to be quite effective for pro4 monomers, but they were not ideal for several reasons. Occasionally, precipitate would form in the reaction mixture and the yield of fully closed product was low. We also discovered that for oligomers containing hin*(2S4R7R9R)* or pip5(2S5S) the DKP formation between monomers under 20% piperidine in dimethylformamide was very slow or undetectable.
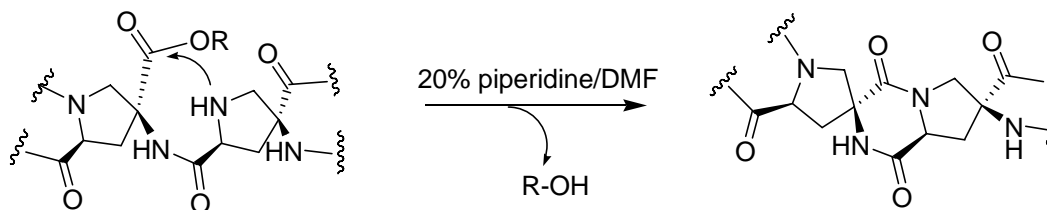
Scheme 9: Diketopiperazine formation in a bis-peptide by 20% piperidine/DMF catalyzed aminolysis

The rate of DKP formation is known to be sensitive to the stereochemistry and nature of the substituents on the forming DKP ring.[171] This would rationalize a big difference observed in rates of DKP closure with various monomers. An obvious solution would have been to carry out the DKP closure at higher temperature. Unfortunately we couldn't use high temperatures or long reaction times to drive the aminolysis reaction towards completion because DKPs tend to epimerize under basic conditions.[172] It was for this reason that we undertook this search for an appropriate bifunctional catalyst for DKP closure.

Apart from being a base catalyzed reaction, aminolysis is also known to be catalyzed by bifunctional catalysts including carboxylic acids[171, 173, 174] as well as neutral compounds,[175] such as 1,2,4 triazole and 2-pyridone. One advantage of using a bifunctional catalyst is that the reaction conditions utilized are either neutral or mildly acidic. These reaction conditions are not conducive for epimerization. Thus we could use long reaction time or high temperature to accelerate the DKP formation without fear of epimerization.

There are numerous reports on the use of bifunctional catalysts for aminolysis and a wide range of compounds have demonstrated catalytic ability as catalyst. These examples are largely for bimolecular reactions and include carboxylate anion,[171] 2-hydroxypyridine,[175-178] DMAP,[179] imidazole,[175] nucleosides,[180] cyanide,[181] 1,2,4-triazole[175] and catechol.[182] There are also some reports of intramolecular variant which involve the formation of five- and six-membered rings.[171, 173, 183] After a careful survey of available options we selected acetic acid for its simplicity. Acetic acid has been discovered by Gisin and Merrifield[171] to accelerate DKP formation in dipeptides. We also selected 2-hydroxypyridine[175] because of its catalytic activity in a variety of reactions. (Figure 12)
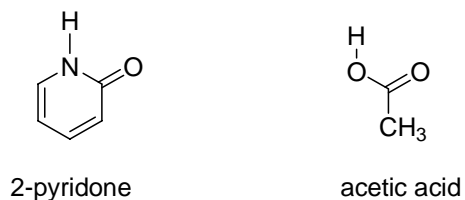
Figure 12: Bifunctional catalysts used in present study

As pointed out earlier, another problem with DKP formation was that occasionally intermediates precipitated out of the solution that we believe stalled any further DKP formation. We reasoned that by closing DKPs on resin, the solubility problem could be avoided. Any byproducts of the reaction could be easily washed away, yielding expected rigidified products with high purity. Also, the oligomer could be further functionalized while is still attached to the resin that would further reduce the number of reaction and purification steps needed.

3.1   STUDIES ON DKP FORMATION

In order to explore different solvents, catalyst concentrations and temperatures we chose to close the diketopiperazines on solid support and measure the kinetics thereof. As DKP are closed on resin an equimolar amount of alcohol is formed that passes into solution in which the resin is suspended. We reasoned that if this alcohol was a UV chromophore, the extent of DKP closure could be estimated by measuring the amount of released alcohol. *p*-Nitrobenzylalcohol was chosen for these kinetic studies because of high absorbance and ease of ester formation. Accordingly, monomer **32** and **33** were obtained from Fmoc amino acid intermediates **29** and **13** respectively, in a 2-step procedure that involved ester formation via nucleophilic substitution by

carboxylate at *p*-nitrobenzyl bromide followed by unmasking of carboxylic acid functionality with TFA as shown in Scheme 10.
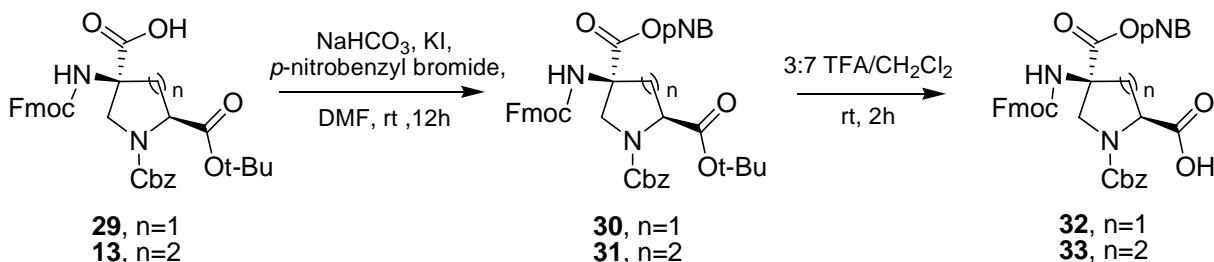
Scheme 10: Synthesis of pNB ester version of monomers

Also we needed to expose a secondary amine after the solid phase assembly on each monomer so that DKP formation could be carried out while the oligomer is still attached to solid support. This was accomplished using monomers **35** and **36** that were obtained by exchanging a Cbz protecting group with a Boc group[184] on pro4(2S4S) and pip5(2S5S) monomers (Scheme 11).
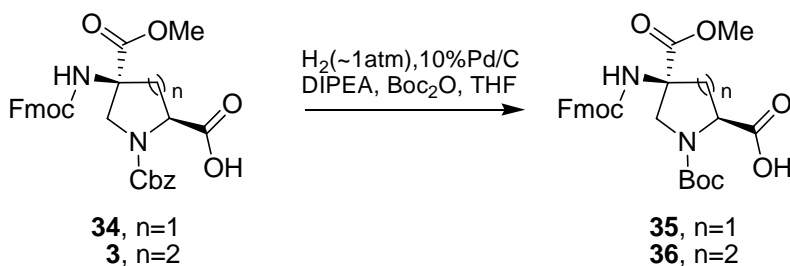
Scheme 11: Cbz to Boc exchange for the synthesis of monomers **35** and **36**

We assembled all 4 possible combinations of bis-amino acid dimers **37a-d**, using monomers **32**, **33**, **35** and **36** on TFMSA cleavable but TFA stable MBHA[185] resin. Our goal was to find the combination that gave the slowest reaction rate by measuring the kinetics of DKP formation in a flow-cell containing resin bound dimers **37a-d** and optimize the reaction

conditions for this dimer. This was to make sure that upon using these optimized reaction conditions the DKP formation on resin was complete for all monomers. We hypothesized that this could be accomplished by quantifying the amount of *para*-nitrobenzyl alcohol in the effluent as different catalyst solutions were flowed over the resin at varying temperatures (Figure 13). This was to be followed by optimization of the catalyst solutions against the slowest combination and find conditions under which all diketopiperazines close rapidly.
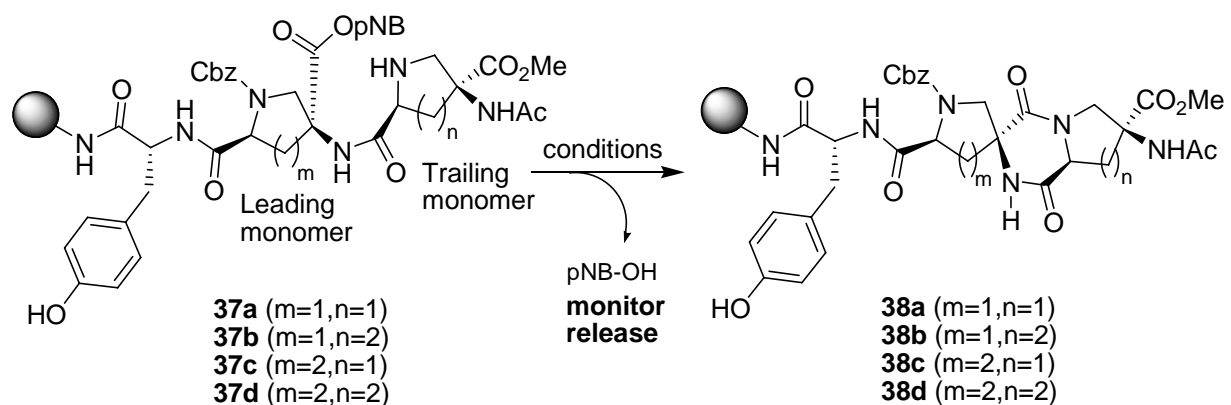
Figure 13: On resin diketopiperazine formation reaction with bis-amino acid dimers

3.1.1 Effect of monomer combination

A series of diketopiperazine closures experiments was performed using two bifunctional catalysts, 2-pyridone and acetic acid, to examine how the nature of the monomers affects the rate of intramolecular aminolysis. The kinetic data obtained were used to calculate half-lives for the aminolysis reaction in each set of experiments (Table 1).

Gisin and Merrifield[171] found that the maximum rate of acetic acid catalyzed DKP formation occurred at an AcOH concentration of 80 mM. We used the same concentration for

our experiments as well. Deutero acetic acid was used because epimerization of **38a-d** would give rise to an increase in molecular weight of at least one Dalton.

Rony and coworkers[175] studied the aminolysis of 4-nitrophenyl acetate by n-butylamine in benzene and concluded that 2-pyridone provided the greatest acceleration and the rate of reaction increased with the concentration of catalyst. We chose 50 mM as a starting point because at this concentration *o*-xylene becomes nearly saturated with 2-pyridone. Some triethyl amine was also added to the catalytic solution to minimize dimerization of 2-pyridone. Addition of a base lowers the dimerization constant by preferentially solvating monomeric form of 2-pyridone.[175]

Table 1: Half-lives of DKP formation using 2-pyridone and acetic acid as catalysts

DKP closure sequence (Figure 13)	Half life $t_{1/2}$ (min) for	
	50 mM 2-pyridone, 1mM Et$_3$N, o-xylene, 130 °C	80 mM AcOD, DMF, 100 °C
pro4-pro4(37a→38a)	<4	6.5
pro4-pip5(37b→38b)	<4	12
pip5-pro4(37c→38c)	15	16
pip5-pip5(37d→38d)	17	78

A comparison of half lives observed for different combinations of monomers showed that 2-pyridone and acetic acid are both competent bifunctional catalysts under the given conditions (Table 1). An 80 mM solution of acetic acid-*d* in dimethylformamide at 100 °C is a good catalyst

for the formation of **38a-c** but four times slower for the formation of **38d**. This indicated that for acetic acid, the rate of DKP formation is dependent on both monomers, leading and trailing.

A similar trend was observed with 50 mM 2-pyridone in *o*-xylene at 130 °C as catalyst, except that the dependence on the leading monomer, i.e. the one that carries the ester functionality was more prominent. When the dimers **38a-d** were cleaved from the resin, no epimerization was observed in any experiments.

3.1.2 Effect of temperature and concentration on catalysis by 2-pyridone

Initially it appeared that 2-pyridone is more effective than acetic acid in accelerating the DKP formation and could be a viable solution to our DKP formation problems. In order to confirm this we examined the effect of temperature and concentration of 2-pyridone on the rate of formation of **38c**. (Table 2).

Table 2: The half-life of DKP formation for the formation of **38c**

Reaction conditions	Half life $t_{1/2}$ (min)
10 mM 2-pyridone, 1 mM Et$_3$N, toluene, 100 °C	158
50 mM 2-pyridone, 1 mM Et$_3$N, toluene, 100 °C	72
50 mM 2-pyridone, 1 mM Et$_3$N, o-xylene, 130 °C	15

The data showed that 2-pyridone at 10 mM concentration was not an effective catalyst at 100 °C. Increasing the catalyst concentration 5-fold to 50 mM accelerated the reaction but only by a factor of 2. We attributed this moderate increase to the tendency of 2-pyridone to dimerize

in non-polar solvents.[186] Increasing the concentration only helps in pushing the equilibrium between its active form (monomer) and inactive form (dimer) towards the dimer. Also, the solubility of 2-pyridone was not much higher than 50 mM in *o*-xylenes and there was little room for improvement.

3.1.3   Solvent and temperature effect on catalysis by acetic acid

To explore more optimal acetic acid catalyzed DKP formations conditions, we investigated the effect of solvent and temperature on AcOD catalyzed formation of **38b** (Table 3). The concentration of acetic acid was kept unchanged throughout the comparative experiments to simplify the interpretation of the observed trends.

Table 3: The solvent and temperature effect on DKP formation in **37b** for 80 mM AcOD as catalyst

Temperature (T °C)	Half life, $t_{1/2}$ (min) for	
	DMF	o-xylene
40	126	n/a
70	31	115
100	12	18
130	<4	<2

As anticipated, increasing the temperature accelerates the rate of DKP formation in both solvents. However, the temperature effect was stronger in non polar solvent i.e. *o*-xylene. At lower temperatures the reaction was faster in DMF (e.g. 70 °C) but at higher temperatures *o*-xylene accelerated reaction more than DMF. Dimethylformamide is not considered a suitable reaction medium at elevated temperatures as it decomposes above 100 °C. On the other hand *o*-xylene doesn't have this limitation and can be safely used at temperatures up to 130-135 °C.

From the above analysis, we concluded that 80 mM AcOD in *o*-xylene at 130 °C served as an effective catalyst. We used these conditions for sequence **37d,** that represents a pip5-pip5 combination, the half-life was found to be 12.5 minutes. This entailed that more than 1.5 hour (7 half-lives) was needed to ensure > 99 % DKP closure. This prompted us to continue the search for even better reaction conditions for aminolysis.

3.1.4   Effect of added triethyl amine on catalysis by acetic acid

The work of Capasso and co-workers[187] suggested that triethylammonium acetate was at least ten times faster at catalyzing DKP formation than acetic acid by itself. Following their lead, we examined the effect of adding triethylamine to the catalyst solution and found that DKP formation was accelerated by a factor of two to three in the formation of **38d** (Table 4) relative to when no triethylamine was added.

Table 4: The half life of diketopiperazine formation in the reaction **37d→38d** exploring different concentrations of acetic acid and triethylamine.

Solvent: o-xylene, Temperature: 130 °C	Half life $t_{1/2}$ (min)
80 mM AcOD	12.5
50 mM AcOD	9.5
50 mM AcOD + 50 mM Et$_3$N	5
100 mM AcOD + 50 mM Et$_3$N	4.3
1 mM Et$_3$N	266

Giralt and coworkers[188] have shown that trifluoroacetic acid inhibited the DKP formation via aminolysis reaction. It is likely that in Capasso's studies[187] the triethylamine served to neutralize the acidic trifluoroacetate salt of the dipeptides that underwent diketopiperazine formation. In our system, we free-base our amines on solid support by washing the deprotected resin with triethylamine in dimethylformamide prior to diketopiperazine closure. This could explain the moderate increase in the rate of aminolysis observed for our systems. Nonetheless, this 2 to 3 fold acceleration provided by addition of triethylamine was sufficient to drive the DKP closure reaction in pip5-pip5 dimer to completion in less than 20 minutes. We believe that Et$_3$N helps in DKP formation by neutralizing the secondary amines and the carboxylic acid catalyzes the aminolysis reaction.

3.2   ATTEMPTED ON-RESIN DKP CLOSURE WITH METHYL ESTER

Next we wanted to test if methyl ester versions of pro4 and pip5 monomers could be used for DKP closure as *p*-nitrobenzyl ester version of monomers (**32** and **33**) couldn't be used without retooling the monomer synthesis. *p*-Nitrobenzyl ester is sensitive to hydrogenolysis, that is used to exchange the Cbz group with a Boc group during the synthesis of the monomer. For our strategy of on-resin DKP to be effective this swapping is highly desired as the Boc group can be quantitatively removed on MBHA resin by 1:1 TFA/DCM to free the secondary amine for DKP closure. If successful, we could use the existing methyl ester versions of monomers, without a need to retool the synthesis of monomers.
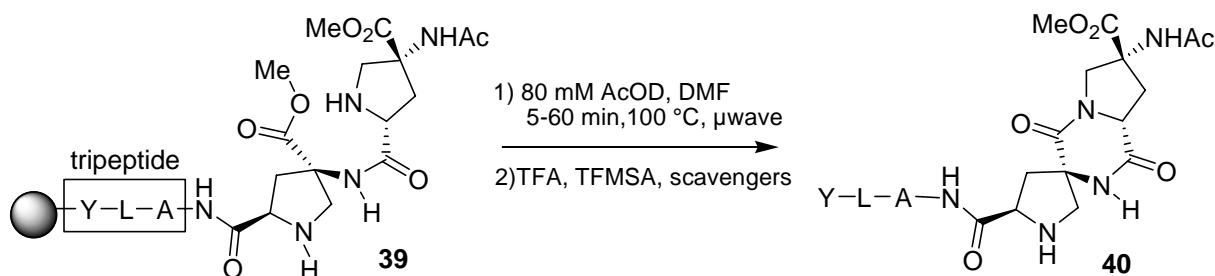
Figure 14: DKP closure between two pro4 monomers with methyl esters

The answer came from a series of experiments performed in collaboration with Megan Macalla, a fellow graduate student in research group. She measured the rate of closure of a pro4-pro4 dimer using methyl ester bearing monomers (Figure 14). In this case, the intramolecular aminolysis reaction was between a secondary amine and a methyl ester rather than a secondary amine and a *p*-nitrobenzyl ester such as **32**. The results showed that for pro4-pro4 combinations under microwave irradiation and 80 mM AcOD in *o*-xylene as catalyst, the use of methyl ester in place of *p*-nitrobenzyl ester slows down the rate of DKP formation by a factor of 5.5.

By using 5.5 as a scaling factor, we projected that the half-life for pip5-pip5 combinations with methyl esters using the optimized reaction conditions (100 mM AcOD, 50 mM Et₃N in *o*-xylene at 130 °C, µwave) should be 20-30 minutes.
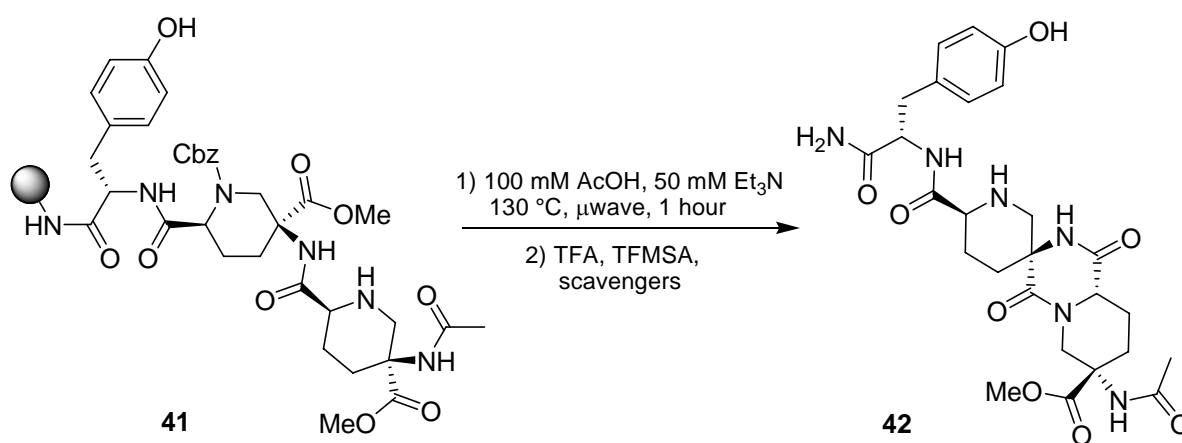
Figure 15: On-resin DKP closure using µwave for a dimer of pip5 (2S5S) monomers with methyl ester.

To test this prediction we assembled a dimer **41** from two pip5(2S5S)(OMe) monomers on MBHA resin and subjected it to microwave irradiation in presence of 100 mM AcOH and 50 mM Et₃N in o-xylene at 130 °C for 1 hr. (Figure 15) The oligomer was then cleaved from the resin using TFMSA. The analysis of the product by HPLC-MS revealed complete conversion to the expected product **42** without any side product or epimerization.

Buoyed by this favorable result, we assembled a short oligomer (4-mer) from pip5(2S5S)(OMe) monomers **3** and attempted DKP closure under the conditions as utilized for dimers. To our surprise, even after 8 hours of microwave heating we obtained a little product with mostly a mixture of products that corresponded to one failed DKP formation.

We hypothesized that this failure to close DKP in an oligomer other than a dimer can be attributed to the difference in reaction environment felt by different pairs of monomers

undergoing DKP closure. A pair of monomers preceded or followed by a monomer might need to overcome a higher energy barrier for DKP formation than the pair without a preceding or following monomer. This scenario is further complicated by the statistical probability that DKP formation between a pair of monomers could take place in any order thus changing the energy landscape for later DKP formations. This result forced us to explore ways to further improve our DKP formation methodology that could overcome this probable decrease in rate of DKP formation for longer sequences.

3.3   2,2,3,3 TETRAFLUORO PROPYL ESTERS TO ACCELERATE DKP FORMATION

Bimolecular aminolysis of activated esters has been studied in great detail by Menger et al.[189, 190] They showed that in a non polar medium, the rate determining step is the breakdown of the tetrahedral intermediate to yield amide product and an alcohol. This suggested that the rate of aminolysis can be accelerated by using a more activated ester i.e. the corresponding alcohol has a lower pKa value. That would convert the alcohol into a better leaving group and thus accelerate the collapse of tetrahedral intermediate.

Methyl alcohol has a pKa value of 15.5. On the other hand the pKa value for *p*-nitrobenzyl alcohol is only 13.6 and thus it is a better leaving group than methanol. This difference of 1.9 units in pKa values is sufficient to account for the observed slower rate of DKP formation for methyl ester version of monomers than *p*-nitrobenzyl ester versions that we used for the optimization experiments. This suggested that by using an alcohol of lower pKa value for the ester formation we could further enhance the rate of DKP formation.

60

As observed during optimization studies, the rate enhancement provided by *p*-nitrobenzyl esters is good enough to affect DKP closure between two pip5(2S5S) monomer. However *p*-nitrobenzyl ester is incompatible with our on-resin DKP formation strategy. This forced us to try out other alcohols with lower pKa values for the ester formation. These alcohols with their corresponding pKa values are shown in Figure 16.
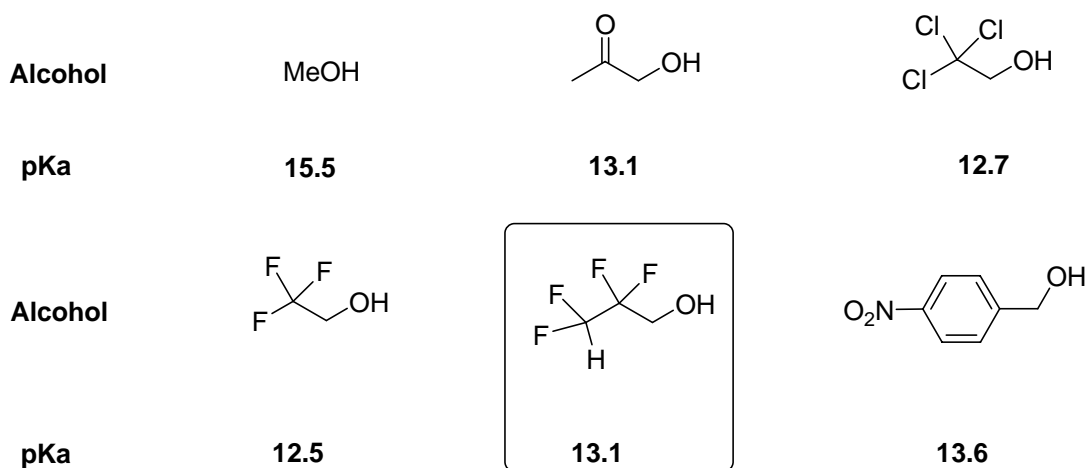
Figure 16: pKa's of alcohols screened for feasibility of DKP closure (Source: SciFinder Scholar).

We explored trifluoroethyl, trichloroethyl and acetoxy ester versions of the pip5(2S5S) monomer and found that they are not suitable for synthesis of the oligomers as they react with piperidine and DBU during the assembly of oligomers. After an extensive search we found that 2,2,3,3-tetrafluoro propyl esters are a good compromise between stability towards piperidine (or DBU) and reactivity in DKP formation.

3.3.1 Synthesis of TFP ester version of pro4(2S4S) and pip5(2S5S) monomer

We developed the second generation monomers **47** and **48**, TFP ester versions of pro4(2S4S) and pip5(2S5S) as a replacement for the methyl esters version of our first generation monomer **35** and **36**. The Fmoc protected amino acid **29** (and **13**) was esterified with 2,2,3,3 tetrafluoro propanaol using DCC in the presence of catalytic DMAP and the *t*-Bu group was subsequently removed by treatment with 3:7 TFA/DCM to give **45** (and **46**), the Cbz protected version of the monomer. Then the Cbz group was exchanged with a Boc group under hydrogenolysis conditions to yield monomer **47** (and **48**) which is suitable for oligomer assembly for on-resin DKP formation (Scheme 12). In a similar manner, we have also synthesized **64** and **65**, the TFP ester versions of pro4(2S4R) and pip5(2S5R) respectively as shown in Scheme 14 (Experimental Section).
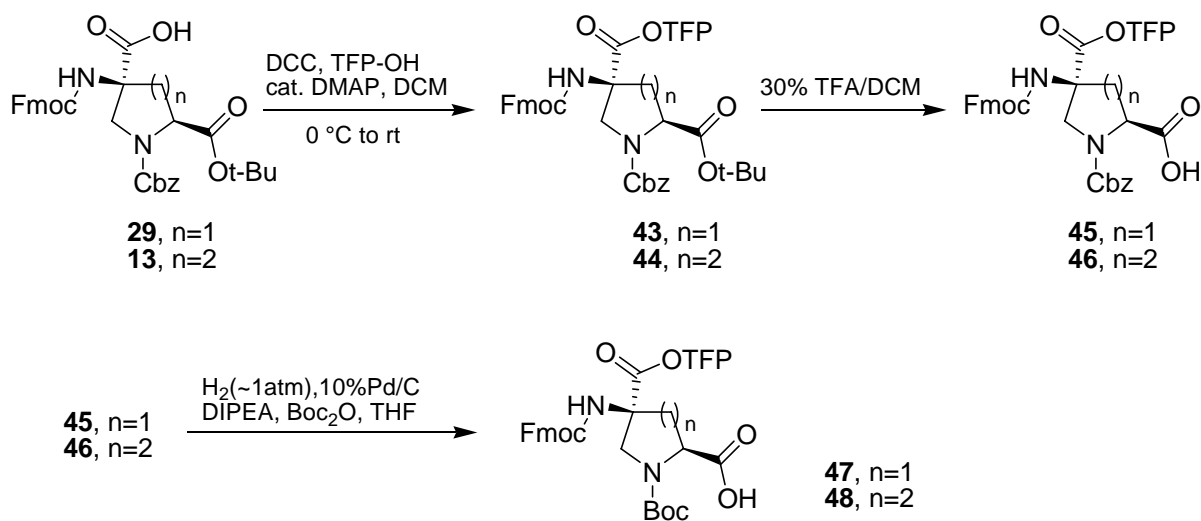
Scheme 12: Synthesis of 2nd generation of pro4(2S4S) and pip5(2S5S) monomers

3.3.2 A test of new DKP closure conditions against pip5(2S5S) pentamer

To test our best catalysis conditions, we assembled a pentamer **49** from pip5(2S5S) monomers **48** on a MBHA resin by using standard Fmoc solid phase synthesis methodology. We removed the Boc protecting group on each monomer and neutralized the amine to form intermediate **49**. The resin bound open oligomer **49** was suspended in 100 mM AcOD, 50 mM Et_3N and exposed to microwaves at 130°C for 30 minutes (Scheme 13). The oligomer was cleaved from the resin by treatment with TFMSA and the resulting product was characterized by C_{18} reverse phase HPLC with mass spectrometry (Figure 17). The major peak was the desired product **50**. Two small peaks representing intermediates that had failed to close one diketopiperazine were also observed but there was no evidence of epimerization of **50**.
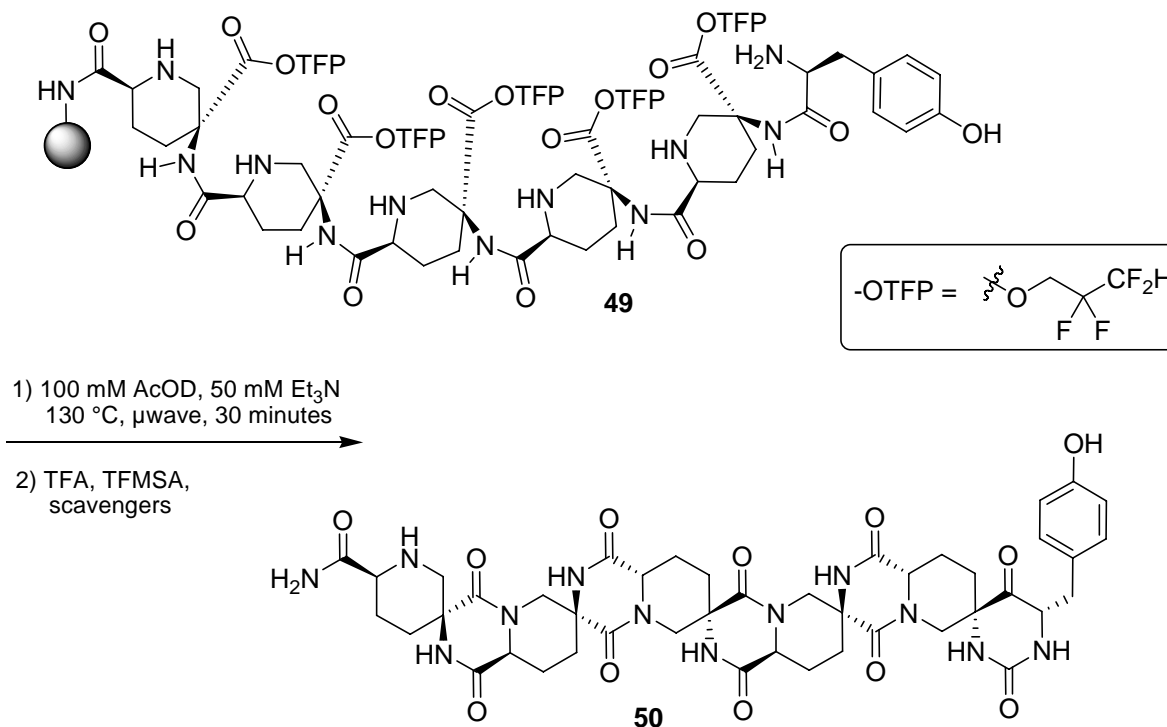
Scheme 13: A test of DKP formation on pentamer synthesized from pip5(2S5S)(OTFP) monomers
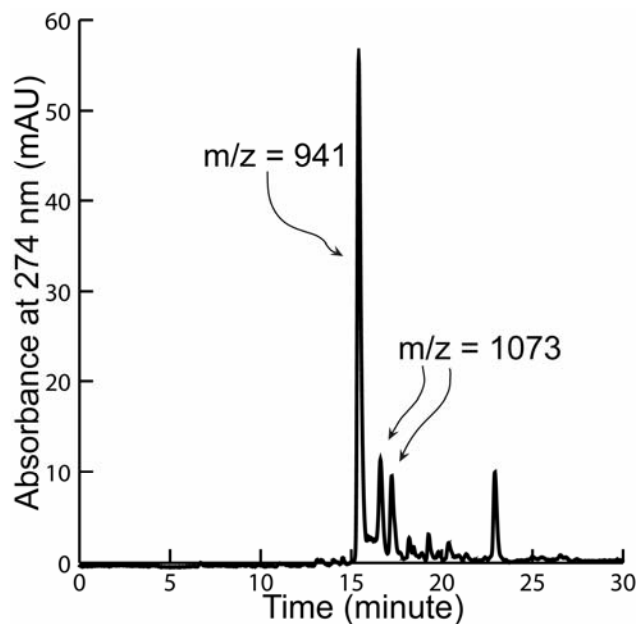
Figure 17: The unpurified reverse phase C$_{18}$ HPLC chromatograms of **50** (0.1% HCO$_2$H, 0-25% AcN over 30 min). The main peak is the desired product (m/z=941).

This result showed that we can simultaneously close five DKP rings in a homooligomer consisting of the most difficult combination that is between pip5(2S5S) monomers, in less than 30 minutes. In later experiments we observed that microwave irradiation was not necessary and similar results can be obtained with conventional heating in a flow cell.

3.4   DKP CLOSURE IN SMALL HETEROSEQUENCES BY ACOH/ET$_3$N CATALYSIS

We then set out to synthesize a small library of structurally diverse bis-peptide oligomers containing pip5(2S5S) and pro4(2S4S) monomers and test the efficacy of our newly optimized

conditions for diketopiperazine formation. We designed four hetero sequences **51-54** and assembled them on hydroxymethyl polystyrene resin[191] (Figure 18) by standard Fmoc solid phase peptide synthesis methodolgy. This was followed by on resin diketopiperazine formation in a flow cell apparatus catalyzed by 100 mM AcOH and 50 mM Et$_3$N in *o*-xylene at 130 °C.
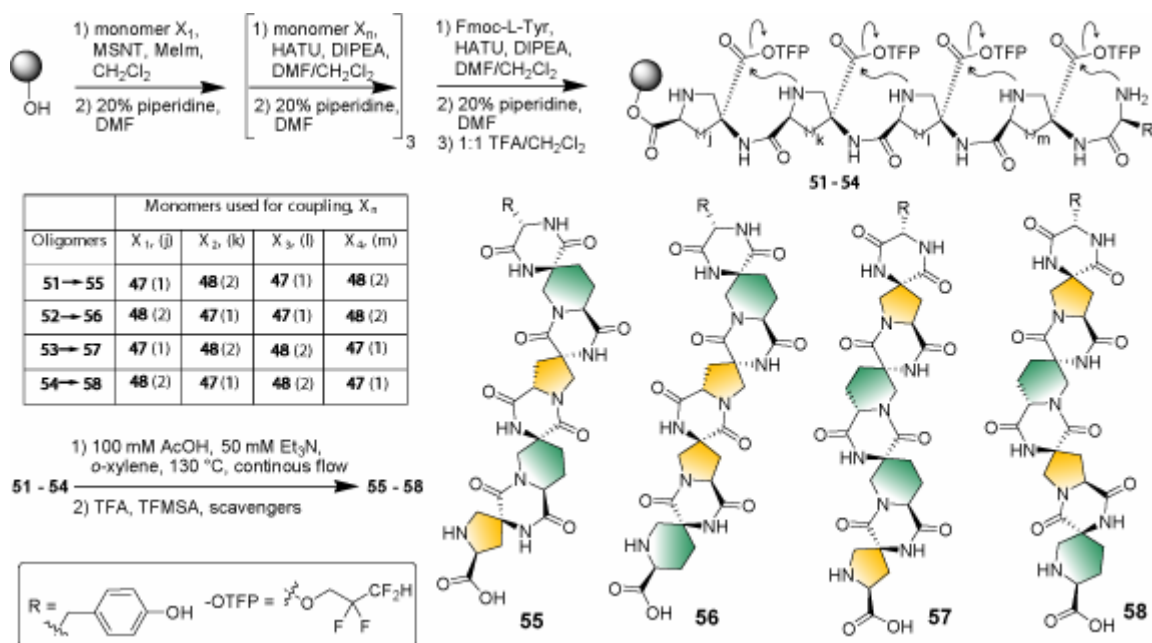
Figure 18: Assembly of short hetero oligomers and on resin diketopiperazine formation by continous flow method using optimized catalytic conditions.

The resin cleavage products **55-58** were purified by C$_{18}$ reverse phase preparative HPLC characterized by high resolution mass spectrometry. The analysis of the crude products before purification by C$_{18}$ reverse phase HPLC reveals that in all four cases diketopiperazine formation was very clean. Only trace amounts of any products with one diketopiperazine ring unclosed were detected. A representative chromatogram for oligomer **58** is shown in Figure 19. The

oligomers **55**, **56**, **57** and **58** gave rise to high resolution mass spectra with m/z = 762.2927, 762.2844, 762.2880 and 762.2865 respectively (calculated 762.2847).
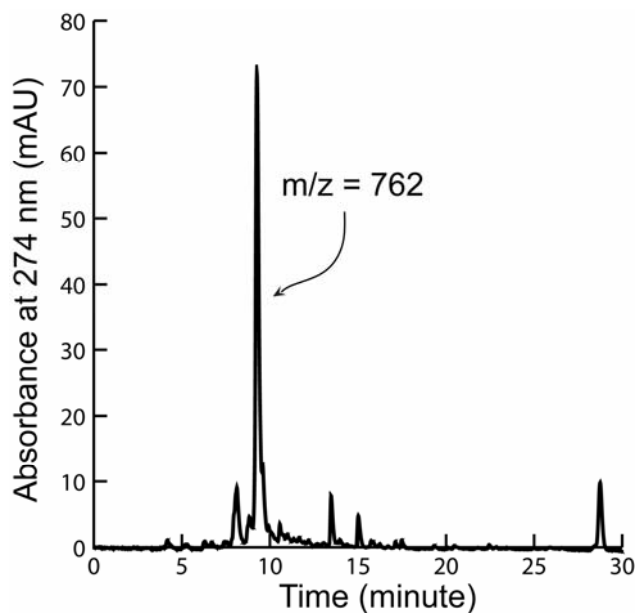
Figure 19: The unpurified reverse phase C_{18} HPLC chromatograms of **58** (0.1% HCO_2H, 0-25% AcN over 30 min). The main peak is the desired product (m/z=762).

These results confirmed that these new AcOD/Et$_3$N catalyzed microwave assisted and continuous flow conditions for DKP closure were good for all combinations of monomers **47** and **48**. Now we could close multiple diketopiperazines on solid support with no evidence of epimerization.

3.5   SUMMARY

We explored bifunctional catalysts for DKP closure on solid support. A range of reaction conditions were screened against combinations of pro4(2S4S) and pip5(2S5S) monomers. As observed in previous chapter, pip5-pip5 combination was found to be the slowest one. We optimized AcOD/Et$_3$N catalyzed, microwave assisted and continuous flow conditions for simultaneously closing multiple diketopiperazines on solid support with no evidence of epimerization. By developing the 2nd generation monomers **47** and **48** that carry a TFP ester in place of a methyl ester, we further enhanced the rate of DKP formation. As a proof of the viability of these new reaction conditions we assembled and performed DKP closure on a pentamer **50** made of pip5(2S5S) and small heteroligomers **55-58** consisting of various combinations of pro4(2S4S) and pip5(2S5S) monomers in less than 1 hour.

3.6   EXPERIMENTAL METHODS

3.6.1   General procedures

THF was distilled from Na/benzophenone under nitrogen atmosphere. CH_2Cl_2 was distilled from CaH_2. All other reagents were used as received unless otherwise noted. All the reactions were carried out in flame-dried or oven-dried glassware under nitrogen atmosphere unless otherwise noted.

Column chromatography was performed either manually using 32-63 D (60 Å particle size) grade silica gel or using commercially available normal phase flash chromatography silica gel columns on automated purification system. For a typical purification, the compound was dissolved in a minimum amount of dichloromethane and after mixing with celite, the solvent was removed by rotary evaporation. The resulting solid mixture was transferred to a 10 g or 40 g loading column. To obtain best results, any residual solvent was removed by drying under reduced pressure. Analytical TLC analysis was performed on Silica Gel plates (250 μm thickness).

NMR experiments were performed on 300 MHz spectrometer. Chemical shifts (δ) are reported in parts per million (ppm) relative to DMSO-d_6 residual solvent peaks. If possible, rotational isomers were resolved by obtaining spectra at 77 °C (350K) in DMSO-d_6. IR spectra were obtained on a FT-IR instrument. Optical rotations were obtained at ambient temperature (23 ± 2 °C). HPLC-MS analysis was performed on a Waters Xterra C_{18} column (3.5 μm packing, 4.6 mm x 150 mm) coupled to a Mass Spectrometer (ESI source). The elemental composition of

purified compounds was confirmed by the spectrums obtained on a high resolution mass spectrometer with an electrospray ion source (HRESIQTOFMS). Purification by preparative HPLC was carried out on a semiprep C_{18} column (5μm packing, 10 mm x 100 mm).

Solid phase chemistry was performed on a home-built manual synthesizer. Dry dichloromethane used in coupling reactions was obtained from distillation over CaH_2. Diisopropylethyl amine (DIPEA) was distilled under nitrogen sequentially from ninhydrin and potassium hydroxide and stored over molecular sieves (4 Å). Resins for solid phase synthesis were purchased from NovaBiochem. All other reagents and dry solvents were obtained from various commercial sources and used as such. All solid phase reactions were mixed by bubbling argon through the reaction mixture.

3.6.2   Synthesis of monomers

(2S,4S)-4-(9H-Fluoren-9-ylmethoxycarbonylamino)-proline-1,2,4-tricarboxylic   acid   1-benzyl ester 4- (*p*-nitro)benzyl ester 2-tert-butyl ester (30)

A suspension of **29** (418 mg, 0.71 mmol), KI (119 mg,0.71 mmol, 1 equiv.) and NaHCO$_3$ (57 mg, 0.67 mmol, 0.9 equiv.) was prepared in anhydrous DMF (5 mL, 7 mL per mmol of substrate) in a 25 mL round bottom flask under N_2 atmosphere. To this suspension *p*-nitrobenzyl bromide (383 mg, 1.8 mmol, 2.5 equiv.) was added in one portion. The stirring was continued at room temperature and the reaction progress was monitored by HPLC-MS. After completion of the reaction (about 10 hours), water (15 mL) was added to the reaction mixture and extracted with EtOAc (30mL + 2x10 mL). All the organic layers were combined and washed with brine (10 mL). This solution was dried over anhydrous Na_2SO_4, filtered and concentrated by rotary evaporation. The crude product was mixed with celite and then purified by automated flash

chromatography (10 gm silica column; Solvent A: Hexanes, Solvent B: EtOAc; Gradient elution: 0-60 CVs, solvent B 5% to 35%). The fractions that contain the desired compound were combined and concentrated by rotary evaporation. The residual solvent was removed by overnight drying under reduced pressure to yield **30** (411 mg, 5.7 mmol, 80%) as a white foam: $[\alpha]^{23}_D$ = +11.0 (*c* 1.15, CHCl$_3$); IR (film) ν_{max} 3317, 2977, 1711, 1523, 1449, 1417, 1347, 1259, 1156, 749, 740, 697 cm^{-1}; ^{1}H NMR (300 MHz, 77 °C, DMSO-*d$_6$*) δ 8.07 (d, *J* = 8.4 Hz, 2H), 8.00 (s, 1H), 7.85 (d, *J* = 7.5 Hz, 2H), 7.64 (d, *J* = 7.5 Hz, 2H), 7.53 (d, *J* = 8.4 Hz, 2H), 7.26-7.42 (m, 9H), 5.22 (br s, 2H), 5.08 (br s, 2H), 4.03-4.39 (m, 5H), 3.64 (d, *J* = 11.4 Hz, 1H), 2.87 (br m, 1H), 2.33 (br m, 1H), 1.37 (s, 9H); ^{13}C NMR (75.4 MHz, 20 °C, DMSO-*d$_6$*): mixture of rotamers δ 171.0, 170.1, 169.8, 155.8, 153.5, 153.2, 146.9, 143.4, 143.1, 140.6, 136.5 and 136.3, 128.4, 128.1, 127.8, 127.7, 127.5, 127.4, 127.2, 126.9, 125.0, 123.2, 120.0, 81.0, 66.2 (CH$_2$), 65.8 (CH$_2$), 65.5 (CH$_2$), 63.1 and 62.2, 58.3 and 58.0 (CH), 54.7 and 54.3 (CH$_2$), 46.4 (CH), 38.6 and 37.6 (CH$_2$), 27.4 and 27.3 (CH$_3$, 3C); HPLC-MS: MeCN (0.05% Formic acid) / water (0.1% Formic Acid), 5% to 95% MeCN over 30 min; flow rate 0.80 mL/min; UV detection at 274 nm; t$_R$ for **30** 29.09 min; HRESIQTOFMS calcd for C$_{40}$H$_{39}$N$_3$O$_{10}$Na (M + Na$^+$) 744.2533, found 744.2532.

(2S,5S)-5-(9H-Fluoren-9-ylmethoxycarbonylamino)-piperidine-1,2,5-tricarboxylic acid 1-benzyl ester 5-(*p*-nitro)benzyl ester 2-tert-butyl ester (31)

129 mg (0.21 mmol) of **13** yielded 112 mg (0.16 mmol, 76%) of **31** as a white foam according to the procedure given above for **30**: $[\alpha]^{23}_D$ = -9.1 (*c* 1.5, CHCl$_3$); IR (film) ν_{max} 3333, 3030, 2955, 1716, 1521, 1449, 1347, 1317, 1254, 749, 741, 667 cm^{-1}; ^{1}H NMR (300 MHz, 77 °C, DMSO-*d$_6$*) δ 8.06 (d, *J* = 8.7 Hz, 2H), 7.85 (d, *J* = 7.5 Hz, 2H), 7.80 (s, 1H), 7.65 (d, *J* = 7.5 Hz, 2H), 7.52

(d, J = 8.4 Hz, 2H), 7.39 (dd, J= 7.5,7.5 Hz, 2H), 7.26-7.31 (m, 7H), 5.17 (br s, 2H), 5.08 (br s, 2H), 4.71 (br d, J = 13.5 Hz, 1H), 4.64 (m, 1H), 4.30-4.33 (m, 2H), 4.16 (t, J = 6.6 Hz, 1H) 2.99 (br d, J = 13.2 Hz, 1H), 2.24 (br d, J = 13.5 Hz, 1H), 2.04 (br d, J = 14.1 Hz, 1H), 1.86 (br m, 1H), 1.63 (br dd, J = 12.9, 12.9, Hz, 1H), 1.42 (s, 9H); ^{13}C NMR (75.4 MHz, 20 °C, DMSO-d_6): mixture of rotamers δ 170.9, 169.8, 169.5, 155.1, 155.0, 154.7, 146.9, 143.6, 143.5, 140.7, 136.6, 128.3, 128.2, 127.7, 127.6, 127.2, 126.9, 125.0, 123.3, 120.1, 81.4, 66.4 (CH_2), 65.6 (CH_2), 64.8 (CH_2), 56.3, 56.2, 53.7 and 53.5(CH), 46.6 (CH_2), 46.5 (CH), 29.0 and 28.8 (CH_2), 27.5 and 27.4 (CH_3, 3C), 22.4 and 22.3 (CH_2); HPLC-MS: MeCN (0.05% Formic acid) / water (0.1% Formic Acid), 5% to 95% MeCN over 30 min; flow rate 0.80 mL/min; UV detection at 274 nm; t_R for **31**, 29.50 min; HRESIQTOFMS calcd for $C_{41}H_{41}N_3O_{10}Na$ (M + Na$^+$) 758.2690, found 758.2698.

(2S,4S)-4-(9H-Fluoren-9-ylmethoxycarbonylamino)-proline-1,2,4-tricarboxylic acid 1-benzyl ester 4- (*p*-nitro)benzyl ester (32)

205 mg (0.28 mmol) of **30** was dissolved in 3:7 mixture of TFA/ DCM (6 mL, 20 mL per mmol of substrate) and stirring was continued for 2 hours at room temperature. After confirming the disappearance of substrate by TLC (5:1 $CHCl_3$/MeOH, visualized under UV), the reaction mixture was diluted with toluene (6 mL) and concentrated by rotary evaporation. This step of adding toluene and evaporation *in vacuo* was repeated one additional time to ensure complete removal of TFA. The crude product was mixed with celite and then purified by automated flash chromatography (10 gm silica column; Solvent A: $CHCl_3$, Solvent B: 10% $CHCl_3$ in MeOH; Gradient elution: 0-60 CVs, solvent B 0% to 100%). The fractions that contain the desired compound were combined and concentrated by rotary evaporation. The residual solvent was removed by overnight drying under reduced pressure to yield **32** (175 mg, 0.26 mmol, 93%) as a

white foam: $[\alpha]^{23}_D$ = -18.0 (*c* 2.4, CHCl$_3$); IR (film) ν_{max} 3307, 3033, 2953, 1709, 1523, 1450, 1422, 1348, 1263, 749, 741, 697 cm^{-1}; ^{1}H NMR (300 MHz, 77 °C, DMSO-*d$_6$*) δ 8.05 (d, *J* = 8.4 Hz, 3H, overlap with Fmoc-NH-), 7.84 (d, *J* = 7.5 Hz, 2H), 7.65 (d, *J* = 7.5 Hz, 2H), 7.52 (d, *J* = 8.4 Hz, 2H), 7.27-7.42 (m, 9H), 5.22 (br s, 2H), 5.08 (br s, 2H), 4.13-4.37 (m, 5H), 3.61 (d, *J* = 11.4 Hz, 1H), 2.90 (br m, 1H), 2.33 (br m, 1H); ^{13}C NMR (75.4 MHz, 20 °C, DMSO-*d$_6$*): mixture of rotamers δ 172.7, 172.4, 171.3, 156.0, 153.7, 153.5, 147.0, 143.6, 143.2, 140.7, 136.6, 128.5, 128.3, 127.9, 127.6, 127.5, 127.0, 125.2, 123.3, 120.1, 79.2, 66.3 (CH$_2$), 66.0 (CH$_2$), 65.5 (CH$_2$), 63.0 and 62.2, 57.8 and 57.5 (CH), 54.9 and 54.5 (CH$_2$), 46.5 (CH), 38.7 and 37.6 (CH$_2$); HPLC-MS: MeCN (0.05% Formic acid) / water (0.1% Formic Acid), 5% to 95% MeCN over 30 min; flow rate 0.80 mL/min; UV detection at 274 nm; t$_R$ for **32**, 25.21 min; HRESIQTOFMS calcd for C$_{36}$H$_{31}$N$_3$O$_{10}$Na (M + Na$^+$) 688.1907, found 688.1906.

(2S,5S)-5-(9H-Fluoren-9-ylmethoxycarbonylamino)-piperidine-1,2,5-tricarboxylic acid 1-benzyl ester 5- (*p*-nitro)benzyl ester (33)

112 mg (0.15 mmol) of **31** yielded 95 mg (14.0 mmol, 92%) of **33** as a white foam according to the procedure given above for **32**: $[\alpha]^{23}_D$ = -6.4 (*c* 0.8, CHCl$_3$); IR (film) ν_{max} 3333, 3030,2955, 1716, 1521, 1449, 1347, 1317, 1254, 749, 741, 667 cm^{-1}; ^{1}H NMR (300 MHz, 77 °C, DMSO-*d$_6$*) δ 8.05 (d, *J* = 8.4 Hz, 2H), 7.85 (d, *J* = 7.2 Hz, 2H), 7.78 (s, 1H), 7.65 (d, *J* = 7.2 Hz, 2H), 7.52 (d, *J* = 8.1 Hz, 2H), 7.27-7.42 (m, 9H), 5.15 (br s, 2H), 5.07 (br s, 2H), 4.70-4.74 (m, 2H), 4.29 (d, *J* = 6.6 Hz, 2H), 4.16 (t, *J* = 6.6 Hz, 1H) 3.05 (br d, *J* = 13.2 Hz, 1H), 2.25 (br d, *J* = 13.2 Hz, 1H), 2.08 (br d, *J* = 11.4 Hz, 1H), 1.88 (br m, 1H) 1.63 (br dd, *J* = 12.9, 12.9, Hz, 1H); ^{13}C NMR (75.4 MHz, 20 °C, DMSO-*d$_6$*): mixture of rotamers δ 172.3, 172.2, 171.0, 155.2, 155.0, 154.7, 146.9, 143.7, 143.6, 140.7, 136.7, 128.4, 128.3, 127.7, 127.6, 127.2, 127.1, 127.0, 125.1, 123.3,

120.1, 79.2, 66.4 (CH$_2$), 65.7 (CH$_2$), 64.8 (CH$_2$), 56.4 and 56.3, 53.0 (CH), 46.5 (CH$_2$), 46.4 (CH), 29.3 (CH$_2$), 22.5 (CH$_2$); HPLC-MS: MeCN (0.05% Formic acid) / water (0.1% Formic Acid), 5% to 95% MeCN over 30 min; flow rate 0.80 mL/min; UV detection at 274 nm; t$_R$ for **33**, 25.75 min; HRESIQTOFMS calcd for C$_{37}$H$_{33}$N$_3$O$_{10}$Na (M + Na$^+$) 702.2064, found 702.2042.

(2S,4S)-5-(9H-Fluoren-9-ylmethoxycarbonylamino)-proline-1,2,4-tricarboxylic acid 1-benzyl ester 4-(2,2,3,3-tetrafluoro) propyl ester 2-tert-butyl ester (43)

Fmoc protected amino acid **29** (9.57 g, 16.3 mmol) was dissolved in dry DCM (163 mL, 10mL per mmol) in a 500 mL round bottom flask under N$_2$ atmosphere. To this solution, DMAP (100 mg, 0.82 mmol, 0.05 equiv.) and 2,2,3,3-tetraflouro propanol (2.93 mL, 32.6 mmol, 2 equiv.) were added in one portion. The reaction mixture was cooled in an ice bath under N$_2$ and DCC (4.04 g, 19.6 mmol, 1.2 equiv.) was added to the reaction flask in one portion. The reaction mixture was allowed to warm up to room temperature and stirring was continued overnight. Disappearance of the substrate was confirmed by TLC analysis (5:1 CHCl$_3$: MeOH, observed under UV). The reaction was quenched by an addition of 10% acetic acid in DCM (20 mL) and solvent was removed via rotary evaporation. The residue was mixed with 1:1 EtOAc / hexanes (100 mL) mixture and filtered through sintered funnel to remove insoluble byproduct DCU. The filtrate was concentrated, mixed with celite and then purified by automated flash chromatography (two separate 40 gm silica columns; Solvent A: Hexanes, Solvent B: EtOAc; Gradient elution: 0-5 CVs, solvent B 5% followed by 5-45 CVs, solvent B 5% to 35%). The fractions that contain the desired product were combined, concentrated and residual solvent was removed by drying overnight under reduced pressure to yield **43** (9.7 g, 13.84 mmol, 85%) as a white foam; [α]^{23}$_D$ = +2.9 (*c* 1.09, CHCl$_3$); IR (film) ν$_{max}$ 3307, 2979, 1712, 1525, 1450, 1419,

1258, 1157, 1109, 759, 741, 698 cm^{-1}; ^{1}H NMR (300 MHz, 77 °C, DMSO-d_6) δ 7.99 (s, 1H), 7.85 (d, J = 7.8 Hz, 2H), 7.66 (d, J = 7.5 Hz, 2H), 7.31-7.40 (m, 9H), 6.40 (tt, J = 52.2 Hz, J = 5.1 Hz, -CF$_2$CF$_2$H, 1H) 5.08 (br s, 2H), 4.56 (t, J = 13.8 Hz, -CH$_2$CF$_2$-, 2H), 4.28-4.42 (m, 3H), 4.19 (t, J = 6.4 Hz, 1H), 4.03 (d, J = 11.4 Hz, 1H), 3.61 (d, J = 11.4 Hz, 1H), 2.82 (br, 1H), 2.32 (br, 1H), 1.35 (br s, 9H); ^{13}C NMR (75.4 MHz, 20 °C, DMSO-d_6): mixture of rotamers δ 170.1, 169.7, 159.2, 143.5, 140.6, 136.5, 136.3, 128.2, 128.1, 127.6, 127.5, 127.2, 126.8, 124.9, 119.9, 109.0 (tt, ^1J = 248 Hz, ^2J = 34 Hz, CH), 80.9, 66.2 (CH$_2$), 65.7 (CH$_2$), 63.0 and 62.1, 60.2 (t, ^2J = 28 Hz, CH$_2$), 58.3 and 57.9 (CH), 54.5 and 54.1 (CH$_2$), 46.4 (CH), 38.7 and 37.3 (CH$_2$), 27.4 (CH$_3$, 3C); HPLC-MS: MeCN(0.05% Formic acid) / water (0.1% Formic Acid), 5% to 95% MeCN over 30 min; flow rate 0.80 mL/min; UV detection at 274 nm; t_R for **43**, 29.13 min; HRESIQTOFMS calcd for C$_{36}$H$_{36}$N$_2$O$_8$F$_4$Na (M + Na$^+$) 723.2305, found 723.2295.

(2S,5S)-5-(9H-Fluoren-9-ylmethoxycarbonylamino)-piperidine-1,2,5-tricarboxylic acid 1-benzyl ester 5- (2,2,3,3-tetrafluoro) propyl ester 2-tert-butyl ester (44)

4.0 g (6.66 mmol) of **13** yielded 3.97 g (5.55 mmol, 83%) of **44** as a white foam according to the procedure given above for **43**: $[\alpha]^{23}_D$ = -14.7 (c 0.9, CHCl$_3$); IR (film) v_{max} 3316, 2977, 1761,1729, 1526, 1450, 1321, 1255, 1118,759,741, 698 cm^{-1}; ^{1}H NMR (300 MHz, 77 °C, DMSO-d_6) δ 7.84 (d, J = 7.8 Hz, 3H,overlap with Fmoc-NH-), 7.67 (d, J = 7.5 Hz, 2H), 7.30-7.43 (m, 9H), 6.38 (tt, J = 52.2, 5.1 Hz, -CF$_2$CF$_2$H, 1H) 5.12 (br s, 2H), 4.19-4.70 (m, 4H), 4.35 (d, J = 6.3 Hz, 2H), 4.21 (t, J = 6.3 Hz, 1H), 2.95 (br d, J = 12.9 Hz, 1H), 2.17 (br d, J = 13.2 Hz, 1H), 2.05 (br d, J = 12.0 Hz, 1H), 1.82 (m, 1H) 1.62 (br dd, J = 12.9, 12.9, Hz, 1H), 1.42 (br s, 9H); ^{13}C NMR (75.4 MHz, 20 °C, DMSO-d_6): mixture of rotamers δ 170.0, 169.6, 169.4, 155.1, 155.0, 154.7, 143.6, 143.5, 143.4, 140.7, 136.6, 136.5, 128.2, 127.7, 127.5, 127.2, 126.9, 124.9,

120.0, 81.4, 79.1, 66.3 (CH$_2$), 65.5 (CH$_2$),59.7 (CH$_2$), 56.3 and 56.2, 53.6 and 53.4 (CH), 46.6 (CH), 46.5 (CH$_2$), 28.8 (CH$_2$), 27.5 (CH$_3$, 3C), 22.2 (CH$_2$); HPLC-MS: MeCN (0.05% Formic acid) / water (0.1% Formic Acid), 5% to 95% MeCN over 30 min; flow rate 0.80 mL/min; UV detection at 274 nm; t$_R$ for **44**, 29.23 min; HRESIQTOFMS calcd for C$_{37}$H$_{38}$N$_2$O$_8$F$_4$Na (M + Na$^+$) 737.2462, found 737.2423.

(2S,4S)-5-(9H-Fluoren-9-ylmethoxycarbonylamino)-proline-1,2,4-tricarboxylic acid 1-benzyl ester 4- (2,2,3,3-tetrafluoro) propyl ester (45)

9.7 g (13.84 mmol) of **43** yielded 8.55 g (13.26 mmol, 96%) of **45** as a white foam according to the procedure given above for **32**: [α]$^{23}_D$ = -30.0 (*c* 0.81, CHCl$_3$); IR (film) ν$_{max}$ 3306, 3034, 1713, 1526, 1450, 1422, 1260, 1193, 1109, 759, 742, 697 cm^{-1}; ^{1}H NMR (300 MHz, 77 °C, DMSO-d_6) δ 8.26 (s, 1H), 7.85 (d, *J* = 7.5 Hz, 2H), 7.66 (d, *J* = 7.5 Hz, 2H), 7.31-7.40 (m, 9H), 6.40 (tt, *J* = 52.2 Hz, *J* = 5.1 Hz, -CF$_2$CF$_2$*H*, 1H) 5.09 (br s, 2H), 4.57 (t, *J* = 13.8 Hz, -C*H$_2$*CF$_2$-, 2H), 4.33-4.36 (m, 3H), 4.20 (t, *J* = 6.6 Hz, 1H), 4.31 (d, *J* = 11.4 Hz, 1H), 3.57 (d, *J* = 11.4 Hz, 1H), 2.85 (br, 1H), 2.31 (br, 1H); ^{13}C NMR (75.4 MHz, 20 °C, DMSO-d_6): mixture of rotamers δ 172.5, 172.1, 170.3, 155.7, 153.5, 153.3, 143.5, 140.6, 136.5, 128.2, 128.1, 127.7, 127.5, 127.3, 126.9, 125.0, 119.9, 109.0 (tt, ^{1}*J* = 248 Hz, ^{2}*J* = 34 Hz, CH), 66.2 (CH$_2$), 65.8 (CH$_2$), 62.8 and 62.0, 60.2 (t, ^{2}*J* = 28 Hz, CH$_2$), 57.6 and 57.3 (CH), 54.6 and 54.2 (CH$_2$), 46.5 (CH), 38.8 and 37.5 (CH$_2$); HPLC-MS: MeCN(0.05% Formic acid) / water (0.1% Formic Acid), 5% to 95% MeCN over 30 min; flow rate 0.80 mL/min; UV detection at 274 nm; t$_R$ for **45**, 24.75 min; HRESIQTOFMS calcd for C$_{32}$H$_{28}$N$_2$O$_8$F$_4$Na (M + Na$^+$) 667.1679, found 667.1681.

(2S,5S)-5-(9H-Fluoren-9-ylmethoxycarbonylamino)-piperidine-1,2,5-tricarboxylic acid 1-benzyl ester 5- (2,2,3,3-tetrafluoro) propyl ester (46)

3.88 g (5.43 mmol) of **44** yielded 3.17 g (4.81 mmol, 89%) of **46** as a white foam according to the procedure given above for **32**: $[\alpha]^{23}_D$ = -13.5 (*c* 1.5, CHCl$_3$); IR (film) ν_{max} 3316, 3037, 1716, 1523, 1450, 1317, 1255, 1118,759,742, 698 cm^{-1}; ^{1}H NMR (300 MHz, 77 °C, DMSO-*d$_6$*) δ 7.86 (d, *J* = 7.2 Hz, 2H), 7.81 (1H), 7.66 (d, *J* = 7.2 Hz, 2H), 7.30-7.43 (m, 9H), 6.37 (tt, *J* = 52.2, 5.1 Hz, -CF$_2$CF$_2$*H,* 1H) 5.11 (br s, 2H), 4.42-4.72 (m, 4H), 4.33 (d, *J* = 6.6 Hz, 2H), 4.20 (t, *J* = 6.6 Hz, 1H) 3.00 (br d, *J* = 13.2 Hz, 1H), 2.19 (br d, *J* = 13.2 Hz, 1H), 2.08 (br d, *J* = 14.1 Hz, 1H), 1.84 (m, 1H) 1.63 (ddd, *J* = 12.9, 12.9, 3.0 Hz, 1H); ^{13}C NMR (75.4 MHz, 20 °C, DMSO-*d$_6$*): mixture of rotamers δ 172.0, 170.0, 155.1, 154.7, 143.6, 143.5 and 143.4, 140.6, 136.7 and 136.5, 128.2, 127.7, 127.5, 127.1, 127.0, 126.9, 124.9, 120.0, 79.1, 66.4 (CH$_2$), 65.6 (CH$_2$),59.7 (CH$_2$), 56.3 and 56.2, 53.0 and 52.7 (CH), 46.5 (CH), 46.4 (CH$_2$), 28.9 (CH$_2$), 22.1 (CH$_2$); HPLC-MS: MeCN (0.05% Formic acid) / water (0.1% Formic Acid), 5% to 95% MeCN over 30 min; flow rate 0.80 mL/min; UV detection at 274 nm; t$_R$ for **46**, 25.47 min; HRESIQTOFMS calcd for C$_{32}$H$_{28}$N$_2$O$_8$F$_4$Na (M + Na$^+$) 681.1836, found 681.1802.

(2S,4S)-5-(9H-Fluoren-9-ylmethoxycarbonylamino)-proline-1,2,4-tricarboxylic acid 1- tert-butyl ester 4- (2,2,3,3-tetrafluoro) propyl ester (47)

Intermediate **45** (8.4 g, 13.1 mmol) was dissolved in dry THF (10 mL per mmol of substrate) in a 250 mL round bottom flask. Boc$_2$O (8.6 g, 39.3 mmol, 3 equiv.) was added to this solution in one portion and this was followed by a careful addition of 10 wt % Pd/C (840 mg, 10% by wt. of substrate). The reaction mixture was degassed by applying vacuum using an aspirator and backfilled with H$_2$ via balloon. This cycle of degassing and backfilling was repeated a few times

and stirring was continued under H_2 atmosphere (~ 1 atm.) at room temperature. The reaction progress was monitored by HPLC. In order to speed up the reaction DIPEA (1.73 mL, 10.8 mmol, 0.8 equiv.) was added after a few hours and stirring was further continued under H_2 atmosphere. After confirming the disappearance of **45** (about 2 days) by HPLC, the reaction mixture was filtered through filter paper under reduced pressure and residual Pd/C was washed several times with THF to recover most of the product. The filtrates were combined and concentrated by rotary evaporation. The resulting crude product was mixed with celite and then purified by automated flash chromatography (120 g silica column; Solvent A: $CHCl_3$ with 0.1% AcOH, Solvent B: 10% MeOH/ $CHCl_3$ with 0.1% AcOH; Gradient elution: 0-2 CVs, solvent A 100% followed by 2-18 CVs, solvent B 0% to 100%). The fractions containing the desired product were combined and concentrated. Any residual acetic acid was azeotropically removed by mixing with hexane followed by rotary evaporation. Any residual solvent was further removed by drying overnight under reduced pressure to yield **47** (7.2 g, 11.8 mmol, 90%) as a white foam: $[\alpha]^{23}_D$ = -54.3 (*c* 1.35, $CHCl_3$); IR (film) ν_{max} 3304, 2980, 1760, 1724, 1530, 1451, 1409, 1369, 1259, 1111, 759, 742 cm^{-1}; ^1H NMR (300 MHz, 77 °C, DMSO-d_6) δ 8.07 (br s, 1H), 7.85 (d, *J* = 7.5 Hz, 2H), 7.66 (d, *J* = 7.5 Hz, 2H), 7.32-7.41 (m, 4H), 6.40 (tt, *J* = 52.2 Hz, *J* = 5.1 Hz, -CF_2CF_2H, 1H), 4.57 (t, *J* = 13.8 Hz, -CH_2CF_2-, 2H), 4.32-4.37 (m, 2H), 4.18-4.23 (m, 2H), 4.03 (d, *J* = 11.4 Hz, 1H), 3.47 (d, *J* = 11.4 Hz, 1H), 2.82 (br, 1H), 2.20 (br, 1H), 1.38 (br s, 9H); ^{13}C NMR (75.4 MHz, 20 °C, DMSO-d_6): mixture of rotamers δ 172.8, 172.5, 170.5, 155.7, 152.9, 152.5, 143.5, 140.6, 127.5, 126.9, 124.9, 119.9, 109.0 (tt, ^1J = 248 Hz, ^2J = 34 Hz, CH), 79.2, 65.7 (CH_2), 62.7 and 61.9, 60.1 (t, ^2J = 28 Hz, CH_2), 57.5 and 57.2 (CH), 54.4 and 54.1 (CH_2), 46.5 (CH), 39.0 and 37.6 (CH_2), 27.7 (CH_3, 3C); HPLC-MS: MeCN(0.05% Formic acid) / water (0.1% Formic Acid), 5% to 95% MeCN over 30 min; flow rate 0.80 mL/min; UV

detection at 274 nm; t_R for **47**, 24.21 min; HRESIQTOFMS calcd for $C_{29}H_{30}N_2O_8F_4Na$ (M + Na^+) 633.1836, found 633.1835.

(2S,5S)-5-(9H-Fluoren-9-ylmethoxycarbonylamino)-piperidine-1,2,5-tricarboxylic acid 1-tert-butyl ester 5- (2,2,3,3-tetrafluoro) propyl ester (48)

3.07 g (4.66 mmol) of **46** yielded 2.03 g (3.25 mmol, 70%) of **48** as a white foam according to the procedure given above for **47**: $[\alpha]^{23}_D$ = -12.5 (*c* 1.26, CHCl$_3$); IR (film) ν_{max} 3316, 2978, 1716, 1524, 1450, 1420, 1369, 1319, 1255, 1118, 759, 741 cm^{-1}; ^{1}H NMR (300 MHz, 77 °C, DMSO-*d$_6$*) δ 7.86 (d, *J* = 7.5 Hz, 2H), 7.77 (s, 1H), 7.67 (d, *J* = 7.2 Hz, 2H), 7.30-7.44 (m, 4H), 6.39 (tt, *J* = 52.2, 5.1 Hz, -CF$_2$CF$_2$*H,* 1H), 4.46-4.58 (m, 4H), 4.32 (d, *J* = 6.6 Hz, 2H), 4.33 (t, *J* = 6.6 Hz, 1H) 2.94 (br d, *J* = 13.5 Hz, 1H), 2.19 (br d, *J* = 13.8 Hz, 1H), 1.99-2.07 (m, 1H), 1.86 (m, 1H) 1.63 (ddd, *J* = 12.9, 12.9, 3.6 Hz, 1H), 1.40 (s, 9H); ^{13}C NMR (75.4 MHz, 20 °C, DMSO-*d$_6$*): mixture of rotamers δ 172.4, 170.2, 170.1, 155.2, 154.1, 143.6, 140.7, 127.6, 127.0, 125.0, 120.1, 79.4, 79.1, 65.6 (CH$_2$), 59.8 and 59.7 (CH$_2$), 56.4 and 56.3, 53.4 (CH), 46.5 (CH), 45.8 (CH$_2$), 29.2 (CH$_2$), 27.8 (CH$_3$, 3C), 22.2 (CH$_2$); HPLC-MS: MeCN (0.05% Formic acid) / water (0.1% Formic Acid), 5% to 95% MeCN over 30 min; flow rate 0.80 mL/min; UV detection at 274 nm; t_R for **48**, 25.23 min; HRESIQTOFMS calcd for $C_{30}H_{32}N_2O_8F_4Na$ (M + Na^+) 647.1992, found 647.2028.

(2S,5S)-5-(9H-Fluoren-9-ylmethoxycarbonylamino)-piperidine-1,2,5-tricarboxylic acid 1-tert-butyl ester 5- methyl ester (36)

280 mg (0.5 mmol) of **3** yielded 198 mg (0.38 mmol, 76%) of **36** as a white foam according to the procedure given above for **47**: $[\alpha]^{23}_D$ = -17.8 (*c* 0.5, CHCl$_3$); IR (film) ν_{max} 3316, 2977, 1716,

1525, 1450, 1421, 1369, 1319, 1255, 1118, 759, 741 cm^{-1}; ^{1}H NMR (300 MHz, 77 °C, DMSO-d_6) 7.86 (d, J = 7.2 Hz, 2H), 7.68 (d, J = 7.2 Hz, 2H), 7.58 (s, 1H), 7.30-7.44 (m, 4H), 4.59 (m, 1H), 4.49 (d, J = 13.5 Hz, 1H), 4.32 (d, J = 6.6 Hz, 2H), 4.20 (t, J = 6.6 Hz, 1H), 3.59 (br s, 3H), 2.95 (d, J = 13.5 Hz, 1H), 2.20 (br d, J = 13.5 Hz, 1H), 1.81-2.02 (m, 2H), 1.54 (ddd, J = 12.6, 12.6, 4.2 Hz, 1H); ^{13}C NMR (75.4 MHz, 20 °C, DMSO-d_6): mixture of rotamers δ 172.2, 171.7, 154.9, 153.9, 143.6, 140.6, 127.5, 126.9, 125.0, 120.0, 79.4, 79.2, 65.4 (CH$_2$), 56.2, 52.1 (CH), 51.8 (CH$_3$), 46.5 (CH), 45.9 (CH$_2$), 29.2 (CH$_2$), 27.8 (CH$_3$, 3C), 22.3 (CH$_2$); HPLC-MS: MeCN (0.05% Formic acid) / water (0.1% Formic Acid), 5% to 95% MeCN over 30 min; flow rate 0.80 mL/min; UV detection at 274 nm; t_R for **36**, 22.91 min; HRESIQTOFMS calcd for C$_{28}$H$_{32}$N$_2$O$_8$Na (M + Na$^+$) 547.2056, found 547.2066.

Scheme 14: Synthesis of TFP ester version of pro4(2S4R) and pip5(2S5R) monomers

(2S,4R)-5-(9H-Fluoren-9-ylmethoxycarbonylamino)-proline-1,2,4-tricarboxylic   acid   1-benzyl ester 4- (2,2,3,3-tetrafluoro) propyl ester 2-tert-butyl ester (60)

4.0 g (6.82 mM) of **59** yielded 4.28 g (6.11 mM, 89%) of **60** as a white foam according to the procedure given for **43**; $[\alpha]^{23}_D$ = -39.9 (*c* 0.96, CHCl$_3$); IR (film) ν_{max} 3306, 2979, 1762, 1724, 1529, 1451, 1414, 1370, 1260, 1152, 1110, 759, 742 cm^{-1}; ^{1}H NMR (300 MHz, 77 °C, DMSO-d_6) δ 8.04 (br s, 1H), 7.85 (d, *J* = 7.5 Hz, 2H), 7.65 (d, *J* = 7.5 Hz, 2H), 7.31-7.40 (m, 9H), 6.41 (tt, *J* = 52.2 Hz, *J* = 5.1 Hz, -CF$_2$CF$_2$*H*, 1H) 5.08 (br s, 2H), 4.56 (t, *J* = 13.8 Hz, -C*H$_2$*CF$_2$-, 2H), 4.36-4.40 (m, 2H), 4.30 (dd, *J* = 8.3, 8.3 Hz, 1H), 4.21 (t, *J* = 6.4 Hz, 1H), 4.02 (d, *J* = 11.4 Hz, 1H), 3.73 (d, *J* = 11.4 Hz, 1H), 2.67 (br, 1H), 2.26 (br, 1H), 1.37 (br s, 9H); ^{13}C NMR (75.4 MHz, 20 °C, DMSO-d_6): mixture of rotamers δ 170.2, 169.8, 168.9, 155.4, 153.4, 143.5, 140.6, 136.4, 136.2, 128.1, 127.7, 127.5, 127.3, 126.8, 124.8, 120.1, 109.0 (tt, ^1J = 248 Hz, ^2J = 34 Hz, CH), 81.1 and 80.9, 66.2 (CH$_2$), 65.6 (CH$_2$), 63.4 and 62.6, 60.2 (t, ^2J = 28 Hz, CH$_2$), 58.4 and

57.8 (CH), 54.2 and 53.6 (CH$_2$), 46.5 (CH), 38.7 and 37.6 (CH$_2$), 27.3 (CH$_3$, 3C); HPLC-MS: MeCN(0.05% Formic acid) / water (0.1% Formic Acid), 5% to 95% MeCN over 30 min; flow rate 0.80 mL/min; UV detection at 274 nm; t_R for **60**, 28.79 min; ES-LRMS m/z (ion) calculated 723.3 (M + Na$^+$), observed 723.0;

(2S,4R)-5-(9H-Fluoren-9-ylmethoxycarbonylamino)-proline-1,2,4-tricarboxylic acid 1-benzyl ester 4- (2,2,3,3-tetrafluoro) propyl ester (62)

4.28 g (6.11 mM) of **60** yielded 3.55 g (5.51 mM, 90%) of **62** as a white foam according to the procedure as given for **32**: $[\alpha]^{23}_D$ = -31.0 (c 0.88, CHCl$_3$); IR (film) ν_{max} 3306, 3034, 1761, 1721, 1529, 1450, 1425, 1262, 1109, 758, 743, 697 cm^{-1}; ^{1}H NMR (300 MHz, 77 °C, DMSO-d_6) δ 8.22 (s, 1H), 7.85 (d, J = 7.5 Hz, 2H), 7.65 (d, J = 7.5 Hz, 2H), 7.31-7.40 (m, 9H), 6.42 (tt, J = 52.2 Hz, J = 5.1 Hz, -CF$_2$CF$_2$H, 1H) 5.08 (br s, 2H), 4.57 (t, J = 13.8 Hz, -CH$_2$CF$_2$-, 2H), 4.37-4.40 (m, 3H), 4.21 (t, J = 6.4 Hz, 1H), 4.05 (d, J = 11.4 Hz, 1H), 3.75 (d, J = 11.4 Hz, 1H), 2.71 (br, 1H), 2.31 (br, 1H); ^{13}C NMR (75.4 MHz, 20 °C, DMSO-d_6): mixture of rotamers δ 172.5, 172.2, 168.9, 155.5, 153.9, 153.5, 143.5, 140.6, 136.4, 128.2, 127.9, 127.7, 127.5, 127.2, 127.0, 124.8, 119.9, 109.0 (tt, ^1J = 248 Hz, ^2J = 34 Hz, CH), 66.2 (CH$_2$), 65.7 (CH$_2$), 63.5 and 62.8, 60.2 (t, ^2J = 28 Hz, CH$_2$), 57.7 and 57.2 (CH), 54.1 and 53.7 (CH$_2$), 46.5 (CH), 38.9 and 37.7 (CH$_2$); HPLC-MS: MeCN(0.05% Formic acid) / water (0.1% Formic Acid), 5% to 95% MeCN over 30 min; flow rate 0.80 mL/min; UV detection at 274 nm; t_R for **62**, 25.87 min; ES-LRMS m/z (ion), calculated 667.2 (M + Na$^+$), observed 666.9;

(2S,4R)-5-(9H-Fluoren-9-ylmethoxycarbonylamino)-proline-1,2,4-tricarboxylic acid 1- tert-butyl ester 4- (2,2,3,3-tetrafluoro) propyl ester (64)

3.4 g (5.3 mM) of **62** yielded 2.84 g (4.65 mM, 88%) of **64** as a white foam according to the procedure given for **47** : $[\alpha]^{23}_{D}$ = -54.3 (*c* 1.35, CHCl$_3$); IR (film) ν_{max} 3304, 2980, 1760, 1724, 1530, 1451, 1409, 1369, 1259, 1111, 759, 742 cm^{-1}; ^{1}H NMR (300 MHz, 77 °C, DMSO-*d$_6$*) δ 8.07 (br s, 1H), 7.85 (d, *J* = 7.5 Hz, 2H), 7.66 (d, *J* = 7.5 Hz, 2H), 7.32-7.41 (m, 4H), 6.41 (tt, *J* = 52.2 Hz, *J* = 5.1 Hz, -CF$_2$CF$_2$*H*, 1H), 4.57 (t, *J* = 13.8 Hz, -C*H$_2$*CF$_2$-, 2H), 4.37 (d, *J* = 6.6 Hz, 2H), 4.18-4.28 (m, 2H), 3.94 (d, *J* = 11.4 Hz, 1H), 3.66 (d, *J* = 11.4 Hz, 1H), 2.64 (m, 1H), 2.25 (m, 1H), 1.40 (br s, 9H); ^{13}C NMR (75.4 MHz, 20 °C, DMSO-*d$_6$*): mixture of rotamers δ 173.0, 172.5, 169.1, 155.5, 153.4, 152.7, 143.5, 140.6, 127.5, 126.9, 124.8, 119.9, 109.0 (tt, ^1J = 248 Hz, ^2J = 34 Hz, CH), 79.4, 65.6 (CH$_2$), 63.4 and 62.7, 60.1 (t, ^2J = 28 Hz, CH$_2$), 57.5 and 57.2 (CH), 53.6 (CH$_2$), 46.5 (CH), 39.0 and 37.7 (CH$_2$), 27.7 (CH$_3$, 3C); HPLC-MS: MeCN(0.05% Formic acid) / water (0.1% Formic Acid), 5% to 95% MeCN over 30 min; flow rate 0.80 mL/min; UV detection at 274 nm; t_R for **64**, 25.55 min; ES-LRMS m/z (ion), calculated 633.2 (M + Na$^+$), observed 633.0;

(2S,5R)-5-(9H-Fluoren-9-ylmethoxycarbonylamino)-piperidine-1,2,5-tricarboxylic acid 1-benzyl ester 5- (2,2,3,3-tetrafluoro) propyl ester 2-tert-butyl ester (61)

3.86 g (5.42 mM) of **24** yielded 3.79 g (5.31 mM, 98%) of **61** as a white foam according to the procedure given for **43**; $[\alpha]^{23}_{D}$ = -17.9 (*c* 0.94, CHCl$_3$); IR (film) ν_{max} 3326, 2977, 1729, 1522, 1450, 1369, 1285, 1155, 1111,741 cm^{-1}; ^{1}H NMR (300 MHz, 77 °C, DMSO-*d$_6$*) δ 7.85 (d, *J* = 7.5 Hz, 2H), 7.74 (s, 1H), 7.65 (d, *J* = 7.5 Hz, 2H), 7.28-7.42 (m, 9H), 6.38 (tt, *J* = 52.2 Hz, *J* = 5.1 Hz, -CF$_2$CF$_2$*H*, 1H) 5.12 (br s, 2H), 4.74 (m, 1H), 4.50-4.60 (m, 3H), 4.04-4.27 (m, 3H), 3.30

(br, 1H), 1.87-2.15 (m, 3H) 1.65 (m, 1H), 1.41 (br s, 9H); ^{13}C NMR (75.4 MHz, 20 °C, DMSO-d_6): mixture of rotamers δ 171.3, 169.7 and 169.5, 155.6, 143.8, 143.6, 140.7, 136.5, 136.4, 128.3, 128.1, 127.8, 127.6, 127.3, 127.0, 125.2, 125.0, 120.1, 81.6, 66.5 (CH$_2$), 65.8 (CH$_2$),59.8 (CH$_2$), 56.9 and 56.7, 53.7and 53.2 (CH), 46.5 and 46.4 (CH), 43.7 (CH$_2$), 28.0 (CH$_2$), 27.5 (CH$_3$, 3C), 20.7 (CH$_2$); HPLC-MS: MeCN(0.05% Formic acid) / water (0.1% Formic Acid), 5% to 95% MeCN over 30 min; flow rate 0.80 mL/min; UV detection at 274 nm; t_R for **61**, 29.35 min; ES-LRMS m/z (ion) calculated 737.3 (M + Na$^+$), observed 737.2;

(2S,5R)-5-(9H-Fluoren-9-ylmethoxycarbonylamino)-piperidine-1,2,5-tricarboxylic acid 1-benzyl ester 5- (2,2,3,3-tetrafluoro) propyl ester (63)

3.7 g (5.2 mM) of **61** yielded 2.94 g (4.47 mM, 86%) of **63** as a white foam according to the procedure given for **32**: [α]$^{23}_D$ = -10.9 (*c* 1.15, CHCl$_3$); IR (film) ν_{max} 3324, 3034, 1717, 1520, 1450, 1285, 1190, 759, 742, 697 cm^{-1}; ^{1}H NMR (300 MHz, 77 °C, DMSO-d_6) δ 7.87 (d, *J* = 7.5 Hz, 2H), 7.80 (s, 1H), 7.66 (d, *J* = 7.5 Hz, 2H), 7.24-7.42 (m, 9H), 6.42 (tt, *J* = 52.2 Hz, *J* = 5.1 Hz, -CF$_2$CF$_2$*H*, 1H) 5.05 (br s, 2H), 4.82 (m, 1H), 4.51-4.63 (m, 3H), 4.18-4.28 (m, 3H), 3.39 (br, 1H), 2.04-2.18 (m, 3H) 1.69 (m, 1H); ^{13}C NMR (75.4 MHz, 20 °C, DMSO-d_6): mixture of rotamers δ 171.9, 171.3, 155.5, 143.7, 143.5, 140.6, 136.6, 136.4, 128.4, 128.2, 127.8, 127.7, 127.2, 127.1, 125.3, 125.0, 120.2, 109.2 (tt, ^1J = 248 Hz, ^2J = 34 Hz, CH), 79.2, 66.6 (CH$_2$), 65.9 (CH$_2$),59.9 (t, ^2J = 28 Hz, CH$_2$), 56.9 and 56.7, 53.2and 52.7 (CH), 46.6 and 46.4 (CH), 44.2 and 43,8 (CH$_2$), 28.3 and 27.8 (CH$_2$), 20.6 and 20.8 (CH$_2$); HPLC-MS: MeCN(0.05% Formic acid) / water (0.1% Formic Acid), 5% to 95% MeCN over 30 min; flow rate 0.80 mL/min; UV detection at 274 nm; t_R for **63**, 25.87 min; ES-LRMS m/z (ion), calculated 681.2 (M + Na$^+$), observed 681.0;
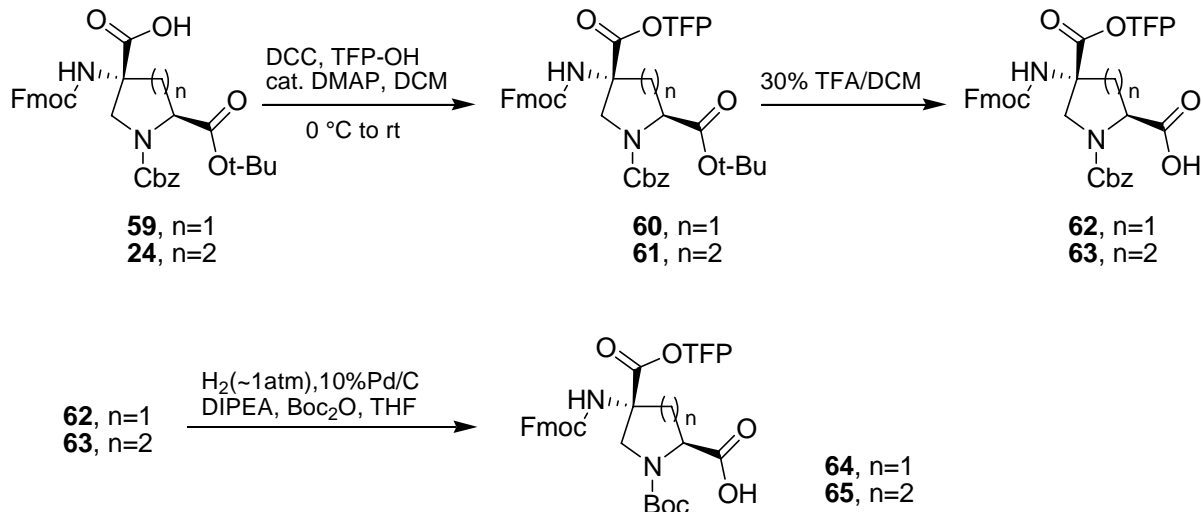
(2S,5R)-5-(9H-Fluoren-9-ylmethoxycarbonylamino)-piperidine-1,2,5-tricarboxylic acid 1-tert-butyl ester 5- (2,2,3,3-tetrafluoro) propyl ester (65)

2.86 g (4.34 mM) of **63** yielded 2.13 g (3.41 mM, 79%) of **65** as white foamy solid according to the procedure given for **47**: $[\alpha]^{23}_D$ = -7.7 (*c* 0.83, CHCl$_3$); IR (film) ν_{max} 3317, 2978, 1717, 1519, 1451, 1369, 1268, 1154, 1113, 759, 742 cm^{-1}; ^{1}H NMR (300 MHz, 77 °C, DMSO-d_6) δ 7.85 (d, *J* = 7.5 Hz, 2H), 7.78 (d, *J* = 7.5 Hz, 2H), 7.64 (s, 1H), 7.29-7.43 (m, 4H), 6.40 (tt, *J* = 52.2 Hz, *J* = 5.1 Hz, -CF$_2$CF$_2$*H*, 1H) 4.71 (br s, 1H), 4.49-4.65 (m, 3H), 4.13-4.28 (m, 3H), 3.26 (br d, *J* = 13.0 Hz, 1H), 1.94-2.08 (m, 3H), 1.60-1.69 (m, 1H), 1.34 (s, 9H); ^{13}C NMR (75.4 MHz, 20 °C, DMSO-d_6): mixture of rotamers δ 172.1, 171.4, 155.4, 154.4, 143.5, 140.5, 127.5, 126.9, 124.9, 124.8, 119.9, 109.0 (tt, ^1J = 248 Hz, ^2J = 34 Hz, CH), 79.1, 65.7 (CH$_2$),59.6 (t, ^2J = 28 Hz, CH$_2$), 56.7, 51.6 (CH), 46.4 (CH), 43.6 (CH$_2$), 28.4 and 28.0 (CH$_2$), 27.7 (CH$_3$, 3C) 20.4 (CH$_2$); HPLC-MS: MeCN(0.05% Formic acid) / water (0.1% Formic Acid), 5% to 95% MeCN over 30 min; flow rate 0.80 mL/min; UV detection at 274 nm; t$_R$ for **65**, 24.91 min; ES-LRMS m/z (ion), calculated 647.2 (M + Na$^+$), observed 646.9;

3.6.3 Solid phase assembly of dimers for kinetics measurements
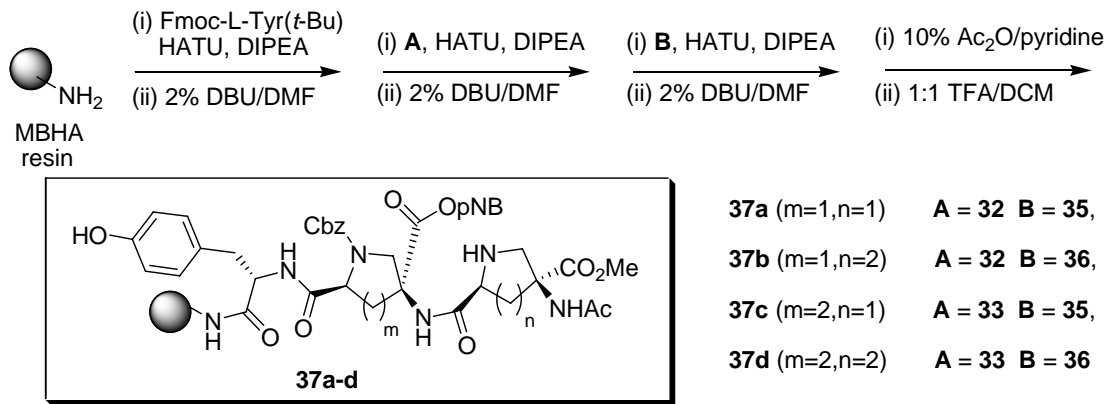
Figure 20: Assembly of bis-amino acid dimers

General procedure A: Washing

In a typical washing sequence, the resin was washed 5 times with DCM and DMF alternately. This was followed by a final wash with DCM.

General procedure B: HATU coupling

In a 1.5 mL polypropylene micro centrifuge vial the amino acid (as given) was dissolved in a solution of 20% DCM/ DMF (as given). To this mixture was added DIPEA (as given) followed by HATU (as given). The resulting coupling mixture was mixed briefly and immediately added to the SPPS reaction vessel carrying the resin. After mixing for the given amount of time, the resin was drained and washed according to the general procedure (A).

General procedure C: Fmoc deprotection by piperidine

To the SPPS reactor carrying the resin added 1000 μL of a solution of 2% DBU in DMF. After 5 minutes of mixing, a volume of 40 μL of deprotection mixture was withdrawn and diluted 50 fold with a solution of 20% piperidine in DMF. A UV-visible spectroscopic analysis of the piperidine-fluorenyl adduct was performed and the absorbance at 301 nm ($\varepsilon = 7800$ M^{-1}cm^{-1}) was recorded. This value of the absorbance was used to estimate coupling yield. Following the Fmoc deprotection, the resin was washed according to general procedure (A).

General procedure D: Capping of the residual free amine

To the SPPS reactor carrying the resin added 250 μL of a solution of 10% acetiic anhydride in pyridine. After 5 minutes of mixing, the resin was drained and washed according to the general procedure (A).

General procedure E: Fmoc deprotection by DBU

To the SPPS reactor carrying the resin added 1000 μL of a solution of 20% piperidine in DMF. After 20 minutes of mixing, a volume of 40 μL of deprotection mixture was withdrawn and diluted 50 fold with a solution of 20% piperidine in DMF. A UV-visible spectroscopic analysis of the piperidine-fluorenyl adduct was performed and the absorbance at 301 nm ($\varepsilon = 7800$ M^{-1}cm^{-1}) was recorded. This value of the absorbance was used to estimate coupling yield. Following the Fmoc deprotection, the resin was washed according to general procedure (A).

General procedure F: Boc and t-Bu protecting group removal

Boc and t-Bu protecting groups were removed by treating the resin with 1mL of 1:1 TFA/DCM (2 x 15 minute). The resin was washed with CH_2Cl_2 and MeOH several times and then neutralized by washing a few times with 10% Et_3N/CH_2Cl_2. The resin was washed again with CH_2Cl_2 and MeOH several times, followed by only CH_2Cl_2.

General procedure G: DKP closure via flow-cell method

A few beads of resin carrying oligomer sequence were transferred to the PTFE tubing of flow cell apparatus and the catalytic solution (as given) was pumped through the resin for the desired amount of time at a given temperature. The resin was recovered and transferred to a 1 mL polypropylene SPPS reactor. The resin was washed with CH_2Cl_2, and MeOH several times, followed by only CH_2Cl_2 and then dried under reduced pressure overnight.

General procedure H: DKP closure via microwave irradiation method

A few beads of resin carrying oligomer sequence were placed in a 10 mL microwave reaction vessel (10mL capacity, glass) containing 5 mL of a given solution. The vessel was capped and placed in the microwave reactor (CEM Discover) and irradiated (300 W maximum power, T° C, 5 min ramp) with continuous stirring. After desired time interval the vessel was removed from the microwave reactor and the resin was transferred to a 1 mL polypropylene SPPS reactor. The resin was washed with CH_2Cl_2, and MeOH several times, followed by only CH_2Cl_2 and then dried under reduced pressure overnight.

General procedure I: Oligomer cleavage from resin via TFMSA method

The reactor carrying the resin was kept in ice bath and added 25 µL thioanisole, 12.5 µL 1,2-Ethanedithiol (EDT), and 250 µL TFA. The cleavage mixture was allowed to stir for 5 min and 25 µL of TFMSA was added. The stirring was continued for 1 h at 0° C followed by 1 h at room temperature. The cleavage mixture was dripped into 50 mL of ether in an eppendorf centrifuge tube that caused the desired product to precipitate out. This precipitate was converted into pellet form by centrifugation for 30 min at 4 °C at 3200 rpm. Ether was decanted, precipitate was dissolved in 200 µL of TFA, and product was precipitated a second time from ether. After centrifugation Ether was decanted and residual precipitate pellet was prepared for analysis by air drying for a few minutes.

Assembly of oligomer 37a

A quantity of 23 mg of MBHA resin (14.6 µmol free amine, 0.62 mmol loading) was transferred to a 1 mL polypropylene solid phase peptide synthesis (SPPS) reaction vessel and allowed to swell in DMF for 30 minutes.

Fmoc-L-Tyr(t-Bu)-OH (13.1 mg, 28.5 µmol) was dissolved in 20% CH_2Cl_2/DMF (143 µL) and coupled for 2 hours according to general procedure (B) by using DIPEA (9.9 µL, 57 µmol) and HATU (10.8 mg, 28.5 µmol). Any residual free amine was capped according to general procedure (D). The terminal Fmoc group was deblocked by general procedure (C). The coupling yield was estimated as quantitative.

Monomer **32** (19.4 mg, 28.5 µmol) was dissolved in 20% CH_2Cl_2/DMF (143 µL) and coupled for 2 hours according to general procedure (B) by using DIPEA (9.9 µL, 57 µmol) and HATU (10.8 mg, 28.5 µmol). The resin was subjected to a second coupling reaction under

identical conditions. Any residual free amine was capped according to general procedure (D). The terminal Fmoc group was deblocked by general procedure (C).

Monomer **35** (19.4 mg, 28.5 μmol) was dissolved in 20% CH_2Cl_2/DMF (143 μL) and coupled for 2 hours according to general procedure (B) by using DIPEA (9.9 μL, 57 μmol) and HATU (10.8 mg, 28.5 μmol). The resin was subjected to a second coupling reaction under identical conditions. The terminal Fmoc group was deblocked by general procedure (C). The coupling yield was estimated as 95%. The terminal amine was acylated according to general procedure (D). The acylation procedure (D) was repeated one additional time to ensure complete acylation. The resin was prepared for Boc group cleavage by washing with MeOH and DCM alternately followed by drying under reduced pressure.

Boc and *t*-Bu protecting group were removed by general procedure (F) and resin was dried under reduced pressure. Other bis-amino acid oligomers (**37b**, **37c** and **37d**) were synthesized in the same manner by following general procedures A, B, C and D.

Flow Cell Apparatus for DKP closure studies
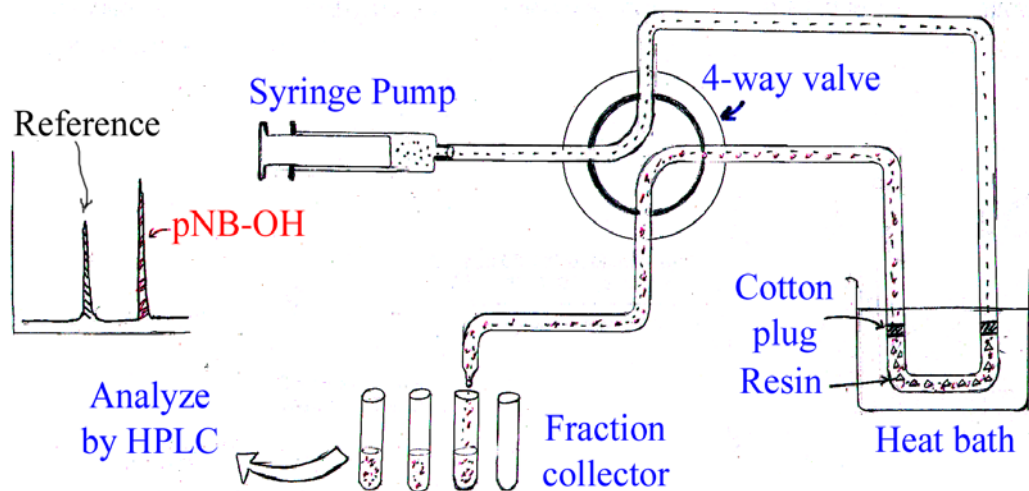
Figure 21: Schematic Diagram of the flow cell set up for the kinetic measurements.

The above shown simple set up in Figure 21 for the measurement of half-life for DKP closure reaction was assembled from the PTFE tubings and connectors. All the connections were made by thin tubing with inner diameter 0.75 mm. For flow cell a small piece of tubing (15 mm) with inner diameter 1.55 mm was used. This tubing was filled with a few beads of resin (2-5 mg) that were held in place by cotton plugs at both ends. The oil bath was maintained at desired temperature by using a digital temperature controller. The eluant was prepared by dissolving approximately 20 µM of reference compound (9-fluorenemethanol) in the desired catalytic solvent mixture. The resin was allowed to swell by pumping blank solvent. After a few minutes the flow cell tube carrying the resin was removed from the loop and rest of the system was allowed to equilibrate by pumping the eluant. The flow cell was inserted back into the loop, lowered into a preheated oil-bath at desired temperature and flow rate was set at 100 µL per minute. After a wait of 5 minutes (compensating for the dead volume of tubing from resin to collector) the fractions were collected at desired interval by using automatic fraction collector.

General procedure for measurement of kinetics of diketopiperazine formation

A few beads of resin (2-3 mg) carrying desired dimer (e.g. **37c**) were loaded in a homemade flow cell apparatus and catalysis solution (e.g. 80 mM AcOD in DMF) was flowed over the resin at a constant flow rate (100 µL/min) at desired temperature (e.g. 100 °C). The fractions were collected at 15 minute interval, and analyzed by analytical HPLC. Areas under the peaks were recorded for the reference and the *p*-nitrobenzyl alcohol that were used to estimate the half lives for the corresponding reaction under a given set of conditions as discussed below.
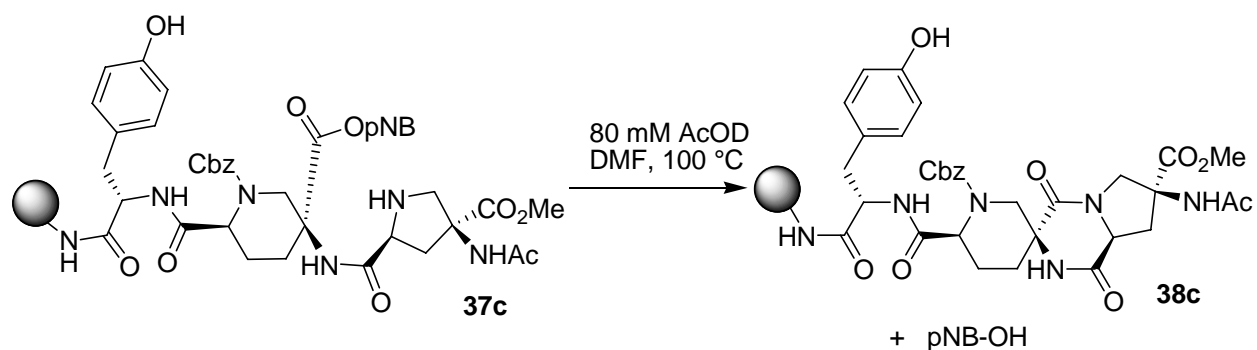
Figure 22: Diketopiperazine formation for sequence **37c**

Overall aminolysis reaction can be represented as

X → Y + Z

Since catalyst is flowed over the resin at a fixed rate, it can be safely assumed that the reaction follows first order reaction rate equation

$$d[Y]/dt = -d[X]/dt = k[X]$$ (1)

The quantity being measured in our experiments is the area under the curve (I) for the released amount of p-nitrobenzyl alcohol (Y). Hence (I) at any time t represents amount of Y released for a time interval t-Δt to t. Thus,

$$I = a\{[Y]_t - [Y]_{t-\Delta t}\}$$

$$I = a\{[X] \ -[X]_t - [X] \ +[X]_{t-\Delta t}\}$$

$$I = a\{[X]_{t-\Delta t} - [X]_t\}$$

However general solution for eq.1 is given by

$$[X]_t = [X]_0 e^{-kt}$$

$$\Rightarrow I = a[X]_0 \{e^{-k(t-\Delta t)} - e^{-kt}\}$$

$$\Rightarrow I = a[X]_0 (e^{k\Delta t} - 1)e^{-kt}$$

$$\Rightarrow I = Ae^{-kt} \qquad \text{where A} = a[X]_0 (e^{k\Delta t} - 1), \text{ is constant as long as } \Delta t \text{ is a constant}$$

$$\Rightarrow \ln I = -kt + \ln A$$

Therefore if the plot lnI against time t gives a straight line, than the aminolysis reaction does follow

first order reaction rate equation and halflife for this transformation is given by

$$t_{1/2} = \ln 2 / k = 0.693 / k$$

Since $[X]_0$ appears as a constant it can be chosen arbitrarily without affecting the calculation of half lives. Also we normalized the area under the curve for *p*-nitrobenzyl alcohol (I) by dividing it by the area under the curve for reference, I_{ref} to remove any discrepancies arising due to instrumental errors.

Table 5: Data obtained from on resin DKP closure for oligomer **37c**

t (min)	I (mAU*sec)	I_{ref} (mAU*sec)	$I'=(I/I_{ref})$	$\ln I'$
15	746.9	1640.7	0.455	-0.787
30	1877.6	2451.2	0.766	-0.267
45	896.7	2414.3	0.371	-0.990
60	460.8	2472.4	0.186	-1.68
75	238.7	2417.4	0.0987	-2.315
90	144.2	2464.3	0.0585	-2.838
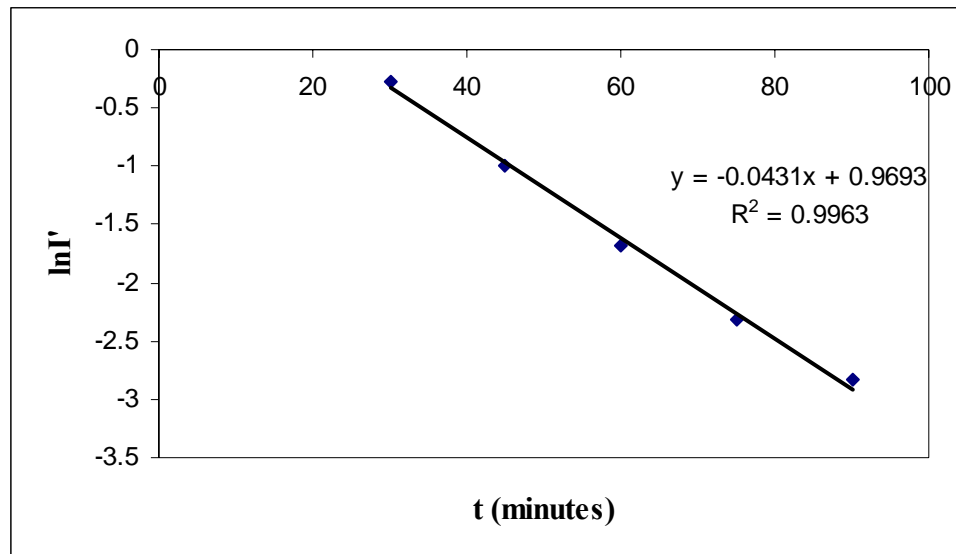
Figure 23: Graph of **ln(I')** vs. Time **t**

From graph, k = 0.0431 min^{-1}

Hence half life, $t_{1/2}$ = 0.693/k

$t_{1/2}$ = 0.693/0.0431 = 16.1 minutes

Post DKP closure analysis

To confirm that the DKP formation was complete and find the evidence of epimerization, the resin bound oligomer **38c** was recovered and cleaved by TFMSA method according to general procedure (I). (Figure 24) The product **66** was recovered in pallet from and dissolved in 200 µL of 1:1 acetonitrile/water. A part of this solution (10 µL) was injected into HPLC-MS for analysis.

HPLC-MS: column, Waters XTerra MS C_{18} column 4.6 mm x 150 mm; mobile phase, MeCN (0.05% Formic acid) / water (0.1% Formic Acid), 5% to 95% MeCN over 30 min; flow rate 0.80 mL/min; UV detection at 220 nm; t_R for **66**, 10.194 min; ES-LRMS m/z (ion), calculated 545.2(M + H$^+$) observed 545.0.
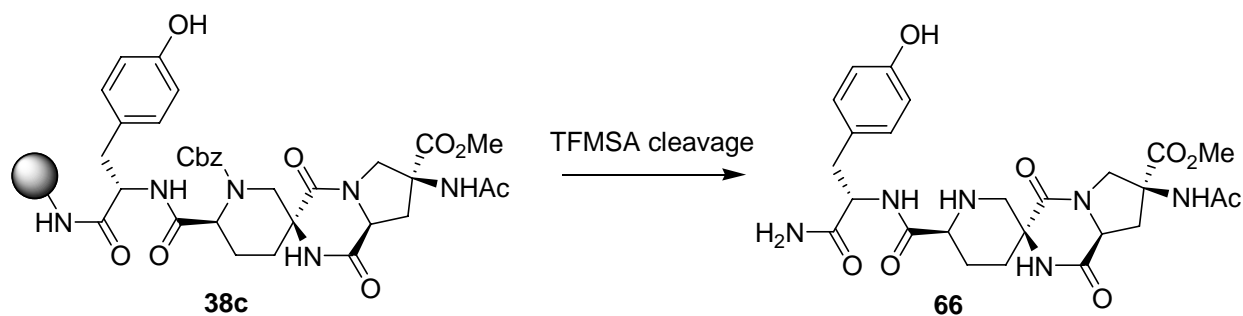
Figure 24: Cleavage of the product **66** following the DKP formation reaction
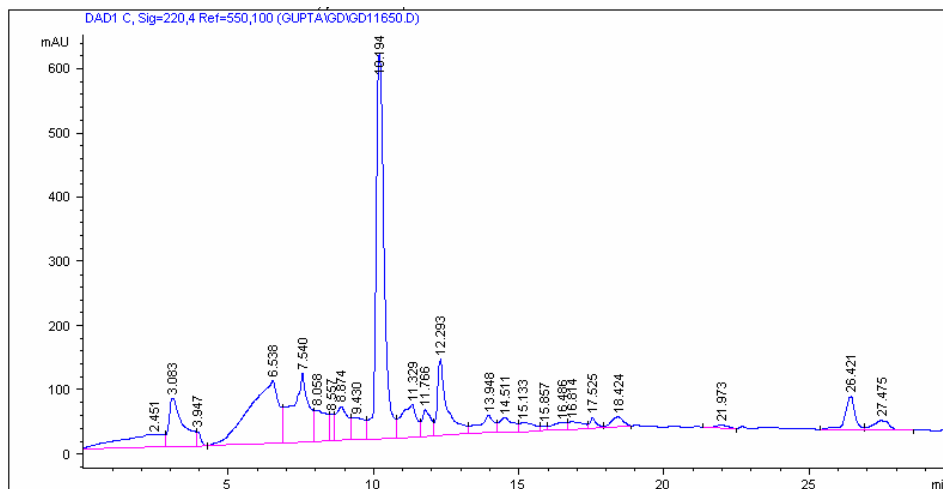
Figure 25: Chromatogram of the cleaved product **66** at 220 nm.

94

Solid phase assembly of homooligomer 49 on MBHA resin
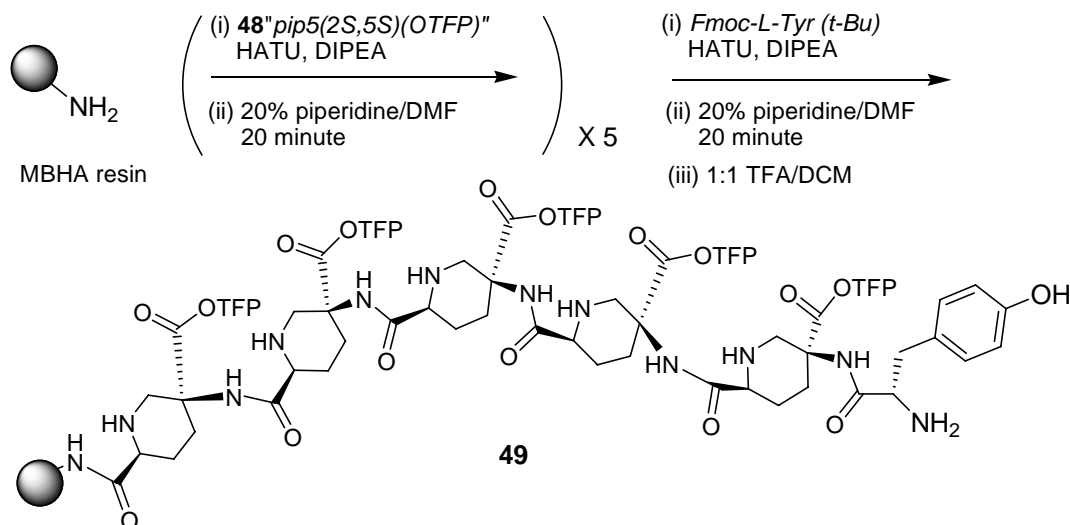
Figure 26: Assembly of homo-oligomer **49**

A quantity of 10 mg of MBHA resin (0.62 mmol/g loading, 6.2 μmol free amine) was transferred to a 1 mL polypropylene solid phase peptide synthesis (SPPS) reaction vessel and allowed to swell in DMF for 30 minutes.

Monomer **48** (7.7 mg, 12.4 μmol) was dissolved in 20% CH_2Cl_2/DMF (62 μL) and coupled for 2 hours according to general procedure (B) by using DIPEA (4.8 μL, 27.3 μmol) and HATU (4.7 mg, 12.4 μmol). The resin was subjected to a second coupling reaction under identical conditions. Any residual free amine was capped according to general procedure (D). The terminal Fmoc group was deblocked by general procedure (E).

The above given sequence for coupling of monomer **48** was repeated four times. Coupling yields were estimated to be >90% based on Fmoc deprotection step.

Fmoc-L-Tyr(*t*-Bu)-OH (8.5 mg, 18.6 μmol) was dissolved in 20% CH_2Cl_2/DMF (93 μL) and coupled for 2 hours according to general procedure (B) by using DIPEA (7.1 μL, 40.9 μmol)

and HATU (7.1 mg, 18.6 μmol). Any residual free amine was capped according to general procedure (D).

The terminal Fmoc group was deblocked by general procedure (C). The coupling yield was quantitative.

Boc and *t*-Bu protecting group were removed by general procedure (F) and resin was dried under reduced pressure. The DKP closure was performed by suspending the resin in a solution of 100 mM AcOH and 50 mM Et$_3$N in o-xylene in a microwave oven at 130° C according to general procedure (G).

After recovery the resin bound oligomer **49** was cleaved by TFMSA method as given in general procedure (I). The product **50** was recovered in pallet from and dissolved in 200 μL of 1:1 Acetonitrile/water. 10 μL of this solution was injected into HPLC-MS for analysis. HPLC-MS: column, Waters XTerra MS C$_{18}$ column 4.6 mm x 150 mm; mobile phase, MeCN(0.05% Formic acid) / water (0.1% Formic Acid), 0% to 25% MeCN over 30 min; flow rate 0.80 mL/min; UV detection at 274 nm; t$_R$ for **50**, 16.03 min; ES-LRMS m/z (ion), Calculated 941.4 (M + H$^+$), observed 941.2;

Assembly of heterooligomers 51-54 and DKP closure

Each of the hetero oligomers **51-54** was assembled on hydroxymethyl polystyrene resin (0.98 mmol/g loading) on 20 mg scale. Monomer X$_1$ was attached to the hyroxymethylpolystyrene resin using MSNT/MeIm method, as described in Novabiochem catalogue.

The resin was transferred to a 1 mL polypropylene SPPS reaction vessel and allowed to swell in dry CH$_2$Cl$_2$ for 10 minutes. In case of oligomer **54,** 25 mg of **48** (40 μmol, 2 equiv.) were dissolved in 300 μL of dry CH$_2$Cl$_2$. To this solution 2.3 μL of MeIm (28 μmol, 1.4 equiv.)

and 12 mg of MSNT (40 µmol) were added. This coupling solution was mixed briefly and added to the pre swelled resin. After mixing for 30 minutes, the coupling solution was drained and the resin was washed several times with MeOH and CH_2Cl_2 alternately. Any unreacted alcohol groups were capped by treatment with 500 µL of 10% Ac_2O in pyridine for 5 minutes. The resin was drained and washed several times with MeOH and CH_2Cl_2, followed by only CH_2Cl_2.

Other monomers, X_{2-4} followed by Fmoc-L-Tyr(t-Bu)OH were coupled sequentially using HATU following a procedure similar to the one as described for oligomer **49**. After the removal of terminal Fmoc group, residual Boc and t-Bu protecting groups were removed by general procedure (F) and resins were dried under reduced pressure prior to DKP closure.

The resins carrying desired sequence **51-54** were subjected to DKP closure at 130 °C by flow cell method (200 µL/min) according to general procedure (G) by flowing catalytic solution of 100 mM AcOH and 50 mM Et_3N in *o*-xylene over the resin for 2 hours.

After recovery, the resin bound oligomer **51** (and **52-54**) was cleaved by TFMSA method as given in general procedure (I). After single precipitation the product **55** (and **56-58**) was obtained in a pallet from and immediately dissolved in ~ 1mL of 10% acetonitrile in water. 10 µL of this solution was injected into analytical HPLC-MS for analysis and rest was purified by preparative reverse phase HPLC on a Varian ProStar 500 HPLC system with a Varian Chrompack Micrsorb 100-C_{18} column (8 µm packing; 21.5mm x 50mm): mobile phase MeCN(0.05% Formic acid) / water (0.1% Formic Acid), 0% to 25% MeCN over 30 min; flow rate 15 mL/min; UV detection at 274 nm). The product containing fractions were combined and lyophilized to yield the desired rigidified oligomers **55-58** as fluffy white powders. HRESIQTOFMS calcd for $C_{35}H_{40}N_9O_{11}$ (M + H^+) 762.2847, found 762.2927 for **55**, found 762.2844 for **56**, found 762.2880 for **57**, found 762.2865 for **58**.

Analytical HPLC-MS (before purification): column, Waters XTerra MS C_{18} column 4.6 mm x 150 mm; mobile phase, MeCN(0.05% Formic acid) / water (0.1% Formic Acid), 0% to 25% MeCN over 30 min; flow rate 0.80 mL/min; UV detection at 220 and 274 nm; t_R for **55**, 9.7 min; t_R for **56**, 8.6 min; t_R for **57**, 10.1 min; t_R for **58**, 9.3 min; ES-LRMS calcd for $C_{35}H_{40}N_9O_{11}$ (M + H$^+$) 762.3, found 762.2 for **55, 56, 57, 58.**

3.6.4 HPLC chromotograms for the oligomers before purification.
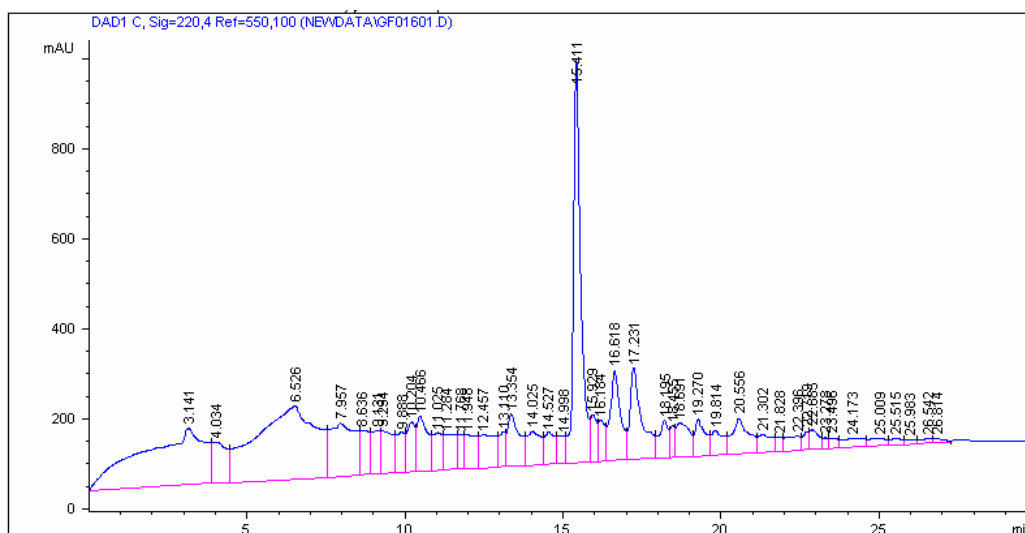
Figure 27: HPLC chromatogram for homo-oligomer **50** at 220 nm
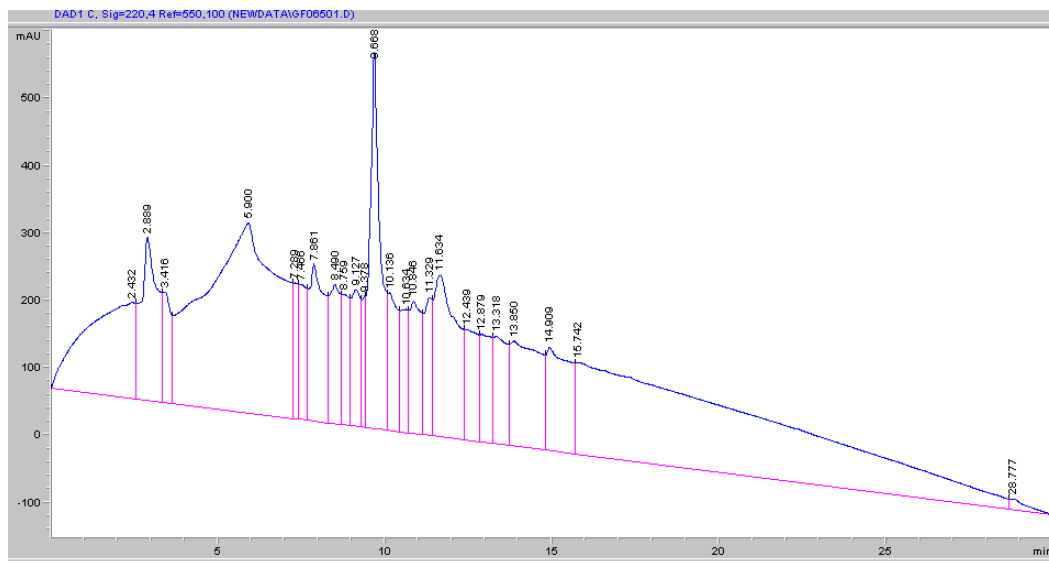
Figure 28: HPLC chromatogram for hetero-oligomer **55** at 220 nm
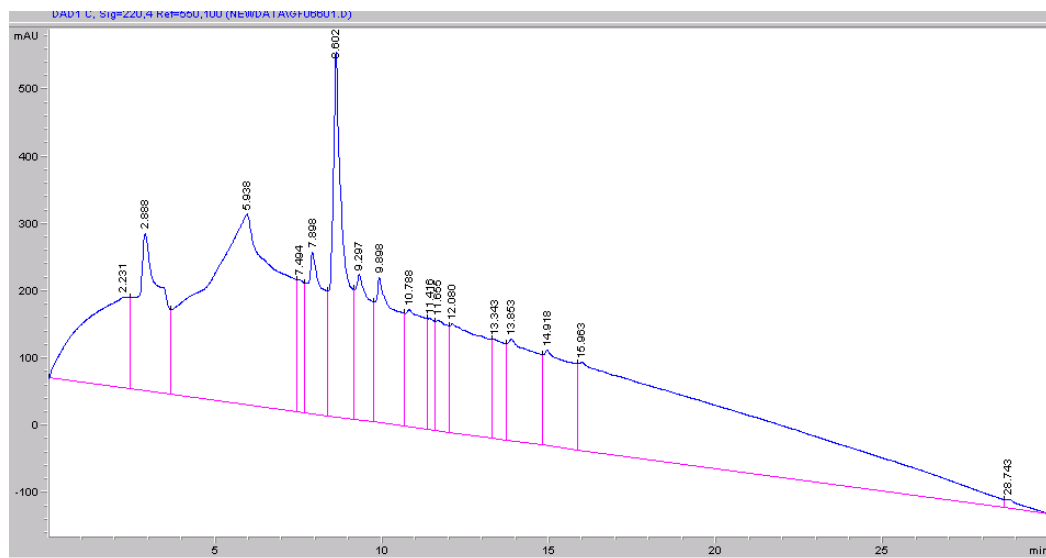
Figure 29: HPLC chromatogram for hetero-oligomer **56** at 220 nm
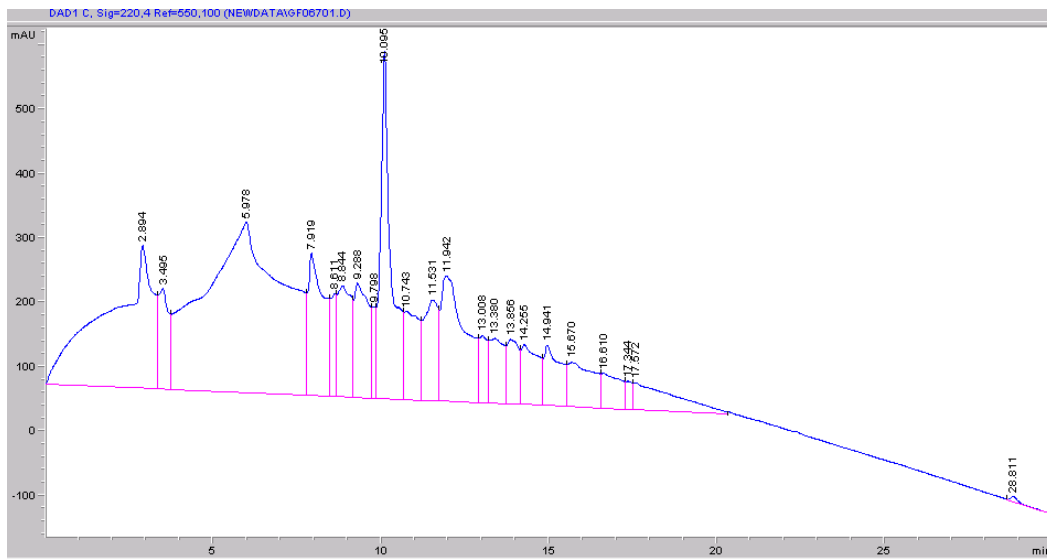
Figure 30: HPLC chromatogram for hetero-oligomer **57** at 220 nm
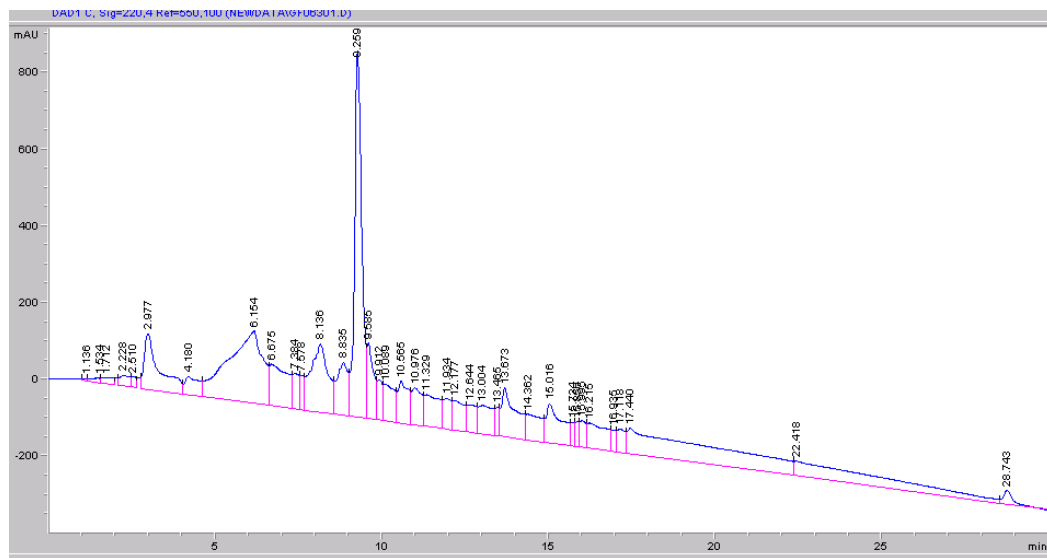
Figure 31: HPLC chromatogram for hetero-oligomer **58** at 220 nm

4.0 SYNTHESIS OF A CARBOXYLATE FUNCTIONALIZED BIS-AMINO ACID

MONOMER

Oligomers that adopt well-defined three-dimensional structures have attracted a great deal of interest in the past decade.[10-12] Functionalized oligomers that present proteogenic and nonproteogenic functional groups from a structurally defined backbone have found many applications.[192] Functionalized amphipathic β-peptides have demonstrated antifungal and antimicrobial activities and mixed β-peptide foldamers have been developed that bind protein surfaces.[193-195] Functionalized peptoids have also demonstrated antimicrobial activity and are being developed as mimics of lung surfactant proteins.[196, 197] Phenylene ethynylene foldamers have demonstrated molecular recognition of small molecules.[198] In our own laboratory, we have developed a functionalized oligomer that acts as a molecular switch under the control of metal exchange.[199] An essential requirement toward the development of more sophisticated applications for shape-persistant oligomers is the development of monomers that carry proteogenic and nonproteogenic chemical functionality.

As described previously in chapters 1 and 2, in our laboratory, we have developed a synthetic approach to a unique class of oligomers called bis-peptides.[200] We synthesize stereochemically pure, cyclic bis-amino acid monomers and couple them through pairs of amide bonds to create spiro-ladder oligomers (bis-peptides) with programmable three-dimensional shapes. Bis-peptides are assembled by using solid phase peptide synthesis and they are trivially

functionalized on their two ends through the incorporation of amino acids at the beginning or the end of a bis-peptide synthesis.

To enable the development of more highly functionalized bis-peptides we need to develop synthetic approaches to incorporate functionality into the bis-peptide backbone. The approach that we have described in this chapter is to create the functionalized bis-amino acid "proAc(2S3S4R)"[114] that carries a protected carboxylic acid functional group on its cyclic core. This approach is general and can be easily extended to incorporate other functional groups.

We chose carboxylic acid group for our first synthesis as it is a very versatile proteogenic functional group found in aspartic acid and glutamic acid. It plays an essential role in enzyme catalysis such as part of the Asp-His-Ser catalytic triad in proteases and esterases.[201] Miller and co-workers have demonstrated that carboxylic acids on chiral scaffolds can carry out asymmetric epoxidation of alkenes.[202, 203] It is a polar group that is solvated well by water and it can be activated and further functionalized through the formation of amides and esters.

In this chapter we describe the synthesis of the first functionalized bis-amino acid monomer proAc(2S3S4R) **67** that carries an acetyl side chain. This monomer was incorporated into oligomer **84** to assess the monomer's amenability for Fmoc-SPPS. Finally, two-dimensional NMR and computational experiments were performed to determine the conformational preference of this new functionalized monomer **67**.

4.1 SYNTHESIS OF FUNCTIONALIZED MONOMER

4.1.1 Approaches to alkylation

Our synthesis of proAc series of monomers starts from *trans*-4-hydroxy-(S)-proline **6** the same starting material used in the synthesis of pro4 and pip5 monomers. The simplest approach would have been to alkylate the ketone intermediate **5** used for the synthesis of pro4[108, 109] and pip5[112] monomers at β–carbon and follow subsequent synthetic steps to the final monomer (Figure 32). Numerous methods are available for ketone alkylation and two approaches that are most prevalent are via enolate formation or via enamine formation.
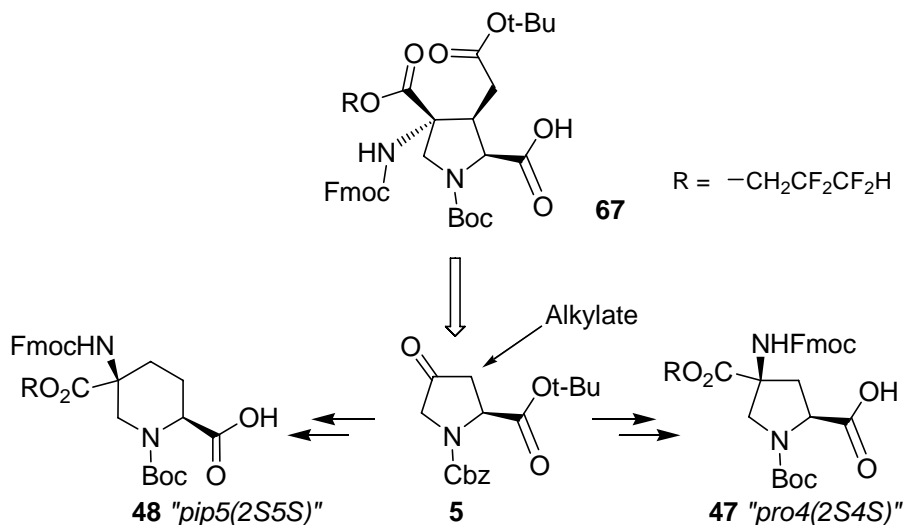
Figure 32: Retrosynthetic approach to a functionalized monomer

Enamine based approaches do not require strong acidic or basic conditions and are generally performed at ambient temperature or with mild heating. However, strongly activated

electrophiles are required for alkylation. Initially we tried a few approaches for alkylation based on enamine chemistry[204] but without any success.

Enolates are easily formed by treating a ketone with strong bases such as organolithium compounds and are easily alkylated with an electrophile. This approach could be utilized to access a large number of alkylated bis-amino acids as a variety of electrophiles are commercially available. Unfortunately we could not utilize ketone **5** for enolate based alkylations. A major concern for us was that the strong bases used could cause epimerization at α-carbon (C-2) of amino-acid moiety in **5**. Furthermore, the secondary amine of ketone **5** is protected with a Cbz protecting group that reacts with organolithiums. Another convenient *N*-protecting group, the Boc group is stable under alkylation conditions, but offers little protection against epimerization. Also, amino ketones protected with carbamates show poor regioselectivity towards alkylation (C-3 vs C-5).[205]

4.1.2   The Pf protecting group

This prompted us to find an effective substitute for Cbz protecting group that not only is stable to alkylation conditions but also protects against any racemization. We built on the work of Rapoport and Lubell,[206-210] who have made extensive use of the 9-phenylfluoren-9-yl (Pf) as a nitrogen protecting group for regio- and stereoselective alkylation of various amino acid, amino aldehyde and amino ketone derivatives. The phenylfluorenyl group offered us several advantages over other protecting group (such as carbamates): It simulatenously masked the secondary amine, prevented enolization at carbon next to nitrogen (C-5), protected the stereochemical configuration of the α-carbon, and protected the adjacent benzyl ester from attack by nucleophiles and base hydrolysis (Figure 33). Furthermore, the Pf protecting group is very stable

to solvolysis and can withstand mild acids unlike the trityl protecting group and is easily removed by hydrogenolysis. We found that the introduction of Pf protecting group also facilitated NMR analysis because it did not produce amide rotamers associated with carbamate protecting groups. We noted that all the intermediates isolated during the synthesis that carried Pf protecting group were easy to crystallize. Since Pf protecting group is an excellent UV chromophore, we could utilize RP-HPLC very effectively for the monitoring and optimization of reactions.
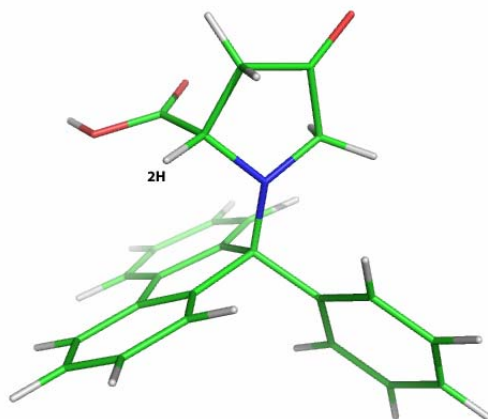
Figure 33: The steric bulk of 9-phenylfluoren-9-yl (pf) group provides protection to functional groups in its periphery including α-proton (2H) of ketone **70**

4.1.3   Alkylation of ketone 70 via enolate formation

We used the Rapoport and Lubell's chemistry to convert *trans*-4-hydroxy-L-proline **6** into ketone **70** through a three-step procedure that included the conversion of **6** to its benzyl ester,[210, 211] protection of the secondary amine with a phenylfluorenyl group,[208] and oxidation of the

alcohol by using Swern oxidation[212, 213] to produce the ketone **70**. We deliberately chose benzyl ester for the protection of carboxylic acid functionality as it can be simultaneously deprotected in a single step while swapping a Pf group with a Boc group under hydrogenolysis conditions as described later.

α-Bromo acetic acid protected with *t*-butyl group was chosen as the electrophile so that the carboxylic acid functionality could be unmasked by treatment with TFA after the monomer has been incorporated into an oligomeric sequence. For alkylation, we used a protocol similar to the one reported by Poisson et al. [214] The ketone **70** was treated with *n*-BuLi in THF:HMPA at -78 ºC and the resulting enolate was added to a suspension of $BrCH_2CO_2t$-Bu and NaI in THF at -40 ºC. The enolate was formed exclusively at the 3-position of the pyrrolidine ring consistent with previous reports.[214] We obtained a diastereomeric mixture of ketones **72a** and **72b** in a 10:1 ratio as determined by C_{18} reverse phase (RP) HPLC-MS analysis and 1D proton NMR. After separation of the diastereomers by silica gel chromotography, the stereochemistry of each diastereomer was tentatively assigned by comparing the coupling constants between Hα and Hβ for the respective ketones (J = 6.1 Hz for **72a** and J = 8.2 Hz for **72b**) with those reported previously for similar alkylated ketone derivatives (Scheme 15).[214, 215]
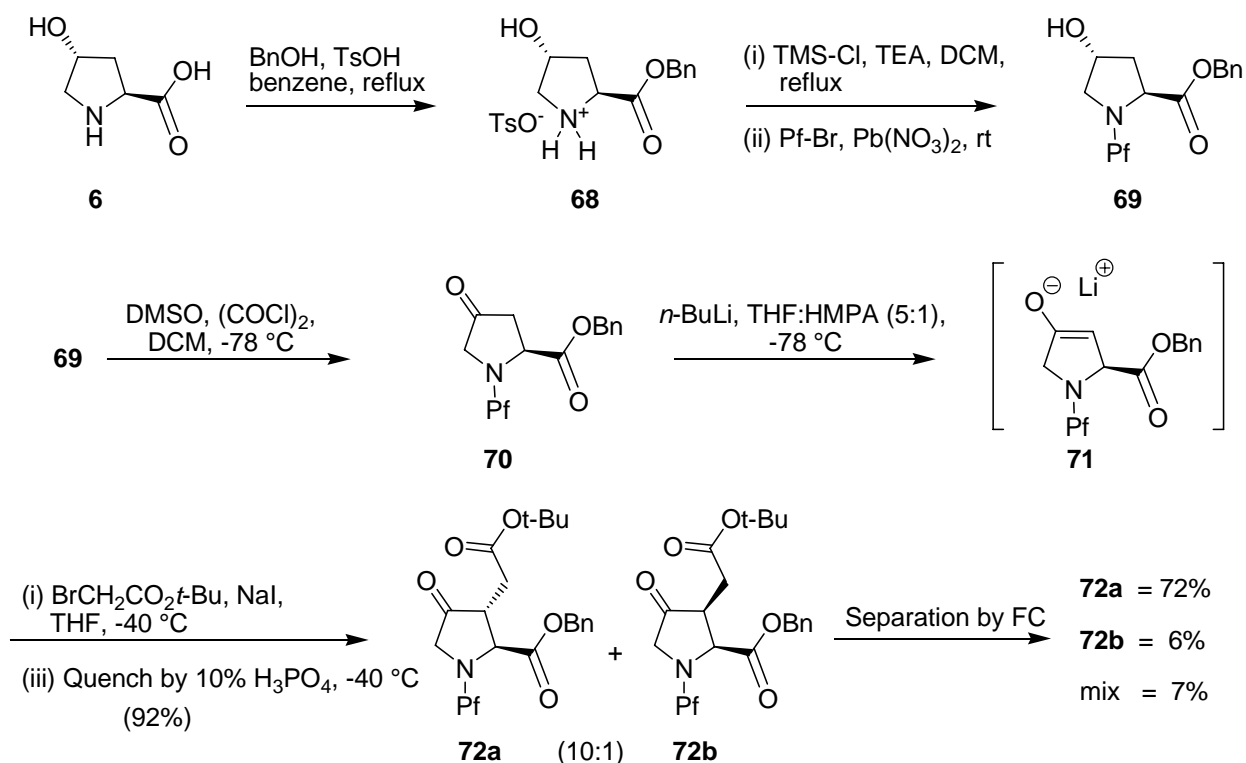
Scheme 15: Synthesis of diastereomeric alkylated ketones **72a** and **72b**

We noted that the diasteromeric ratio was very sensitive to the reaction temperature employed and the order of addition of reactants as observed generally with enolate alkylations. Upon reversing the order of addition i.e. adding the solution of the electrophile at -40 ºC to the preformed enolate at -78 ºC followed by warming the reaction to -40 ºC a ratio of 3:2 for **72a** and **72b** was obtained albeit in lower yields. Moreover, flash chromatography purification of crude product did not result in good separation.

The alkylation of enolate with BrCH$_2$CO$_2$t-Bu at -40 ºC represents a bottleneck in the overall process of synthesizing monomer **67**.We found that the combined yield of **72a** and **72b** decreased significantly when we carried the reaction out on scales larger than 100 mmol and in particular in round-bottomed flasks larger than 100 mL. We believe that this is because of poor temperature control in larger volumes.

4.1.4 Reduction of alkylated ketones with trichloromethylanion

Both diastereomers **72a** and **72b** could lead to useful carboxylate functionalized bis-amino acids with different stereochemistry. Our attempts to use the Bucherer-Bergs reaction[142, 143] reaction to convert alkylated ketones **72a** or **72b** to their corresponding hydantoins failed. However, unalkylated ketone **70** easily reacted under similar reaction conditions to yield corresponding hydantoins. This led us to conclude that the steric hinderance from the alkyl side chain is the reason for this inertness of alkylated ketones toward the Bucherer-Bergs reaction and an alternative method was needed for the installation of the second amino acid functionality.

In 1992 Corey and Link[216] reported a mild protocol for the conversion of a ketone to trichlorocarbinols, that on treatment with a basic solution of azide undergoe a Jocic rearrangement[217] to yield a carboxylic acid. Later Pedregal et al.[218] reported an efficient method for the synthesis of trichlorocarbinols that involved reduction of a ketone with a trichloromethyl anion. This trichloromethyl anion is formed by the reaction of chloroform with LiHMDS in THF at -78 ºC. This methodology has been previously used by us[111] to synthesize quarternary amino acid derivatives.

On reduction with trichloromethyl anion, the major ketone **72a** yielded two diastereomeric products **73a** and **73b** in a ratio of 3:2 as determined by RP-HPLC-MS analysis and 1D proton NMR (Scheme 16). Unfortunately, this mixture of two diastereomeric trichlorocarbinols was very difficult to separate by silica chromotography. We succesfully isolated these trichlorocarbinols **73a** and **73b** by flash chromotography at mg scale to obtain pure analytical samples, but our attempts to isolate two diastereomeric products in useful gram quantities failed repeatedly. This limitation turned our attention towards the minor ketone **72b**.
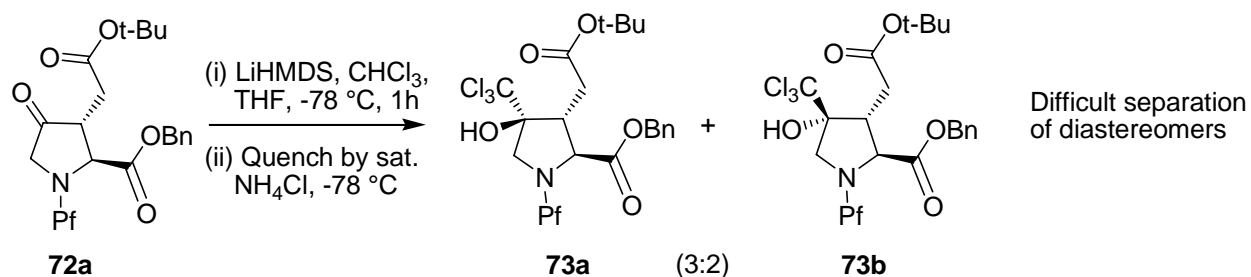
Scheme 16: Reduction of major ketone **72b** with trichloromethyl anion

We hypothesized that because of the relative cis orientation of substituents at C2 and C3, the Re face of the ketone will be highly shielded against approach of an anion towards the trigonal carbon C4 along the Burgi-Denitz trajectory (Figure 34b). The incoming bulky trichloro anion would preferably attack from the Si face which could translate into very high diastereoselectivity. As envisioned, the reaction of ketone **72b** with trichlormethyl anion yielded only the single diasteremer **74** as evidenced by RP-HPLC-MS and 1D proton NMR.
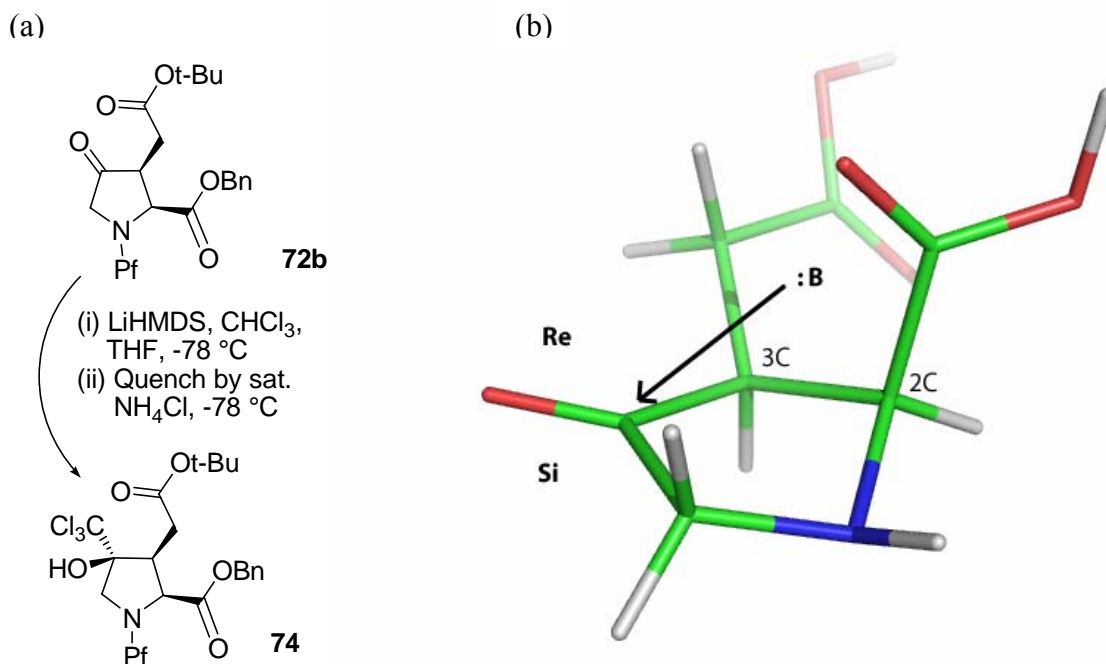
Figure 34: (a) Reduction of minor ketone **72b** with trichloromethyl anion leads to a single product **74**. (b) Incoming anion can add from the Si face only as approach from the Re face (shown by an arrow) is blocked.

4.1.5 Enrichment of minor alkylated ketone

As described earlier, the alkylation of ketone **70** yields ketone **72b** only as a minor diastereomer. We explored a deprotonation-protonation protocol for reversing the stereochemistry of an alkylated ketone previously developed by Sardina et al.[215] This involved the treatment of an alkylated ketone with n-BuLi at -78 °C followed by quenching with acetic acid. This method was very effective but only at mg scale. Upon scaling up to gram scale, it resulted in poor yields as a significant amount of the alkylated ketone **72a** was being converted to an unknown side product. We attributed this to the high strength of n-BuLi base that could wreak havoc if the reaction

mixture warms above -78 ºC because of the poor temperature control as is generally the case with large scale reactions. We searched for a milder organolithium base for deprotonation that has the capacity to deprotonate the alkylated ketone but is mild enough to tolerate slight variation in temperature. We found that the combination of LiHMDS for deprotonation and saturated NH$_4$Cl solution for quenching worked best.

To increase the amount of ketone intermediate **72b** that we could produce, we carried out a controlled epimerization at carbon 3 by treating the 10:1 mixture of **72a** and **72b** with lithium bis(trimethylsilyl)amide (LiHMDS) at -78 ºC for 1 h followed by quenching by rapidly adding saturated ammonium chloride to the reaction mixture at -78 ºC. The resulting diastereomeric mixture had a more useful ratio of **72a** and **72b** of 1:2. The two diastereomers were then separated by silica gel chromatography.

We believe that this poor stereoselectively of the enolate protonation process was due to the small size of incoming electrophile that was proton. Because of its small size, incoming proton does not see much steric interaction from either of the faces. This was in contrast to initial alkylation by BrCH$_2$CO$_2$*t*-Bu, a bulky nucleophile, which proceeded with high stereoselectivity.
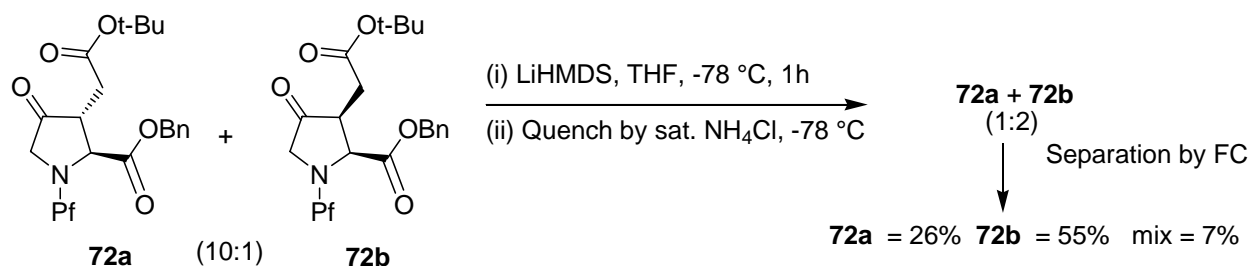
Scheme 17: Deprotonation-protonation protocol for the enrichment of minor ketone **72b**

Toward the synthesis of carboxyl functionalized bis-amino acid **67** we converted the ketone **72b** to a protected amino ester. We achieved this by reducing the ketone **72b** to trichloromethylcarbinol **74**. In Pedregal et al.'s procedure,[218] LiHMDS was added to a precooled solution of the ketone and chloroform in THF. The base that is being added to chloroform in the presence of a ketone, has two chemical species to react with (Scheme 18). It can either deprotonate chloroform or deprotonate at C3 on the alkylated ketone **72b** to give enolate **75**. The fraction of the ketone that is converted to an enolate cannot be reduced with trichloromethyl anion and upon quenching gives rise to both diasteromeric ketones **72a** and **72b** thus reducing the recovered yield of the desired trichlorocarbinol **74**. This was supported by the observation that the addition of more LiHMDS after the reaction had stopped (as observed by HPLC) did not result in more product. One way to avoid this competitive deprotonation would have been to preform the trichlomethyl anion and add the ketone to this solution. Indeed, we saw no epimerization at C3 indicating no enolization occurred, but yields could not be improved beyond 20% even though 5 fold initial excess of anion was used. We concluded that the trichloromethyl anion is very unstable and needs to react with ketone immediately upon its formation.
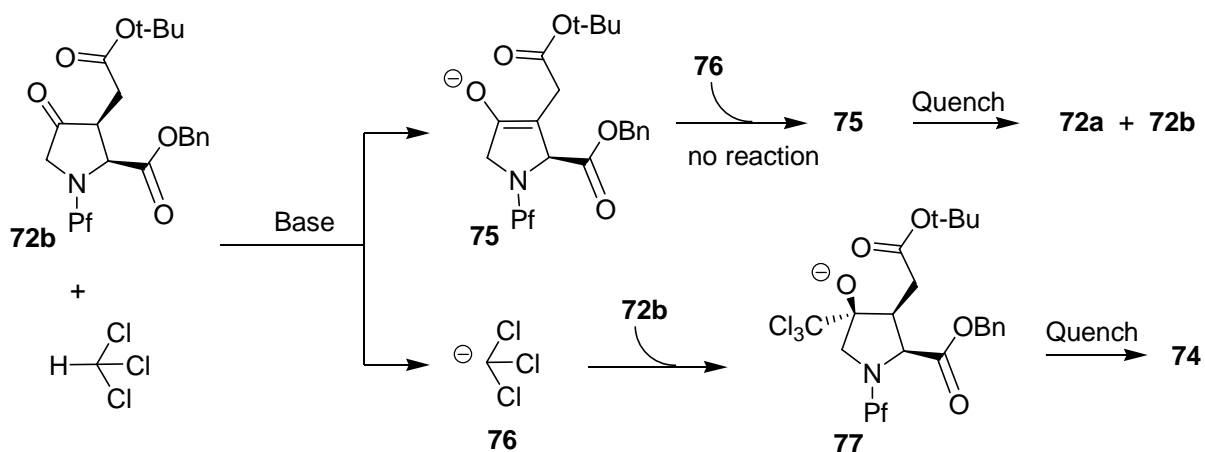
Scheme 18: Two reaction pathways during the reduction of alkylated ketone **72b** by trichloromethyl anion and their end products

We optimized the reaction conditions and found that the best yields are obtained by a slow addition of 2 equiv of LiHMDS solution to a precooled solution of alkylated ketone in a 1:2 mixtures of chloroform and THF. We also determined that the reaction stops after first few minutes by that time most of the ketone has been reduced to trichlorocarbinol. Unreacted ketone was easily recovered by silica gel column chromatography. Alternatively, the crude product was taken to the next step without any interference from unreacted ketones.

4.1.6 Synthesis of the amino acid intermediate 79
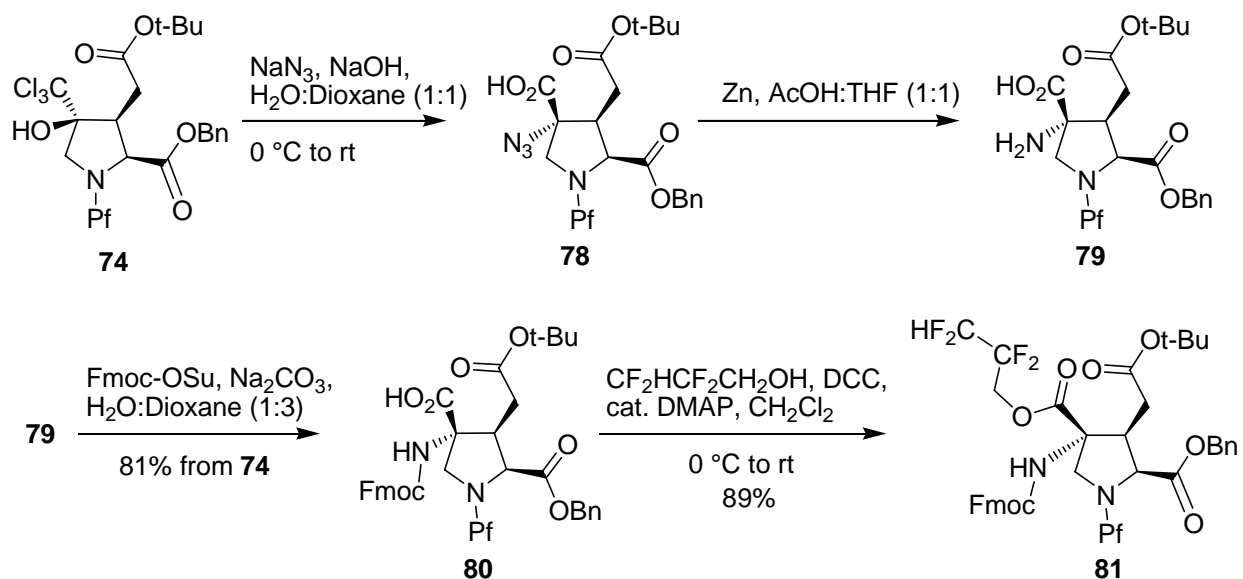
Scheme 19: Synthesis of a fully protected ester intermediate **81**

Upon treatment with a basic aqueous solution of sodium azide, the trichlorocarbinol **74** underwent a Jocic rearrangement to yield azido acid **78** with an inversion of configuration. The best results were obtained when an ice-cooled solution of sodium azide and sodium hydroxide was added to an ice-cooled solution of trichlorocarbinol in dioxane. If any of the two solutions were added at room temperature, an undesired hydroxyacid **82** was formed in varying amounts

113

(Scheme 18). Also, an excess of sodium azide and sodium hydroxide (5 equiv each) was required to ensure that the reaction is complete within a day and has no side products. We couldn't use strong mineral acids e.g. HCl, to quench the reaction as they are incompatible with azides. A simple aqueous workup minus quenching step led to the partition of the product azido-acid **78** into organic as well as into aqueous layer. After experimenting with a series of quenching conditions, we found that upon quenching the reaction mixture with a small volume of saturated NH_4Cl solution, the entire product could be forced into organic layer as desired. The crude product **78** thus obtained could be taken to next step without any complication.
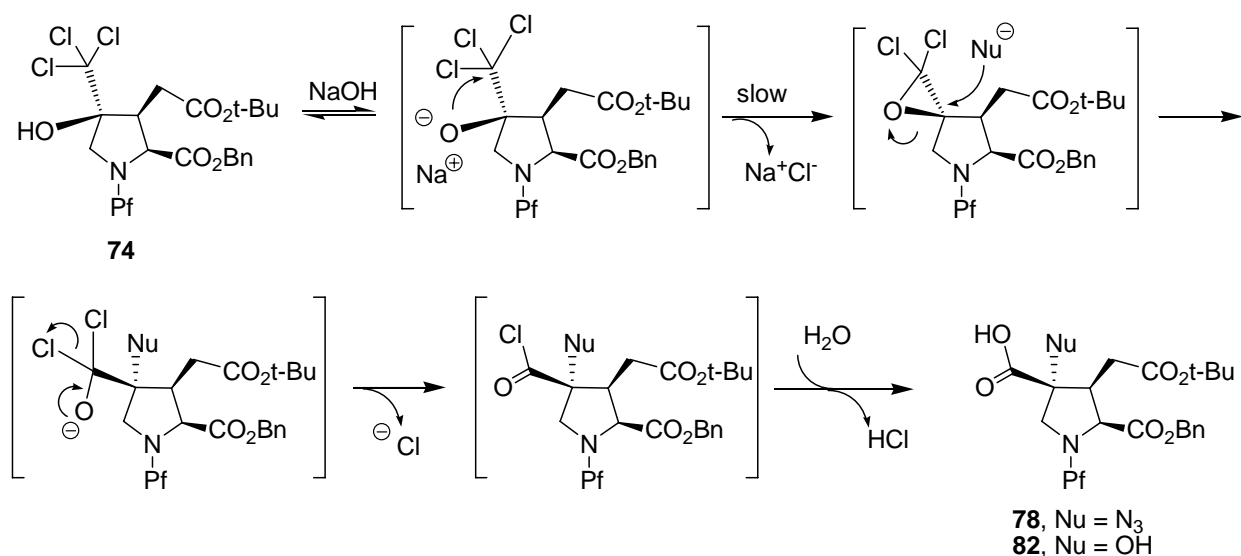
Figure 35: Mechanism of a Jocic Reaction: Formation of azide intermediate **78** and undesired hydroxyl-acid side product **82**

The azide **78** was then reduced to the amine **79** using Zn/AcOH. We determined that to achieve quantitative reduction within a day, 20-30 wt% (with respect to **78**) of Zn was optimum. When we tried to speed up the reaction by adding more Zn, a significant amount of over-reduced product i.e. complete removal of azide was observed. In one such optimization experiment where

we used 45 wt% of Zn, the reaction was complete within 1.5 h. However, 23% of the azide **78** was lost as over-reduced undesired product (as determined by RP-HPLC). The crude amino-acid product **79** obtained after the removal of acetic acid could be used for next step without any further purification.

4.1.7 Synthesis of fully protected intermediate 81

We protected amine functionality of **79** with 9-fluorenylmethyl *N*-succinimidyl carbonate (Fmoc-Su) to form **80**. It was necessary to keep the reaction mixture homogenous throughout the course of the reaction by adjusting the ratio of water and dioxane. The Fmoc protected amino acid **80** was purified by silica gel chromatography and a portion was crystallized from hexanes/ethyl acetate. The X-ray determined structure revealed that the stereochemistry was as shown for compound **80** and consistent with our tentative assignment using NMR.
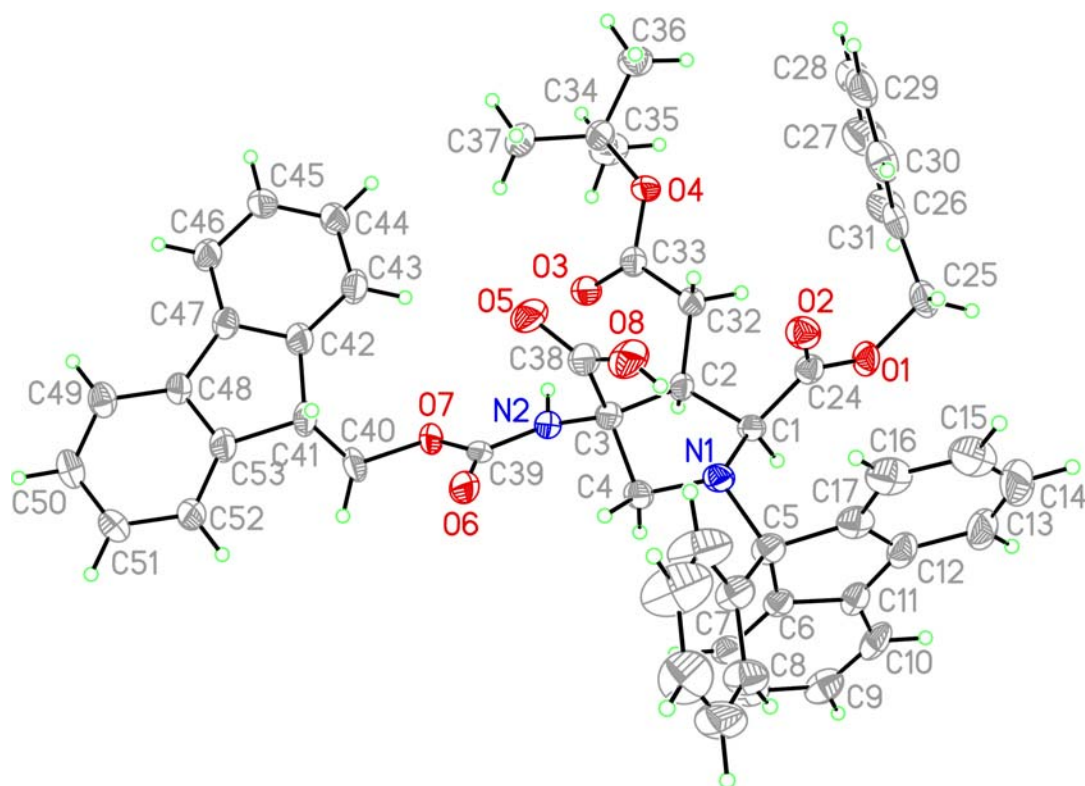
Figure 36: X-ray crystallographic structure of intermediate **80**

Compound **80** was then treated with 1,3-dicyclohexylcarbodiimide (DCC)/4-(dimethylamino)pyridine (DMAP) and 2,2,3,3-tetrafluoropropanol to yield ester **81**. We found that the yield of this reaction was moderately affected by the purity of **80**. When the esterification was performed on crude intermediate **80**, obtained after Fmoc protection step, the reaction was incomplete (~ 14% unreacted **80** as determined by HPLC) and the isolation of the desired product **81** was difficult.

4.1.8 Pf to Boc group exchange

Finally the Pf protecting group was exchanged for a Boc protecting group while simultaneously removing the benzyl protecting group to unmask the carboxylic acid for coupling. Use of *N,N-*

diisopropylethylamine (DIPEA) as an additive in this reaction reduced the reaction time from a week to less than a day. The best result was obtained when the reaction mixture was allowed to equilibrate for 2-3 h before the addition of DIPEA. If DIPEA was added to the reaction mixture at the onset of the reaction with other reagents, a significant amount of a side product (~ 30%) formed. This was a result of an incomplete Boc protection of the secondary amine and could not be converted into monomer **67** without isolating it from the crude product. After final purification we obtained the desired monomer **67** as a white foam in an overall 38% yield from the ketone **72b** (Scheme 20).
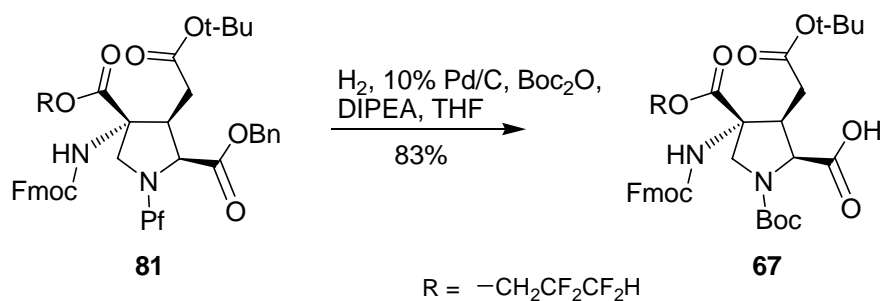
Scheme 20: Conversion of intermediate **81** into the functionalized monomer **67**

Only three purification columns are required through the synthesis from ketone **70.** The synthesis we describe is well optimized and highly reproducible for the scale of 850 mg of monomer **67**. All the reactions have been well optimized and are individually scalable to multigram synthesis. The synthesis of **67** identified that the enolate alkylation (to form **72a** and **72b)** alongwith the subsequent purification, and the trichloromethyl anion reduction (to form **74)** are potential bottlenecks.

4.2   SYNTHESIS OF THREE-MER INCORPORATING A PROAC(2S3S4R)

MONOMER

4.2.1   Solid phase assembly of a short oligomer

We incorporated **67** into a heterosequence of three bis-amino acid monomers using solid phase synthesis protocols that we have previously developed for synthesizing bis-peptides.[108, 112] The oligomeric sequence (*L*)Leu-pro4(2S4S)-proAc(2S3S4R)-pro4(2S4S)-(*L*)Tyr was assembled on 2-chlorotritylchloride resin[219] (50 mg scale). The leucine residue was used to enhance the lipophilicity of the oligomer and the tyrosine residue provides a UV-chromophore to facilitate purification and characterization. After the attachment of leucine to the resin, each subsequent residue was activated as the 1-hydroxy-7-azabenzotriazole (-OAt) ester[149] for coupling to the growing oligomer on solid support. Quantitative coupling of the first pro4(2S4S) monomer was achieved through double coupling of 2 equiv with respect to the resin loading. The next coupling of proAc(2S3S4R) to the pro4(2S4S) monomer proved to be difficult. After screening a range of coupling methods and reagents we concluded that our general coupling method that involves activating monomer as the -OAt ester gives the best results (up to 45% after double coupling with 3 equiv for 4 h). This may be due to the additional hindrance of the *t*-Bu protected acetyl side chain. Recently, our group has reported acyl transfer based coupling methodology for the coupling of sterically hindered amino acids that could be utilized to overcome this problem.[220]

The subsequent coupling of pro4(2S4S) monomer to proAc(2S3S4R) monomer was quanititaive. After coupling tyrosine and removal of the terminal Fmoc group, the oligomer was cleaved from the resin with trifluoroacetic acid (TFA)/CH_2Cl_2. After removal of TFA, the oligomer **83** was lypholized to remove any traces of TFA (Scheme 21).
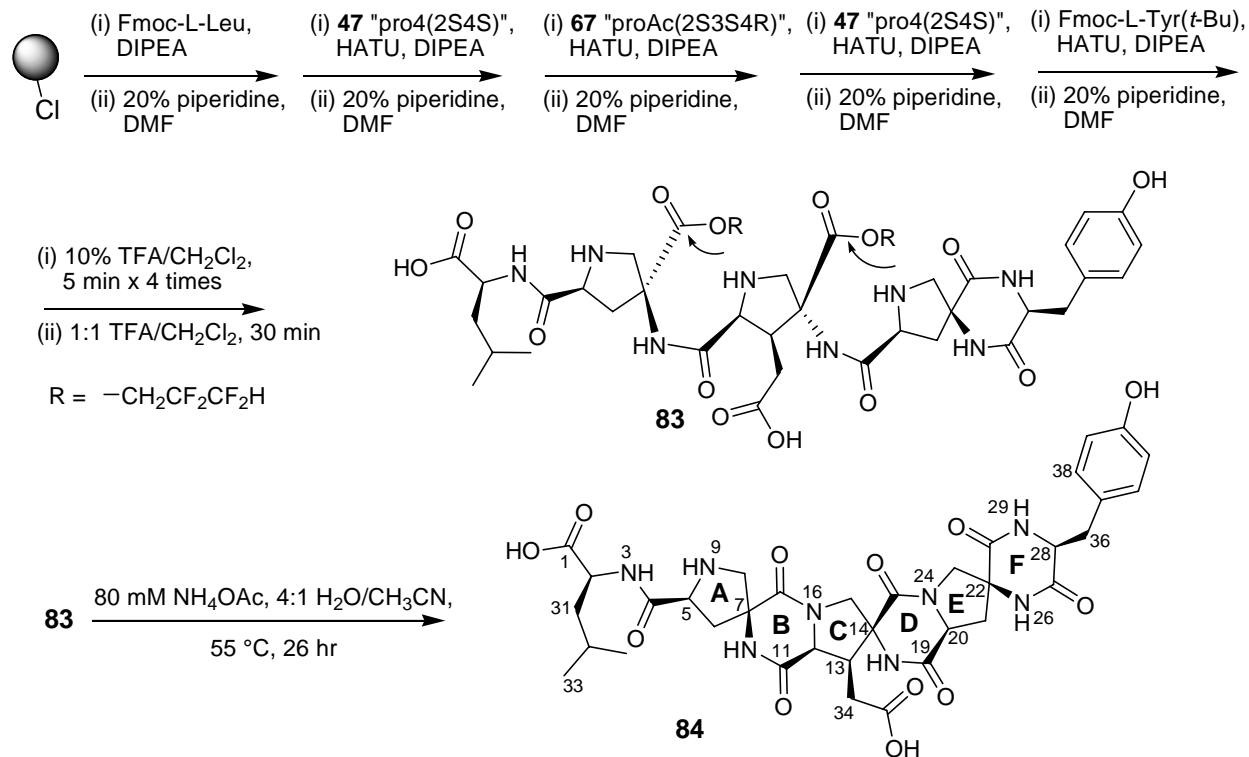
Scheme 21: Solid phase assembly of a short oligomer **84** with proAc(2S3S4R) monomer

(The hydrogens on compound **84** are labeled with the number of the heavy atom to which they are attached. The hydrogens of methylenes are labeled "α" if they go into the page and "β" if they come out.)

To form the remaining two diketopiperazine (DKP) rings, **83** was dissolved in an 80 mM solution of ammonium acetate in 20% acetonitrile/water and heated in an oven at 55 °C. The reaction progress was monitored by RP-HPLC-MS. After 26 h, analysis of the reaction mixture revealed a major peak for the desired product **84** and no trace of **83** or any intermediates. The crude oligomer was purified by preparative C$_{18}$ RP-HPLC and after lypholization, **84** was obtained as a white powder that we used for NMR studies and high-resolution mass spectrometry (Scheme 21).
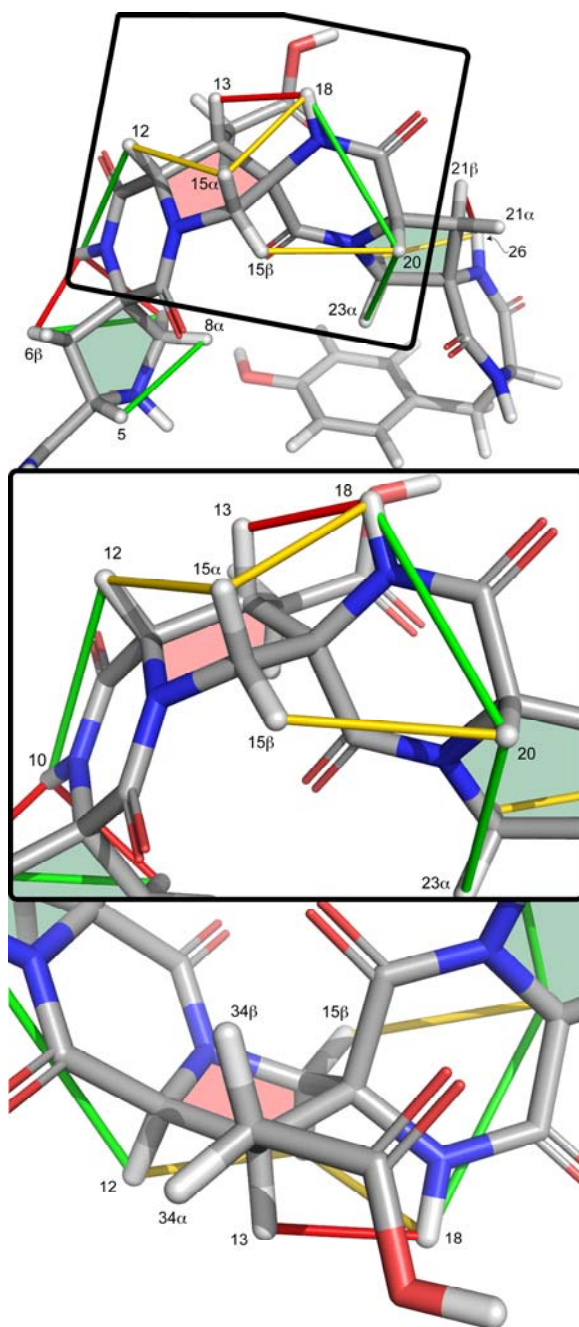
Figure 37: The AMBER94 energy minimized structure of bis-peptide **84** that is most consistent with the superimposed ROESY correlations.

(The sequence is (L)-Leu-pro4(2S4S)-proAc(2S3S4R)-pro4(2S4S)-(L)-Tyr and the pyrrolidine rings are shaded green, red, and green, respectively. The inset figures are a close-up of the second monomer (proAc(2S3S4R), red). The colors of the ROESY correlation lines are color-coded based on their intensity (red = strong, yellow = medium, green = weak).)

4.2.2 Solution phase NMR structure and conformational analysis

For NMR experiments, the oligomer **84** was dissolved in 350 µL dimethyl sulfoxide-d_6 and 5 µL trifluoroacteic acid was added to protonate all basic groups. We carried out a series of two-dimensional NMR experiments (COSY, TOCSY, ROSEY, HMQC, and HMBC) and assigned the hydrogen and carbon chemical shifts using SPARKY.[166] The NMR data confirmed the expected connectivity and stereochemistry.

We carried out a stochastic conformational[144] search in vacuo using the AMBER94[145] force field within the molecular mechanics package MOE.[146] The lowest energy conformation is shown in Figure 37; ROESY correlations between non-*J*-coupled protons are superimposed on the structure sorted by intensity, classified as strong, medium, and weak. The conformational search revealed two closely spaced lowest energy conformers (separated by 0.22 kcal/mol) differing in conformation of the pyrolidine ring A. The ROESY correlations for pyrolidine ring A were consistent with this in that they did not support a single conformation.

In the case of pyrolidine ring C, amide proton H18 shows a strong correlation with H13 but only a medium correlation with H15α. There is a medium intensity correlation between H15α and H12. We also observe a medium strength correlation between H20 and H15β. These correlations are in agreement with the structure shown.

The ROESY correlations of pyrrolidine ring E are consistent with the envelop conformation shown. It is identical with the envelop conformation that we have previously seen for a pro4(2S4S) monomer followed by an (*S*)-tyrosine.[108, 110] The amide proton H26 shows a strong correlation with H21β and a medium correlation with H23β. A weak correlation of H20 with H23α further supports this conformation. We did not observe ROESY correlations between

the tyrosine aromatic hydrogens and H23α and H23β as seen in previous structures;[108, 110] this may be because this structure was determined in DMSO rather than water, which would promote a hydrophobic interaction between the aromatic tyrosine and the methylene 23.
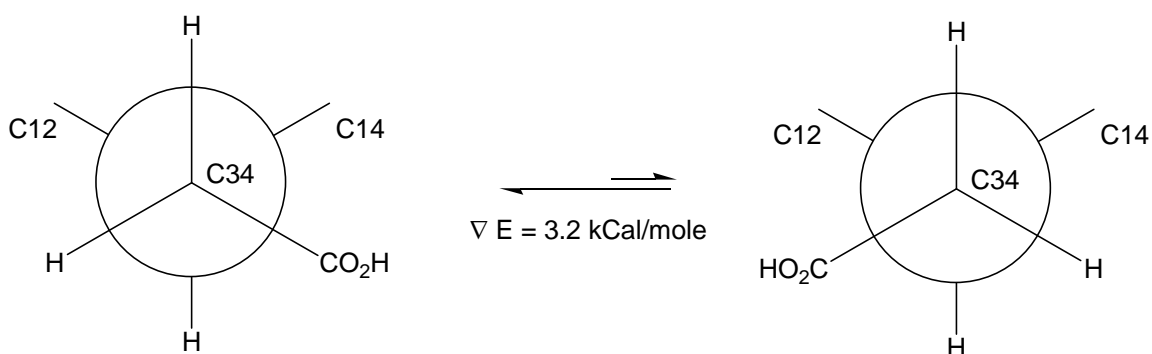
Figure 38: Two probable conformations of the acetyl group that are consistent with ROESY correlations seen for oligomer **84**

The acetyl side chain appears to prefer a single rotamer because we observe a 3 Hz (gauche) and 11.5 Hz (anti) $J_{1,3}$ coupling constant between H13 to H34α and H13 to H34β. We cannot absolutely assign the chemical shift of H34α and H34β and so there are two possible conformations consistent with these chemical shifts. The conformation shown in Figure 37 is the lower energy rotamer by 3.2 kcal/mol.

4.3   CONCLUSION

In conclusion, we have developed a synthesis for a carboxylate functionalized bis-amino acid, proAc(2S3S4R). We demonstrated that it can be incorporated into bis-peptides, determined the structure of a short bis-peptide oligomer that contains it, verified its stereochemical configuration, and determined its conformational preference. The synthesis of this monomer is general and can be used to incorporate other functional groups.

4.4   EXPERIMENTAL METHODS

4.4.1   General methods

All the reagents, including dry solvents, were obtained from various commercial sources and used as such. All the moisture sensitive reactions were carried out in flame-dried or oven-dried glassware under an argon atmosphere unless otherwise noted.

Analytical TLC analysis was performed on silica gel plates (250 μm thickness). Flash chromatography was performed using custom made columns (50 g, I.D. 26 mm or 170g, I.D. 47 mm) packed with 32-63 D (60 Å particle size) grade silica gel on an automated purification system. For difficult separations, oven-dried silica (kept in oven for 2 days at 120-130 °C and immediately used after cooling inside a desiccator) was used as indicated in preparative methods. For a typical purification, the compound was dissolved in a minimum amount of dichloromethane and mixed with celite. Dichloromethane was removed by rotary evaporation. The resulting solid mixture was transferred to a 40 g empty loading column and further dried overnight under reduced pressure to remove any residual solvent. In the case of purifications where multiple columns connected in series were used, CVs are reported with respect to the size of an individual column not the entire series.

NMR experiments were performed on a 500 MHz spectrometer. In the case of oligomer **84**, a special 5 mm Shigemi tube matched for DMSO was used. For all other experiments, standard 5 mm NMR tubes were used. Chemical shifts (δ) are reported in parts per million (ppm) relative to $CDCl_3$, DMSO-d_6 or acetone-d_6 residual solvent peaks. If required, rotational isomers

were resolved by obtaining spectra at 77 °C (350K) in DMSO-d_6. Analysis of 1D NMR spectra was performed using commercially available processing software NUTS. IR spectra were obtained on an FT-IR instrument. Optical rotations were obtained at ambient temperature (26 ± 1 °C).

The elemental composition of purified compounds was confirmed by spectra obtained on a high resolution mass-spectrometer with an electrospray ion source (HRESIQTOFMS). The elemental composition of oligomer **84** was confirmed by spectra obtained on a LTQ Orbitrap – Hybrid FT mass spectrometer (HRLTQ-Orbitrap).

4.4.2   HPLC-MS procedures

HPLC-MS analysis was performed on a C_{18} reverse-phase column (3.5 μm packing, 4.6 mm x 150 mm) coupled to a mass spectrometer (ESI source). Purification by preparative HPLC was carried out on a semiprep C_{18} column (5μm packing, 19 mm x 100 mm). HPLC mobile phase: Solvent A "water (0.1% formic acid)", Solvent B "acetonitrile (0.05% formic acid)". Method 05_95 indicates that a gradient was run with initial composition of solvent A 95% and B 5% to solvent A 5% and B 95% over 30 min. Method 05_100xx indicates that a gradient was run with initial composition of solvent A 95% and B 5% to solvent B 100% over 32 min and solvent B 100% was continued for an additional 8 min. The analytical HPLC-MS was run at a flow rate of 0.8 mL/min while the preparative HPLC was run at 18 mL/min of mobile phase.

4.4.3 Monomer synthesis

(2*S*,3*R*)-Benzyl 3-((tert-butoxycarbonyl)methyl)-4-oxo-1-(9-phenyl-9*H*-fluoren-9-yl)pyrrolidine-2-carboxylate (72a) and (2*S*,3*S*)-Benzyl 3-((tert-butoxycarbonyl)methyl)-4-oxo-1-(9-phenyl-9*H*-fluoren-9-yl)pyrrolidine-2-carboxylate (72b).

The ketone **70** (4.6 g, 10 mmol) was placed in an oven-dried 50-mL round-bottomed flask and dissolved in dry THF (20 mL) under argon. HMPA (4 mL) was added and the solution was cooled to -78 °C in an acetone/dry ice bath. After equilibrating for 15 min, a 1.6 M solution of *n*-BuLi in hexanes (6.3 mL, 1 equiv) was slowly added to the reaction mixture via syringe pump (0.5 mL/min). The stirring was continued for an additional 30 min to ensure the complete conversion of ketone **70** to the corresponding enolate.

In the meantime, a solution of the electrophile was prepared as follows: NaI (0.75 g, 5 mmol, 0.5 equiv) was suspended in dry THF (20 mL) under argon flow in an oven-dried 100-mL round-bottomed flask. *t*-Butyl bromoacetate (4.4 mL, 30 mmol, 3 equiv) was added and the reaction mixture was stirred at rt for 5 min. The resulting milky suspension was further cooled to -40 °C in an acetonitrile/dry ice bath for 15 min.

The preformed enolate (at -78 °C) was transferred to the reaction flask containing the electrophile suspension (at -40 °C) via cannula and the reaction mixture was stirred for an additional 3 hours at -40 °C. The reaction was quenched by a quick addition of 10 % (v/v) phosphoric acid solution (10 mL, at rt) to the reaction mixture at -40 °C. The quenched reaction mixture was allowed to warm to room temperature. The resulting suspension was further diluted with water (50 mL) and extracted with EtOAc (500 mL). The organic layer was washed with 1:1 brine/water (50 mL) followed by brine (25 mL). After drying over anhydrous Na_2SO_4 for 30 min, the organic layer was decanted and concentrated to dryness by rotary evaporation under

reduced pressure. The crude product was purified via automated flash chromatography (2 x 50 g columns connected in series with silica; solvent A: hexanes; solvent B: EtOAc; gradient elution: 0-5 CVs "solvent A 100%" followed by 5-45 CVs "solvent B 0% to 50%"). All the fractions that showed UV absorbance at 301 nm were pooled together and concentrated by rotary evaporation. The resulting oil was further dried under reduced pressure overnight to yield a mixture of diastereomeric products **72a** and **72b** in a ratio of 10:1 (on the basis of 1H NMR spectrum and HPLC chromatogram at 301 nm) as a white foam (5.3 g, 9.2 mmol, 92%).

HPLC-MS. Method: 05_100xx; UV detection at 301 nm; **72a** t_R = 30.9 min, m/z (ion) 596.3 (M + Na$^+$, expected 596.2), **72b** t_R = 31.1 min, m/z (ion) 596.3 (M + Na$^+$, expected 596.2).

A portion of the mixture of compounds **72a** and **72b** (2.1 g, 3.7 mmol) obtained from the purification step above was placed in an oven-dried 50-mL round-bottomed flask and dissolved in dry THF (18 mL) under argon. The solution was cooled to -78 °C in an acetone/dry ice bath. After equilibrating for 15 min, a 1 M solution of LiHMDS in THF (4.4 mL, 1.2 equiv) was slowly added to the reaction mixture via syringe pump (1 mL/min). The stirring was continued for an additional 1 h after which the reaction was quenched by a quick addition of saturated NH$_4$Cl solution (5 mL, at room temperature) to the reaction mixture at -78 °C. The quenched reaction mixture was allowed to warm to room temperature. The resulting suspension was further diluted with water (50 mL) and extracted with EtOAc (250 mL). The organic layer was washed with 1:1 brine/water (50 mL) followed by brine (25 mL). After drying over anhydrous Na$_2$SO$_4$ for 30 min, the organic layer was decanted and concentrated by rotary evaporation under reduced pressure. The resulting oil was further dried under reduced pressure overnight to yield a mixture of diastereomeric products **72a** and **72b** in a ratio of 1:2 (as determined by HPLC chromatogram at 301 nm) as a yellow foam.

HPLC-MS: Method: 05_100xx; UV detection at 301 nm; **72a** t_R = 30.9 min, *m/z* (ion) 596.3 (M + Na$^+$, expected 596.2), **72b** t_R = 31.1 min, *m/z* (ion) 596.3 (M + Na$^+$, expected 596.2).

The crude product was purified by automated flash chromatography (4 x 50 g columns connected in series packed with oven-dried silica; solvent A: hexanes; solvent B: EtOAc; gradient elution: 0-5 CVs "solvent A 100%" followed by 5-75 CVs "solvent B 0% to 40%"). The fractions were analyzed by HPLC. On the basis of the analysis, the relevant fractions were divided into three parts (pure **72a**, pure **72b** and mixture) and pooled together separately. The three pools were concentrated by rotary evaporation and the resulting oils were further dried under reduced pressure overnight to yield pure **72a** (0.54 g, 0.9 mmol, 26%), pure **72b** (1.15 g, 2.0 mmol, 55%), and a mixture of **72a** and **72b** (0.14 g, 0.2 mmol, 7%), all as white foams (overall recovery 88%).

More polar **72a**:

¹H NMR (500.1 MHz, CDCl$_3$): δ 7.66–7.13 (m, 18H), 4.60 (d, *J* = 12.5 Hz, 1H), 4.36 (d, *J* = 12.5 Hz, 1H), 3.82 (d, *J* = 17.6 Hz, 1H), 3.49 (d, *J* = 17.6 Hz, 1H), 3.49 (d, *J* = 5.9 Hz, 1H), 2.82 (m, 1H), 2.40–2.31 (m, 2H), 1.260 (s, 9H). **¹³C NMR** (125.8 MHz, CDCl$_3$): δ 212.0, 172.4, 169.7, 146.1, 144.7, 141.6, 141.1, 140.6, 135.4, 129.0, 128.6, 128.5, 128.2, 128.1, 127.9, 127.9, 127.8, 127.5, 127.1, 126.1, 120.4, 120.1, 81.5, 75.9, 66.4 (CH$_2$), 63.8 (CH), 55.8 (CH$_2$), 49.3 (CH), 34.4 (CH$_2$), 27.9 (CH$_3$, 3C). **IR**(thin film): 3031, 1760, 1717, 1584, 1261, 959, 735. [α]$^{27}_D$ -68.0 (*c* 0.53, CHCl$_3$). **HRMS-ES** (*m/z*): calcd for C$_{37}$H$_{35}$NO$_5$Na$^+$ (M + Na$^+$) 596.2413, found 596.2407.

Less polar **72b**:

¹H NMR (500.1 MHz, CDCl$_3$): δ 7.63 (dd, J = 17.2, 7.5 Hz, 2H), 7.41–7.20 (m, 14H), 7.13 (m, 2H), 4.61 (d, J = 12.4 Hz, 1H), 4.55 (d, J = 12.4 Hz, 1H), 4.07 (d, J = 8.2 Hz, 1H), 3.83 (d, J = 17.8 Hz, 1H), 3.57 (dd, J = 17.8, 1.0 Hz, 1H), 3.05 (dddd, J = 9.1, 8.2, 5.0, 1.0 Hz, 1H), 2.54 (dd, J = 17.6, 5.0 Hz, 1H), 1.81 (dd, J = 17.6, 9.1 Hz, 1H), 1.27 (s, 9H). **¹³C NMR** (125.8 MHz, CDCl$_3$): δ 212.4, 171.3, 170.3, 147.1, 145.6, 141.9, 141.2, 139.9, 135.3, 128.9, 128.7, 128.5, 128.3, 128.2, 127.8, 126.9, 126.8, 125.4, 120.4, 120.3, 81.1, 75.7, 66.2 (CH$_2$), 62.1 (CH), 54.1 (CH$_2$), 48.2 (CH), 31.0 (CH$_2$), 27.9 (CH$_3$, 3C). **IR**(thin film): 3035, 1761, 1717, 1584, 1264, 1164, 959, 737. $[\alpha]^{27}_D$ -110 (c 0.55, CHCl$_3$). **HRMS-ES** (m/z): calcd for C$_{37}$H$_{35}$NO$_5$Na$^+$ (M + Na$^+$) 596.2413, found 596.2397.

(2S,3S,4S)-Benzyl 3-(($tert$-Butoxycarbonyl)methyl)-4-(trichloromethyl)-4-hydroxy-1-(9-phenyl-9H-fluoren-9-yl)pyrrolidine-2-carboxylate (74).

The pure alkylated ketone **72b** (1.06 g, 1.85 mmol) was placed in an oven-dried 50-mL round-bottomed flask and dissolved in dry THF (18.5 mL) under argon. Dry CHCl$_3$ (9.2 mL) was added and the solution was cooled to -78 °C in an acetone/dry ice bath. After equilibrating for 30 minutes, 1M solution of LiHMDS in THF (3.7 mL, 2 equiv) was slowly added to the reaction mixture via syringe pump (0.5 mL/min). The stirring was continued for an additional 2 h after which the reaction was quenched by a quick addition of saturated NH$_4$Cl solution (5 mL, at room temperature) to the reaction mixture at -78 °C. The quenched reaction mixture was allowed to warm to room temperature. The resulting suspension was further diluted with water (20 mL) and extracted with EtOAc (250 mL). The organic layer was washed with 1:1 brine/water (25 mL) followed by brine (25 mL). After drying over anhydrous Na$_2$SO$_4$ for 30 min, the organic layer

was decanted and concentrated to dryness by rotary evaporation under reduced pressure. The crude product was purified by automated flash chromatography (3 x 50 g columns connected in series packed with oven-dried silica; solvent A: hexanes; solvent B: EtOAc; gradient elution: 0-5 CVs "solvent A 100%" followed by 5-75 CVs "solvent B 0% to 40%"). The fractions were analyzed by HPLC. On the basis of the analysis, the relevant fractions were divided into three parts (pure **74**, pure **72b,** and mixture of **74**, **72b** and **72a**) and pooled together separately. The three pools were concentrated by rotary evaporation and the resulting oils were further dried under reduced pressure overnight to yield pure product **74** (0.81 g, 1.17 mmol, 63%), recovered ketone **72b** (0.15 g, 0.26 mmol, 14%), and the mixture of **74**, **72b**, and isomerized ketone **72a** **(**0.17 g, ~15%), all as white foams (overall recovery ~92%). The stereochemistry for **74** was back-assigned after the determination of the stereochemistry at the quaternary center of intermediate **80** by X-ray crystallography.

HPLC-MS: Method: 05_100xx; UV detection at 301 nm; **74** t_R = 32.8 min, m/z (ion) 692.2 (100%), 694.2 (95.9%) (M + H$^+$ expected 692.2 and 694.2, characteristic for the –CCl$_3$ group).

^{1}H NMR (500.1 MHz, CDCl$_3$): δ 7.62 (dd, J = 7.0, 7.0 Hz, 2H), 7.52–7.18 (m, 14H), 7.09 (m, 2H), 5.31 (s, 1H), 4.78 (d, J = 12.4 Hz, 1H), 4.51 (d, J = 12.4 Hz, 1H), 3.83 (d, J = 9.4 Hz, 1H), 3.81 (d, J = 10.5 Hz, 1H), 3.62 (d, J = 10.5 Hz, 1H), 3.34 (ddd, J = 9.4, 8.2, 5.0, Hz, 1H), 2.89 (dd, J = 18.0, 5.0 Hz, 1H), 1.91 (dd, J = 18.0, 9.1 Hz, 1H), 1.16 (s, 9H). **^{13}C NMR** (125.8 MHz, CDCl$_3$): δ 176.1, 170.1, 146.3, 146.1, 141.5, 140.6, 140.3, 134.5, 128.9, 128.9, 128.6, 128.6, 128.5, 128.4, 128.3, 128.2, 127.8, 127.6, 127.2, 127.0, 125.9, 120.4, 120.2, 103.1, 88.2, 80.9, 75.5, 67.3 (CH$_2$), 65.2 (CH), 59.5 (CH$_2$), 42.8 (CH), 31.8 (CH$_2$), 27.8 (CH$_3$, 3C). **IR**(thin film): 3391, 3062, 2976, 2936, 2877, 1727, 1451, 1368, 1257, 1156, 1065, 909, 794, 735. $[\alpha]^{27}_D$ -97.3

(*c* 0.42, CHCl₃). **HRMS-ES** (*m/z*): calcd for $C_{38}H_{36}Cl_3NO_5Na^+$ (M + Na⁺) 714.1557, found 714.1564.

(2*S*,3*S*,4*R*)-2-((Benzyloxy)carbonyl)-3-((*tert*-butoxycarbonyl)methyl)-4-azido-1-(9-phenyl-9*H*-fluoren-9-yl)pyrrolidine-4-carboxylic Acid (78).

The pure intermediate **74** (0.83 g, 1.2 mmol) was placed in a 50-mL round-bottomed flask and dissolved in dioxane (12 mL). The reaction flask was cooled in an ice bath for 2 min and a solution (precooled to 0 °C) of NaN_3 (390 mg, 6 mmol, 5 equiv) and NaOH (240 mg, 6 mmol, 5 equiv) in water was added drop by drop. Additional dioxane (3–4 mL) was added to dissolve any starting material that precipitates out upon addition of aqueous solution. The stirring was continued and the reaction progress was monitored by HPLC: a small volume (5 µL) was withdrawn from the reaction flask, diluted with MeOH (45 µL), and filtered through a Spin-X centrifuge filter. We injected a portion of this solution (5 µL) into HPLC-MS for analysis (method: 05_100xx, UV detection at 301 nm; **78** t_R = 30.4 min, *m/z* (ion) 645.2 and 667.2 (M + H⁺ expected 645.3 and M + Na⁺ expected 667.3), **74** t_R = 32.7 min). After completion (ca. 9 h, as indicated by the absence of the peak corresponding to **74**), the reaction was quenched by the addition of saturated NH_4Cl solution (10 mL). The resulting mixture was further diluted with water (50 mL) and extracted with EtOAc (500 mL). The organic layer was washed with 1:1 brine/water (50 mL) followed by brine (25 mL). After drying over anhydrous Na_2SO_4 for 30 min, the organic layer was decanted and concentrated to dryness by rotary evaporation under reduced pressure. Any residual solvent was removed by drying under reduced pressure to yield crude product **78** as a yellow foam (0.81 g). This crude product was taken to the next step without any further purification. For characterization, the above reaction was repeated at 0.30

mmol scale and the resulting crude product was purified by automated flash chromatography (50 g silica column; solvent A: hexanes with 0.1% AcOH, solvent B: EtOAc with 0.1% AcOH; gradient elution: 0–5 CVs "solvent B 10%" followed by 5–45 CVs "solvent B 10% to 60%"). The desired fractions were pooled together and concentrated by rotary evaporation. To remove residual acetic acid, the purified product was redissolved in EtOAc (200 mL) and washed with water (2 x 20 mL). The organic layer was further washed with brine (20 mL) and after drying over anhydrous sodium sulfate for 20 min, solvent was removed by rotary evaporation under reduced pressure. The resulting oil was further dried under reduced pressure overnight to yield the desired product **78** (172 mg, 0.26 mmol, 87%) as a white foam.

^{1}H NMR (500.1 MHz, CDCl$_3$): δ 7.75 (d, J = 7.6 Hz, 1H), 7.57 (d, J = 7.4 Hz, 1H), 7.50–7.06 (m, 16H), 4.69 (d, J = 12.4 Hz, 1H), 4.49 (d, J = 12.4 Hz, 1H), 3.86 (d, J = 9.6 Hz, 1H), 3.55 (d, J = 10.0 Hz, 1H), 3.22 (d, J = 10.0 Hz, 1H), 2.78 (ddd, J = 10.2, 9.6, 4.0 Hz, 1H), 2.44 (dd, J = 17.5, 4.0 Hz, 1H), 2.16 (dd, J = 17.5, 10.2 Hz, 1H), 1.17 (s, 9H). **^{13}C NMR** (125.8 MHz, CDCl$_3$): δ 173.8, 170.1, 169.7, 145.4, 143.5, 141.6, 140.6, 140.0, 134.5, 129.5, 129.2, 128.9, 128.5, 128.4, 128.3, 128.1, 128.1, 128.0, 127.3, 127.1, 126.9, 120.7, 120.1, 81.5, 76.2, 70.9, 67.5 (CH$_2$), 61.6 (CH), 55.9 (CH$_2$), 46.3 (CH), 32.9 (CH$_2$), 27.8 (CH$_3$, 3C). **IR** (thin film): 3061, 3034, 2978, 2936, 2107, 1730, 1451, 1368, 1255, 1157, 909, 737. $[\alpha]^{27}_D$ +124 (*c* 0.47, CHCl$_3$). **HRMS-ES** (*m/z*): calcd for C$_{38}$H$_{36}$N$_4$O$_6$Na$^+$ (M + Na$^+$) 667.2533, found 667.2458.

(2S,3S,4R)-2-((Benzyloxy)carbonyl)-3-((*tert*-butoxycarbonyl)methyl)-4-amino-1-(9-phenyl-9*H*-fluoren-9-yl)pyrrolidine-4-carboxylic Acid (79).

The crude product **75** obtained in the preceding step (0.81 g, all of it) was transferred to a 50-mL round-bottomed flask and dissolved in dry THF (12 mL). AcOH (12 mL) was added to this

solution followed by 0.16 g of Zn dust (20 wt % of **78**). The reaction mixture was stirred at rt and the reaction progress was monitored by HPLC: a small volume (10 µL) was withdrawn from the reaction flask, diluted with MeOH (250 µL), and filtered through a Spin-X centrifuge filter. We injected a portion of this solution (5 µL) into HPLC for analysis (method: 05_100xx, UV detection at 301 nm; **79** t_R = 20.2 min, m/z (ion) 619.2 and 641.2 (M + H$^+$ expected 619.3 and M + Na$^+$ expected 641.3), **78** t_R = 30.4 min). After completion (ca. 3 hours, as indicated by the absence of a peak corresponding to **78**) the reaction mixture was filtered through a filter paper, using a Buchner funnel under reduced pressure. The residual zinc was washed 2-3 times with a THF/AcOH (1:1) mixture to extract any trapped product. All the filtrates were combined and concentrated by rotary evaporation under reduced pressure. To remove residual acetic acid, the residual solid was dissolved in CH_2Cl_2 (5 mL) and diluted with hexanes (20 mL), then the solvent was removed by rotary evaporation under reduced pressure. This process was repeated one more time to ensure complete removal of acetic acid. The resulting glue-like solid was further dried under reduced pressure overnight to yield crude product **79** as a white foam (0.75 g) that was taken to the next step as such. For characterization, a small part of this crude product **79** (35 mg) was dissolved in 1:1 acetonitrile/water (500 µL) and purified by preparative HPLC (method: 05_95, UV detection at 254 nm, t_R = 18.1 min). The products containing fractions from all three injections were pooled and the solvent was removed by lyophilization to yield pure product **79** as fluffy white powder (ca. 30 mg), which was used for the characterization tests.

^{1}H NMR (500.1 MHz, $(CD_3)_2CO$): δ 7.80-7.15 (m, 18H), 4.61 (d, J = 12.6 Hz, 1H), 4.57 (d, J = 12.6 Hz, 1H), 3.93 (d, J = 10.6 Hz, 1H), 3.74 (d, J = 8.2 Hz, 1H), 3.49 (d, J = 10.6 Hz, 1H), 2.79 (ddd, J = 8.8, 8.2, 6.6 Hz, 1H), 2.59 (dd, J = 18.0, 8.8 Hz, 1H), 2.34 (dd, J = 18.0, 6.6 Hz, 1H), 1.302 (s, 9H). **^{13}C NMR** (125.8 MHz, $(CD_3)_2CO$): δ 206.5, 206.3, 206.2, 206.0, 176.1, 172.4,

171.7, 148.5, 147.9, 144.4, 141.4, 141.1, 137.1, 129.6, 129.3, 129.1, 129.1, 129.1, 128.7, 128.5, 128.2, 128.2, 127.9, 126.8, 121.1, 120.7, 81.0, 76.3, 70.3, 66.4 (CH_2), 64.1 (CH), 60.3 (CH_2), 48.5 (CH), 32.7 (CH_2), 28.2 (CH_3, 3C). **IR** (thin film): 3414, 2978, 1720, 1501, 1256, 1155, 909, 735. $[\alpha]^{27}_D$ +19.6 (c 0.28, $CHCl_3$). **HRMS-ES** (m/z): calcd for $C_{38}H_{39}N_2O_6^+$ (M + H$^+$) 619.2808, found 619.2825.

(2S,3S,4R)-2-((Benzyloxy)carbonyl)-3-((tert-butoxycarbonyl)methyl)-4-((9H-fluoren-9-yl)methoxycarbonylamino)-1-(9-phenyl-9H-fluoren-9-yl)pyrrolidine-4-carboxylic Acid (80).
The crude amino acid **79** obtained in the preceding step (0.71 g) was transferred to a 50-mL round-bottomed flask and dissolved in dioxane (about 12 mL). This was followed by the addition of water (6 mL) and sodium carbonate (0.25 g, 2.4 mmol, 2 equiv assuming 100% conversion in the previous 2 steps). More dioxane (5-6 mL) was added to ensure that any precipitated starting material goes back into the solution. To this reaction mixture was added Fmoc-Su in one portion. At this stage the reaction mixture was inhomogeneous. The reaction progress was monitored by HPLC: a small volume (10 µL) was withdrawn from the reaction flask, diluted with MeOH (200 µL), and filtered through a Spin-X centrifuge filter. We injected a portion of this solution (5 µL) into HPLC for analysis (method: 05_100xx, UV detection at 301 nm; **80** t_R = 32.4 min, m/z (ion) 842.3 (M + H$^+$ expected 842.3), **79** t_R = 22.4 min). After completion (ca. 17 h, as indicated by the absence of a peak corresponding to **79**), the reaction mixture was quenched by the dropwise addition of 2 N HCl solution until the reaction mixture was at pH ~ 4 as monitored by pH paper. The resulting clear solution was extracted with EtOAc (200 mL + 50 mL). The combined organic layer was washed with 1:1 brine/water (50 mL) followed by brine (25 mL). After drying over anhydrous Na_2SO_4 for 30 min, the organic layer was decanted and concentrated by rotary

evaporation under reduced pressure. The crude product was purified by automated flash chromatography (50 g silica column; solvent A: hexanes with 0.1% AcOH, solvent B: EtOAc with 0.1% AcOH; gradient elution: 0-5 CVs "solvent B 10%" followed by 5-55 CVs "solvent B 10% to 60%"). The desired fractions were pooled and concentrated by rotary evaporation. To remove the traces of acetic acid, the residual solid was dissolved in CH_2Cl_2 (5 mL) and diluted with hexanes (20 mL), then the solvent was removed by rotary evaporation under reduced pressure. This process was repeated one more time to ensure the complete removal of acetic acid. The resulting oil was further dried under reduced pressure overnight to yield pure product **80** (0.78 g, 0.93 mmol, 81% over three steps, based on **74**) as a white foam. A portion of this product was then recrystallized from ethyl acetates/hexanes to yield small, colorless granular crystals of **80** which were used for NMR and other analyses. X-ray structure determination of these crystals revealed that the stereochemistry of the intermediate **80** is *S* at position 3 and *R* at position 4 (Figure 36, see APPENDIX for crystallographic data in cif format).

¹H NMR (500.1 MHz, CDCl₃): δ 12.470 (br s, 1H), 7.81 (d, *J* = 7.6 Hz, 1H), 7.73 (d, *J* = 7.3 Hz, 2H), 7.61-7.17 (m, 22H), 7.128 (t, *J* = 7.4 Hz, 1H), 6.938 (s, 1H), 4.78 (d, *J* = 12.0 Hz, 1H), 4.42 (m, 1H), 4.34 (d, *J* = 12.0 Hz, 1H), 4.22 (t, *J* = 7.1 Hz, 1H), 4.16 (d, *J* = 8.8 Hz, 1H), 4.10 (m, 1H), 3.57 (d, *J* = 10.5 Hz, 1H), 3.35 (d, *J* = 10.5 Hz, 1H), 3.09 (m, 1H), 2.11 (dd, *J* = 18.0, 10.5 Hz, 1H), 1.91 (br d, *J* = 17.6 Hz, 1H), 1.331 (s, 9H). **¹³C NMR** (125.8 MHz, CDCl₃): δ 172.0, 171.2, 170.8, 155.8, 145.2, 144.1, 143.9, 142.4, 141.9, 141.3, 139.9, 139.7, 134.6, 129.8, 129.3, 129.1, 129.0, 128.8, 128.7, 128.6, 128.3, 128.0, 127.9, 127.7, 127.7, 127.3, 127.2, 127.1, 126.9, 125.5, 125.3, 120.6, 120.0, 82.2, 76.7, 67.2 (CH₂), 67.1 (CH₂), 65.0, 60.6 (CH), 55.8 (CH₂), 47.1 (CH), 42.2 (CH), 33.3 (CH₂), 27.9 (CH₃, 3C). **IR** (thin film): 3339, 3063, 3034, 2978, 1728,

1503, 1450, 1256, 1156, 1056, 909, 737. $[\alpha]^{27}_D$ +143 (*c* 0.54, CHCl$_3$). **HRMS-ES** (*m/z*): calcd for C$_{53}$H$_{49}$N$_2$O$_8{}^+$ (M + H$^+$) 841.3489, found 841.3497.

(2*S*,3*S*,4*R*)-2-Benzyl 4-(2,2,3,3-tetrafluoropropyl) 3-((tert-butoxycarbonyl)methyl)-4-(9*H*-fluoren-9-yl)methoxycarbonylamino)-1-(9-phenyl-9*H*-fluoren-9-yl)pyrrolidine-2,4-dicarboxylate (81).

To a solution of **80** (0.88 g, 1.05 mmol) in dry CH$_2$Cl$_2$ (21 mL, 20 mL per mmol) in a 50-mL round-bottomed flask was added DMAP (13 mg, 0.1 mmol, 0.1 equiv) and 2,2,3,3-tetraflouropropanol (283 µL, 3.15 mmol, 3 equiv). The resulting solution was cooled in an ice bath under argon. To this cooled solution was added DCC (433 mg, 2.1 mmol, 2 equiv) in one portion. The reaction mixture was allowed to warm to room temperature and the stirring was continued overnight. The reaction progress was monitored by HPLC: a small volume (10 µL) was withdrawn from the reaction flask, diluted with MeOH (200 µL), and filtered through a Spin-X centrifuge filter. We injected a portion of this solution (10 µL) into HPLC for analysis (method: 05_100xx, UV detection at 301 nm; **81** t_R = 34.4 min, **80** t_R = 32.4 min). After completion (ca. 18 h, as indicated by the absence of a peak corresponding to **80**), the reaction was quenched by the addition of acetic acid (200 µL) and concentrated to dryness by rotary evaporation. The residual solid was dissolved in 30% EtOAc/hexanes (100 mL) and filtered through a sintered funnel to remove the dicyclohexylurea byproduct. The filtrate was concentrated by rotary evaporation to yield the crude product **81** as a yellow foam. The crude product was purified by automated flash chromatography (2 x 40 g silica columns connected in series; solvent A: hexanes, solvent B: EtOAc; gradient elution: 0-5 CVs "solvent A 100%" followed by 5-45 CVs "solvent B 0% to 30%"). The desired fractions were pooled and

concentrated by rotary evaporation. The resulting oil was further dried under reduced pressure overnight to yield **81** as a white foam (0.89 g, 0.93 mmol, 89%).

^{1}H NMR (500.1 MHz, CDCl$_3$): δ 7.79 (d, J = 7.6 Hz, 1H), 7.73 (d, J = 7.6 Hz, 2H), 7.64-7.17 (m, 23H), 7.06 (t, J = 7.4 Hz, 1H), 6.16 (br t, J = 52.6 Hz, -CF$_2$CF$_2$H, 1H), 4.81 (d, J = 12.0 Hz, 1H), 4.72-4.64 (m, 1H), 4.59 (d, J = 9.1 Hz, 1H), 4.43 (d, J = 12.0 Hz, 1H), 4.35-4.28 (m, 2H), 4.17-4.12 (m, 2H), 3.12 (d, J = 10.0 Hz, 1H), 3.06 (d, J = 10.0 Hz, 1H), 2.66-2.61 (m, 1H), 2.34 (dd, J = 18.3, 11.4 Hz, 1H), 2.05 (br d, J = 17.5 Hz, 1H), 1.384 (s, 9H). **^{13}C NMR** (125.8 MHz, CDCl$_3$): δ 172.9, 169.6, 156.0, 148.0, 144.1, 143.9, 142.3, 141.4, 141.2, 139.3, 135.2, 129.1, 128.9, 128.8, 128.6, 128.6, 127.9, 127.8, 127.5, 127.3, 127.3, 127.1, 127.1, 125.3, 125.2, 120.4, 120.1, 120.0, 109.0 (tt, ^1J = 249 Hz, ^2J = 33 Hz, CH), 82.4, 76.1, 67.2 (CH$_2$), 66.7 (CH$_2$), 64.2, 61.5 (CH), 60.6 (t, ^2J = 30 Hz, CH$_2$), 56.7 (CH$_2$), 47.1 (CH), 44.6 (CH), 32.4 (CH$_2$), 28.0 (CH3, 3C). **IR** (thin film): 3325, 3061, 3034, 2978, 1741, 1509, 1260, 1164, 909, 737. $[\alpha]^{27}_D$ +123 (*c* 0.37, CHCl$_3$). **HRMS-ES** (*m/z*): calcd for C$_{56}$H$_{50}$F$_4$N$_2$O$_8$Na$^+$ (M + Na$^+$) 977.3401, found 977.3438.

(2S,3S,4R)-4-((2,2,3,3-Tetrafluoropropoxy)carbonyl)-1-(*tert*-butoxycarbonyl)-3-((*tert*-butoxycarbonyl)methyl)-4-(9H-fluoren-9-yl)methoxycarbonylamino)pyrrolidine-2-carboxylic Acid (67).

Ester **81** (1.36 g, 1.42 mmol) was transferred to a 100-mL round-bottomed flask and dissolved in dry THF (28 mL). Solid Boc$_2$O (1.0 g, 4.3 mmol) was added to this solution followed by careful addition of 10 wt % Pd/C (136 mg, 10 wt % of **81**) in one portion. The reaction flask was degassed under reduced pressure and backfilled with H$_2$ gas several times. After 1 h of stirring, a catalytic amount of DIPEA (25 µL, 10 mol% of **81**) was added to speed up the reaction. The

process of degassing and backfilling with H_2 gas was repeated and the stirring was continued overnight. The reaction progress was monitored by HPLC: a small volume (10 µL) was withdrawn from the reaction flask, diluted with MeOH (200 µL) and filtered through a Spin-X centrifuge filter. We injected a portion of this solution (10 µL) into HPLC for analysis (method: 05_100xx, UV detection at 301 nm; **67** t_R = 27.7 min, **81** t_R = 34.4 min). After completion (ca. 23 h, as indicated by the absence of the peaks corresponding to **81** or other intermediates), the reaction mixture was mixed with Celite and the solvent was removed by rotary evaporation under reduced pressure. The resulting solid mixture was transferred to a 40 g empty loading column and further dried overnight under reduced pressure to remove any residual solvent. This was followed by purification by automated flash chromatography (2 x 40 g silica columns connected in series; solvent A: CH_2Cl_2 with 0.1% AcOH, solvent B: 5% MeOH in CH_2Cl_2 with 0.1% AcOH; gradient elution: 0-10 CVs "solvent A 100%" followed by 10-50 CVs "solvent B 0% to 100%"). The desired fractions were pooled and concentrated by rotary evaporation. To remove residual acetic acid, the purified product was dissolved in EtOAc (200 mL) and washed with water (2 x 20 mL). The combined organic layer was further washed with brine (20 mL) and after drying over anhydrous sodium sulfate for 20 min, the solvent was removed by rotary evaporation under reduced pressure. The resulting oil was further dried under reduced pressure overnight to yield **67** as a white foam (0.85 g, 1.17 mmol, 83%).

^{1}H NMR (500.1 MHz, 77 °C $(CD_3)_2SO$): δ 12.32 (br s, 1H) 8.141 (s, 1H), 7.87 (d, J = 7.6 Hz, 2H), 7.67 (d, J = 7.6 Hz, 2H), 7.42 (t, J = 7.6 Hz, 2H), 7.33 (m t, J = 7.6, Hz, 2H), 6.39 (tt, J = 52.2, 5.1 Hz, $-CF_2CF_2H$, 1H), 4.58-4.40 (m, 3H), 4.36-4.30 (m, 2H), 4.21 (t, J = 6.8 Hz, 1H), 4.10 (d, J = 11.5 Hz, 1H), 3.68 (d, J = 11.5 Hz, 1H), 3.24 (m, 1H), 2.52 (dd, J = 17.5, 4.7 Hz, 1H), 2.31 (dd, J = 17.5, 9.6 Hz, 1H), 1.42 (s, 9H), 1.38 (s, 9H). **^{13}C NMR** (125.8 MHz, 20 °C

(CD$_3$)$_2$SO): mixture of rotamers δ 171.1 and 170.6, 169.6 and 169.5, 168.7 and 168.6, 155.8, 153.5 and 152.9, 143.7 and 143.5, 140.7, 127.7, 127.1, 125.1, 120.2, 109.0 (t, J = 249 Hz, CH), 80.4 and 80.3, 79.6, 79.5, 65.9 (CH$_2$), 60.3 and 60.0 (CH), 60.3 (CH$_2$), 53.6 and 53.0 (CH$_2$), 46.5 (CH), 43.5 and 42.8 (CH), 32.2 and 32.1 (CH$_2$), 28.0 and 27.8 (CH$_3$, 3C), 27.7 (CH$_3$, 3C). **IR** (thin film): 3318, 3061, 3034, 2978, 1742, 1519, 1260, 1156, 909, 737. [α]^{27}$_D$ +75.9 (*c* 0.34, CHCl$_3$). **HRMS-ES** (*m/z*): calcd for C$_{35}$H$_{40}$F$_4$N$_2$O$_{10}$Na$^+$ (M + Na$^+$) 747.2517, found 747.2444.

4.4.4   Solid phase synthesis

Solid phase chemistry was performed manually. All solid phase reactions were mixed by bubbling argon through the reaction mixture and stirring with a magnetic stir bar at the same time. All the couplings (except the first coupling to resin) were performed in 0.8 M LiCl in 10% dry dichloroethane (DCE)/dry DMF solution.

General procedure A: Washing

In a typical washing sequence, the resin was washed 3 times with DCM and DMF alternately. This was followed by 3 times washing with DCM and IPA alternately and a final wash with DCM.

General procedure B: HATU coupling

In a 1.5 mL polypropylene micro centrifuge vial the amino acid (as given) was dissolved in a solution of 0.8M LiCl in 10% DCE/ DMF (as given). To this mixture was added DIPEA (as given) followed by HATU (as given). The resulting coupling mixture was mixed briefly and

immediately added to the SPPS reaction vessel carrying the resin. After mixing for the given amount of time, the resin was drained and washed according to the general procedure (A).

General procedure C: Fmoc deprotection

To the SPPS reactor carrying the resin a solution of 20% piperidine in DMF (2000 μL) was added. After 15 min of mixing, a known volume of deprotection mixture (40 μL) was withdrawn and diluted 100 fold with DMF. A UV-visible spectroscopic analysis of the piperidine-fluorenyl adduct was performed and the absorbance at 301 nm (ε = 7800 M^{-1}cm^{-1}) was recorded. This value of the absorbance was used to estimate coupling yield. Following the Fmoc deprotection, the resin was washed according to general procedure (A).

General procedure D: Capping of the residual free amine

To the SPPS reactor carrying the resin a solution of 10% acetic anhydride in pyridine (0.5 mL) was added. After 5 min of mixing, the resin was drained and washed according to the general procedure (A).

Assembly of the oligomer 83

The coupling of leucine to 2-chloro-trityl chloride resin was achieved via a procedure similar to the one described in Novabiochem catalogue (2006/07 section 2.17). The resin (50 mg, 1.1 μmole/g loading) were transferred to a 10 mL polypropylene solid phase peptide synthesis (SPPS) reaction vessel and allowed to swell in DMF for 30 min.

In a 1.5 mL polypropylene micro centrifuge vial N-α-Fmoc-L-leucine (38.9 mg, 110 μmol) was dissolved in DCE (550 μL). To this mixture DIPEA (76.7 μL, 440 μmol) was added

and mixed briefly. The resulting coupling mixture was added to the SPPS reaction vessel carrying the resin. After 2 h of mixing, the solution was drained and the resin was washed according to general procedure (A). The terminal Fmoc group was deblocked by general procedure (C). The resin loading was determined as 22 µmoles and was used for all further calculations of reagents.

Monomer **47**, pro4(2S4S) (26.9 mg, 44 µmol, 2 equivalents) was dissolved in 0.8M LiCl in 10% DCE/ DMF solution (220 µL) and coupled for 2 h according to general procedure (B) by using DIPEA (16.9 µL, 97 µmol) and HATU (16.8 mg, 44 µmol). Any residual free amine was capped according to general procedure (D). The terminal Fmoc group was deblocked by general procedure (C). The coupling yield was estimated as 94%.

Monomer **67**, *proAc(2S3S4R)* (16 mg, 22 µmol, 1 equivalent) was dissolved in 0.8M LiCl in 10% DCE/ DMF solution (110 µL) and coupled for 3 h according to general procedure (B) by using DIPEA (8.5 µL, 48 µmol) and HATU (8.4 mg, 22 µmol). The resin was subjected to a second coupling reaction under identical conditions. Any residual free amine was capped according to general procedure (D). The terminal Fmoc group was deblocked by general procedure (C). The coupling yield was estimated as 32%.

Monomer **47**, pro4(2S4S) (26.9 mg, 44 µmol, 2 equivalents) was dissolved in 0.8M LiCl in 10% DCE/ DMF solution (220 µL) and coupled for 1.5 h according to general procedure (B) by using DIPEA (16.9 µL, 97 µmol) and HATU (16.8 mg, 44 µmol). The resin was subjected to a second coupling reaction under identical conditions. Any residual free amine was capped according to general procedure (D). The terminal Fmoc group was deblocked by general procedure (C). The coupling yield was estimated as 100%.

N-α-Fmoc-O-*tert*-butyl-L-tyrosine (20.3 mg, 44 μmol, 2 equivalents) was dissolved in 0.8M LiCl in 10% DCE/ DMF solution (220 μL) and coupled for 1.5 h according to general procedure (B) by using DIPEA (16.9 μL, 97 μmol) and HATU (16.8 mg, 44 μmol). The resin was subjected to a second coupling reaction under identical conditions. Any residual free amine was capped according to general procedure (D). The terminal Fmoc group was deblocked by general procedure (C). The coupling yield was estimated as 96%. The resin was prepared for cleavage by drying under reduced pressure.

The cleavage of the oligomer from resin was affected by treatment of the resin with 10% TFA/DCM (1 mL) for 5 min. The cleavage solution was collected after filtration and the resin was treated again three more times with TFA solution. All filtered solutions were combined in a flask. Additional TFA (3 mL, so that overall composition is 50% TFA by volume) was added and the solution was stirred at room temperature for 30 additional minutes to ensure the complete removal of the Boc and *t*-butyl groups. After dilution with toluene (10 mL), the solvent was removed *in vacuo*. The residual solid was dissolved in 1:1 acetonitrile/water (2 mL). We injected a portion of this solution (5 μL) into HPLC-MS for analysis (Method: 05_95, UV detection at 274 nm; **83** t_R = 8.58 min, m/z (ion) 1031.2 (M + H$^+$ expected 1031.3). The rest of the solution was lypholized to yield crude product **83** as white fluffy powder.

Rigidification of the oligomer 83

The crude oligomer **83** was dissolved in a 100 mM solution of ammonium acetate (1.6 mL). To help the dissolution, some acetonitrile (0.4 mL) was added so that the final concentration of ammonium acetate was 80 mM. The reaction mixture was incubated inside an oven and stirred at 55 °C. In order to monitor the reaction progress, a small volume (5 μL) was withdrawn from the reaction mixture and injected into HPLC-MS for analysis. After 26 h of stirring the reaction was complete as indicated by the absence of **83** and any other intermediates by HPLC-MS (Method: 00_50, UV detection at 274 nm; **84** t_R = 11.2 min, m/z (ion) 767.2 (M + H$^+$ expected 767.3)).

The desired rigidified oligomer **84** was isolated from the reaction mixture by C$_{18}$ reverse phase preparative HPLC chromatography (Method: 00_50, UV detection at 274 nm; **84** t_R = 9.9 min). The fractions containing the desired peak were analyzed by analytical HPLC. All the pure fractions were combined and lypholized to give the desired rigidified oligomer **84** as white fluffy powder (2 - 3 mg).

To ensure the purity, a small quantity of **84** was dissolved in water and analyzed by analytical HPLC-MS (Method: 00_50, UV detection at 274 nm; **84** t_R = 11.2 min, m/z (ion) 767.2 (M + H$^+$ expected 767.3) (Figure 39). **HRMS (LTQ-Orbitrap)** (m/z): calcd for C$_{35}$H$_{43}$N$_8$O$_{12}$$^+$ (M + H$^+$) 767.2995, found 767.2992.
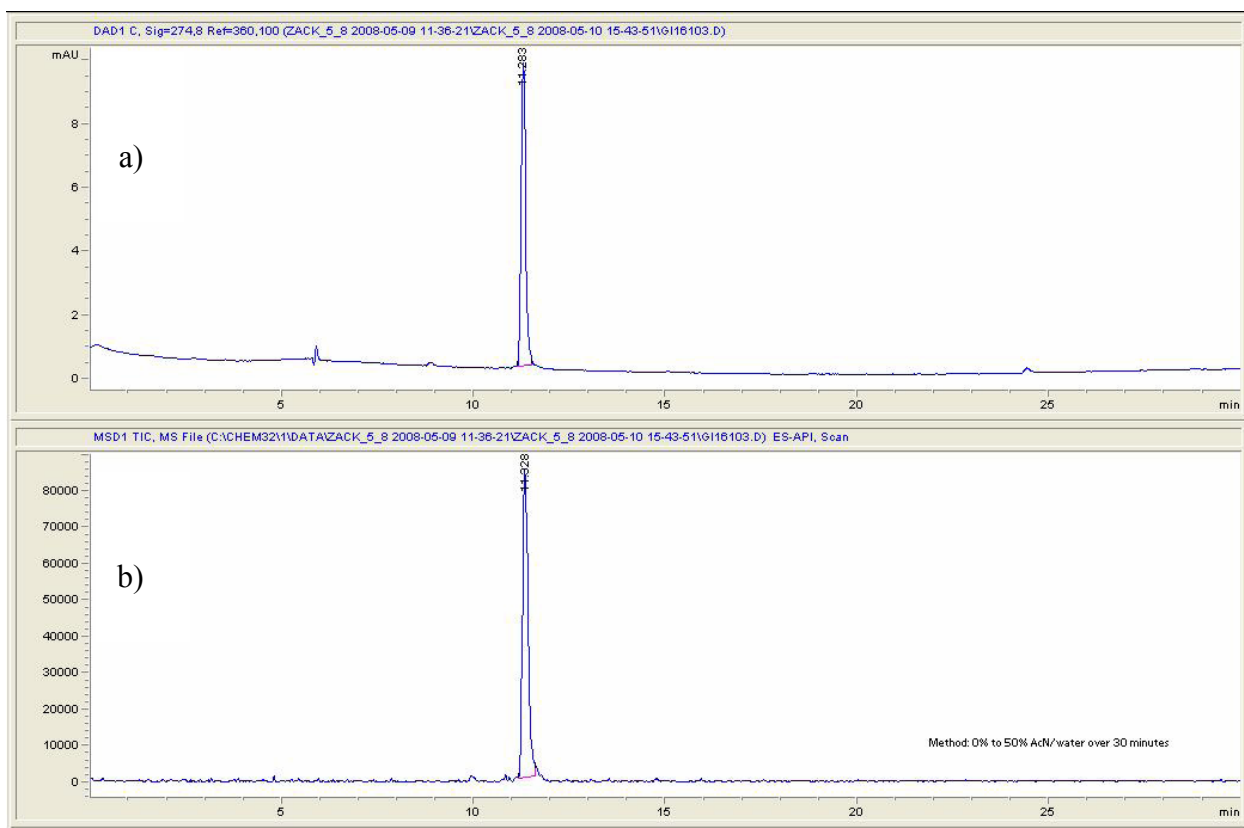
Figure 39: (a) Absorbance (mAU) at 274 nm versus time and (b) corresponding total ion current (TIC) versus time plots from HPLC-MS analysis of purified oligomer **84**.

5.0   FURTHER PROGRESS TOWARDS SYNTHESIS OF FUNCTIONALIZED BIS-
AMINO ACID MONOMER

In chapter 4, we described the synthesis of a functionalized monomer proAc(2S3S4R) from alkylated ketone **72b**. Here, we discuss advances that have been made towards the synthesis of other two stereoisomers, proAc(2S3R4R) and proAc(2S3R4S) that are accessible from alkylated ketone **72a**.

We also report on preliminary experiments towards the synthesis of a functionalized monomer that carries an *N*-methyl imidazolyl side chain. *N*-methyl imidazole (NMI).[221] Small peptides containing *N*-alkyl histidine derivatives are efficient nucleophilic catalysts in enantioselective acylation and phosphorylation reactions.[222] Miller and coworkers[223] have published a comprehensive study where they screened peptide libraries and identified an octapeptide carrying two alkyl imidazole groups that acts as a highly enantioselective acylation catalyst. We believe that we can employ simliar principles of catalytic selectivity and design functionalized bis-peptides that catalyze a variety of chemical reactions. The advantage of bispeptides in studying bifunctional catalysis is that we can alter the distance and relative orientation between functional groups and study the relationship between catalytic function and structure.

Synthetic access to an *N*-methyl imidozolyl carrying monomer will not only add a highly versatile, catalytically useful monomer to our molecular toolkit but also validate the assertion that our synthetic methodology is general.

5.1   SYNTHESIS OF STEREOISOMERS OF PROAC(2S3S4R) MONOMER

5.1.1   Separation of diasteromeric trichlorocarbinols

As illustrated earlier in chapter 4 Scheme 15, ketone **72a** when reduced with trichloromethyl anion yielded a mixture of diastereomeric trichlorocarbinols **73a** and **73b** that were very difficult to separate. To obtain these trichlorocarbinols in useful gram quantities that could be converted to the corresponding monomers, we needed to develop efficient conditions for chromatographic separation.

We attempted several combinations of solvents (e.g. cyclohexanes/EtOAc, hexanes/ether, hexanes/THF) but no separation was observed even after multiple elutions. Hexanes/EtOAc was the only combination that gave any separation of the products upon TLC analysis (minimum 3 elutions are needed). This solvent system was the most economical and convenient as well. We deduced that the most effective and general method will be to improve the separation capacity of silica gel.

When exposed to atmospheric moisture, silica gel gets hydrated and its separation capacity is affected negatively. We hypothesized that if we could re-activate those hydrated sites in silica gel, the separation power could be restored back. To test this, we dried commercially available silica gel in a conventional oven for a given length of time and cooled it in a dessicator

for 2-3 h before loading onto the chromatographic column. We immediately noticed a great improvement in the separation of diasteremoeric trichlorocarbinols. We observed that the best results are obtained for silica gel that has been dried for 2 days in a conventional oven at 130 °C. Further drying does not result in any visible improvement in the separation capacity.

Alkylated ketone **72a** (2.3 g, 4 mmol) was reduced with trichloro anion to yield a mixture of diastereomeric trichlorocarbinols **73a** and **73b** in a ratio of 3:2 as determined by RP-HPLC-MS and NMR. This crude mixture was purified by automated flash chromatography. Four 50g columns connected in series and loaded with pre-dried silica gel were utilized for purification (see experimental section).

We found that upon using dried silica gel, a useful quantity of 1.15 g for **73a** and 0.32 g for **73b** could be recovered. This was in sharp contrast to earlier separation when use of regular silica gel yielded only 22 mg of **73a** and 6 mg of **73b** for a similar scale reaction. This experiment proved that the separation capacity of silica gel can be greatly enhanced by drying. Later we determined that this use of oven dried silica gel improved other difficult separations as well.
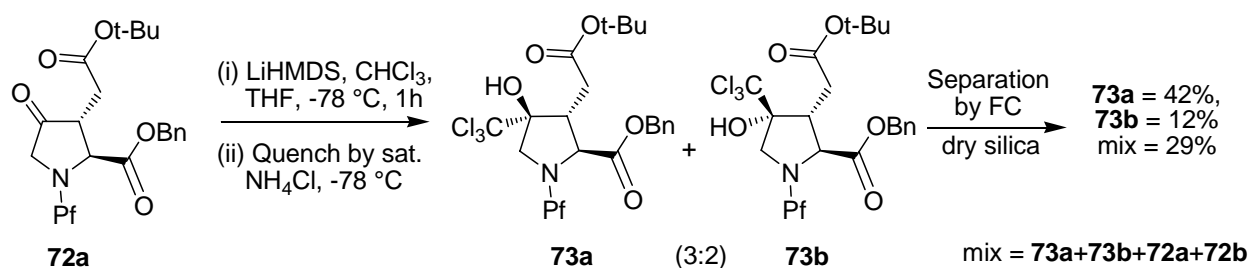
Scheme 22: Use of dry silica gel to improve separation of diasteromeric trichlorocarbinols

5.1.2　Determination of stereochemistry of trichlorocarbinol diastereomers

We used an approach that utilizes the difference in the proximities of the alcoholic –OH to α, β and δ protons of the pyrrolidine ring which is detectable by ROESY or NOESY spectra.[108] This method could not be utilized for the determination of stereochemistry of trichlorocarbinol **74** as only one diastereomer was available. We hypothesized that since ketone **72a** yields both diastereomeric trichlorocarbinols, we could assign stereochemistry based on the differences observed in ROESY spectra.
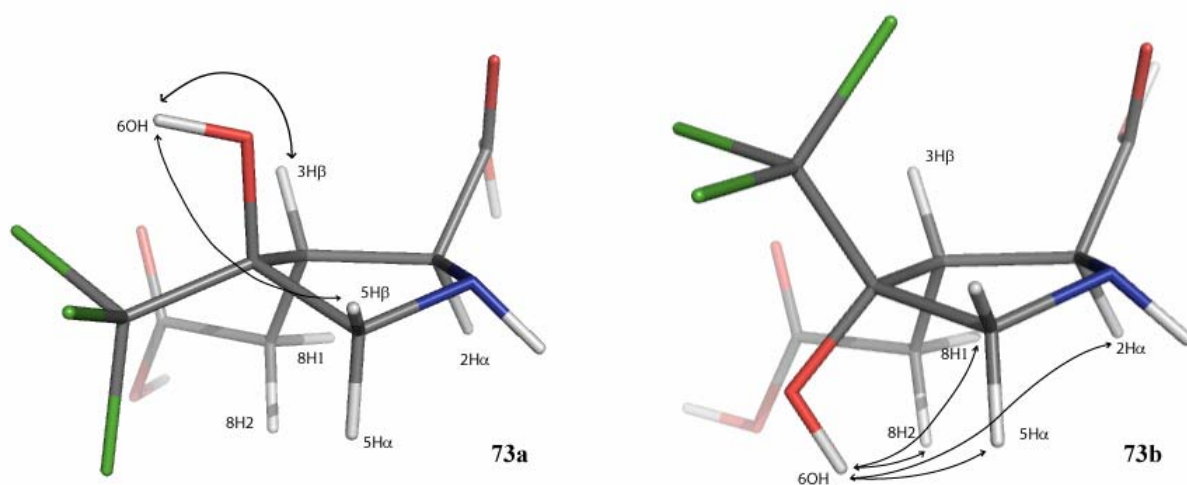
Figure 40: Stereochemistry of tricarbinols **73a** and **73b**: ROESY correlation projected upon corresponding lowest energy conformations as determined by MOE.

2D ROESY spectra were recorded for **73a** and **73b** in CDCl$_3$ at ambient temperature on a 500MHZ NMR instrument. Spectral analysis showed a correlation of alcoholic hydrogen 6OH with 3Hβ and 5Hβ for trichlorocarbinol **73a**. However, for **73b** of the the alcoholic hydrogen 6OH showed a correlation with 5Hα and 2Hα. We also observed correlations of 6OH with side

chain -CH$_2$ hydrogens (8H1 and 8H2). These correlations are justified only if the side chain acyl group, tertiary alcohol and α hydrogen of pyrolidine ring are on the same face for **73b**. Thus we assigned S and R stereochemistry respectively to **73a** and **73b** at quarternary center 4C.

5.1.3   Attempted synthesis of azido-acids

In previous chapter we reported a clean Jocic rearrangement for the trichlorocarbinol **74** that yielded azido acid **78** with an inversion of configuration. We subjected trichlorocarbinol **73a** to the same reaction conditions. To our surprise we received no desired product **85a**. Two major peaks in a ratio of ~5:2 were observed in HPLC chromatogram. The peak at 28.6 min corresponded to hydroxy acid **85b** (m/z = 620 for M + H$^+$) while the peak at 23.5 min indicated hydroxy acid sans t-Bu ester **86b** (m/z = 564 for M + H$^+$ and m/z = 586 for M + Na$^+$).
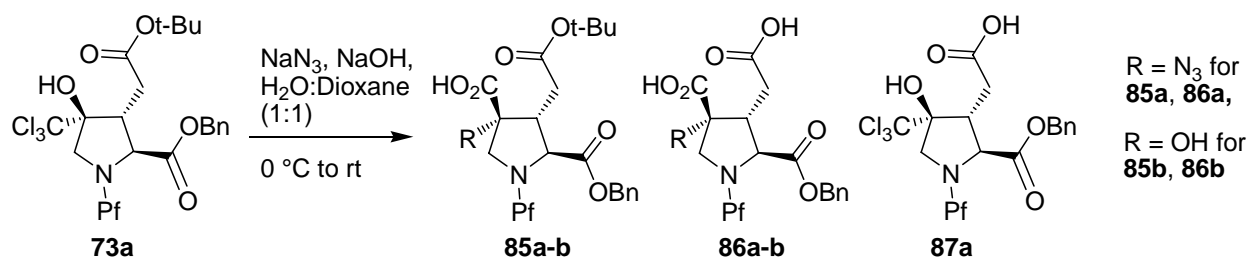
Scheme 23: Products obtained from a Jocic rearrangement on trichlorocarbinol **73a**

We had previously encountered this formation of hydroxy acid side product **82** in the case of the rearrangement of trichlorocarbinol **74** as well but hydrolysis of side chain t-butyl ester was surprising. We tried to change the course of this reaction by decreasing NaOH equivalents from 5 to 2. It slowed down the formation of hydroxyl acid **86a** and subsequent hydrolysis product **86b** significantly but no desired azido-acid **85a** could be produced. Also, we

didn't detect any hydrolyzed trichlorocarbinol **87a** that would have indicated that the hydrolysis of side chain t-butyl group occurs before the rearrangement. Increasing the equivalents of azide from 5 to 8 did not cause any noticeable change in reaction rate.
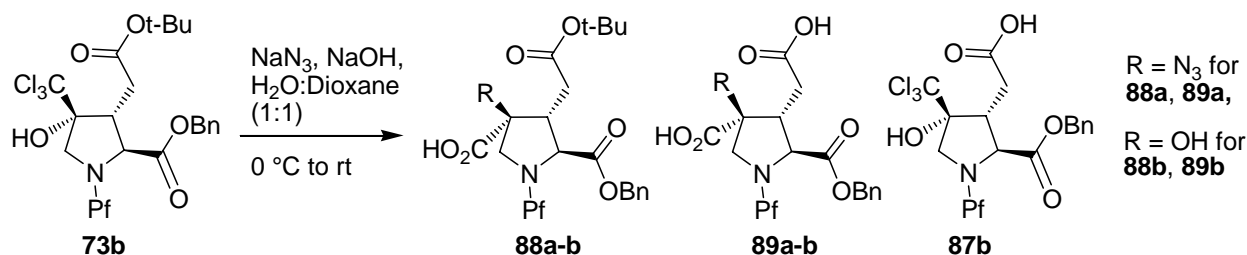
Scheme 24: Products obtained from a Jocic rearrangement on trichlorocarbinol **73b**

Next we performed a Jocic reaction on the minor trichlorocarbinol **73b**. We observed desired azido acid product but the formation of hydroxy acid and the hydrolysis of t-butyl ester was competitive. In one such experiment that was performed at 0.6 mmol scale of **73b** by utilizing a combination of 4 equiv of NaOH and 8 equiv of NaN_3 we found that after 2 days, 4% of **73b** remained unreacted. We detected 7 major peaks of which 6 could be accounted for. The peak at 31 min corresponded to desired product **88a** (30%) while the peak at 28.4 min indicated hydroxyl acid side product **88b** (10%). We also see corresponding hydrolyzed product for trichlorocarbinol **87b** (16%), azido acid **89a** (11%), and hydroxy acid **89b** (13%).

The product distribution observed with three trichlorocarbinols **74**, **73a** and **73b** can be justified based on the relative stereochemistry of the functional groups. We compare hypothetical reaction pathways for Jocic reaction for these stereoisomers in Figure 41. In all three cases overall reaction takes place at the same time scale if similar reaction conditions are utilized. This indicates that the rate determining step i.e. the formation of dichloroepoxides is not influenced by

a change in stereochemistry. This is further supported by the observation that a decrease in NaOH equiv, slows down the reaction but product distribution remains unchanged.
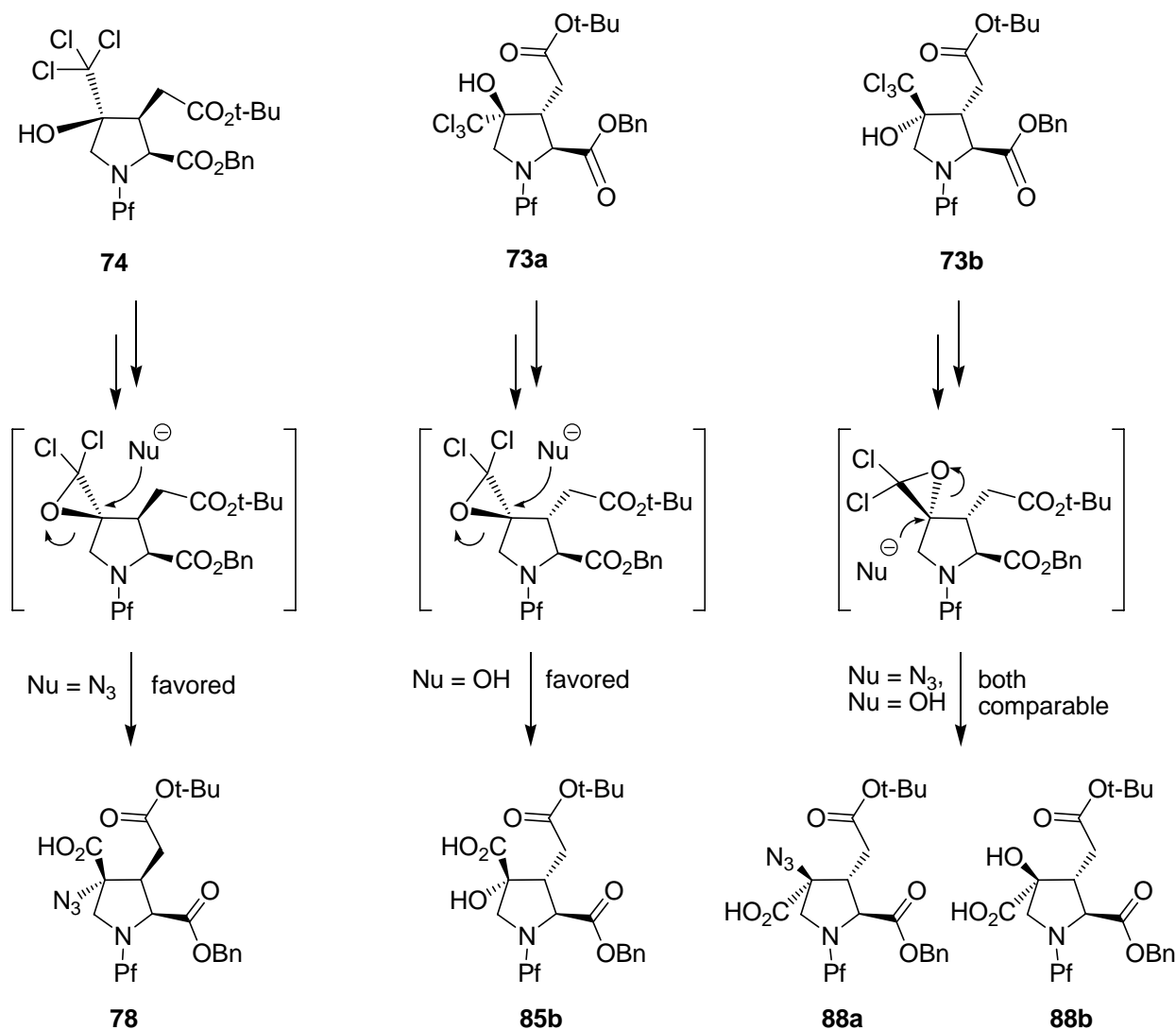
Figure 41: A comparison of pathways that lead to the observed product formations in stereoisomeric trichlorocarbinols

Once dichloroepoxide intermediate is formed the product distribution is governed by the stereochemical factors. In the case of **74** nucleophile attacks from a face that is sterically

unhindered and the desired azido acid is primarily formed. However, for **73a** and **73b** incoming

nucleophile encounters steric hindrance to different extent. In this scenario, a smaller hydroxide

anion becomes a better nucleophile than larger azide anion. For trichlorocarbinol **73a**,

nucleophile sees steric hindrance from neigbouring acetyl side chain that is greater than the steric

hindrance by benzyl ester for trichlorocarbinol **73b**. This translates into a complete formation of

hydroxy acid **85b** from **73a** but only a partial formation of hydroxy acid **88b** from **73b**.

Even though we can rationalize the formation of azido and hyroxy acids in the light of

stereochemical differences, the hydrolysis of t-butyl ester remains perplexing. We do not see any

hydrolysis of trichlorocarbinol **74** or azido acid **78**. In the case of **73a** we observe hydrolysis only

after the hydroxy acid has formed. For **73b** the hydrolysis occurs before the Jocic reaction takes

place. We are unable to explain these observations and a detailed study is needed to completely

understand the true mechanism of various product formations.

We believe that by enhancing the nucleophilicity of azide and/or decreasing the

nucleophilicity of hydroxides we could force the reaction to go on a desired pathway and efforts

are on in this direction.

5.2   SYNTHESIS OF A MONOMER WITH METHYLIMIDAZOLE SIDE CHAIN

Synthesis of a monomer with methylimidazolyl side chain required an electrophile such as 5-

bromomethyl-1-methyl-1 *H*-imidazole **92**. Unlike t-butyl bromoacetate this electrophile needs to

be synthesized. Easiest approach would have been to convert commercially available alcohol **91**

to the corresponding bromide electrophile. However this alcohol is very expensive and since we

needed gram quantities of the electrophile to start this project, we decided to synthesize it from available literature methods.

As shown in Scheme 25 the imidazole alcohol **91** was prepared in 48% yield in two steps from 1, 3-dihydroxyacetone **89** using Collman et. al.'s[224] modification of Rapoport et. al.'s[225] procedure. Next we tried to brominate this alcohol **91** to obtain bromomethyl imidazole **92**. We dissolved the alcohol (obtained in powder form) in a solution of HBr in acetic acid and left it to stir for a couple of days. The reaction mixture was evaporated to dryness by rotary evaporation under reduced pressure leaving behind a red-brown crystalline residue. Unfortunately we were unable to characterize this bromomethyl imidazole **92**. Later, we determined that this bromo derivative was very sensitive to moisture and upon storing decomposed in a few days.
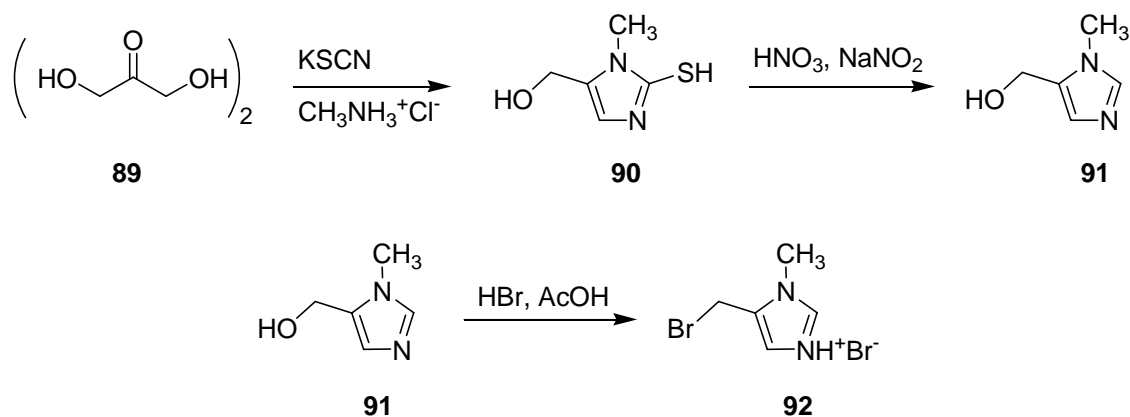
Scheme 25: Synthesis of 5-bromomethyl-1-methyl-1*H*-imidazole electrophile

We hypothesized that the best way to confirm the success of this conversion would be to use this as an electrophile for alkylation of ketone **70** and search for the expected products. The ketone **70** (2.3 g, 5mmol) was treated with *n*-BuLi in THF:HMPA at -78 ºC and the resulting enolate was added to a suspension of crude electrophile **92**, *n*-BuLi (1 equiv) and NaI in THF at -

40 ºC. It was necessary to add n-BuLi to neutralize the HBr salt of the electrophile suspension. We obtained a diastereomeric mixture of ketones **93a** (less polar, t_R = 17.5 min, m/z = 554 for M + H$^+$) and **93b** (more polar, t_R = 17.0 min, m/z = 554 for M + H$^+$) in a 2:1 ratio as determined by RP-HPLC-MS analysis (Figure 44). We also found that the alkylation stalled after 2 h of reaction leaving 34% of ketone **70** unreacted.

We tried to separate two diastereomeric ketones **93a** and **93b** by silica gel FC. Although we could remove unreacted ketone **70** from the crude mixture by using EtOAc/hexanes as eluant, ketones **93a** and **93b** remained inseparable even after repeated attempts. We decided to use this mixture of ketone for next step as such and attempt purification at that stage.

Upon reduction with trichloromethyl anion this mixture of alkylated ketone (**93a** and **93b**) yielded a mixture of diastereomeric trichlorocarbinol. RP-HPLC-MS chromatogram (Figure 45) of the crude reaction mixture showed two nearly overlapping peaks (t_R = 17.9 min and 18.0 min, m/z (ion) 692.2 (100%), 694.2 (95.9%) for M + H$^+$, characteristic for the –CCl$_3$ group). We were able to purify this mixture by silica gel FC by using dichloromethane/MeOH solvent gradient. Although two diastereomers couldn't be separated fully, we were able to obtain a nearly pure sample (78 mg) of trichlorocarbinol **94b** (more polar) as indicated by HPLC-MS (Figure 46).

Next we subjected this trichlorocarbinol **94b** to same sequence of steps that were used for the synthesis of proAc(2S3S4R) monomer from corresponding trichlorocarbinol **74** (Scheme 26). Each reaction was monitored by RP-HPLC-MS and the crude products formed were taken to the next step without any purification.

154
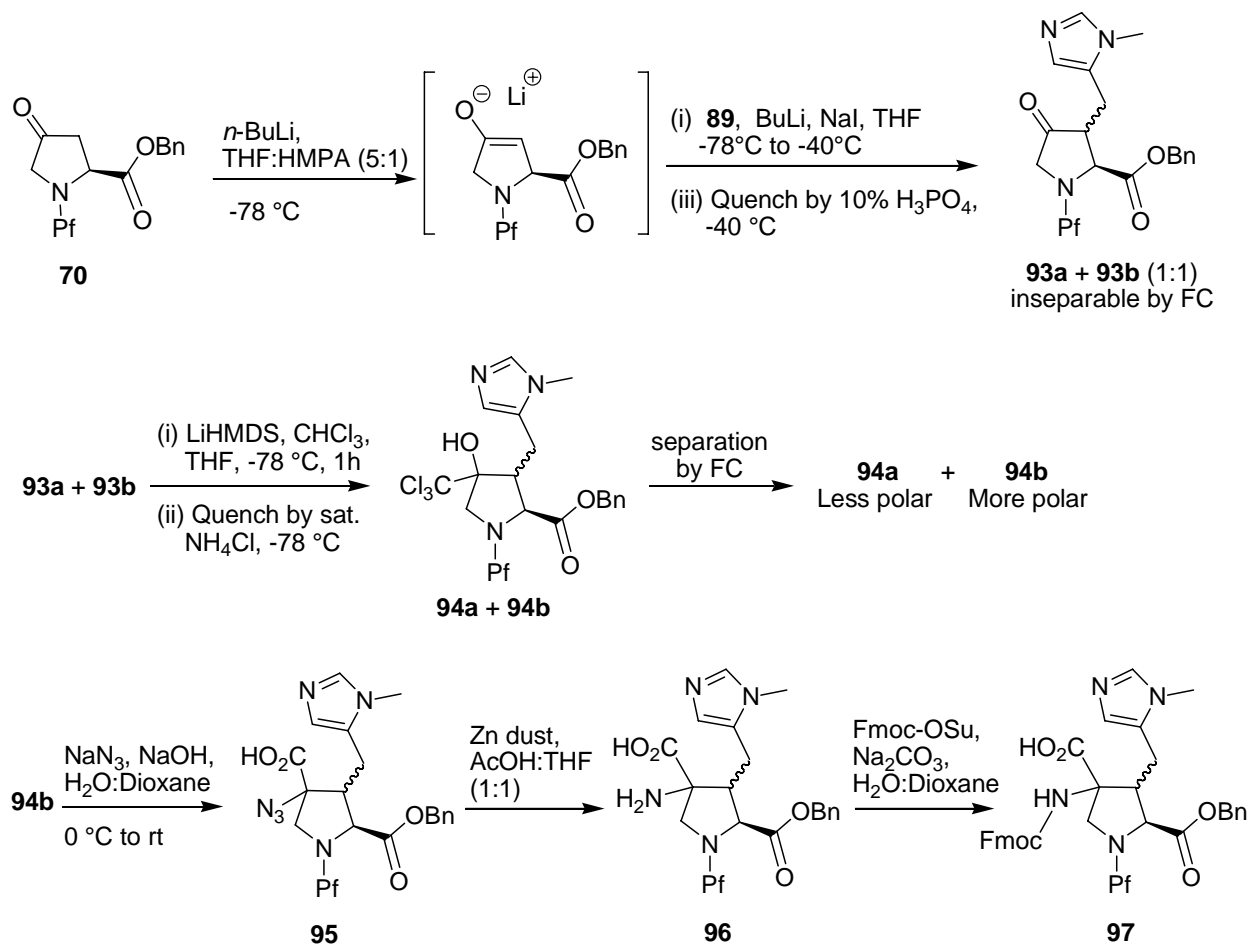
Scheme 26: Synthesis of a methylimidazole functional group bearing bis-amino acid

Trichlorocarbinol **94b** was subjected to Jocic rearrangement reaction conditions that yielded desired azido acid **95** (t_R = 17.7 min, m/z = 625 for M + H$^+$). This azido acid upon reduction with Zn/AcOH gave amino acid **96** (t_R = 13.7 min, m/z = 621 for M + Na$^+$) that was protected with an Fmoc protecting group by Fmoc-OSu to yield the desired protected amino acid **97 (**t_R = 19.3 min, m/z = 821 for M + H$^+$). We could not continue beyond this step as the product **97** was lost during purification.

5.3   CONCLUSION AND FUTURE DIRECTIONS

In this chapter we showed that the development of other stereoisomers of proAc(2S3S4R) was not straightforward. Trichlorocarbinol **73b** gave some azido acid **88a** upon Jocic rearrangement but **73a** yielded hydroxy acid only. We also observed unexpected hydrolysis of side chain t-butyl ester. We are working in the direction of optimizing the formation of azido acids in these cases so that they could be converted to useful monomers.

We also demonstrated a preliminary synthesis of a new monomer that carries a methyl imidazolyl side chain. Although the final monomer could not be obtained we were able to perform all the key steps. We showed that silica gel FC could be used to separate the mixture of trichlorocarbinols **94a** and **94b** and a series of reaction steps can be carried out without any need of purification.

In future we plan to pursue the synthesis of this monomer and other functionalized monomers with various side chains. We will also optimize purification protocol and determine the stereochemistry of trichlorocarbinols **94a** and **94b**. Our group has recently developed a methodology that allows us to incorporate a different functional group on every bis-amino acid monomer within a bis-peptide.[220] We believe that by combining this new approach with the methodology for the synthesis of a functionalized monomer that has been described in chapter 4 and 5, we shall be able to access any desired orientation of functional groups. This will enable us to develop bis-peptides for applications such as multi-functional catalysts, binding and disruption of protein-protein interactions and sophisticated nanodevices.

5.4   EXPRIMENTAL METHODS

For general methods and RP-HPLC-MS methods see chapter 4, experimental section.

5.4.1   Monomer synthesis

(2*S*,3*R*,4*S*)-Benzyl   3-((tert-butoxycarbonyl)methyl)-4-(trichloromethyl)-4-hydroxy-1-(9-phenyl-9H-fluoren-9-yl)pyrrolidine-2-carboxylate (73a) and (2*S*,3*R*,4*R*)-Benzyl 3-((tert-butoxycarbonyl)methyl)-4-(trichloromethyl)-4-hydroxy-1-(9-phenyl-9H-fluoren-9-yl)pyrrolidine-2-carboxylate (73b).

The alkylated ketone **72a** (2.3 g, 4 mmol) was subjected to reduction by trichloromethyl anion as described for the synthesis of trichlorocarbinol **74** from ketone **72b** in the experimental section of chapter 3. The crude product was purified by automated flash chromatography (4 x 50 g columns connected in series packed with oven-dried silica; solvent A: hexanes; solvent B: EtOAc; gradient elution: 0-5 CVs "solvent A 100%" followed by 5-75 CVs "solvent B 0% to 40%"). The fractions were analyzed by HPLC. On the basis of the analysis, the relevant fractions were divided into three parts (pure **73a**, pure **73b** and mixture of **73a**, **73b**, **72a** and **72b**) and pooled together separately. The three pools were concentrated by rotary evaporation and the resulting oils were further dried under reduced pressure overnight to yield pure **73a** (1.15 g, 42%), pure **73b** (0.32 g, 12%), and a mixture (0.69 g) all as white foams.

Less polar **73a**:

HPLC-MS: Method: 05_100xx; UV detection at 301 nm; **73a** t_R = 33.2 min, *m/z* (ion) 692.2 (100%), 694.2 (95.9%) (M + H$^+$ expected 692.2 and 694.2, characteristic for the –CCl$_3$ group).

¹H NMR (500.1 MHz, CDCl₃): δ 7.77 (d, J = 7.3 Hz, 1H), 7.76-7.08 (m, 17H), 6.33 (s, 1H), 4.91 (d, J = 12.3 Hz, 1H), 4.42 (d, J = 12.3 Hz, 1H), 3.77 (d, J = 9.8 Hz, 1H), 3.56 (d, J = 9.8 Hz, 1H), 2.85 (d, J = 2.2 Hz, 1H), 2.73 (br d, J = 12.3 Hz, 1H), 2.64 (dd, J = 15.0, 3.8 Hz, 1H), 1.68 (dd, J = 15.0, 12.3, Hz, 1H), 1.134 (s, 9H). **¹³C NMR** (125.8 MHz, CDCl₃): δ 177.2, 170.0, 147.1, 144.7, 142.0, 140.9, 139.5, 134.8, 129.3, 129.0, 128.8, 128.4, 128.3, 128.2, 128.1, 127.9, 127.6, 127.5, 127.2, 126.5, 120.6, 120.0, 101.4, 87.9, 81.2, 75.9, 67.7 (CH₂), 65.2 (CH), 55.3 (CH₂), 51.0 (CH), 38.0 (CH₂), 27.8 (CH₃, 3C). **IR** (thin film): 3392, 3062, 2978, 2936, 2877, 1725, 1452, 1368, 1256, 1156, 1065, 909, 793, 735. $[\alpha]^{27}_D$ +44.1 (c 0.59, CHCl₃). **HRMS-ES** (m/z): calcd for $C_{38}H_{36}Cl_3NO_5Na^+$ (M + Na⁺) 714.1557, found 714.1542.

More polar **73b**:

HPLC-MS: Method: 05_100xx; UV detection at 301 nm; **73b** t_R = 31.6 min, m/z (ion) 692.2 (100%), 694.2 (95.9%) (M + H⁺ expected 692.2 and 694.2, characteristic for the –CCl₃ group).

¹H NMR (500.1 MHz, CDCl₃): δ 7.66-7.14 (m, 18H), 5.19 (s, 1H), 4.56 (d, J = 12.3 Hz, 1H), 4.28 (d, J = 12.3 Hz, 1H), 4.00 (d, J = 11.5 Hz, 1H), 3.39 (d, J = 8.9 Hz, 1H), 3.27 (m, 1H), 3.17 (d, J = 11.5 Hz, 1H), 2.68 (dd, J = 16.7, 4.4 Hz, 1H), 2.40 (dd, J = 16.7, 5.7 Hz, 1H), 1.23 (s, 9H). **¹³C NMR** (125.8 MHz, CDCl₃): δ 173.1, 172.7, 146.0, 145.6, 142.5, 140.8, 140.6, 135.6, 128.9, 128.7, 128.5, 128.4, 128.2, 128.2, 128.1, 127.8, 127.7, 127.3, 127.2, 126.8, 120.0, 119.9, 105.2, 87.1, 82.5, 76.2, 66.7 (CH), 66.5 (CH₂), 60.4 (CH₂), 45.7 (CH), 33.9 (CH₂), 27.8 (CH₃, 3C). **IR** (thin film): 3391, 3063, 2977, 2936, 2876, 1727, 1451, 1368, 1259, 1156, 1067, 909, 794, 737. $[\alpha]^{27}_D$ -37.8 (c 0.50, CHCl₃). **HRMS-ES** (m/z): calcd for $C_{38}H_{36}Cl_3NO_5Na^+$ (M + Na⁺) 714.1557, found 714.1572.
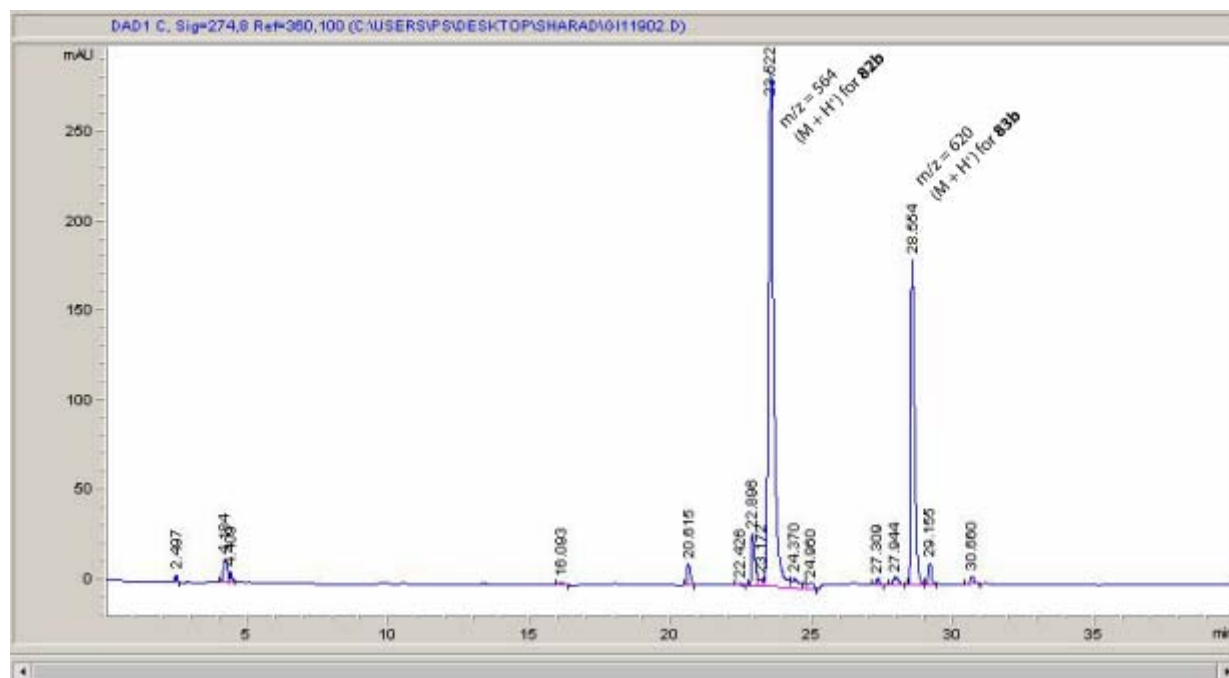
Figure 42: Unpurified RP-HPLC chromatogram at 274 nm for the products obtained after Jocic reaction on **73a**. (Method 05_100xx)
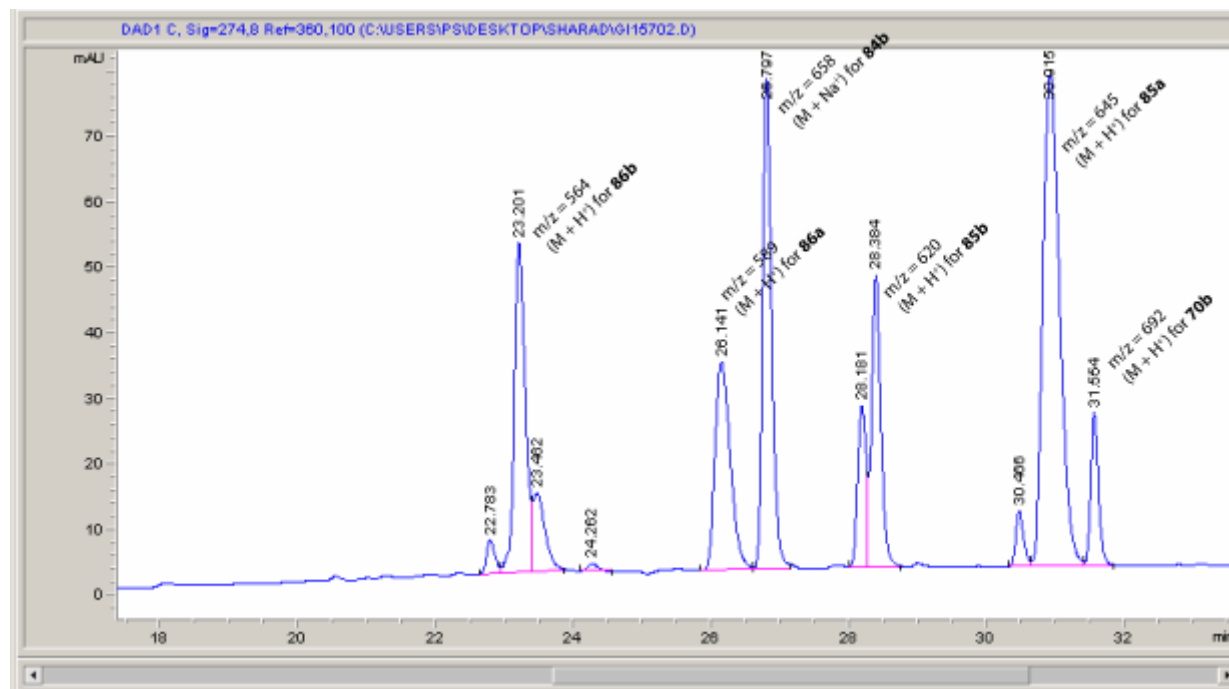
Figure 43: Unpurified RP-HPLC chromatogram at 274 nm for the products obtained after Jocic reaction on **73a**. (Method 05_100xx)

5.4.2 HPLC chromatograms of intermediates toward the synthesis of a monomer with methylimidazole side chain
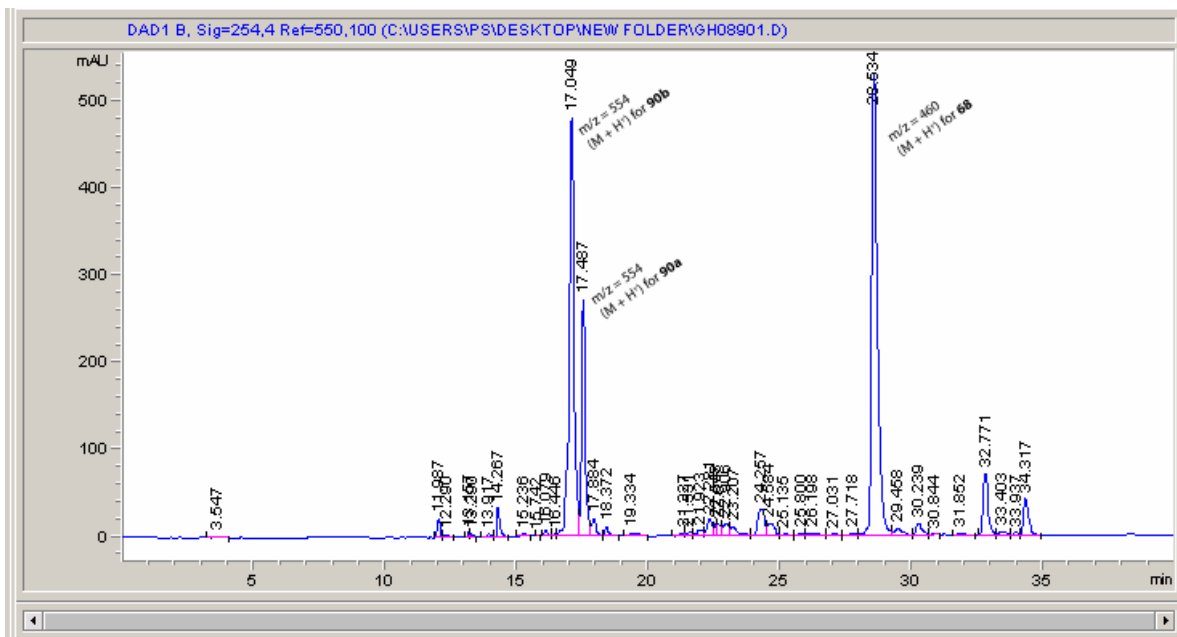
Figure 44: RP-HPLC chromatogram of the crude mixture of products (**93a** + **93b**) obtained after the alkylation of ketone **70** with electrophile **92** at 254 nm. (Method 05_100xx)
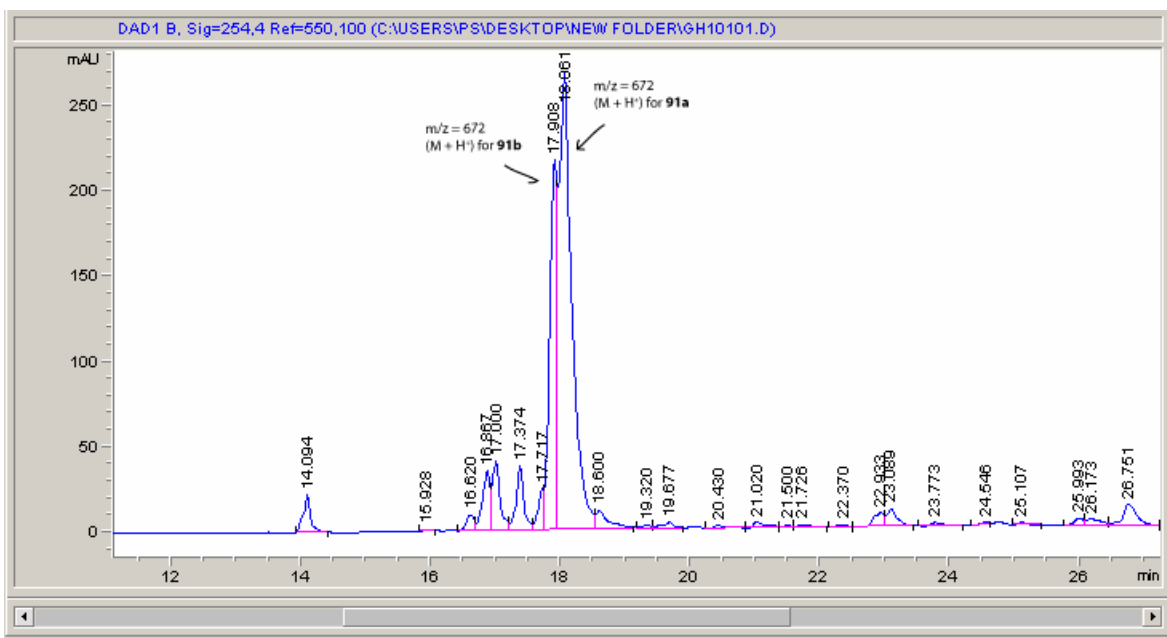
Figure 45: RP-HPLC chromatogram of the crude mixture of products (**94a** + **94b**) obtained after the trichloromethyl anion reduction of mixture of ketones **93a** and **93b** at 254 nm. (Method 05_100xx)
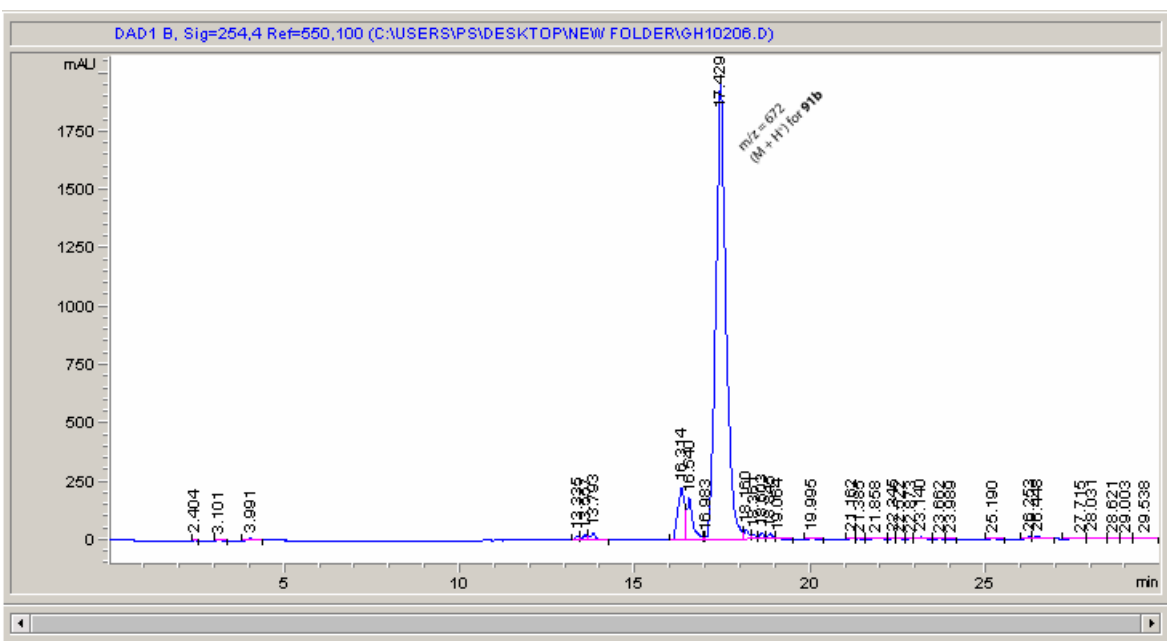
Figure 46: RP-HPLC chromatogram of the pure trichlorocarbinol 9**4b** at 254 nm. (Method 05_95)
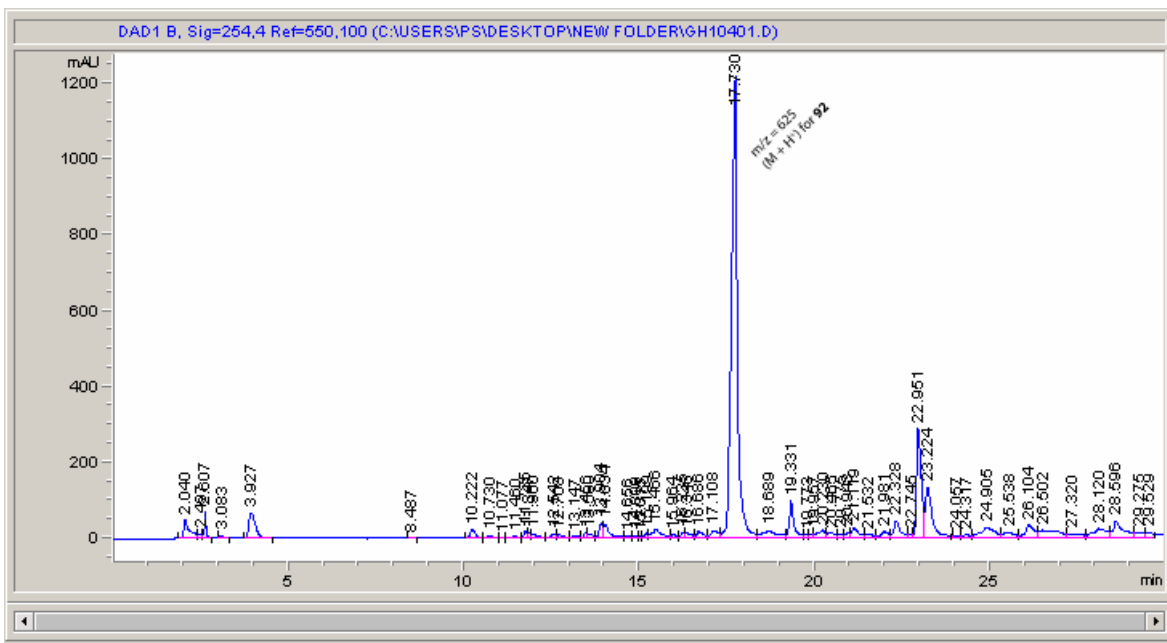
Figure 47: RP-HPLC chromatogram of the unpurified azido acid **95** at 254 nm. (Method 05_95)
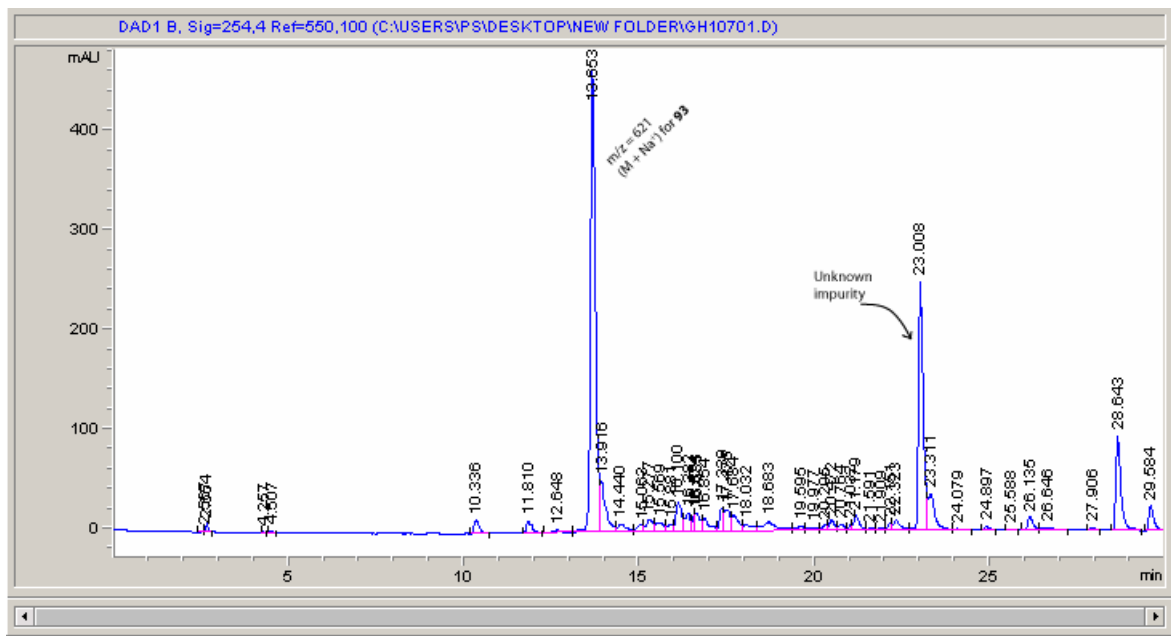
Figure 48: RP-HPLC chromatogram of the unpurified amino acid **96** at 254 nm. (Method 05_95)

Figure 49: RP-HPLC chromatogram of the unpurified Fmoc protected amino acid **97** at 254 nm.

(Method 05_95)
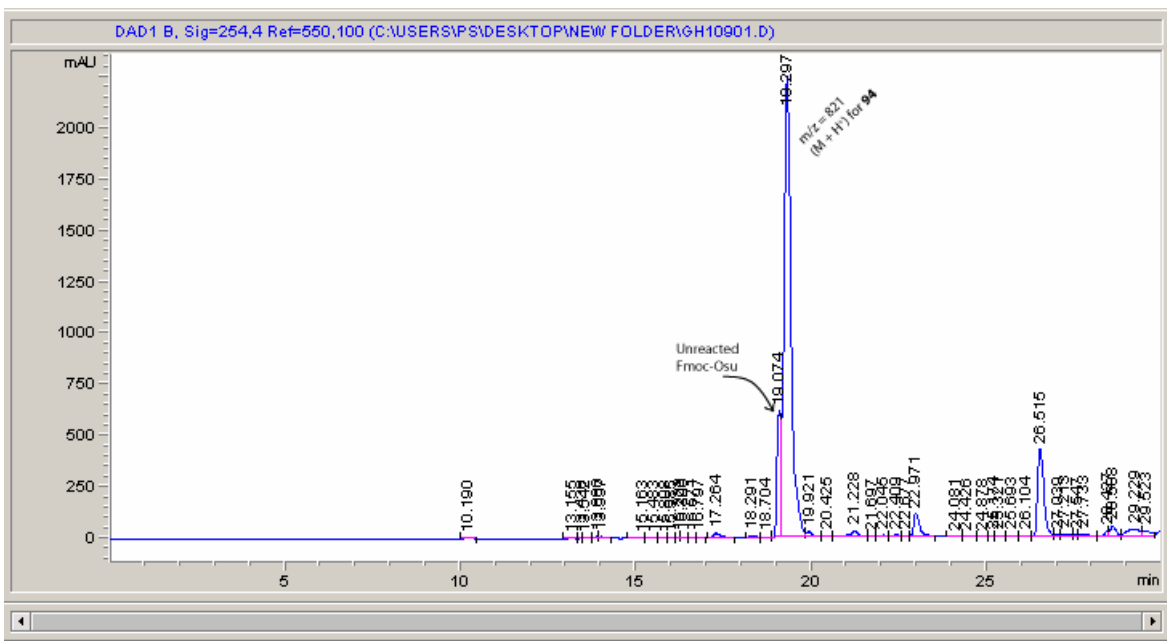
APPENDIX A

1D NMR SPECTRA

The spectra illustrated in this appendix are 1D NMR spectra of the pip5(2S5S)(OBn) **18**, pro4(2S4S)(OTFP) **47**, pip5(2S5S)(OTFP) **48**, and proAc(2S3S4R) **67** monomers and oligomers **22** and **84** that contain them.
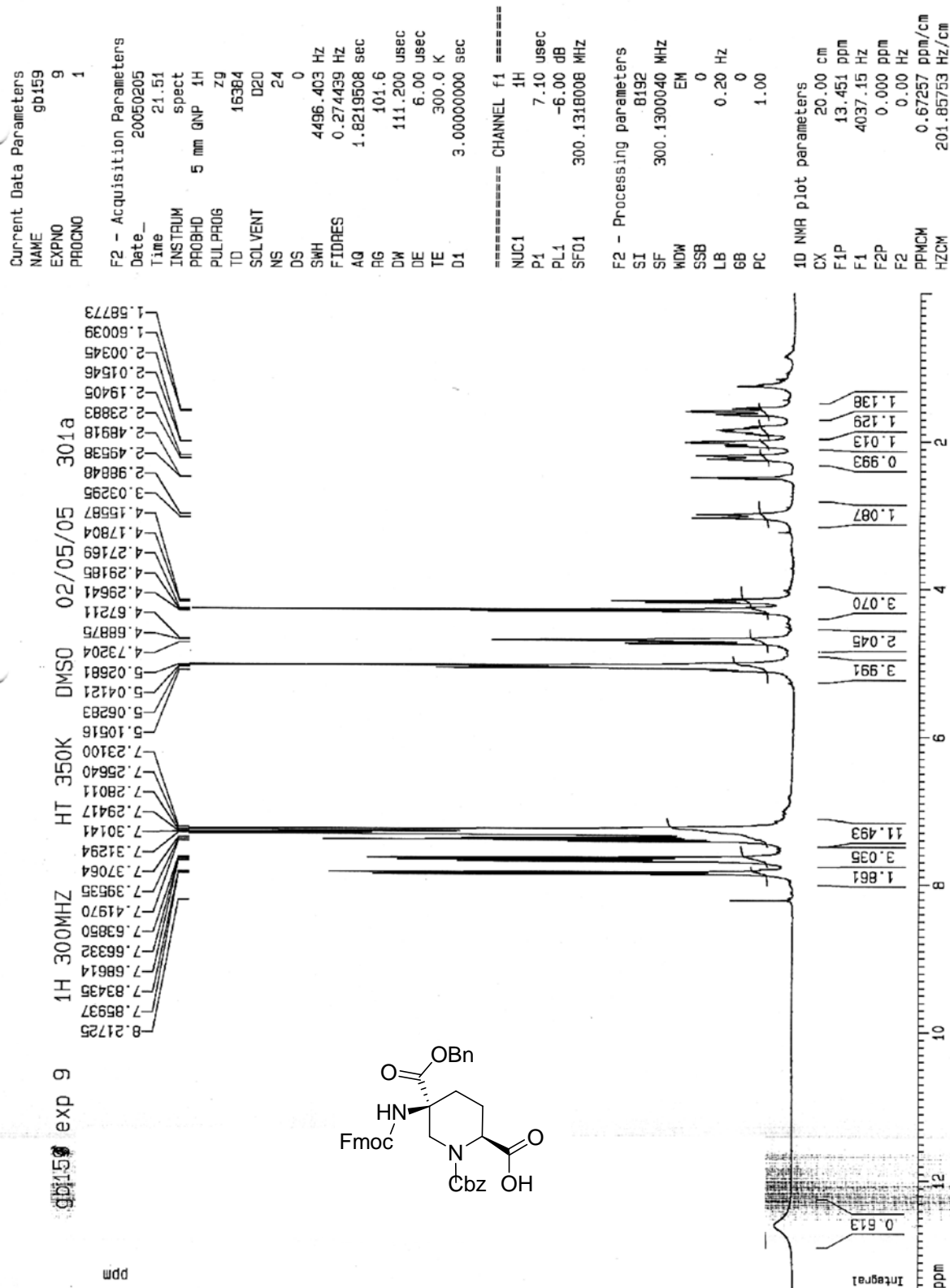
Figure 50: 1H spectrum of compound **18**, 300 MHz, DMSO-d6, 350K

165
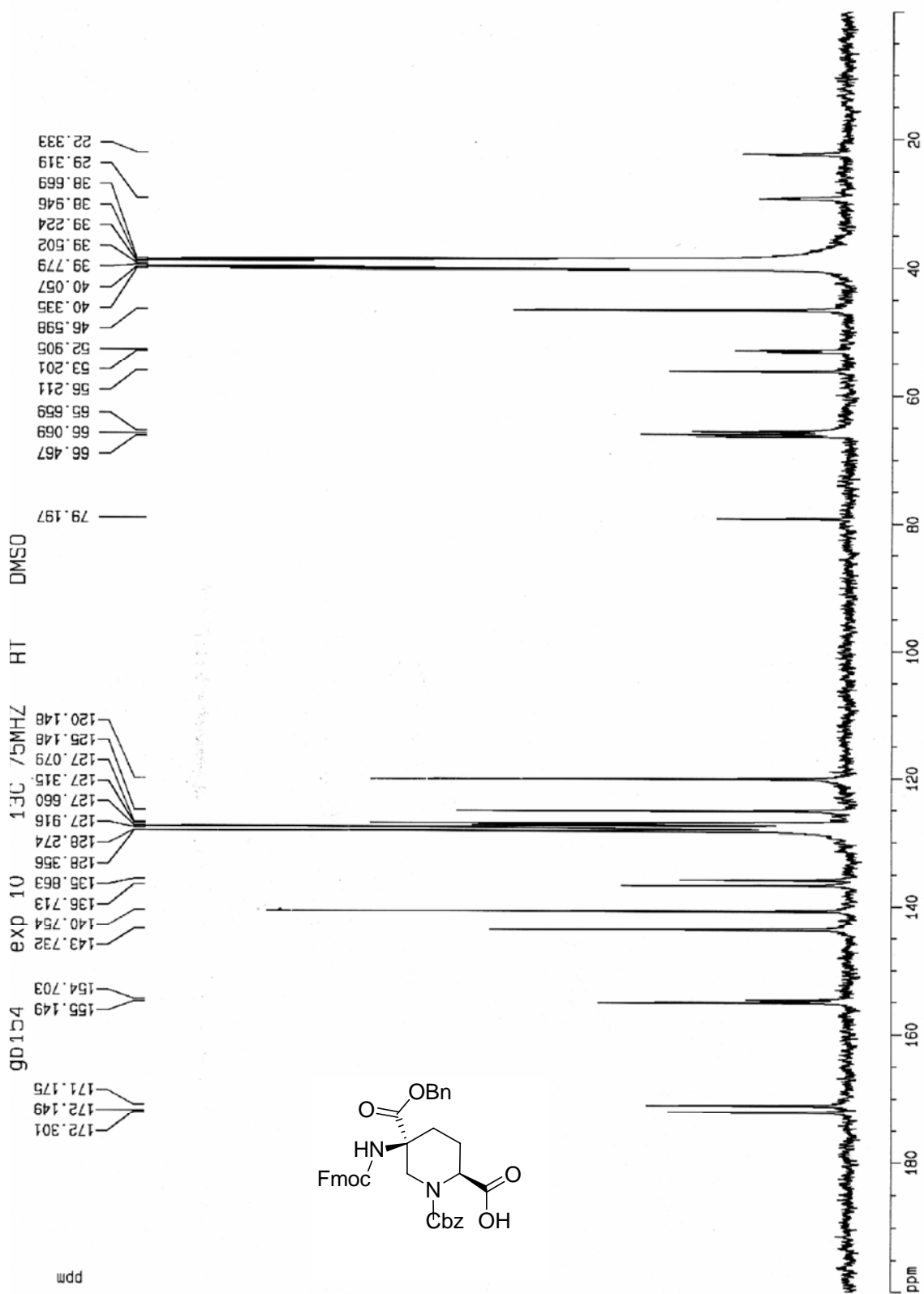
Figure 51: Proton decoupled 13C spectrum of compound **18**, 75.4 MHz, DMSO-*d6* rt

166
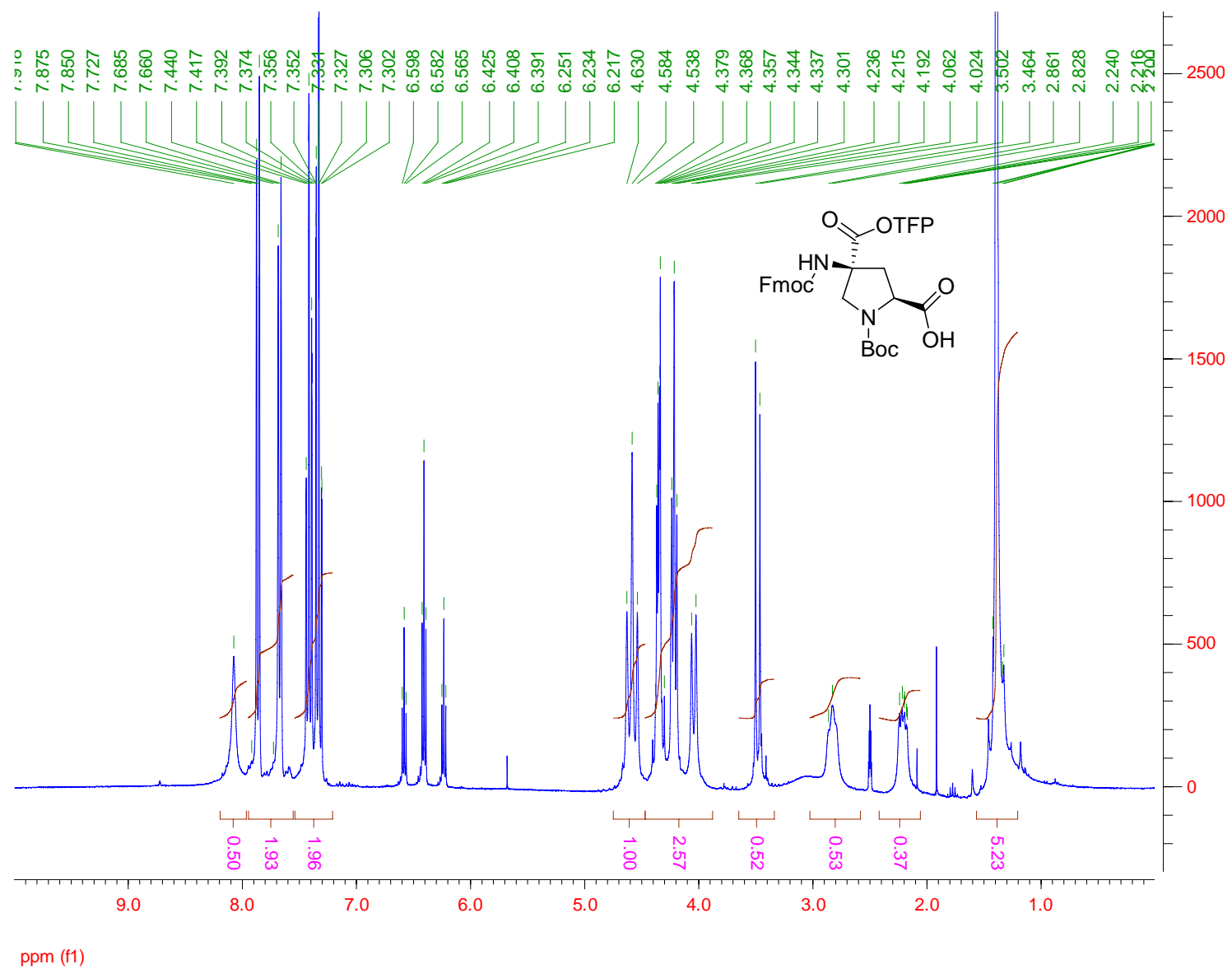
Figure 52: 1H spectrum of compound **47**, 300 MHz, DMSO-d6, 350K

167
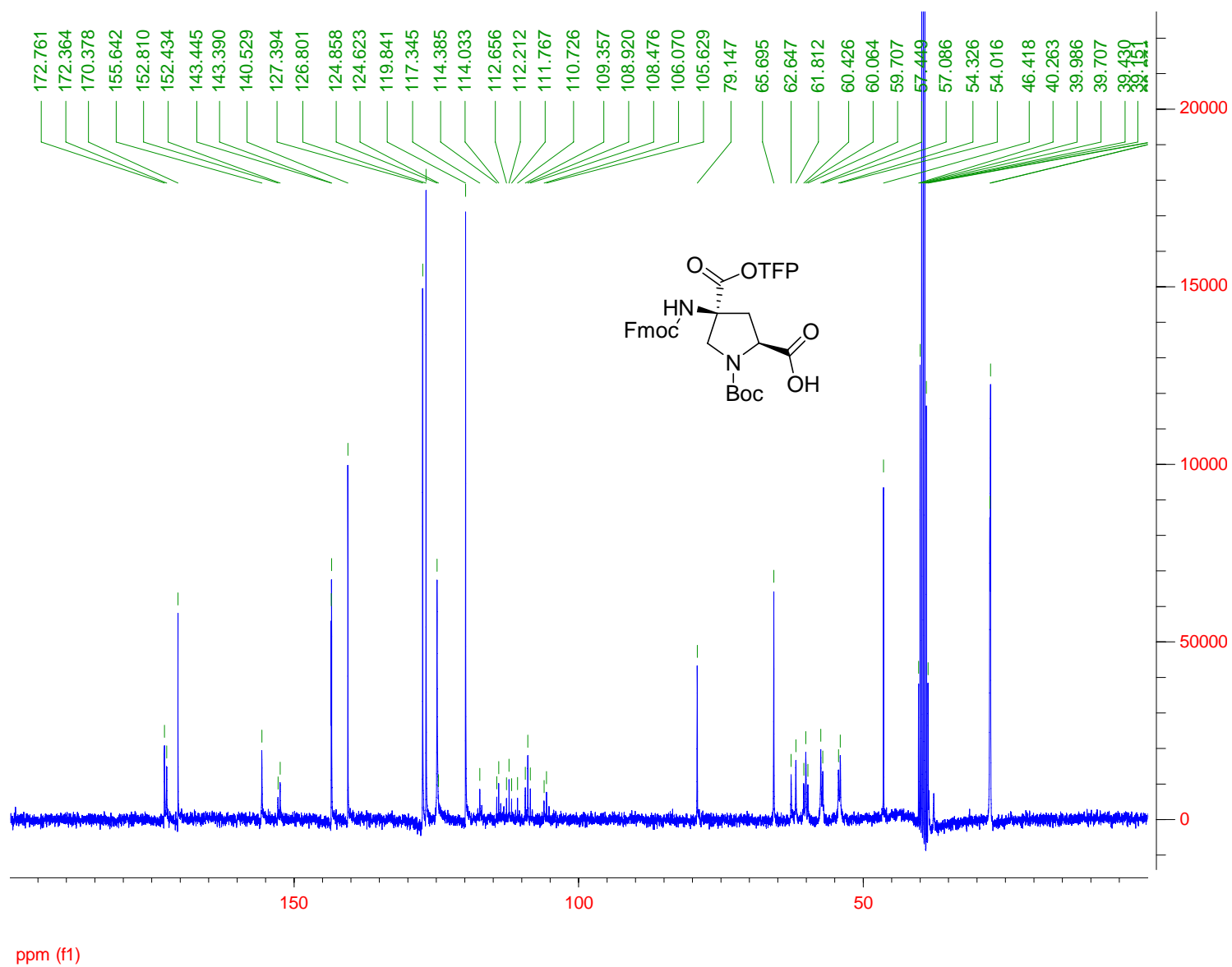
Figure 53: Proton decoupled 13C spectrum of compound **47**, 75.4 MHz, DMSO-*d6* rt

168
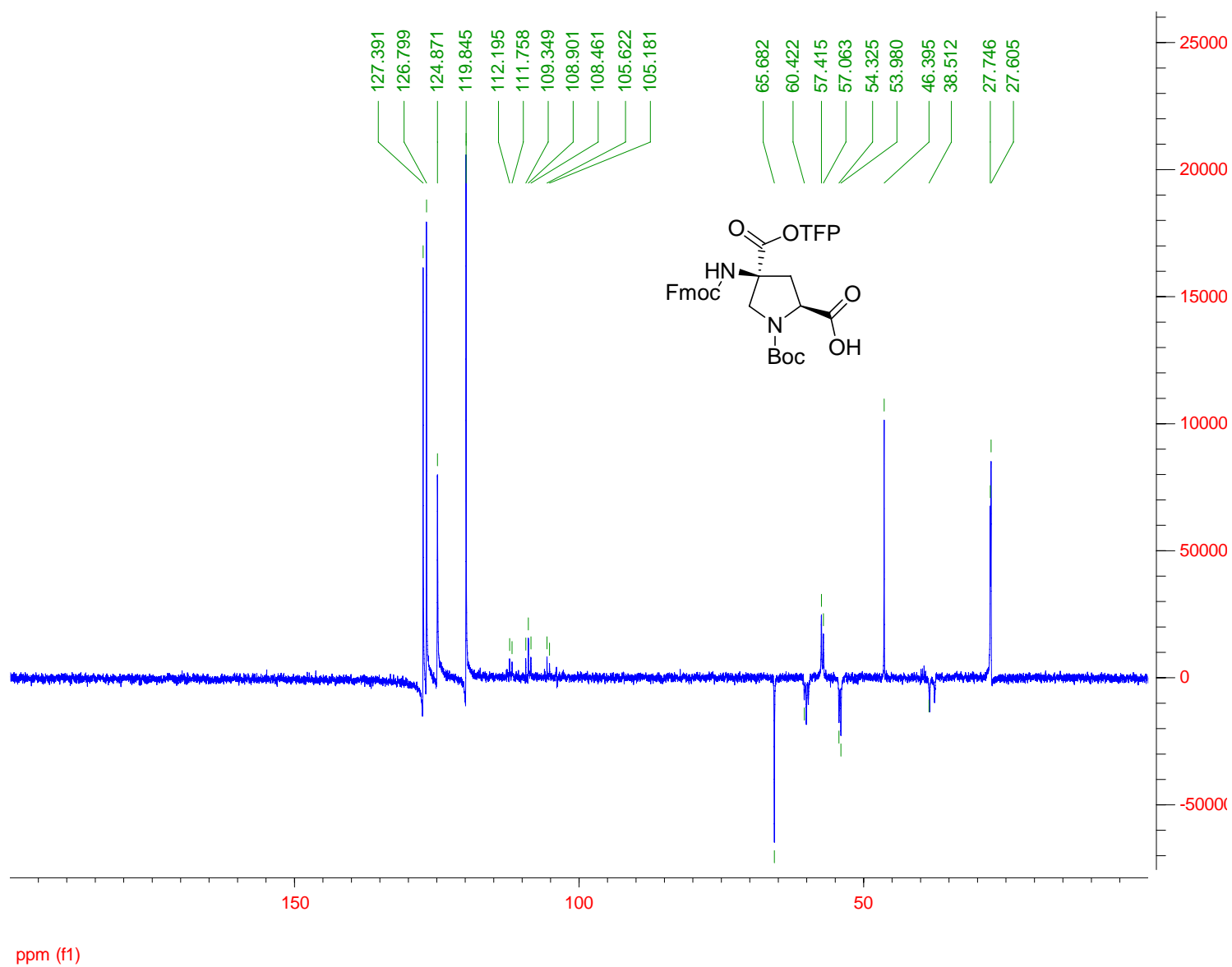
Figure 54: DEPT135 spectrum of compound **47**, 75.4 MHz, DMSO-d6, rt
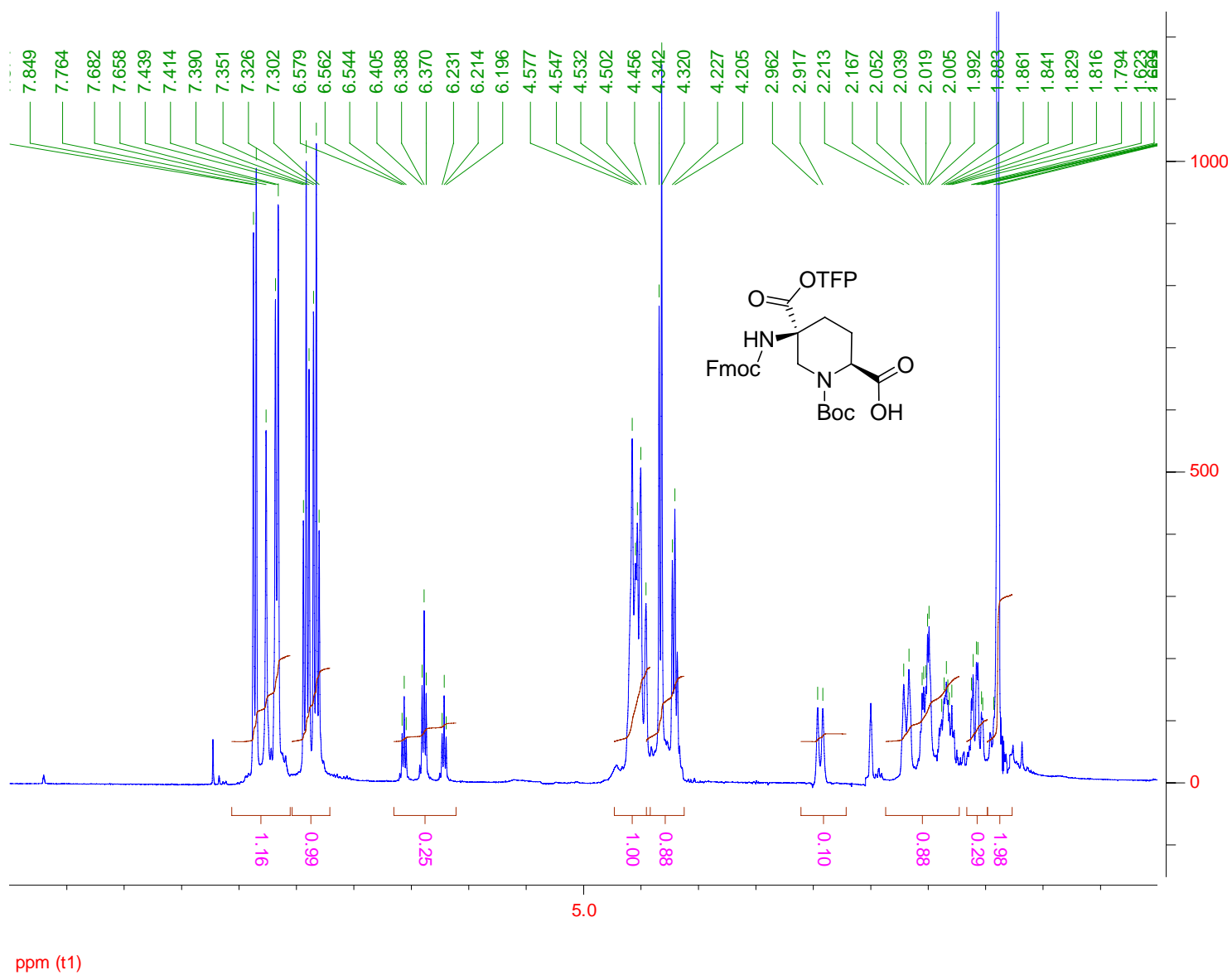
Figure 55: 1H spectrum of compound **48**, 300 MHz, DMSO-d6, 350K
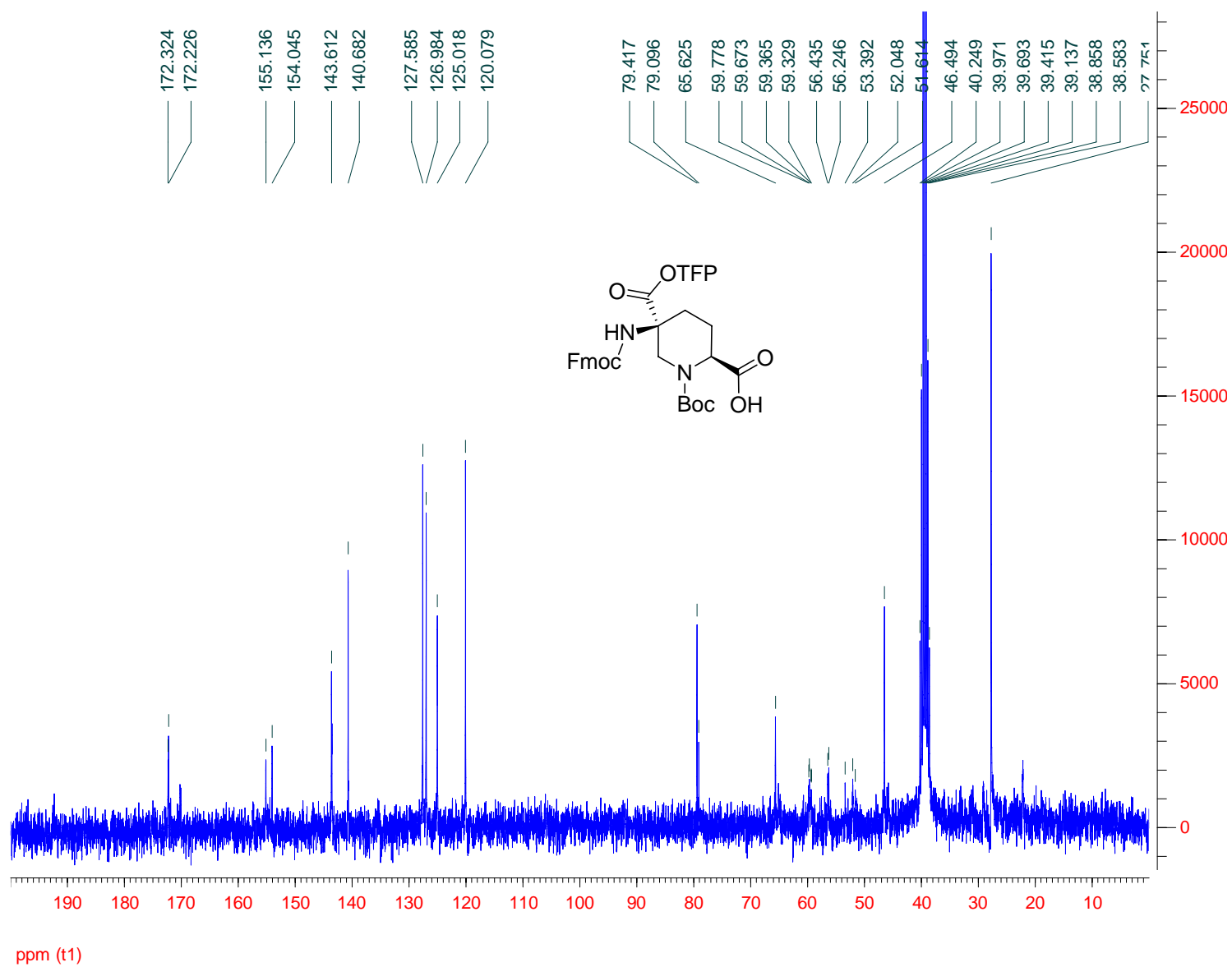
Figure 56: Proton decoupled 13C spectrum of compound **48**, 75.4 MHz, DMSO-d6, rt

171
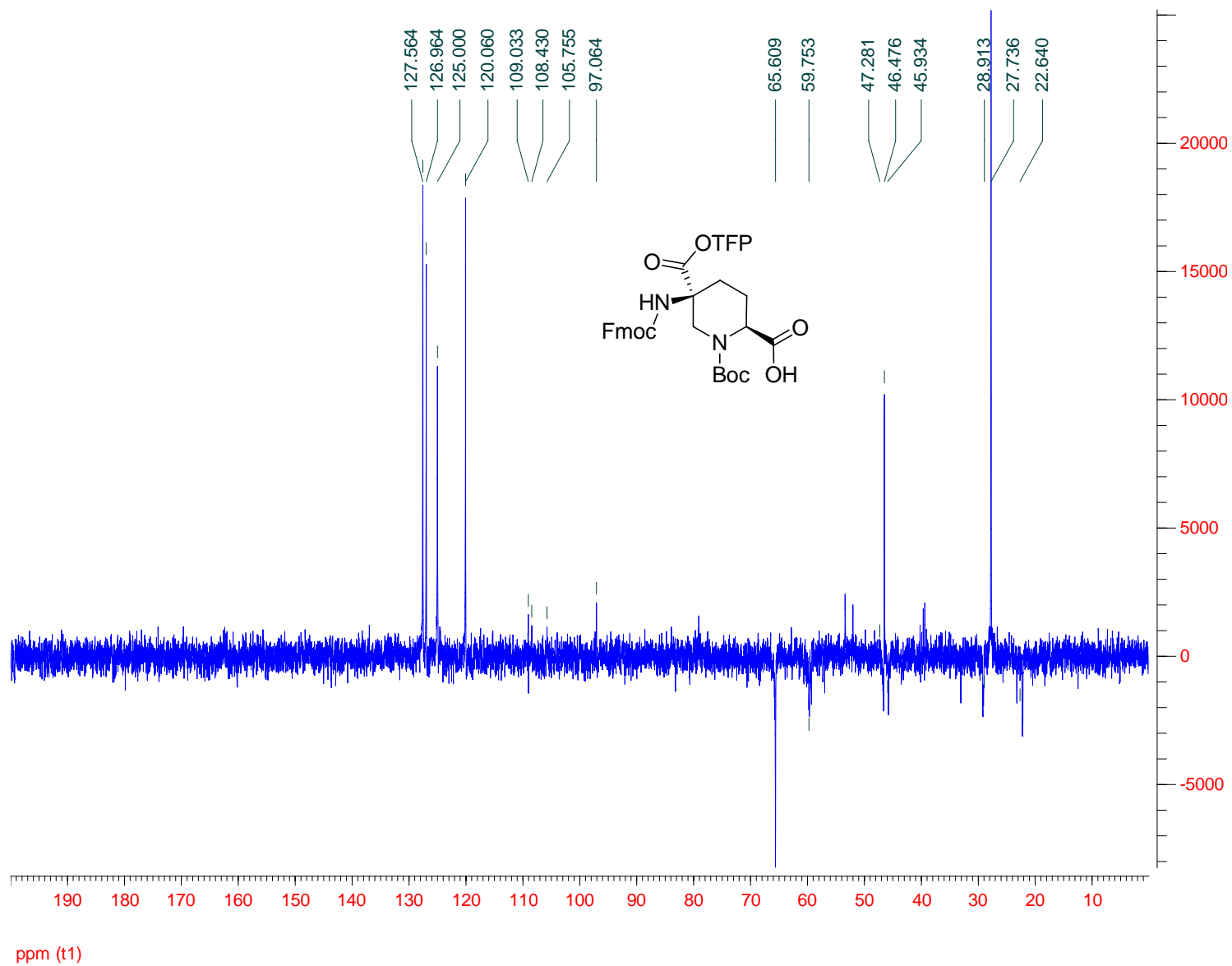
Figure 57: DEPT135 spectrum of compound **48**, 75.4 MHz, DMSO-d6, rt

172
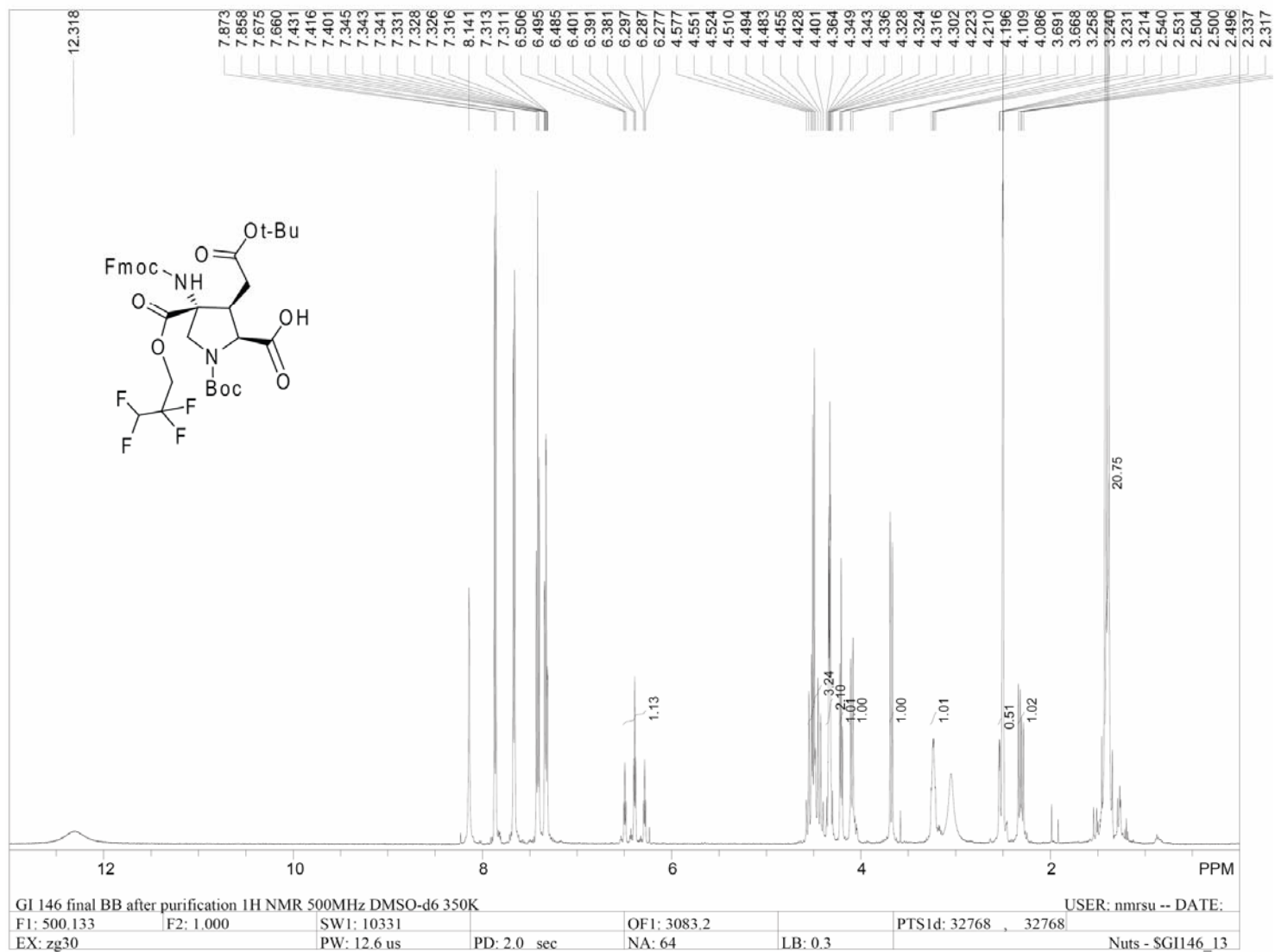
Figure 58: 1H spectrum of compound **67**, 500 MHz, DMSO-*d6*, 350K

173

Figure 59: Proton decoupled 13C spectrum of compound **67**, 125 MHz, DMSO-*d6*, rt

174
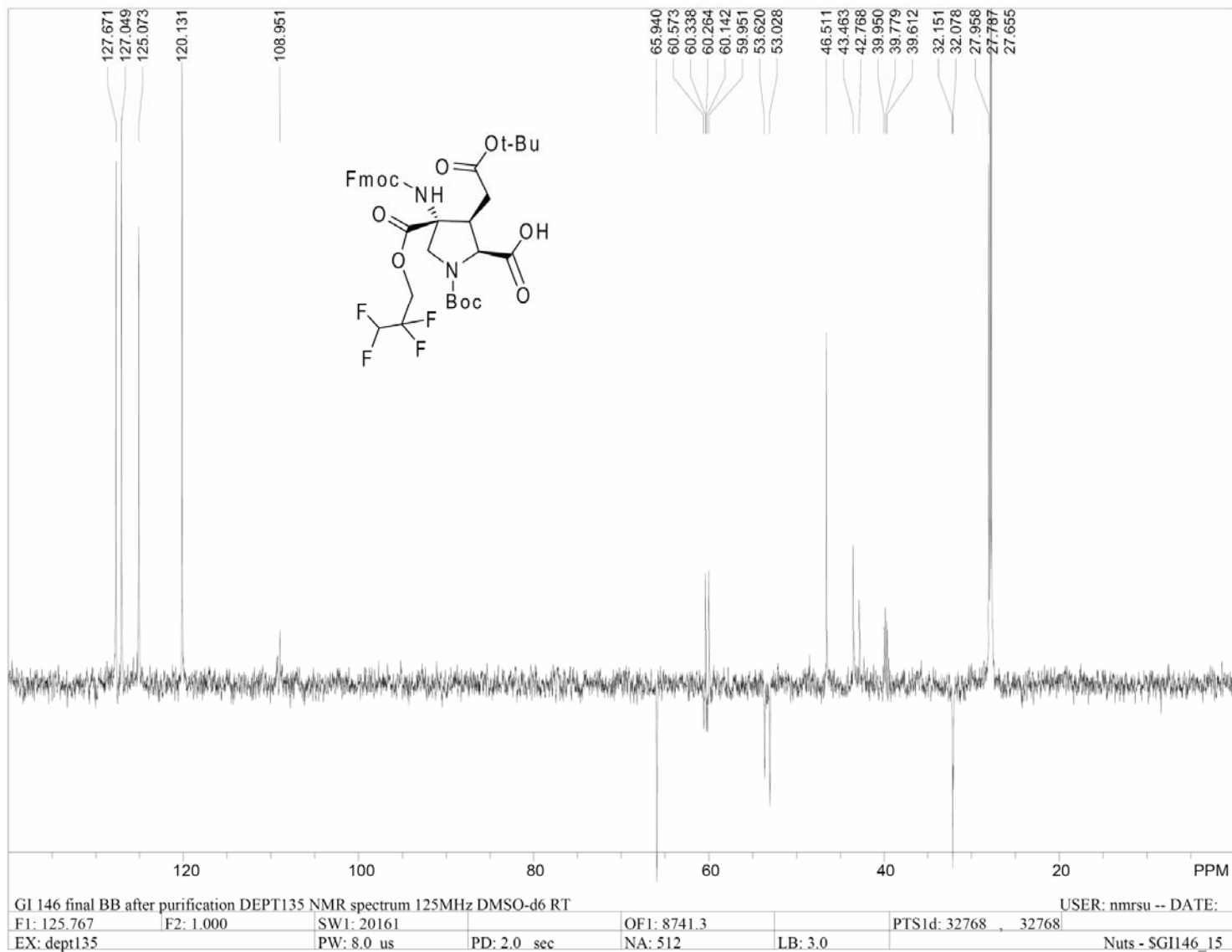
Figure 60: DEPT135 spectrum of compound **67**, 125 MHz, DMSO-*d6*, rt

175

ppm

8.46764
8.43437
8.33355
8.04213
7.27584
7.26138
6.96965
6.95581
6.64660
6.63275
6.96190
4.93921
4.68178
4.65804
4.63878
4.57880
4.04030
4.03545
4.00814
3.97535
3.93203
3.58279
3.09085
3.08086
3.06783
3.05844
2.77566
2.75365
2.63623
2.60131
2.59490
2.57458
2.14043
2.09021
2.06795
1.90418
1.88212
1.77569
1.76850
1.74668
1.15438
0.83422

Oligomer **3**
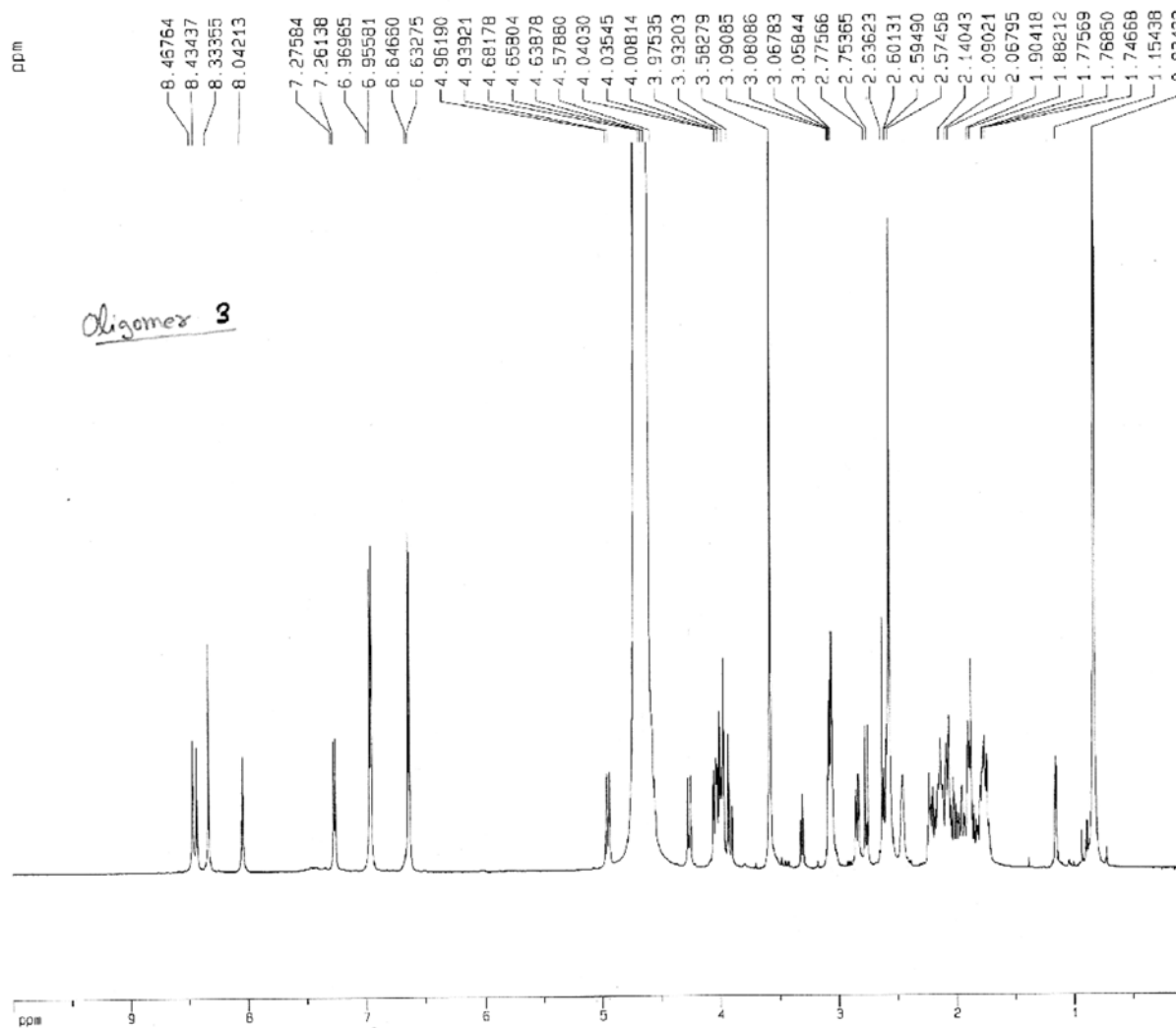
Current Data Parameters
NAME   gc008
EXPNO   20
PROCNO   1

F2 - Acquisition Parameters
Date_   20050124
Time   18.47
INSTRUM   spect
PROBHD   5 mm TBI 1H/
PULPROG   zgpr
TD   65536
SOLVENT   CD2Cl2
NS   64
DS   0
SWH   8992.806 Hz
FIDRES   0.137219 Hz
AQ   3.6438515 sec
RG   28.5
DW   55.600 usec
DE   6.00 usec
TE   290.0 K
D1   1.0000000 sec
d12   0.0000200 sec
d13   0.0000300 sec

=========== CHANNEL f1 ====
NUC1   1H
P1   8.43 usec
PL1   0.00 dB
PL9   55.00 dB
SFO1   600.8328220 MHz

F2 - Processing parameters
SI   65536
SF   600.8300237 MHz
WDW   EM
SSB   0
LB   0.10 Hz
GB   0
PC   1.00

1D NMR plot parameters
CX   20.00 cm
F1P   10.000 ppm
F1   6008.30 Hz
F2P   0.000 ppm
F2   0.00 Hz
PPMCM   0.50000 ppm/
HZCM   300.41501 Hz/c

ppm   9   8   7   6   5   4   3   2   1

Figure 61: 1H spectrum of oligomer **22**, 600 MHz, 90% H_2O / 10% D_2O at rt

176
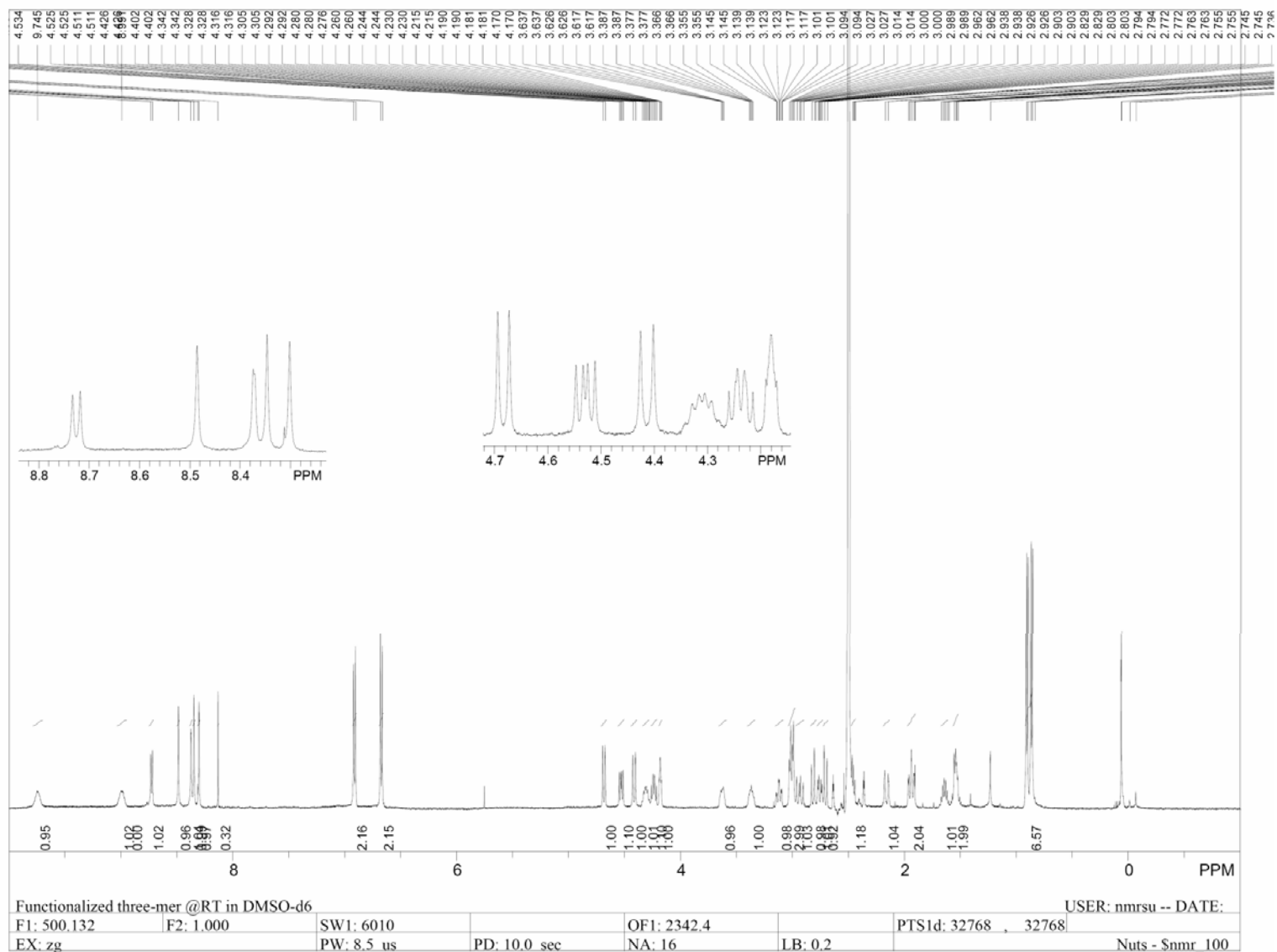
Figure 62: 1H spectrum of oligomer **84**, 500 MHz, DMSO-*d6*, rt

RESONANCE ASSIGNMENT FOR OLIGOMERS

The NMR resonances derived from the 2D-NMR spectra of the oligomers **22** and **84** are tabulated in supplemental tables 1, 2 and 3.

Group: the number corresponding to the place of the residue in the sequence

Heavy atom number: the numerical designation of the atoms in the structures shown in the text.

Atom: the first letter (C or H) designates the nucleus. The following letters are coded as follows;

A = alpha, B = beta, C = gamma, D = delta, E = epsilon

AC = carbonyl carbon adjacent to alpha carbon

CC = carbonyl carbon adjacent to gamma carbon

DC = carbonyl carbon adjacent to gamma carbon

N = amide nitrogen

Shift: chemical shift (on the δ scale)

StDev: the standard deviation of the mean chemical shift for each resonance
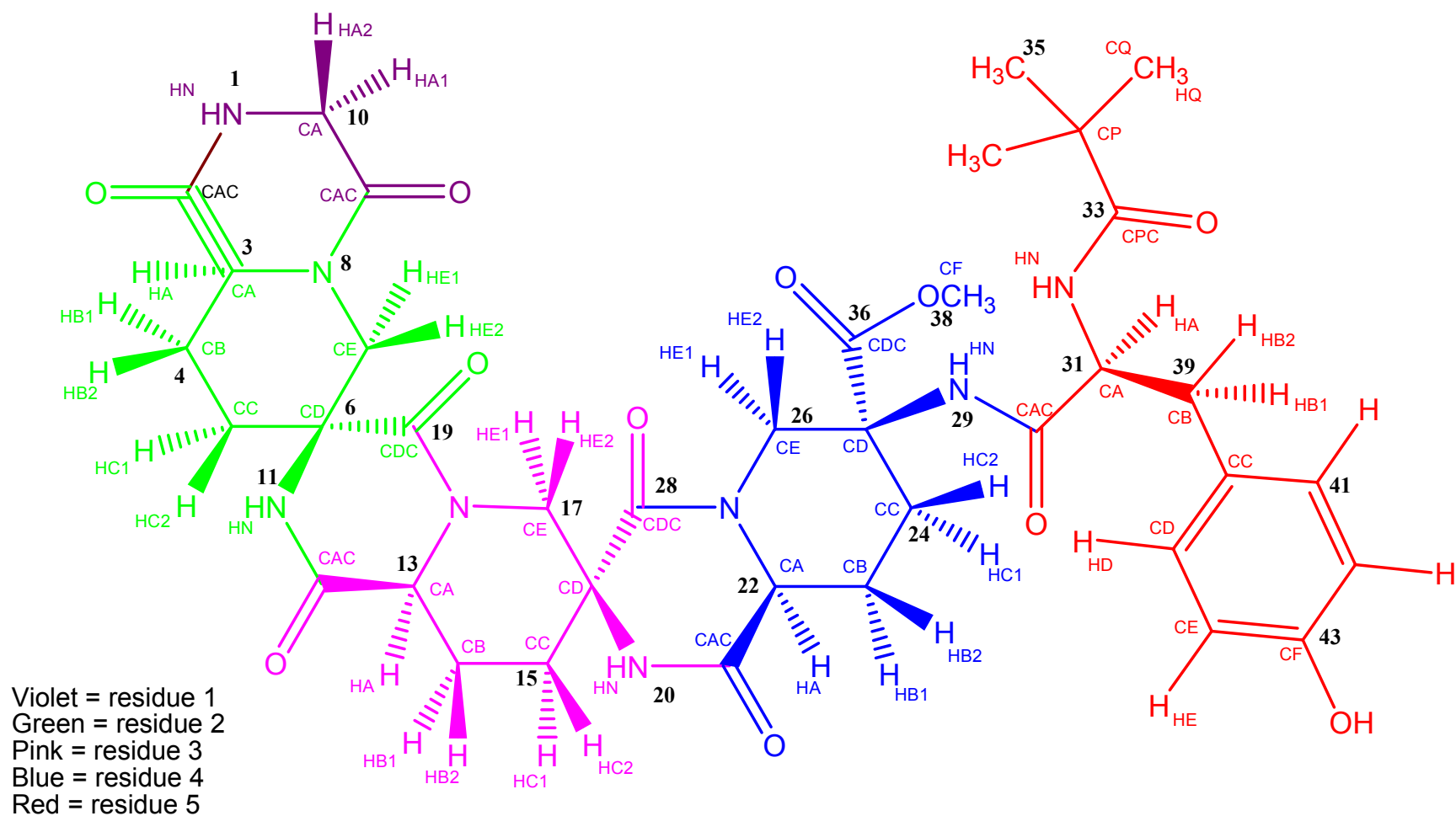
Figure 63: Naming scheme for oligomer **22** used for assigning 2D NMR spectra by SPARKY and corresponding heavy atom numbering scheme used in dissertation.

179

Table 6: Chemical shift assignment and dissertation to Sparky atom name conversion chart for oligomer **22**

(# = number of cross-peaks in COSY/ROESY/HMBC/HMQC spectra involving this nucleus).

Heavy Atom	Group	Atom name	Nuc	Shift	SDev	#	Heavy Atom	Group	Atom name	Nuc	Shift	SDev	#
C10	1	CA	13C	44.806	0.002	3	C22	4	CA	13C	58.332	0.045	2
C9	1	CAC	13C	166.03	0.04	4	C21	4	CAC	13C	169.019	0.067	2
H10α	1	HA1	1H	3.974	0.003	4	C23	4	CB	13C	26.331	0.083	3
H10β	1	HA2	1H	4.03	0.002	5	C24	4	CC	13C	31.73	0.006	2
H1	1	HN	1H	8.075	0.018	7	C25	4	CD	13C	57.969	0.02	2
C3	2	CA	13C	57.471	0.011	2	C36	4	CDC	13C	174.506	0.014	2
C2	2	CAC	13C	166.207	0	1	C26	4	CE	13C	45.386	0	1
C4	2	CB	13C	24.108	0.095	2	C38	4	CF	13C	54.046	0	1
C5	2	CC	13C	35.16	0	1	H22	4	HA	1H	4.098	0.002	11
C6	2	CD	13C	57.214	0	1	H23α	4	HB1	1H	2.198	0.003	4
C19	2	CDC	13C	167.688	0.02	2	H23β	4	HB2	1H	1.803	0.006	6
C7	2	CE	13C	49.687	0	1	H24α	4	HC1	1H	2.005	0.004	5
H3	2	HA	1H	4.033	0.002	10	H24β	4	HC2	1H	2.128	0.001	4
H4α	2	HB1	1H	2.127	0.002	3	H26α	4	HE1	1H	3.126	0.003	4
H4β	2	HB2	1H	1.807	0.003	4	H26β	4	HE2	1H	4.998	0.002	7
H5α	2	HC1	1H	2.07	0.004	5	H38	4	HF	1H	3.629	0.001	2
H5β	2	HC2	1H	1.945	0.002	3	H29	4	HN	1H	8.368	0.025	9
H7α	2	HE1	1H	3.114	0.004	5	C31	5	CA	13C	54.671	0	3
H7β	2	HE2	1H	2.507	0	1	C30	5	CAC	13C	174.446	0.038	3
H11	2	HN	1H	8.477	0.02	6	C39	5	CB	13C	37.457	0.028	4
C13	3	CA	13C	57.047	0	1	C40	5	CC	13C	128.989	0.053	3
C12	3	CAC	13C	168.762	0	1	C41	5	CD	13C	131.307	0.062	4
C14	3	CB	13C	24.474	0.024	2	C42	5	CE	13C	116.204	0.028	3
C15	3	CC	13C	32.586	0	1	C43	5	CF	13C	155.177	0.054	2
C16	3	CD	13C	57.278	0	1	C34	5	CP	13C	39.105	0	1
C28	3	CDC	13C	166.685	0.046	3	C33	5	CPC	13C	182.555	0.013	2
C17	3	CE	13C	51.906	0	1	C35	5	CQ	13C	27.124	0	2
H13	3	HA	1H	4.065	0.002	11	H31	5	HA	1H	4.611	0	4
H14α	3	HB1	1H	2.181	0.002	3	H39α	5	HB1	1H	2.647	0.003	10
H14β	3	HB2	1H	1.84	0.005	5	H39β	5	HB2	1H	2.893	0.002	10
H15α	3	HC1	1H	2.256	0.001	5	H41	5	HD	1H	7.011	0.001	8
H15β	3	HC2	1H	1.941	0.002	4	H42	5	HE	1H	6.689	0.001	5
H17α	3	HE1	1H	2.811	0.003	5	H32	5	HN	1H	7.306	0.017	9
H17β	3	HE2	1H	4.314	0.004	6	H35	5	HQ	1H	0.884	0.001	4
H20	3	HN	1H	8.506	0.022	7							
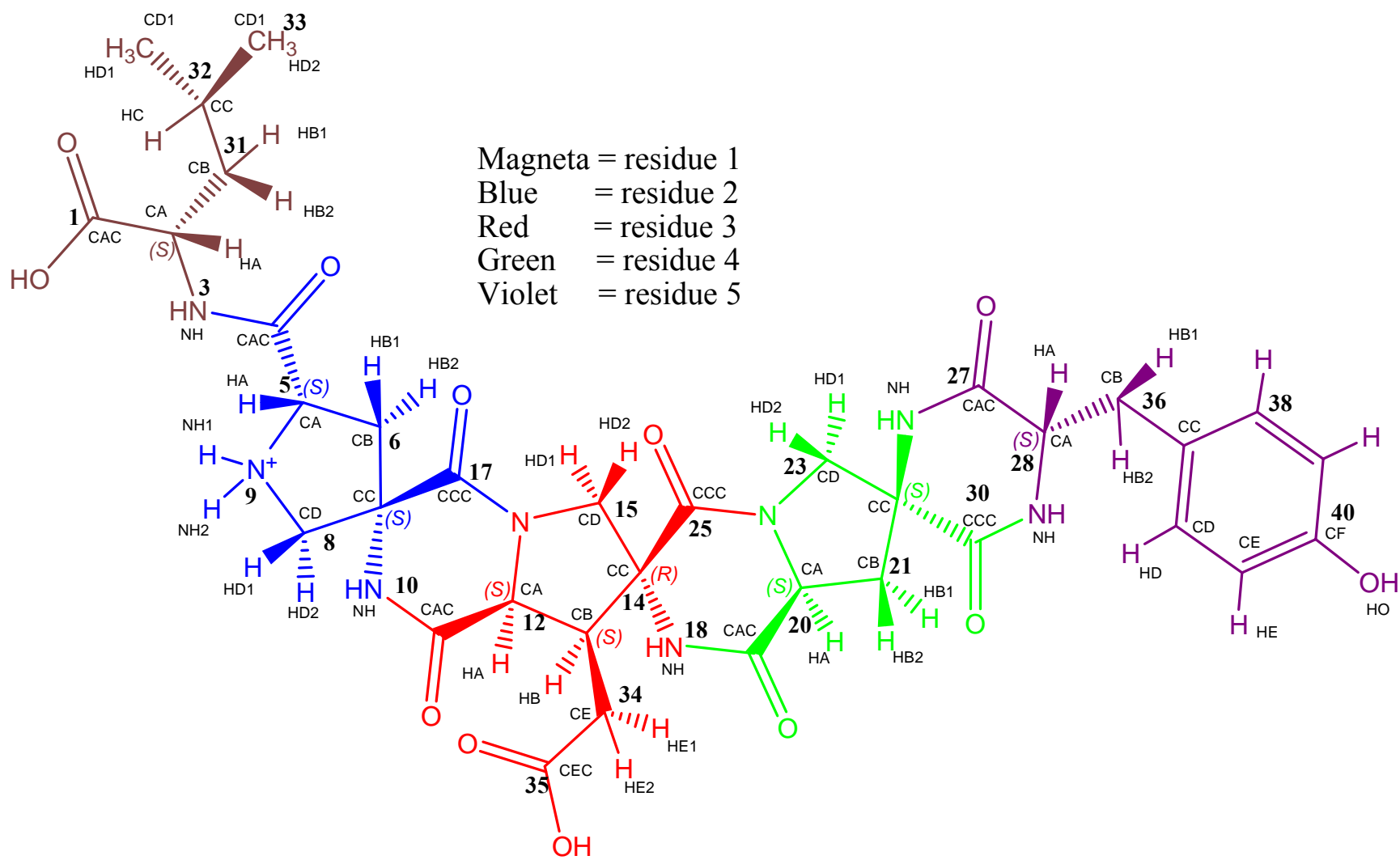
Figure 64: Naming scheme for oligomer **84** used for assigning 2D NMR spectra by SPARKY and corresponding heavy atom numbering scheme used in dissertation

Table 7: Dissertation to Sparky atom name conversion chart and chemical shift assignments for compound **84**. (# = number of cross-peaks in COSY/ROESY/HMBC/HMQC spectra involving this nucleus)

| Group	Atom name	Heavy atom #	Nuc	Shift	SDev	#		Group	Atom name	Heavy atom #	Nuc	Shift	SDev	#
1	CA	2	13C	50.819	0.003	2		3	Ha	12	1H	4.684	0	11
1	CAC	1	13C	172.943	0.003	2		3	Hb	13	1H	3.119	0	7
1	CB	31	13C	39.676	0.001	4		3	Hd1	15α	1H	3.001	0	8
1	CC	32	13C	24.254	0.007	4		3	Hd2	15β	1H	4.414	0	7
1	CD1	33	13C	22.708	0	1		3	He1	34β	1H	2.933	0	7
1	CD2	33	13C	21.129	0	1		3	He2	34α	1H	2.158	0.001	8
1	Ha	2	1H	4.237	0	14		3	NH	18	1H	8.498	0.002	7
1	Hb12	32	1H	1.541	0	9		4	CA	20	13C	57.897	0.002	2
1	Hc	32	1H	1.637	0.001	7		4	CAC	19	13C	167.891	0.006	3
1	Hd1	33	1H	0.906	0	5		4	CB	21	13C	42.048	0	2
1	Hd2	33	1H	0.865	0	5		4	CC	22	13C	58.943	0.011	4
1	NH	3	1H	8.736	0	8		4	CCC	30	13C	169.041	0.012	4
2	CA	5	13C	58.316	0	1		4	CD	23	13C	55.182	0.003	3
2	CAC	4	13C	166.265	0.002	2		4	Ha	20	1H	4.534	0	7
2	CC	7	13C	62.505	0	2		4	Hb1	21α	1H	2.46	0	5
2	CB	6	13C	-	-	-		4	Hb2	21β	1H	1.939	0	5
2	CCC	17	13C	165.331	0	1		4	Hd1	23α	1H	2.703	0	4
2	CD	8	13C	50.829	0	3		4	Hd2	23β	1H	2.816	0	5
2	Ha	5	1H	4.31	0	10		4	NH	26	1H	8.362	0.001	4
2	Hb1	6α	1H	3.006	0	6		5	CA	28	13C	55.398	0.01	3
2	Hb2	6β	1H	1.938	0	11		5	CAC	27	13C	165.745	0.001	2
2	Hd1	8α	1H	3.635	0	7		5	CB	36	13C	37.69	0	3
2	Hd2	8β	1H	3.36	0	8		5	CC	37	13C	156.052	0	2
2	NH	10	1H	8.31	0.002	6		5	CD	38	13C	131.064	0.02	4
2	NH1	9	1H	9.748	0	6		5	CE	39	13C	114.914	0.005	3
2	NH2	9	1H	8.995	0	6		5	CF	40	13C	125.305	0.015	2
3	CA	12	13C	56.018	0.003	4		5	Ha	28	1H	4.181	0	7
3	CAC	11	13C	166.231	0	1		5	Hb1	36α	1H	2.753	0	11
3	CB	13	13C	44.792	0.01	5		5	Hb2	36β	1H	3	0.001	5
3	CC	14	13C	62.622	0.003	4		5	Hd	38	1H	6.912	0	9
3	CCC	25	13C	163.241	0.002	3		5	He	39	1H	6.672	0.001	5
3	CD	15	13C	52.424	0.001	2		5	NH	29	1H	8.389	0	6
3	CE	34	13C	29.719	0	1								
3	CEC	35	13C	173.227	0.004	2								

Table 8: ROESY correlations list for compound **84**.

Assignment	w1	w2	Volume	Intensity
1Hb12-NH	1.531	8.726	-3.87E+05	Medium
1Hc-Ha	1.627	4.227	-1.11E+06	Strong
1Hc-NH	1.637	8.73	-2.95E+05	Medium
1Hd2-Ha	0.87	4.239	-7.01E+05	Medium
2Hb1-1NH	3.006	8.73	-2.25E+05	Weak
2Hb2-Hd2	1.937	3.36	-1.75E+05	Weak
2Hb2-NH	1.938	8.315	-8.86E+05	Strong
4Hb2-4NH	1.931	8.359	-9.94E+05	Strong
2Hd1-Ha	3.626	4.31	-2.05E+05	Weak
2Hd2-NH	3.363	8.31	-1.24E+06	Strong
3Ha-2NH	4.684	8.309	-5.47E+04	Weak
3Hb-NH	3.115	8.495	-1.96E+06	Strong
3Hd1-Ha	3.004	4.68	-4.53E+05	Medium
3Hd1-NH	2.993	8.5	-5.69E+05	Medium
2Ha-1NH	4.304	8.725	-8.97E+05	Strong
3Hd2-4Ha	4.414	4.53	-6.70E+05	Medium
3He1-Ha	2.923	4.689	-2.61E+05	Weak
3He2-NH	2.165	8.5	-1.45E+05	Weak
4Hd1-Ha	2.699	4.531	-1.39E+05	Weak
4Hd2-NH	2.806	8.355	-8.34E+05	Medium
5Hb1-NH	2.749	8.391	-5.34E+05	Medium

APPENDIX C

2D NMR SPECTRA FOR OLIGOMERS
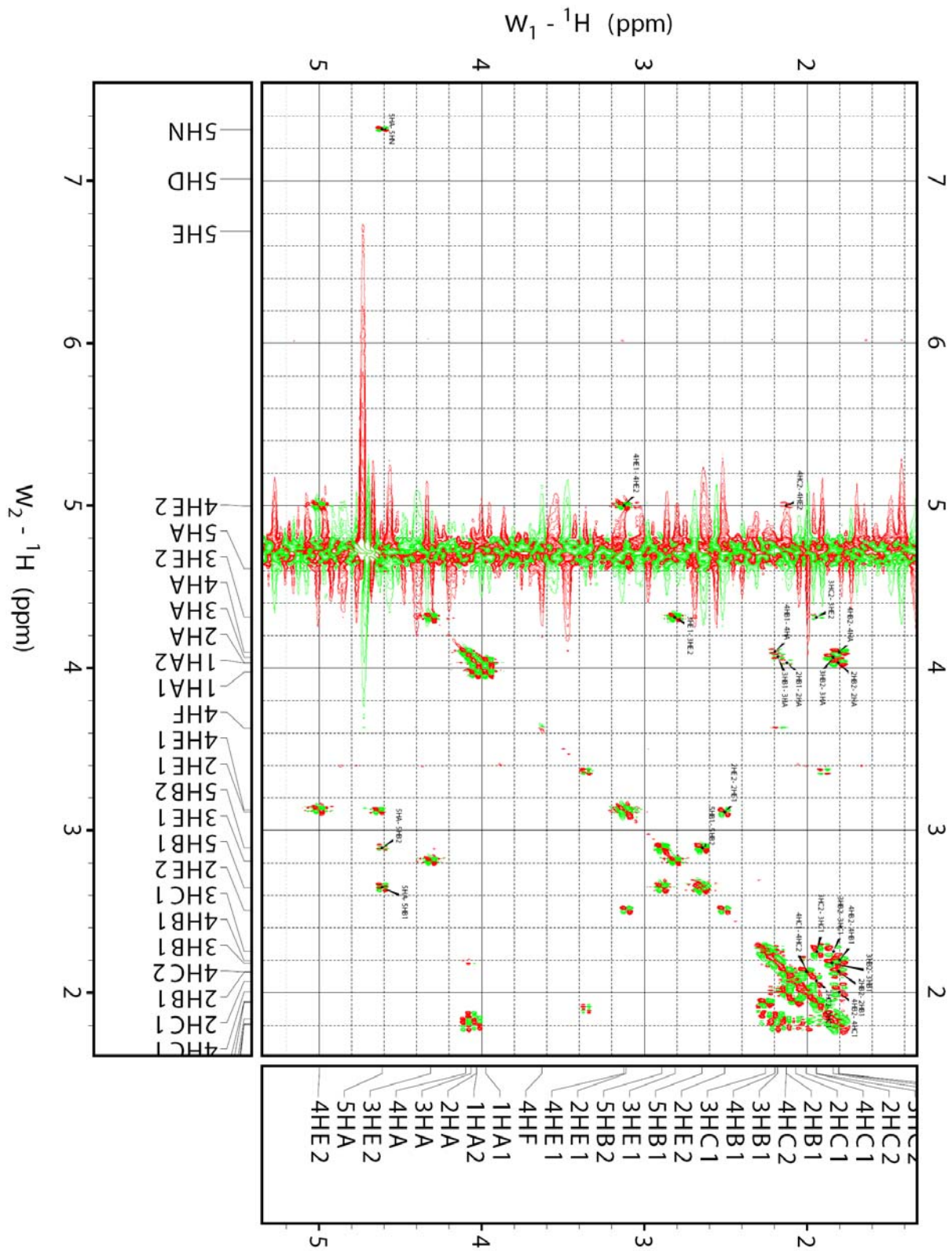
Figure 65: DQF-COSY spectrum of oligomer **22**, 600 MHz, 90% H$_2$O / 10% D$_2$O rt

185
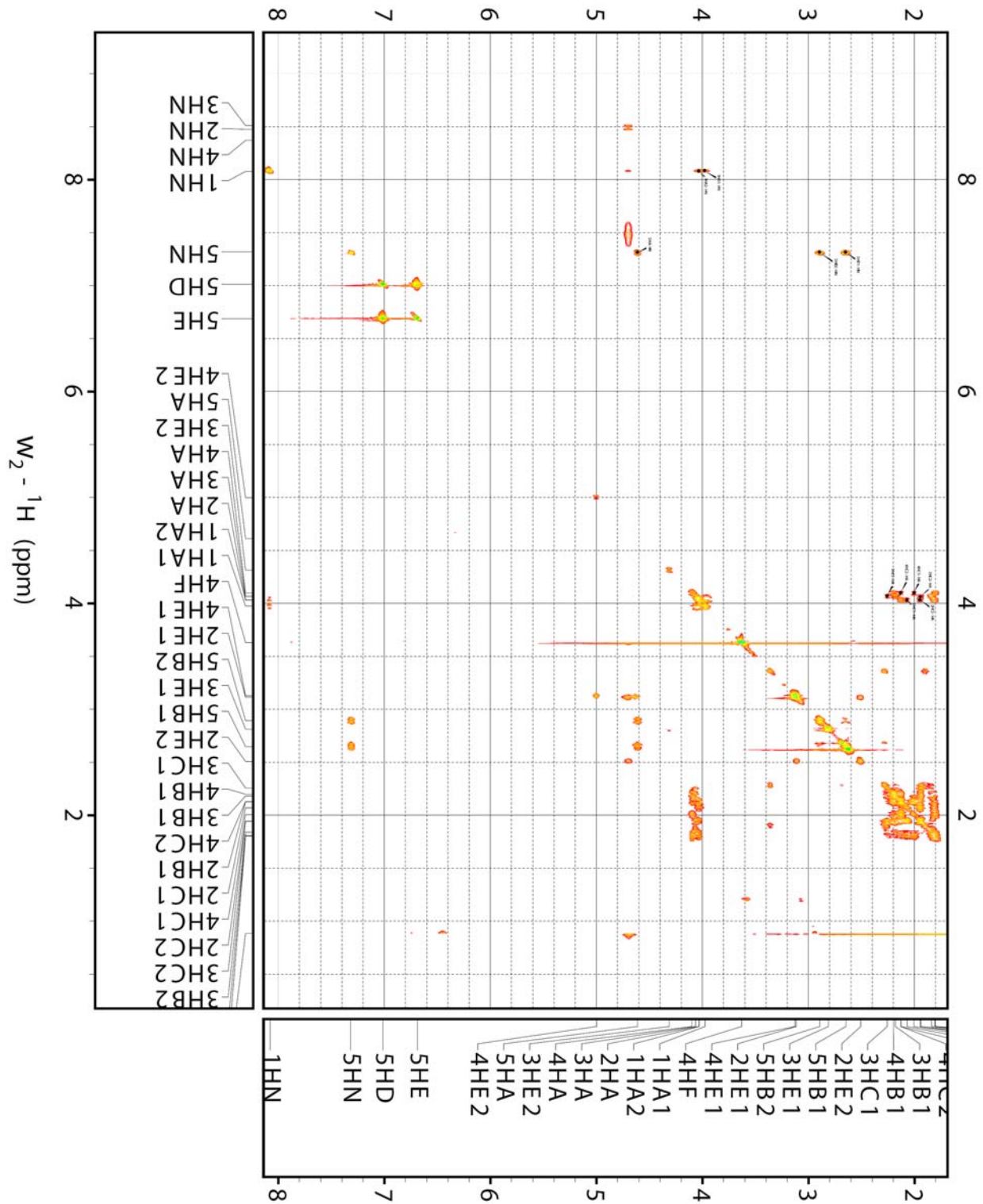
Figure 66: TOCSY spectrum of oligomer **22**, 600 MHz, 90% H$_2$O / 10% D$_2$O rt
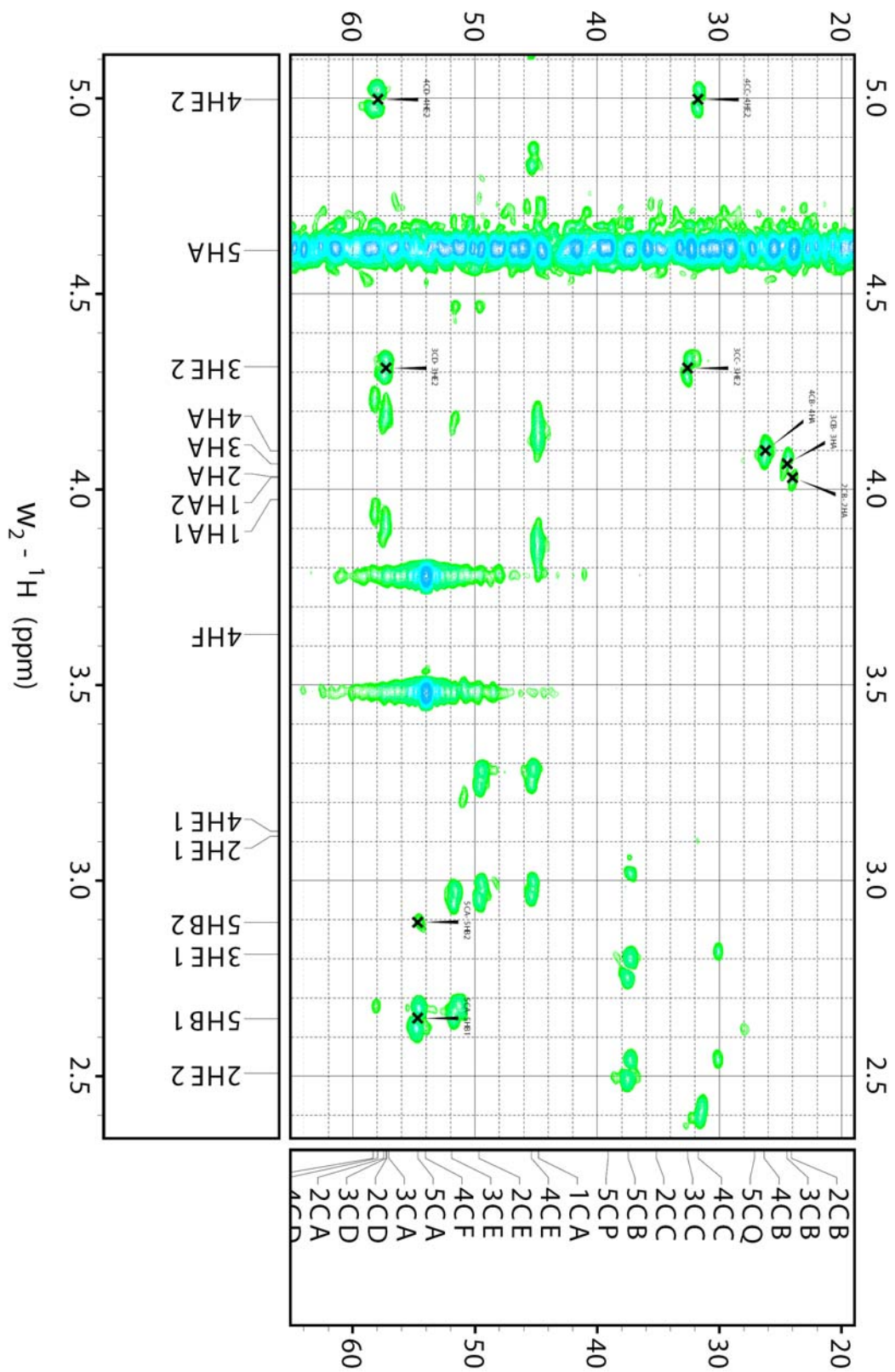
Figure 67: HMBC spectrum (1 of 4) of oligomer **22**, 500 MHz, 90% H$_2$O / 10% D$_2$O rt
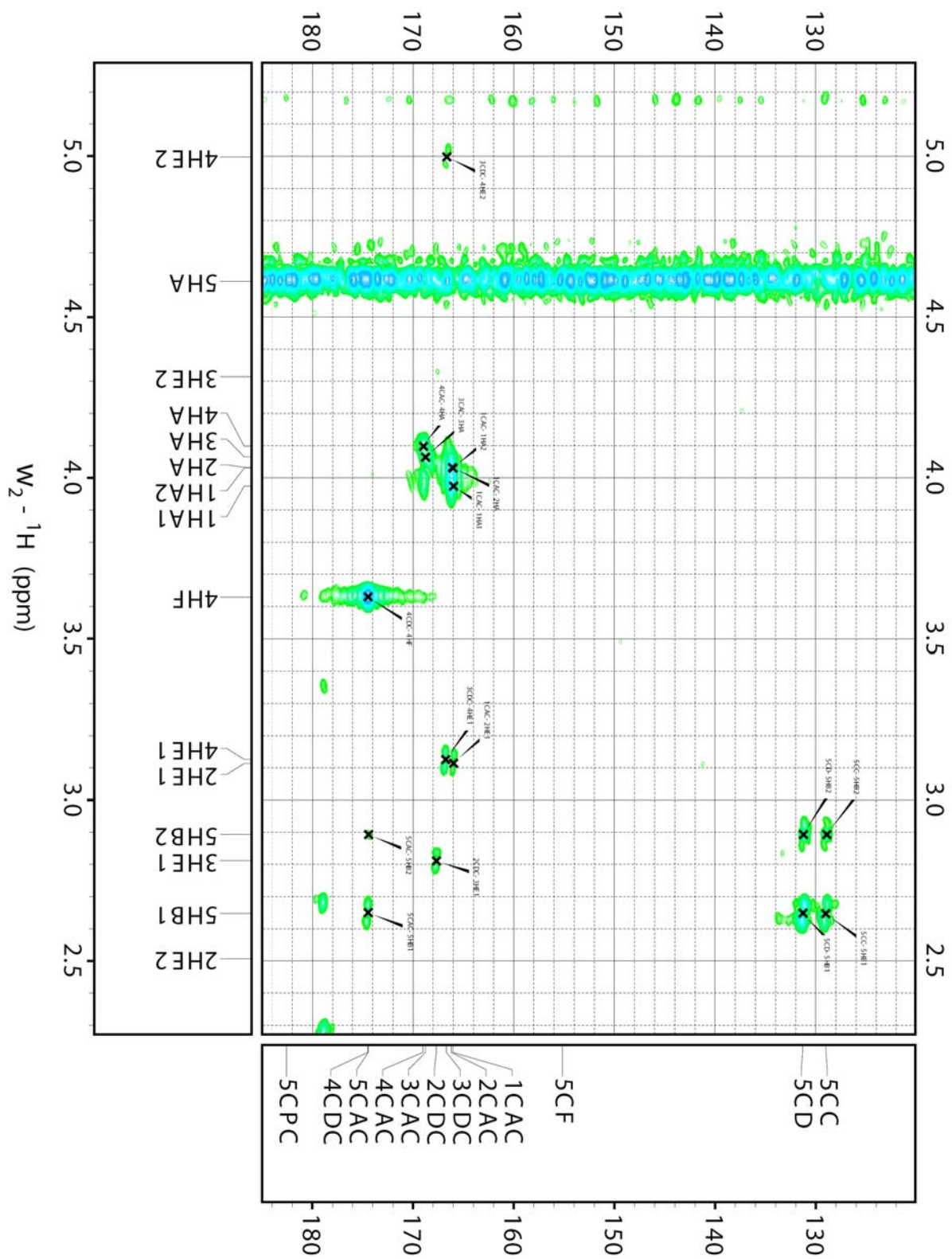
Figure 68: HMBC spectrum (2 of 4) of oligomer **22**, 500 MHz, 90% H$_2$O / 10% D$_2$O rt

188
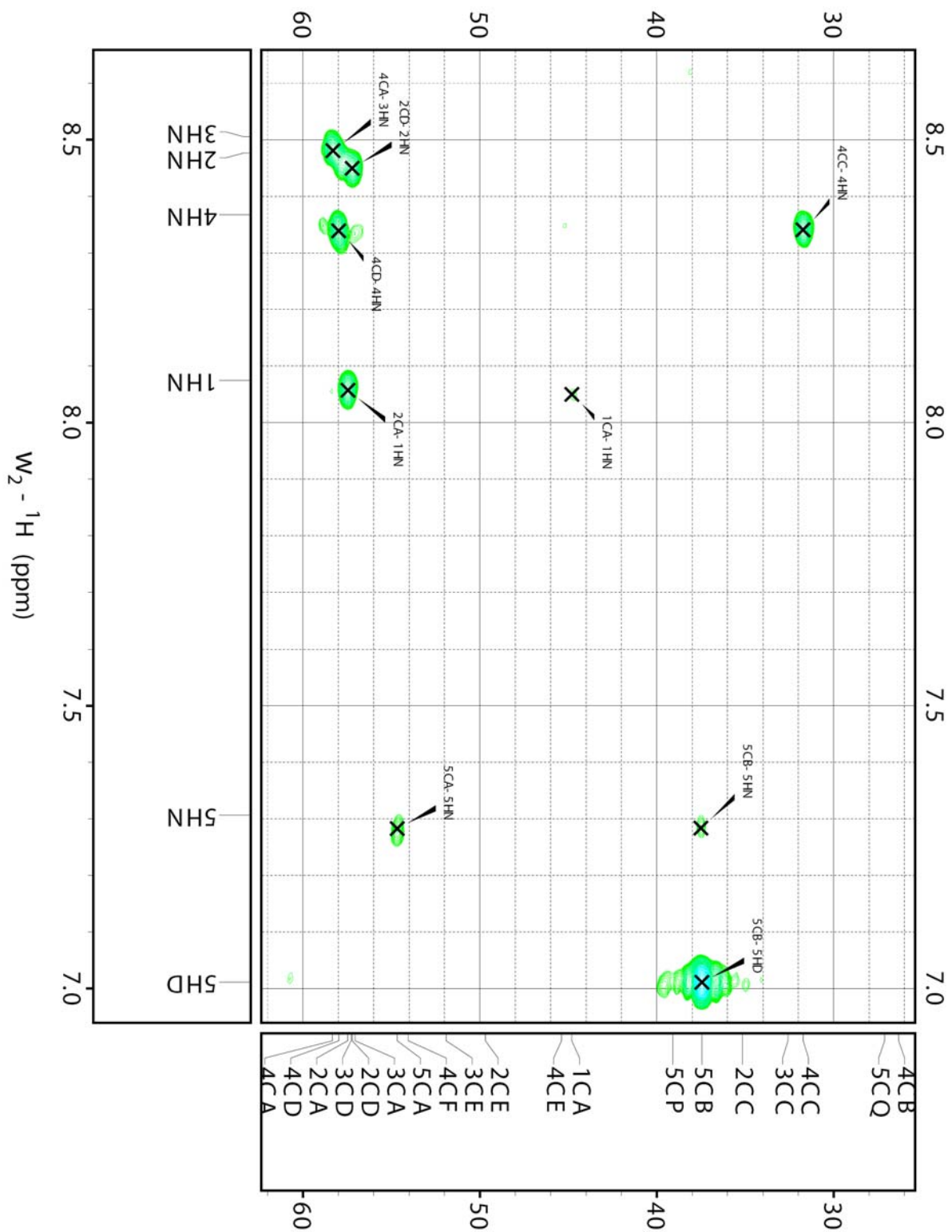
Figure 69: HMBC spectrum (3 of 4) of oligomer **22**, 500 MHz, 90% H$_2$O / 10% D$_2$O rt

Figure 70: HMBC spectrum (4 of 4) of oligomer **22**, 500 MHz, 90% H$_2$O / 10% D$_2$O rt
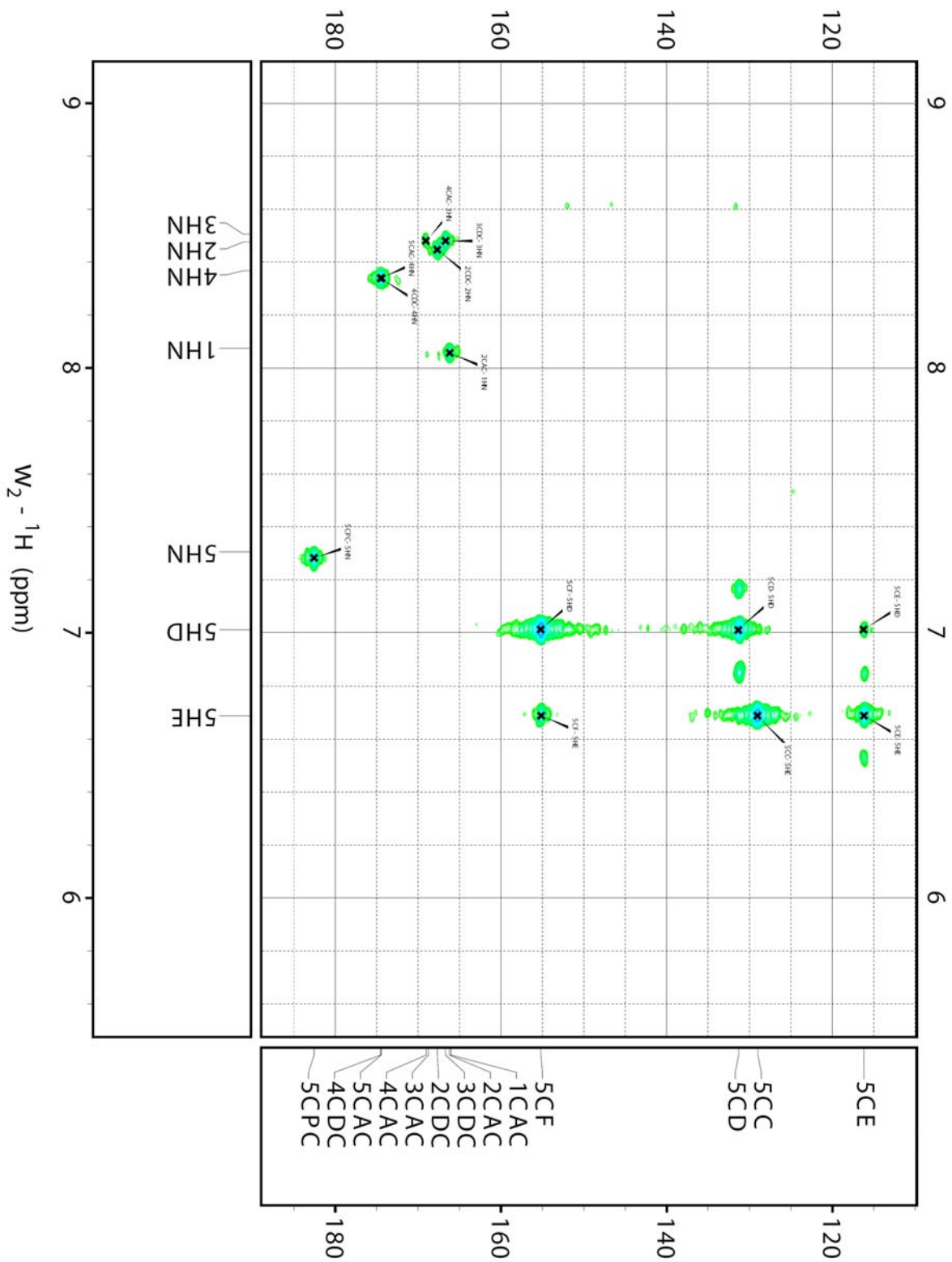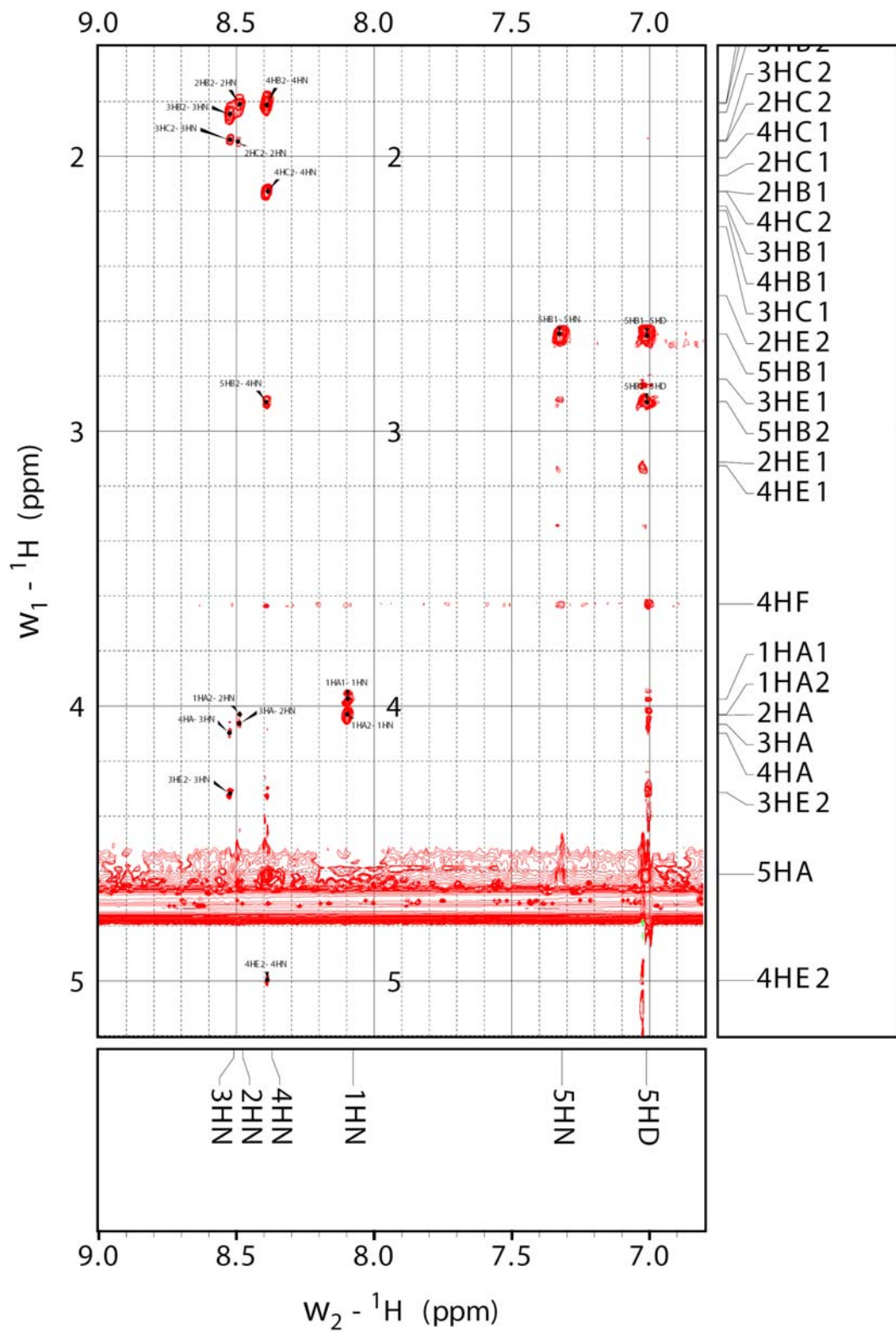
Figure 71: ROESY spectrum (1 of 2) of oligomer **22**, 600 MHz, 90% H$_2$O / 10% D$_2$O rt
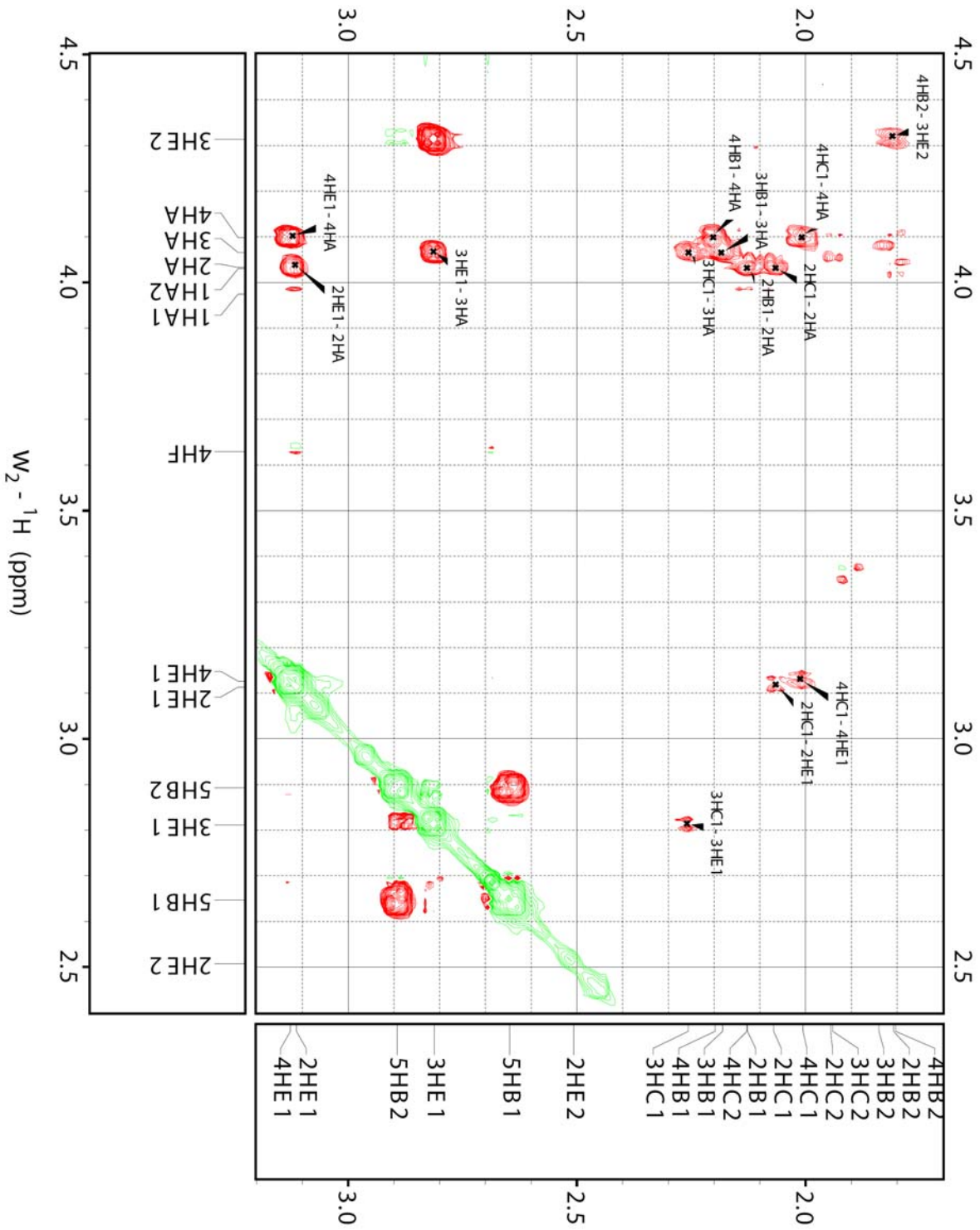
Figure 72: ROESY spectrum (2 of 2) of oligomer **22**, 600 MHz, 90% H$_2$O / 10% D$_2$O rt
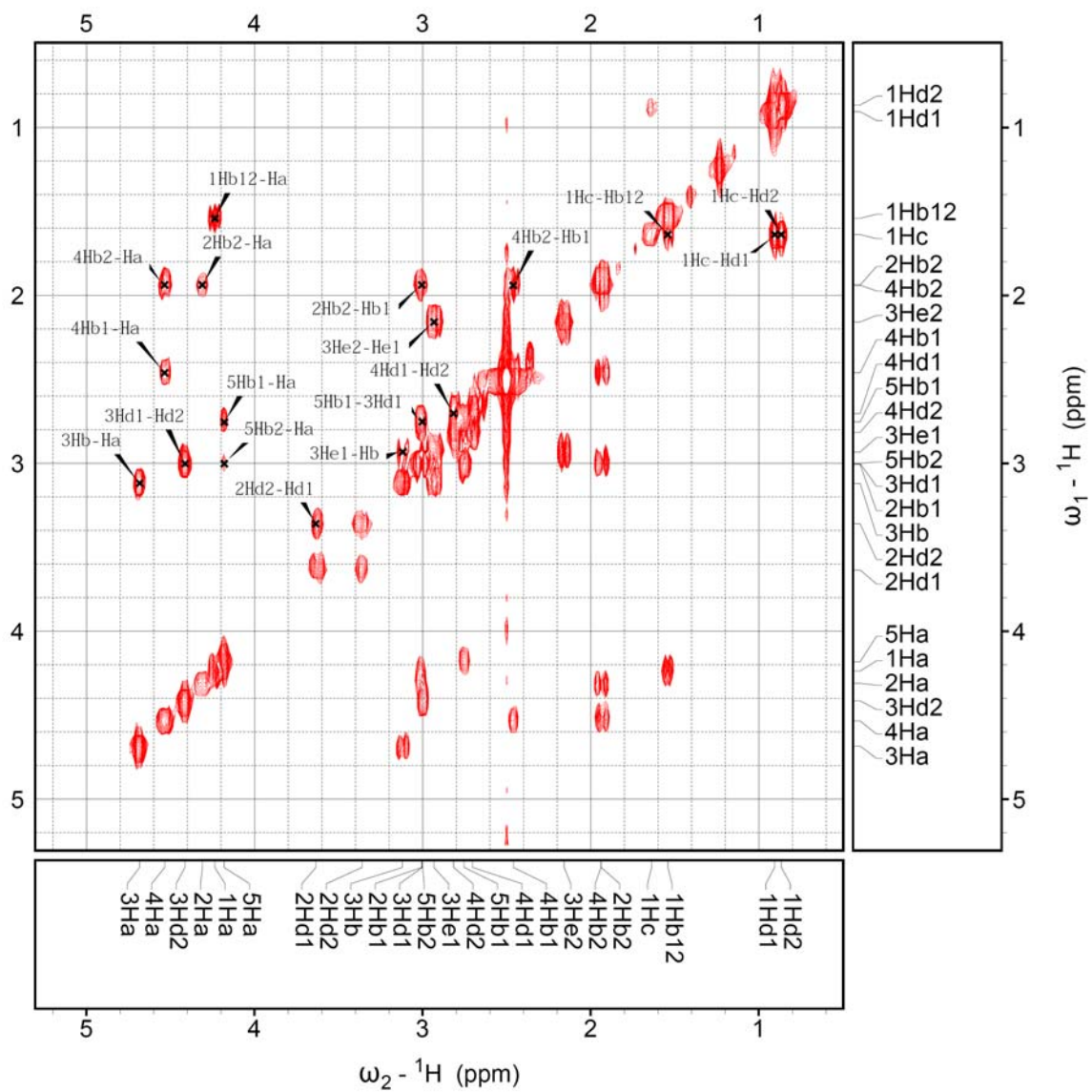
Figure 73: COSY spectrum (1 of 2) of oligomer **84**, 500 MHz, DMSO-*d6,* rt
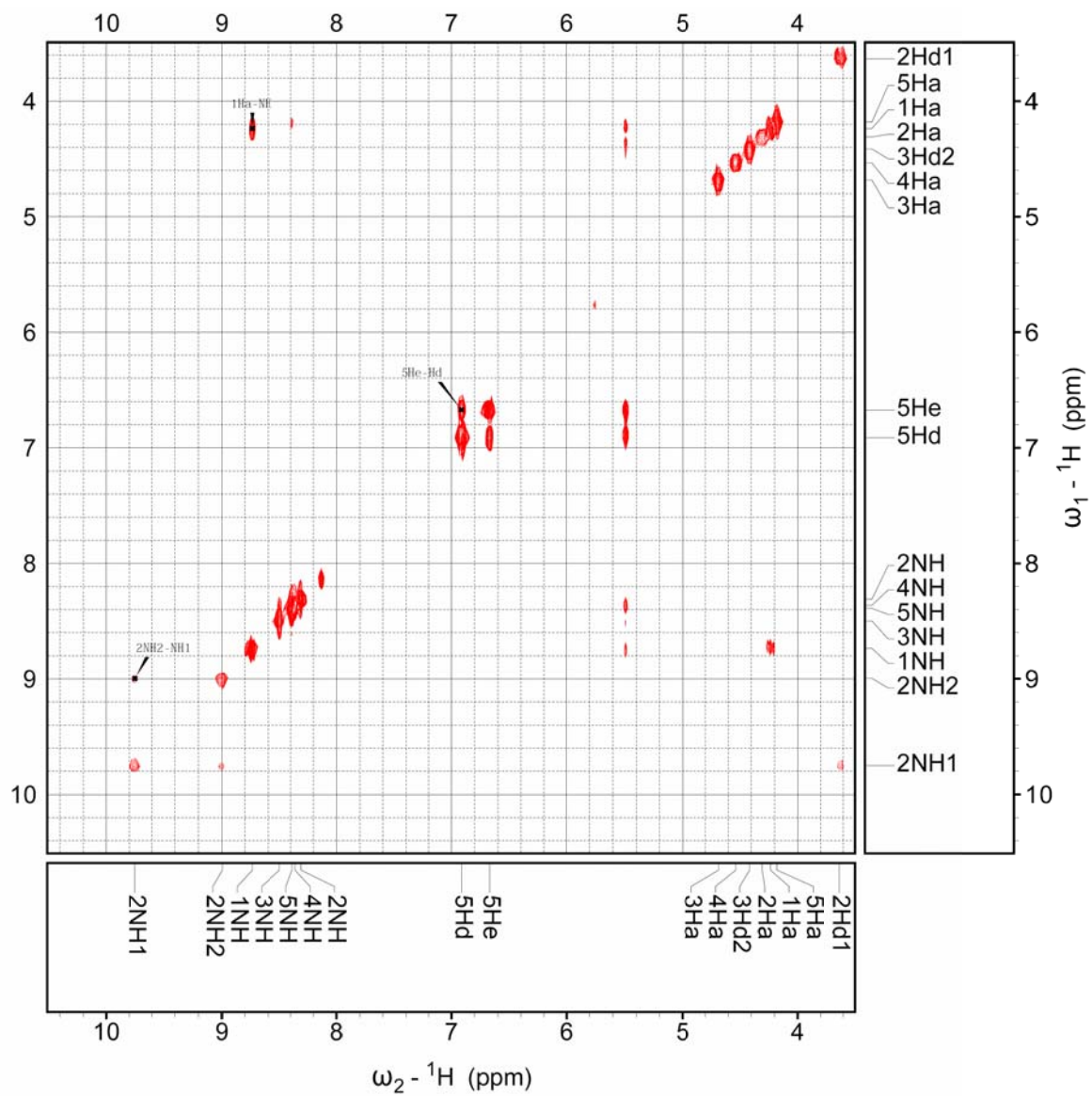
Figure 74: COSY spectrum (2 of 2) of oligomer **84**, 500 MHz, DMSO-*d6,* rt

Figure 75: TOCSY spectrum (1 of 2) of oligomer **84**, 500 MHz, DMSO-*d6,* rt

195
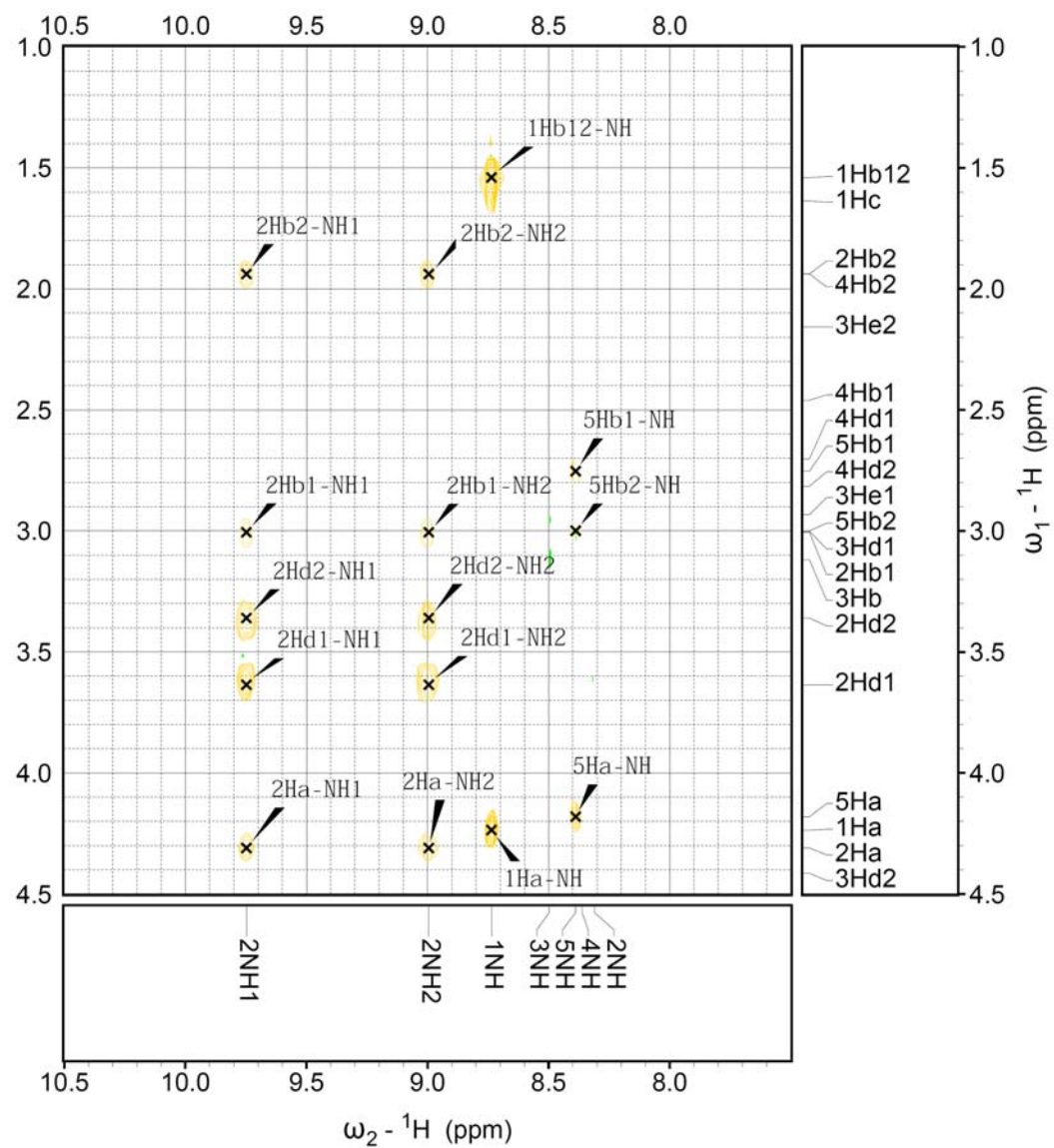
Figure 76: TOCSY spectrum (2 of 2) of oligomer **84**, 500 MHz, DMSO-*d6,* rt
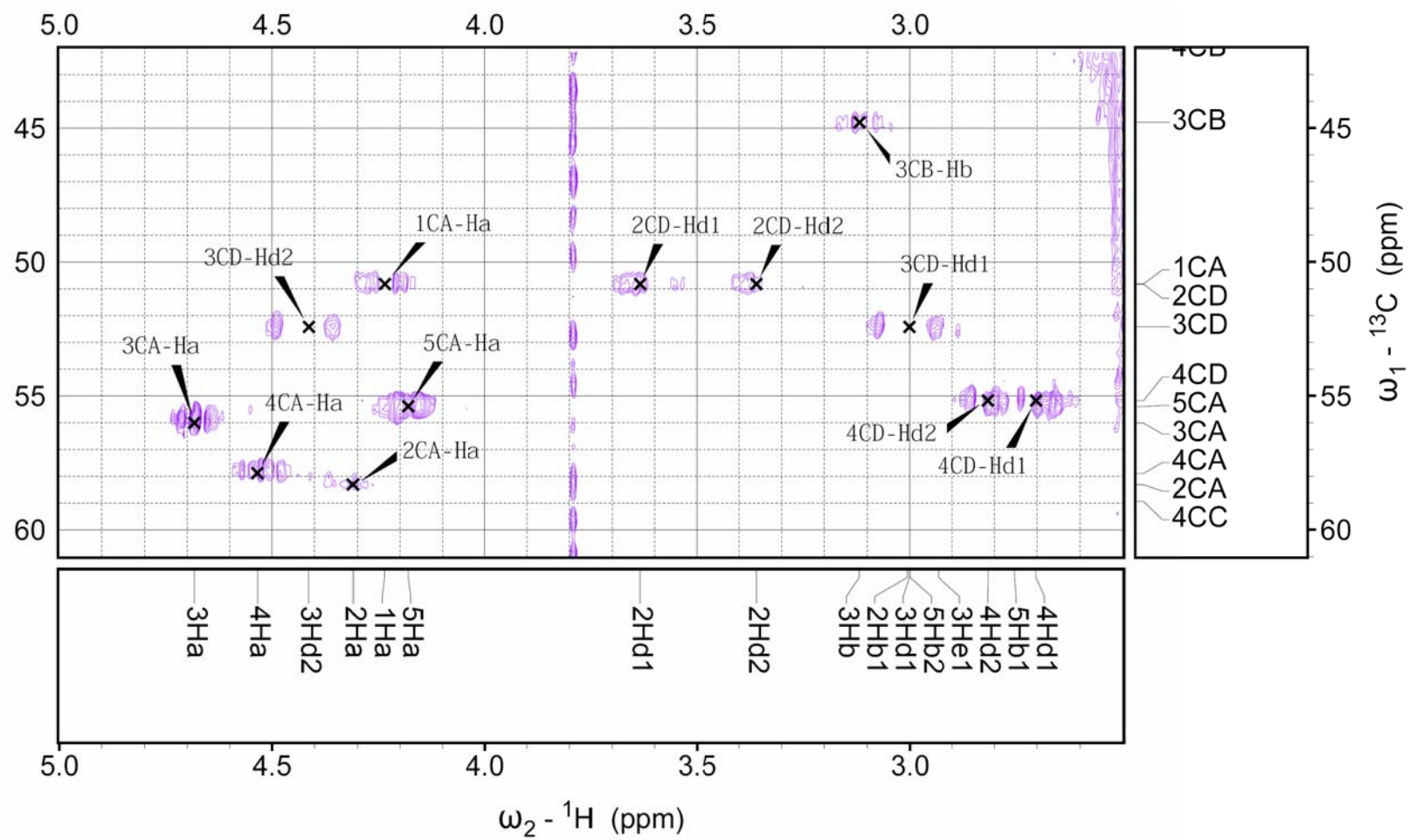
Figure 77: HMQC spectrum (1 of 2) of oligomer **84**, 500 MHz, DMSO-*d6,* rt
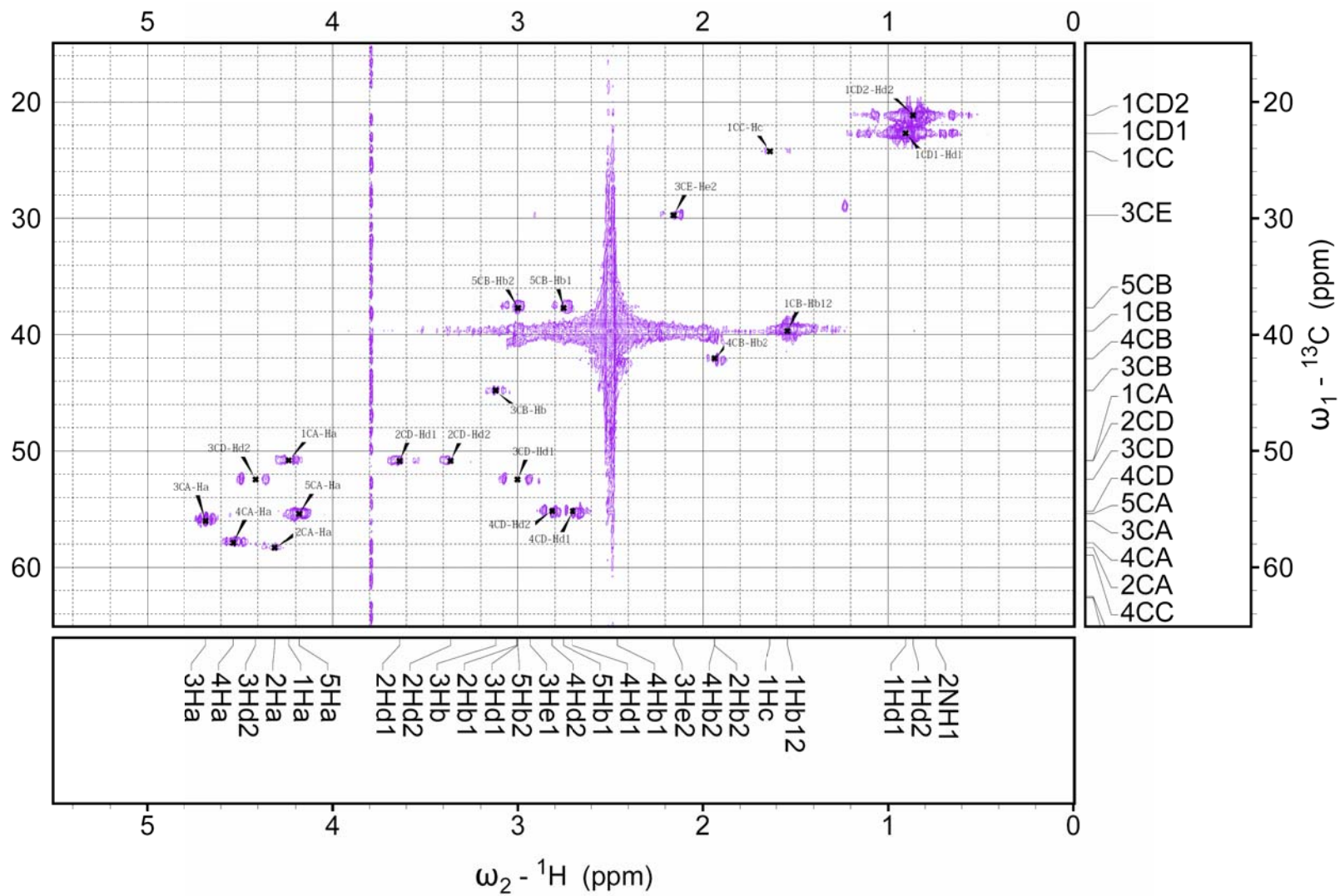
Figure 78: HMQC spectrum (2 of 2) of oligomer **84**, 500 MHz, DMSO-*d6,* rt
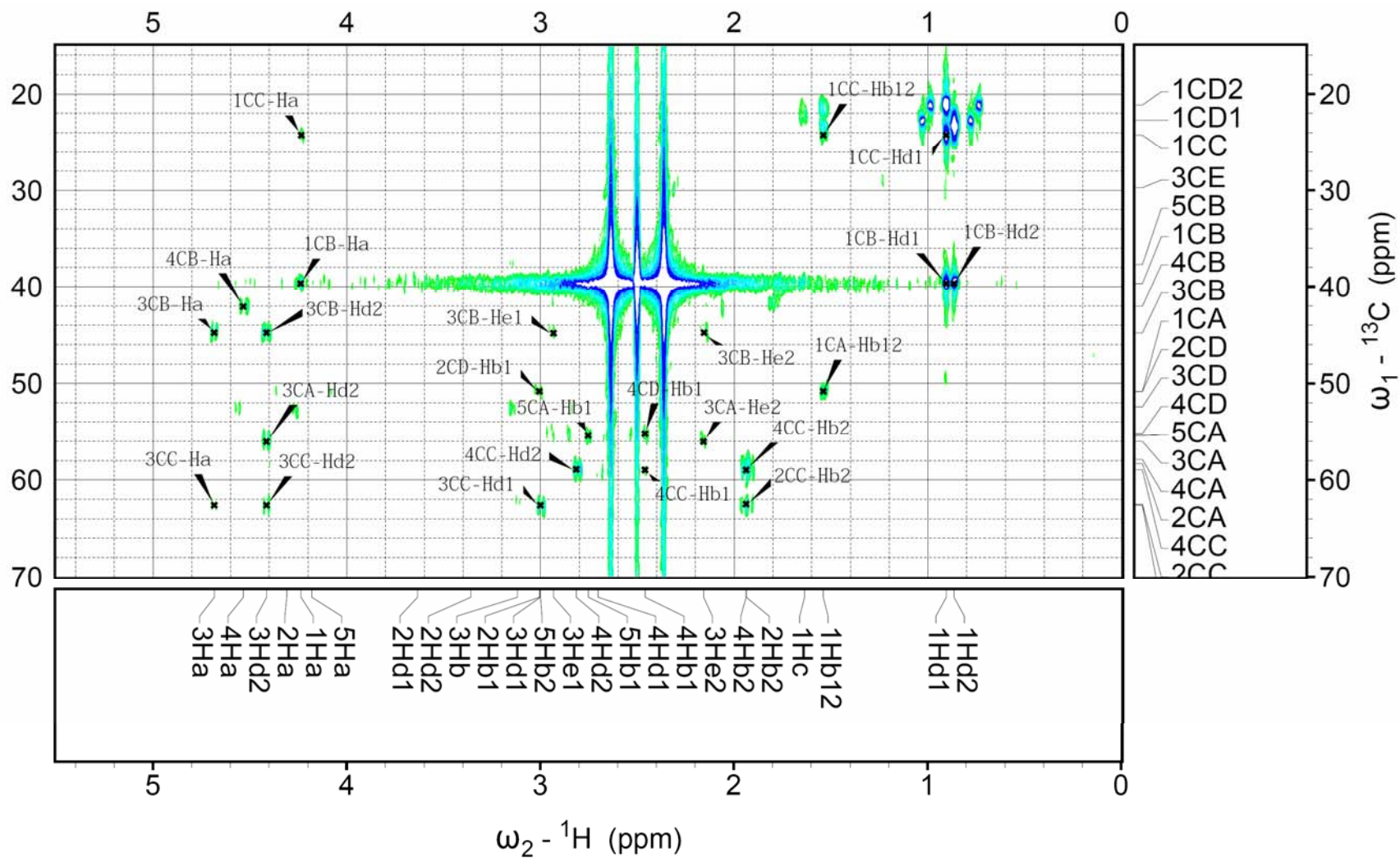
Figure 79: HMBC spectrum (1 of 4) of oligomer **84**, 500 MHz, DMSO-*d6,* rt
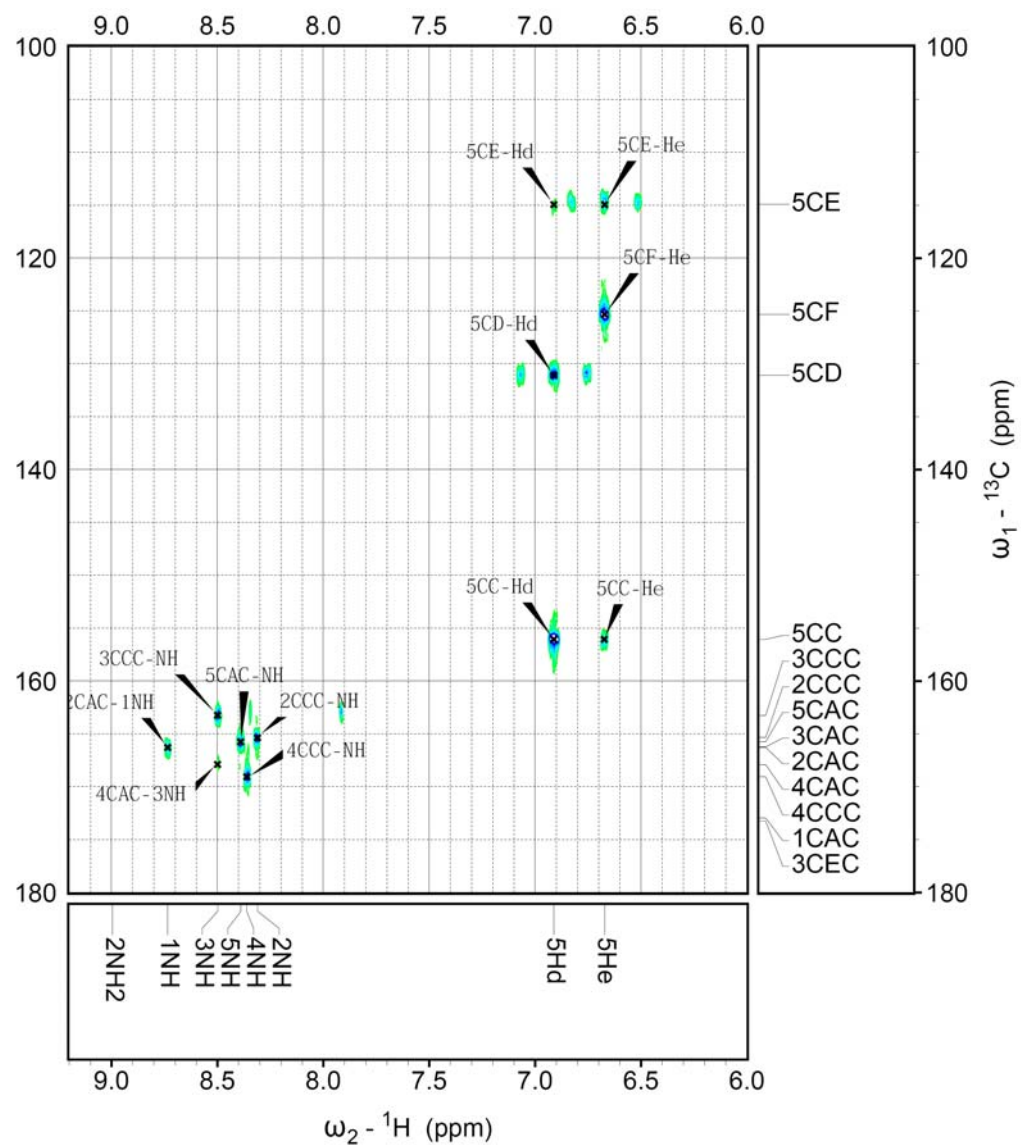
Figure 80: HMBC spectrum (2 of 4) of oligomer **84**, 500 MHz, DMSO-*d6,* rt
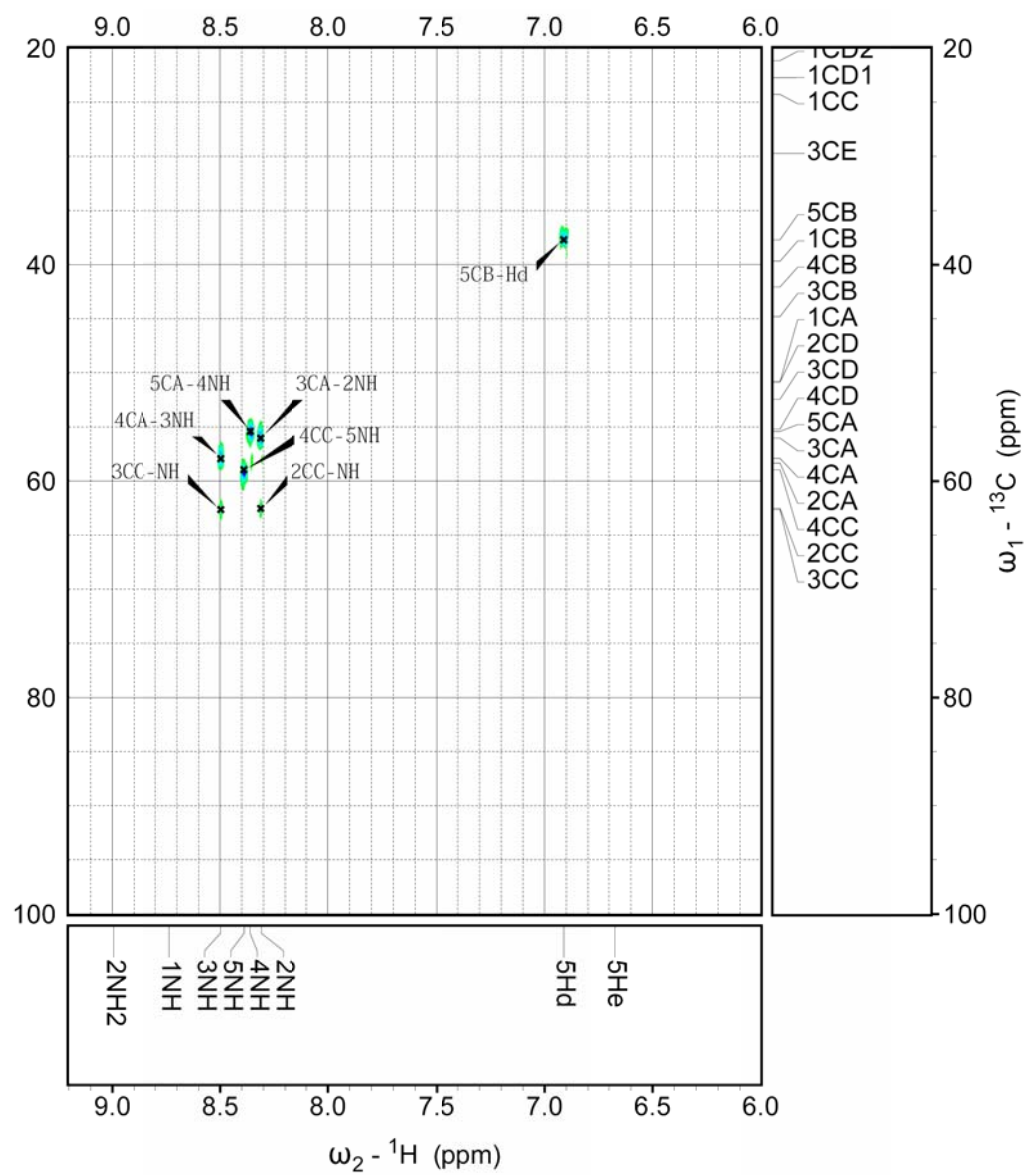
Figure 81: HMBC spectrum (3 of 4) of oligomer **84**, 500 MHz, DMSO-*d6,* rt
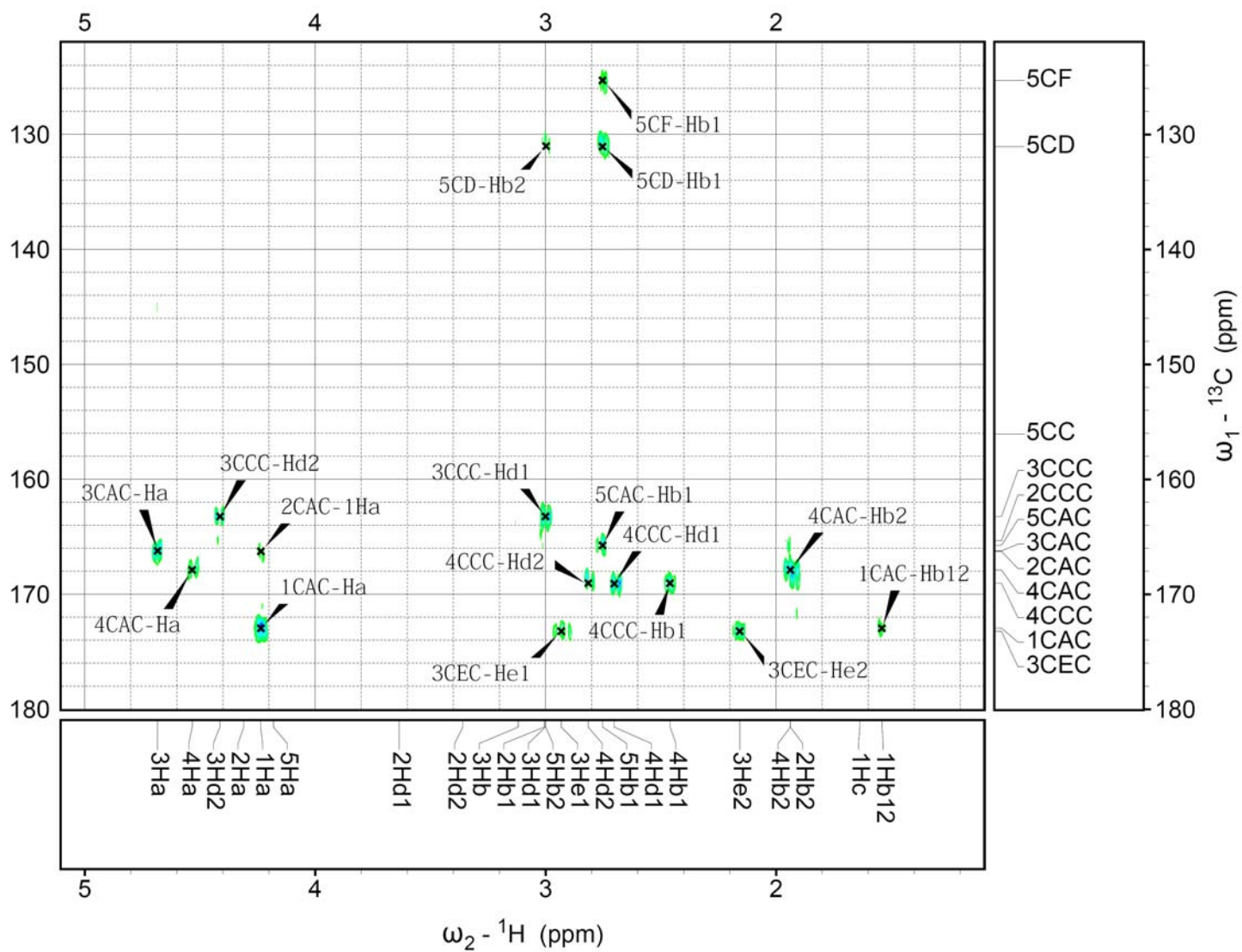
Figure 82: HMBC spectrum (4 of 4) of oligomer **84**, 500 MHz, DMSO-*d6*, rt
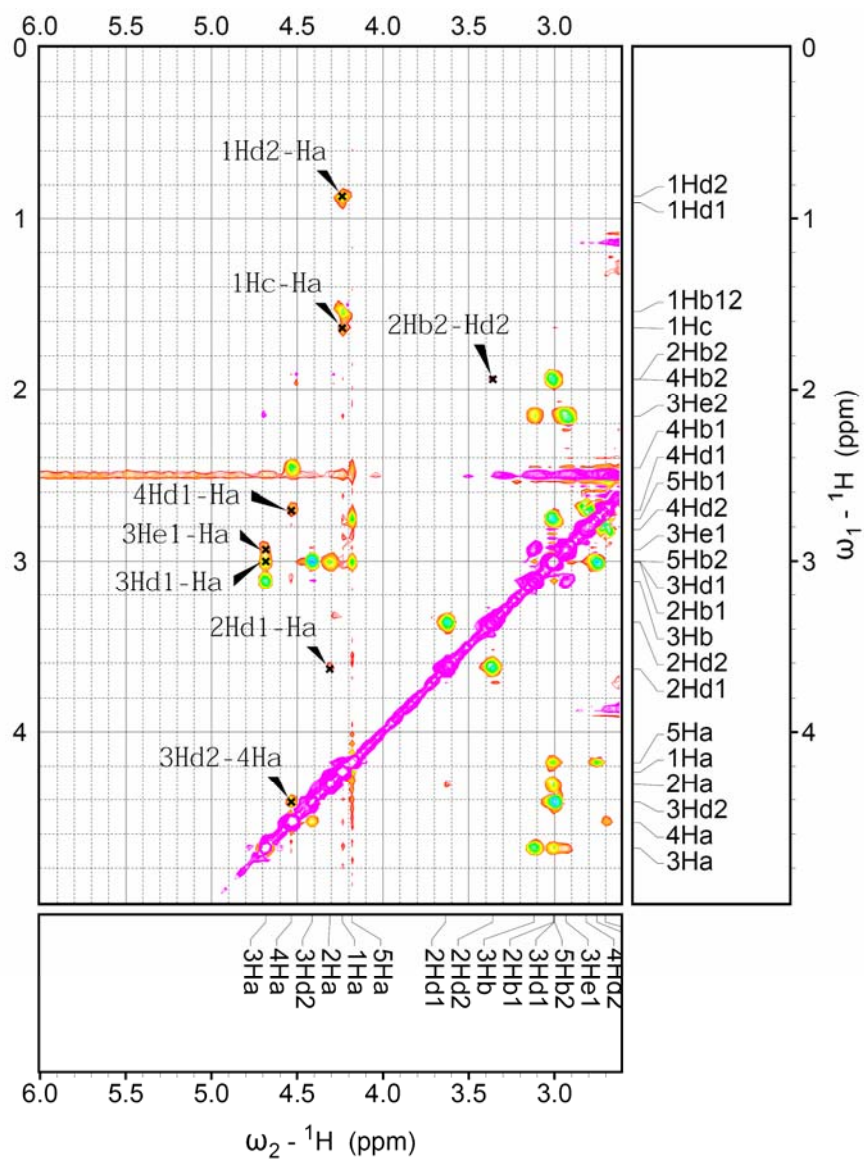
Figure 83: ROESY spectrum (1 of 2) of oligomer **84**, 500 MHz, DMSO-*d6,* rt
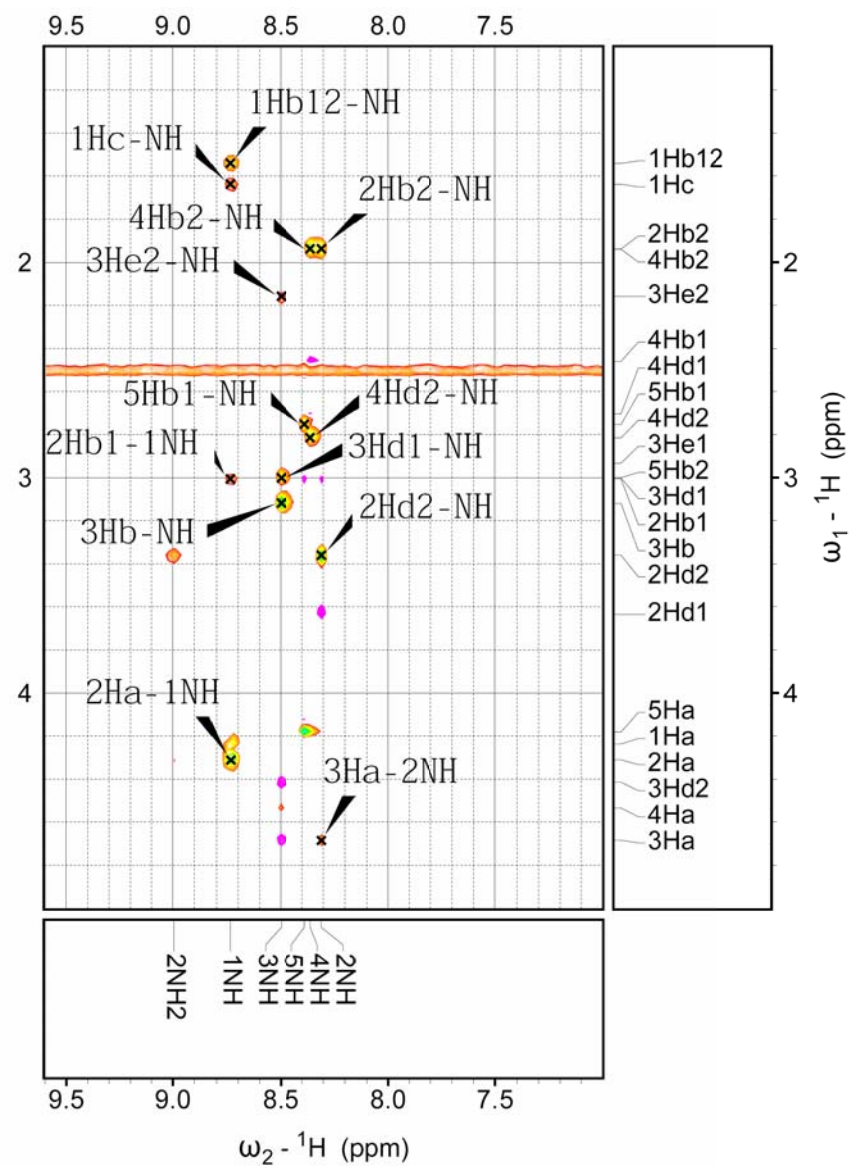
Figure 84: ROESY spectrum (2 of 2) of oligomer **84**, 500 MHz, DMSO-*d6,* rt

APPENDIX D

SPPS SHEMATICS
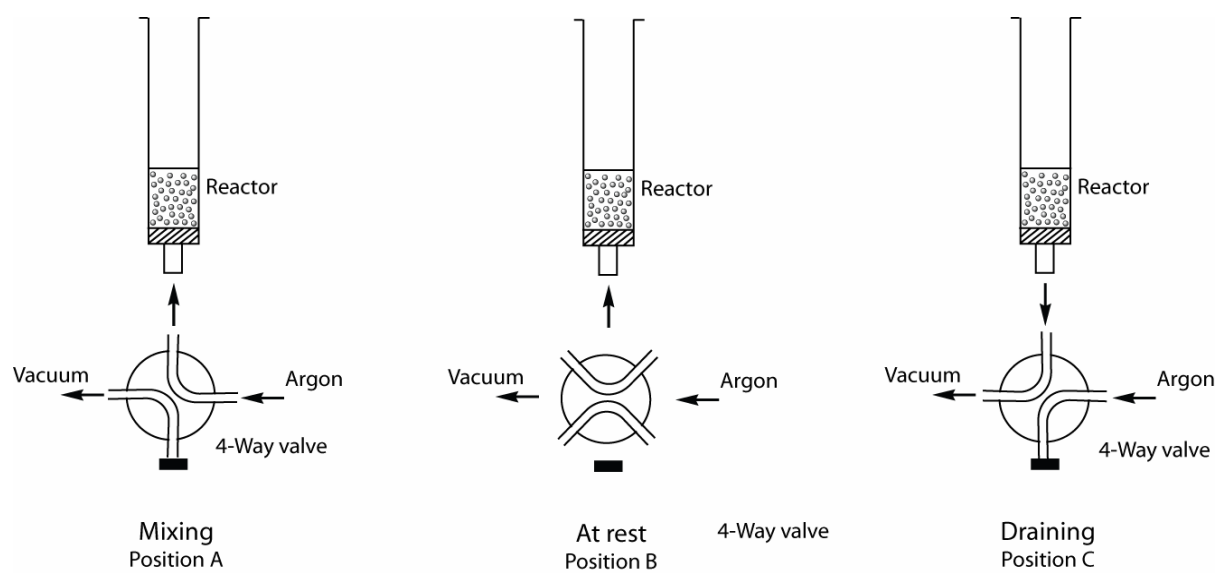
Figure 85: A schematics for solid phase peptide synthesis (SPPS) reactor assembly. Three configurations utilized for the synthesis and corresponding flow directions are shown.

BIBLIOGRAPHY

1.   Goodman, C. M.; Choi, S.; Shandler, S.; DeGrado, W. F. Foldamers as versatile frameworks for the design and evolution of function. *Nature Chemical Biology* **2007,** 3, 252-262.

2.   Horne, W. S.; Price, J. L.; Gellman, S. H. Interplay among side chain sequence, backbone composition, and residue rigidification in polypeptide folding and assembly. *Proceedings of the National Academy of Sciences of the United States of America* **2008,** 105, 9151-9156.

3.   Yoo, B.; Kirshenbaum, K. Peptoid architectures: elaboration, actuation, and application. *Current Opinion in Chemical Biology* **2008,** 12, 714-721.

4.   Robson, B.; Vaithilingam, A., Protein Folding Revisited. In *Molecular Biology of Protein Folding, Pt B*, 2008; Vol. 84, pp 161-202.

5.   DeBartolo, J.; Colubri, A.; Jha, A. K.; Fitzgerald, J. E.; Freed, K. F.; Sosnick, T. R. Mimicking the folding pathway to improve homology-free protein structure prediction. *Proceedings of the National Academy of Sciences of the United States of America* **2009,** 106, 3734-3739.

6.   Voelz, V. A.; Shell, M. S.; Dill, K. A. Predicting Peptide Structures in Native Proteins from Physical Simulations of Fragments. *Plos Computational Biology* **2009,** 5.

7.   DeGrado, W. F.; Summa, C. M.; Pavone, V.; Nastri, F.; Lambardi, A. De novo design and structural charcaterization of proteins and metalloproteins. *Annu. Rev. Biochem.* **1999,** 68, 779-819.

8.   Baker, D. Prediction and design of macromolecular structures and interactions. *Phil. Trans. R. Soc.Lond.B* **2006,** 361, 459-463.

9.   Alexandrova, A. N.; Rothlisberger, D.; Baker, D.; Jorgensen, W. L. Catalytic Mechanism and Performance of Computationally Designed Enzymes for Kemp Elimination. *J. Am. Chem. Soc.* **2008,** 130, 15907-15915.

10.   Gellman, S. H. Foldamers: A manifesto. *Acc. Chem. Res.* **1998,** 31, 173-180.

11.   Hill, D. J.; Mio, M. J.; Prince, R. B.; Hughes, T. S.; Moore, J. S. A Field Guide to Foldamers. *Chem. Rev.* **2001,** 101, 3893-4011.

12.   Kirshenbaum, K.; Zuckermann, K.; Dill, K. A. Designing Polymers that Mimic Biomolecules. *Curr. Opin. Struc. Biol.* **1999,** 9, 530-535.

13.   Rueping, M.; Mahajan, Y.; Sauer, M.; Seebach, D. Cellular uptake studies with beta-peptides. *Chembiochem* **2002,** 3, 257-259.

14.   Harker, E. A.; Schepartz, A. Cell-Permeable beta-Peptide Inhibitors of p53/hDM2 Complexation. *Chembiochem* **2009,** 10, 990-993.

15.   Kritzer, J. A.; Lear, J. D.; Hodsdon, M. E.; Schepartz, A. Helical beta-peptide inhibitors of the p53-hDM2 interaction. *J. Am. Chem. Soc.* **2004,** 126, 9468-9469.

16.   Hardcastle, I. R. Inhibitors of the MDM2-p53 interaction as anticancer drugs. *Drugs of the Future* **2007,** 32, 883-896.

17.   Baldauf, C.; Pisabarro, M. T. Stable hairpins with beta-peptides: Route to tackle protein-protein interactions. *Journal of Physical Chemistry B* **2008,** 112, 7581-7591.

18.   Horne, W. S.; Boersma, M. D.; Windsor, M. A.; Gellman, S. H. Sequence-based design of alpha/beta-peptide foldamers that mimic BH3 domains. *Angewandte Chemie-International Edition* **2008,** 47, 2853-2856.

19.   Harker, E. A.; Daniels, D. S.; Guarracino, D. A.; Schepartz, A. beta-Peptides with improved affinity for hDM2 and hDMX. *Bioorganic & Medicinal Chemistry* **2009,** 17, 2038-2046.

20.   Hintersteiner, M.; Kimmerlin, T.; Garavel, G.; Schindler, T.; Bauer, R.; Meisner, N. C.; Seifert, J. M.; Uhl, V.; Auer, M. A Highly Potent and Cellularly Active beta-Peptidic Inhibitor of the p53/hDM2 Interaction. *Chembiochem* **2009,** 10, 994-998.

21.   Gelman, M. A.; Richter, S.; Cao, H.; Umezawa, N.; Gellman, S. H.; Rana, T. M. Selective binding of TAR RNA by a tat-derived beta-peptide. *Org. Lett.* **2003,** 5, 3563-3565.

22.   Bonnard, V.; Azoulay, S.; Di Giorgio, A.; Patino, N. Polyamide amino acids: a new class of RNA ligands. *Chemical Communications* **2009,** 2302-2304.

23.   Epand, R. F.; Raguse, T. L.; Gellman, S. H.; Epand, R. M. Antimicrobial 14-helical beta-peptides: Potent bilayer disrupting agents. *Biochemistry* **2004,** 43, 9527-9535.

24.   Som, A.; Vemparala, S.; Ivanov, I.; Tew, G. N. Synthetic mimics of antimicrobial peptides. *Biopolymers* **2008,** 90, 83-93.

25.   Miller, C. A.; Abbott, N. L.; de Pablo, J. J. Surface Activity of Amphiphilic Helical beta-Peptides from Molecular Dynamics Simulation. *Langmuir* **2009,** 25, 2811-2823.

26. Fischer, P. M. Peptide, peptidomimetic, and small-molecule antagonists of the p53-HDM2 protein-protein interaction. *International Journal of Peptide Research and Therapeutics* **2006,** 12, 3-19.

27. Aina, O. H.; Liu, R. W.; Sutcliffe, J. L.; Marik, J.; Pan, C. X.; Lam, K. S. From combinatorial chemistry to cancer-targeting peptides. *Molecular Pharmaceutics* **2007,** 4, 631-651.

28. Fear, G.; Komarnytsky, S.; Raskin, I. Protease inhibitors and their peptidomimetic derivatives as potential drugs. *Pharmacology & Therapeutics* **2007,** 113, 354-368.

29. Huther, A.; Dietrich, U. The emergence of peptides as therapeutic drugs for the inhibition of HIV-1. *Aids Reviews* **2007,** 9, 208-217.

30. Li, S.; Xu, W. F. Peptidomimetics and metalloprotease inhibitors as anticancer drugs. *Science in China Series B-Chemistry* **2009,** 52, 535-548.

31. Karle, I. L.; Handa, B. K.; Hassall, C. H. Conformation of cyclic tetra peptide-L-Ser (O-t-Bu)-β-Ala-Gly-L-β-Asp(Ome) containing a 14 membered ring. *Acta Crystallogr. B* **1975,** 31, 555-560.

32. Zuckermann, R. N. The chemical synthesis of peptidomimetic libraries. *Curr. Opin. Struc. Biol.* **1993,** 580-584.

33. Seebach, D.; Overhand, M.; KÃ¼hnle, F. N. M.; Martinoni, B.; Oberer, L.; Hommel, U.; Widmer, H. *Helv. Chim. Acta* **1996,** 79, 913.

34. Cheng, R. P.; Gellman, S. H.; DeGrado, W. F. *Chem. Rev.* **2001,** 101, 3219.

35. Appella, D. H.; Christianson, L. A.; Karle, I. L.; Powell, D. R.; Gellman, S. H. *J. Am. Chem. Soc.* **1996,** 118, 13071.

36. Seebach, D.; Beck, A. K.; Bierbaum, D. J. *Chem. Biodiversity* **2004,** 1.

37. Zega, A. Azapeptides as pharmacological agents. *Current Medicinal Chemistry* **2005,** 12, 589-597.

38. Loser, R.; Frizler, M.; Schilling, K.; Gutschow, M. Azadipeptide nitriles: Highly potent and proteolytically stable inhibitors of papain-like cysteine proteases. *Angewandte Chemie-International Edition* **2008,** 47, 4331-4334.

39. Violette, A.; Averlant-Petit, M. C.; Semetey, V.; Hemmerlin, C.; Casimir, R.; Graff, R.; Marraud, M.; Briand, J. P.; Rognan, D.; Guichard, G. N,N '-linked oligoureas as foldamers: Chain length requirements for helix formation in protic solvent investigated by circular dichroism, NMR spectroscopy, and molecular dynamics. *J. Am. Chem. Soc.* **2005,** 127, 2156-2164.

40.   Fischer, L.; Didierjean, C.; Jolibois, F.; Semetey, V.; Lozano, J. M.; Briand, J. P.; Marraud, M.; Poteau, R.; Guichard, G. Propensity for local folding induced by the urea fragment in short-chain oligomers. *Organic & Biomolecular Chemistry* **2008,** 6, 2596-2610.

41.   Fischer, L.; Lena, G.; Briand, J. P.; Didierjean, C.; Guichard, G. In *Mixing Urea and Amide Bonds: Synthesis and Self-Organization of New Hybrid Oligomers*, 2009; DelValle, S.; Escher, E.; Lubell, W. D., Eds. 2009; pp 39-40.

42.   Baldauf, C.; Gunther, R.; Hofmann, H. J. Helices in peptoids of alpha- and beta-peptides. *Physical Biology* **2006,** 3, S1-S9.

43.   Sharma, G. V. M.; Babu, B. S.; Ramakrishna, K. V. S.; Nagendar, P.; Kunwar, A. C.; Schramm, P.; Baldauf, C.; Hofmann, H. J. Synthesis and Structure of alpha/delta-Hybrid Peptides-Access to Novel Helix Patterns in Foldamers. *Chemistry-a European Journal* **2009,** 15, 5552-5566.

44.   Li, X.; Wu, Y.-D.; Yang, D. α-Aminoxy Acids: New Possibilities from Foldamers to Anion Receptors and Channels. *Acc. Chem. Res.* **2008,** 41, 1428.

45.   Prest, P. J.; Prince, R. B.; Moore, J. S. Supramolecular organization of oligo(m-phenylene ethynylene)s in the solid-state. *J. Am. Chem. Soc.* **1999,** 121, 5933-5939.

46.   Prince, R. B.; Barnes, S. A.; Moore, J. S. Foldamer-based molecular recognition. *J. Am. Chem. Soc.* **2000,** 122, 2758-2762.

47.   Bum, U. H. F. Poly(aryleneethynylene)s. *Macromolecular Rapid Communications* **2009,** 30, 772-805.

48.   Kang, Y. K.; Lee, O. S.; Deria, P.; Kim, S. H.; Park, T. H.; Bonnell, D. A.; Saven, J. G.; Therien, M. J. Helical Wrapping of Single-Walled Carbon Nanotubes by Water Soluble Poly(p-phenyleneethynylene). *Nano Letters* **2009,** 9, 1414-1418.

49.   Hamuro, Y.; Geib, S. J.; Hamilton, A. D. Oligoanthranilamides. Non-peptide subunits that show formation of specific secondary structure. *J. Am. Chem. Soc.* **1996,** 118, 7529-7541.

50.   Hamuro, Y.; Geib, S. J.; Hamilton, A. D. Novel folding patterns in a family of oligoanthranilamides: Non-peptide oligomers that form extended helical secondary structures. *J. Am. Chem. Soc.* **1997,** 119, 10587-10593.

51.   Ziener, U. Self-Assembled Nanostructures of Oligopyridine Molecules. *Journal of Physical Chemistry B* **2008,** 112, 14698-14717.

52.   Mutai, T.; Araki, K. Fluorescent oligopyridines and their photo-functionality as tunable fluorophores. *Current Organic Chemistry* **2007,** 11, 195-211.

53.   Seebach, D.; Ciceri, P. E.; Overhand, M.; Jaun, B.; Rigo, D.; Oberer, L.; Hommel, U.; Amstutz, R.; Widmer, H. Probing the helical secondary structure of short-chain beta-peptides. *Helvetica Chimica Acta* **1996,** 79, 2043-2066.

54.   Seebach, D.; Overhand, M.; Kuhnle, F. N. M.; Martinoni, B.; Oberer, L.; Hommel, U.; Widmer, H. beta-peptides: Synthesis by Arndt-Eistert homologation with concomitant peptide coupling. Structure determination by NMR and CD spectroscopy and by X-ray crystallography. Helical secondary structure of a beta-hexapeptide in solution and its stability towards pepsin. *Helvetica Chimica Acta* **1996,** 79, 913-941.

55.   Seebach, D.; Gademann, K.; Schreiber, J. V.; Matthews, J. L.; Hintermann, T.; Jaun, B.; Oberer, L.; Hommel, U.; Widmer, H. 'Mixed' beta-peptides: A unique helical secondary structure in solution. *Helvetica Chimica Acta* **1997,** 80, 2033-2038.

56.   Seebach, D.; Abele, S.; Sifferlen, T.; Hanggi, M.; Gruner, S.; Seiler, P. Preparation and structure of beta-peptides consisting of geminally disubstituted beta(2,2)- and beta(3,3)-amino acids: A turn motif for beta-peptides. *Helvetica Chimica Acta* **1998,** 81, 2218-2243.

57.   Seebach, D.; Abele, S.; Gademann, K.; Jaun, B. Pleated sheets and turns of beta-peptides with proteinogenic side chains. *Angewandte Chemie-International Edition* **1999,** 38, 1595-1597.

58.   Daura, X.; Gademann, K.; Schafer, H.; Jaun, B.; Seebach, D.; van Gunsteren, W. F. The beta-peptide hairpin in solution: Conformational study of a beta-hexapeptide in methanol by NMR spectroscopy and MD simulation. *J. Am. Chem. Soc.* **2001,** 123, 2393-2404.

59.   Hook, D. F.; Bindschadler, P.; Mahajan, Y. R.; Sebesta, R.; Kast, P.; Seebach, D. The proteolytic stability of 'designed' beta-peptides containing alpha-peptide-bond mimics and of mixed alpha,beta-peptides: Application to the construction of MHC-binding peptides. *Chemistry & Biodiversity* **2005,** 2, 591-632.

60.   Gademann, K.; Seebach, D. Synthesis of cyclo-beta-tripeptides and their biological in vitro evaluation as antiproliferatives against the growth of human cancer cell lines. *Helvetica Chimica Acta* **2001,** 84, 2924-2937.

61.   Nunn, C.; Rueping, M.; Langenegger, D.; Schuepbach, E.; Kimmerlin, T.; Micuch, P.; Hurth, K.; Seebach, D.; Hoyer, D. beta(2)/beta(3)-di- and alpha/beta(3)-tetrapeptide derivatives as potent agonists at somatostatin sst(4) receptors. *Naunyn-Schmiedebergs Archives of Pharmacology* **2003,** 367, 95-103.

62.   Gardiner, J.; Langenegger, D.; Hoyer, D.; Beck, A. K.; Mathad, R. I.; Seebach, D. The enantiomer of octreotate binds to all five somatostatin receptors with almost equal micromolar affinity - A comparison with SANDOSTATIN (R). *Chemistry & Biodiversity* **2008,** 5, 1213-1224.

63.   Gademann, K.; Ernst, M.; Seebach, D.; Hoyer, D. The cyclo-beta-tetrapeptide (beta-HPhe-beta-HThr-beta-HLys-beta-HTrp): Synthesis, NMR structure in methanol solution, and affinity for human somatostatin receptors. *Helvetica Chimica Acta* **2000,** 83, 16-33.

64.   Appella, D. H.; Barchi, J. J.; Durell, S. R.; Gellman, S. H. Formation of short, stable helices in aqueous solution by beta-amino acid hexamers. *J. Am. Chem. Soc.* **1999,** 121, 2309-2310.

65.   Appella, D. H.; Christianson, L. A.; Karle, I. L.; Powell, D. R.; Gellman, S. H. Synthesis and characterization of trans-2-aminocyclohexanecarboxylic acid oligomers: An unnatural helical secondary structure and implications for beta-peptide tertiary structure. *J. Am. Chem. Soc.* **1999,** 121, 6206-6212.

66.   Chung, Y. J.; Huck, B. R.; Christianson, L. A.; Stanger, H. E.; Krauthauser, S.; Powell, D. R.; Gellman, S. H. Stereochemical control of hairpin formation in beta-peptides containing dinipecotic acid reverse turn segments. *J. Am. Chem. Soc.* **2000,** 122, 3995-4004.

67.   Cheng, R. P.; Gellman, S. H.; DeGrado, W. F. beta-peptides: From structure to function. *Chemical Reviews* **2001,** 101, 3219-3232.

68.   Sadowsky, J. D.; Fairlie, W. D.; Hadley, E. B.; Lee, H. S.; Umezawa, N.; Nikolovska-Coleska, Z.; Wang, S. M.; Huang, D. C. S.; Tomita, Y.; Gellman, S. H. (alpha/beta+alpha)-Peptide antagonists of BH3 Domain/Bcl-x(L) recognition: Toward general strategies for foldamer-based inhibition of protein-protein interactions. *J. Am. Chem. Soc.* **2007,** 129, 139-154.

69.   Sadowsky, J. D.; Murray, J. K.; Tomita, Y.; Gellman, S. H. Exploration of backbone space in foldamers containing alpha- and beta-amino acid residues: Developing protease-resistant oligomers that bind tightly to the BH3-recognition cleft of Bcl-x(L). *Chembiochem* **2007,** 8, 903-916.

70.   Horne, W. S.; Gellman, S. H. Foldamers with Heterogeneous Backbones. *Accounts of Chemical Research* **2008,** 41, 1399-1408.

71.   Yang, D.; Ng, F. F.; Li, Z. J.; Wu, Y. D.; Chan, K. W. K.; Wang, D. P. An unusual turn structure in peptides containing alpha-aminoxy acids. *J. Am. Chem. Soc.* **1996,** 118, 9794-9795.

72.   Yang, D.; Qu, J.; Li, B.; Ng, F. F.; Wang, X. C.; Cheung, K. K.; Wang, D. P.; Wu, Y. D. Novel turns and helices in peptides of chiral alpha-aminoxy acids. *J. Am. Chem. Soc.* **1999,** 121, 589-590.

73.   Yang, D.; Li, B.; Ng, F. F.; Yan, Y. L.; Qu, J.; Wu, Y. D. Synthesis and characterization of chiral N-O turns induced by alpha-aminoxy acids. *J. Org. Chem.* **2001,** 66, 7303-7312.

74.   Yang, D.; Qu, J.; Li, W.; Wang, D. P.; Ren, Y.; Wu, Y. D. A reverse turn structure induced by a D,L-alpha-aminoxy acid dimer. *J. Am. Chem. Soc.* **2003,** 125, 14452-14457.

75.   Yang, D.; Qu, J.; Li, W.; Zhang, Y. H.; Ren, Y.; Wang, D. P.; Wu, Y. D. Cyclic hexapeptide of D,L-alpha-aminoxy acids as a selective receptor for chloride ion. *J. Am. Chem. Soc.* **2002,** 124, 12410-12411.

76.   Yang, D.; Li, X.; Sha, Y.; Wu, Y. D. A cyclic hexapeptide comprising alternating alpha-aminoxy and alpha-amino acids is a selective chloride ion receptor. *Chemistry-a European Journal* **2005,** 11, 3005-3009.

77.   Yang, D.; Li, X.; Fan, Y. F.; Zhang, D. W. Enantioselective recognition of carboxylates: A receptor derived from alpha-aminoxy acids functions as a chiral shift reagent for carboxylic acids. *J. Am. Chem. Soc.* **2005,** 127, 7996-7997.

78.   Brown, N. J.; Czyzewski, A. M.; Steinhorn, D. M.; Barron, A. E. In *Peptoid analogues of lung surfactant protein C*, 2007; 2007; pp 432A-432A.

79.   Dohm, M. T.; Ivankin, A.; Brown, N. J.; Liu, C.; Gidalevitz, D.; Barron, A. E. In *Insight into the effect of N-terminal alkylation on the in vitro, surface activity of mixed lipid films containing peptoid mimics of lung surfactant protein C*, 2007; 2007; pp 252A-252A.

80.   Seurynck-Servoss, S. L.; Brown, N. J.; Dohm, M. T.; Wu, C. W.; Barron, A. E. Lipid composition greatly affects the in vitro surface activity of lung surfactant protein mimics. *Colloids and Surfaces B-Biointerfaces* **2007,** 57, 37-55.

81.   Brown, N. J.; Johansson, J.; Barron, A. E. Biomimicry of Surfactant Protein C. *Accounts of Chemical Research* **2008,** 41, 1409-1417.

82.   Brown, N. J.; Wu, C. W.; Seurynck-Servoss, S. L.; Barron, A. E. Effects of hydrophobic helix length and side chain chemistry on biomimicry in peptoid analogues of SP-C. *Biochemistry* **2008,** 47, 1808-1818.

83.   Prince, R. B.; Saven, J. G.; Wolynes, P. G.; Moore, J. S. Cooperative conformational transitions in phenylene ethynylene oligomers: Chain-length dependence. *J. Am. Chem. Soc.* **1999,** 121, 3114-3121.

84.   Heemstra, J. M.; Moore, J. S. Helix stabilization through pyridinium-pi interactions. *Chemical Communications* **2004,** 1480-1481.

85.   Goto, K.; Moore, J. S. Sequence-specific binding of m-phenylene ethynylene foldamers to a piperazinium dihydrochloride salt. *Org. Lett.* **2005,** 7, 1683-1686.

86.   Stone, M. T.; Moore, J. S. Supramolecular chelation based on folding. *J. Am. Chem. Soc.* **2005,** 127, 5928-5935.

87.   Brunsveld, L.; Meijer, E. W.; Prince, R. B.; Moore, J. S. Self-assembly of folded m-phenylene ethynylene oligomers into helical columns. *J. Am. Chem. Soc.* **2001,** 123, 7978-7984.

88.   Cary, J. M.; Moore, J. S. Hydrogen bond-stabilized helix formation of a m-phenylene ethynylene oligomer. *Org. Lett.* **2002,** 4, 4663-4666.

89.   Kubel, C.; Mio, M. J.; Moore, J. S.; Martin, D. C. Molecular packing and morphology of oligo(m-phenylene ethynylene) foldamers. *J. Am. Chem. Soc.* **2002,** 124, 8605-8610.

90.   Ray, C. R.; Moore, J. S., Supramolecular organization of foldable phenylene ethynylene oligomers. In *Poly(Arylene Ethynylene)S: From Synthesis to Application*, 2005; Vol. 177, pp 91-149.

91.   White, S. R.; Sottos, N. R.; Geubelle, P. H.; Moore, J. S.; Kessler, M. R.; Sriram, S. R.; Brown, E. N.; Viswanathan, S. Autonomic healing of polymer composites. *Nature* **2001,** 409, 794-797.

92.   Toohey, K. S.; Sottos, N. R.; Lewis, J. A.; Moore, J. S.; White, S. R. Self-healing materials with microvascular networks. *Nature Materials* **2007,** 6, 581-585.

93.   Yang, J. L.; Keller, M. W.; Moore, J. S.; White, S. R.; Sottos, N. R. Microencapsulation of Isocyanates for Self-Healing Polymers. *Macromolecules* **2008,** 41, 9650-9655.

94.   Yin, H.; Hamilton, A. D. Strategies for targeting protein-protein interactions with synthetic agents. *Angewandte Chemie-International Edition* **2005,** 44, 4130-4163.

95.   Rodriguez, J. M.; Ross, N. T.; Katt, W. P.; Dhar, D.; Lee, G. I.; Hamilton, A. D. Structure and Function of Benzoylurea-Derived alpha-Helix Mimetics Targeting the Bcl-x(L)/Bak Binding Interface. *Chemmedchem* **2009,** 4, 649-656.

96.   Yin, H.; Lee, G. I.; Park, H. S.; Payne, G. A.; Rodriguez, J. M.; Sebti, S. M.; Hamilton, A. D. Terphenyl-based helical mimetics that disrupt the p53/HDM2 interaction. *Angewandte Chemie-International Edition* **2005,** 44, 2704-2707.

97.   Fletcher, S.; Hamilton, A. D. Targeting protein-protein interactions by rational design: mimicry of protein surfaces. *Journal of the Royal Society Interface* **2006,** 3, 215-233.

98.   Saraogi, I.; Hamilton, A. D. alpha-Helix mimetics as inhibitors of protein-protein interactions. *Biochemical Society Transactions* **2008,** 36, 1414-1417.

99.   Saraogi, I.; Hamilton, A. D. Recent advances in the development of aryl-based foldamers. *Chem. Soc. Rev.* **2009,** 38, 1726-1743.

100.   Turkson, J.; Ryan, D.; Kim, J. S.; Zhang, Y.; Chen, Z.; Haura, E.; Laudano, A.; Sebti, S.; Hamilton, A. D.; Jove, R. Phosphotyrosyl peptides block Stat3-mediated DNA binding activity, gene regulation, and cell transformation. *Journal of Biological Chemistry* **2001,** 276, 45443-45455.

101.   Sun, J. Z.; Blaskovich, M. A.; Jain, R. K.; Delarue, F.; Paris, D.; Brem, S.; Wotoczek-Obadia, M.; Lin, Q.; Coppola, D.; Choi, K. H.; Mullan, M.; Hamilton, A. D.; Sebti, S. M. Blocking angiogenesis and tumorigenesis with GFA-116, a synthetic molecule that

inhibits binding of vascular endothelial growth factor to its receptor. *Cancer Research* **2004,** 64, 3586-3592.

102. Sun, J. Z.; Wang, D. A.; Jain, R. K.; Carie, A.; Paquette, S.; Ennis, E.; Blaskovich, M. A.; Baldini, L.; Coppola, D.; Hamilton, A. D.; Sebti, S. M. Inhibiting angiogenesis and tumorigenesis by a synthetic molecule that blocks binding of both VEGF and PDGF to their receptors. *Oncogene* **2005,** 24, 4701-4709.

103. Kim, U. I.; Suk, J. M.; Naidu, V. R.; Jeong, K. S. Folding and Anion-Binding Properties of Fluorescent Oligoindole Foldamers. *Chemistry-a European Journal* **2008,** 14, 11406-11414.

104. Gong, B. Crescent oligoamides: From acyclic "macrocycles" to folding nanotubes. *Chemistry-a European Journal* **2001,** 7, 4336-4342.

105. Gong, B. Hollow Crescents, Helices, and Macrocycles from Enforced Folding and Folding-Assisted Macrocyclization. *Accounts of Chemical Research* **2008,** 41, 1376-1386.

106. Helsel, A. J.; Brown, A. L.; Yamato, K.; Feng, W.; Yuan, L. H.; Clements, A. J.; Harding, S. V.; Szabo, G.; Shao, Z. F.; Gong, B. Highly Conducting Transmembrane Pores Formed by Aromatic Oligoamide Macrocycles. *J. Am. Chem. Soc.* **2008,** 130, 15784-+.

107. Frackenpohl, J.; Arvidsson, P. I.; Schreiber, J. V.; Seebach, D. The outstanding biological stability of beta- and gamma-peptides toward proteolytic enzymes: An in vitro investigation with fifteen peptidases. *Chembiochem* **2001,** 2, 445-455.

108. Levins, C. G.; Schafmeister, C. E. The Synthesis of Functionalized Nanoscale Molecular Rods of Defined Length. *J. Am. Chem. Soc.* **2003,** 125, 4702-4703.

109. Levins, C. G.; Schafmeister, C. E. The Synthesis of Curved and Linear Structures from a Minimal Set of Monomers. *J. Org. Chem.* **2005,** 70, 9002-9008.

110. Levins, C. G.; Brown, Z. Z.; Schafmeister, C. E. Maximizing the Stereochemical Diversity of Spiro-Ladder Oligomers. *Org. Lett.* **2006,** 8, 2807-2810.

111. Habay, S. A.; Schafmeister, C. E. Synthesis of a bis-amino acid that creates a sharp turn. *Org. Lett.* **2004,** 6, 3369-3371.

112. Gupta, S.; Das, B. C.; Schafmeister, C. E. Synthesis of a Pipecolic Acid-Based Bis-amino Acid and Its Assembly into a Spiro Ladder Oligomer. *Org. Lett.* **2005,** 7, 2861-2864.

113. Gupta, S.; Macala, M.; Schafmeister, C. E. Synthesis of structurally diverse bis-peptide oligomers. *J. Org. Chem.* **2006,** 71, 8691-8695.

114. Gupta, S.; Schafmeister, C. E. Synthesis of a Carboxylate Functionalized Bis-Amino acid Monomer. *J. Org. Chem.* **2009,** 74, 3652-3658.

115. Tanaka, H.; Kuroda, A.; Marusawa, H.; Hatanaka, H.; Kino, T.; Goto, T.; Hashimoto, M.; Taga, T. Structure of FK506, a novel immunosuppressant isolated from Streptomyces. *J. Am. Chem. Soc.* **1987,** 109, 5031-3.

116. Rosen, M. K.; Standaert, R. F.; Galat, A.; Nakatsuka, M.; Schreiber, S. L. Inhibition of FKBP rotamase activity by immunosuppressant FK506: twisted amide surrogate. *Science (Washington, D. C., 1883-)* **1990,** 248, 863-6.

117. Emmer, G.; Grassberger, M. A.; Meingassner, J. G.; Schulz, G.; Schaude, M. Derivatives of a Novel Cyclopeptolide. 1. Synthesis, Antifungal Activity, and Structure-Activity Relationships. *J. Med. Chem.* **1994,** 37, 1908-17.

118. Boger, D. L.; Chen, J.-H.; Saionz, K. W. (-)-Sandramycin: Total Synthesis and Characterization of DNA Binding Properties. *J. Am. Chem. Soc.* **1996,** 118, 1629-44.

119. Gupta, S.; Krasnoff, S. B.; Roberts, D. W.; Renwick, J. A. A.; Brinen, L. S.; Clardy, J. Structures of the efrapeptins: potent inhibitors of mitochondrial ATPase from the fungus Tolypocladium niveum. *J. Am. Chem. Soc.* **1991,** 113, 707-9.

120. Toniolo, C. Conformationally restricted peptides through short-range cyclizations. *Int. J. Pept. Protein Res.* **1990,** 35, 287-300.

121. Genin, M. J.; Gleason, W. B.; Johnson, R. L. Design, synthesis, and x-ray crystallographic analysis of two novel spirolactam systems as beta -turn mimics. *J. Org. Chem.* **1993,** 58, 860-6.

122. Matsoukas, J. M.; Agelis, G.; Hondrelis, J.; Yamdagni, R.; Wu, Q.; Ganter, R.; Moore, D.; Moore, G. J.; Smith, J. R. Synthesis and biological activities of angiotensin II, sarilesin, and sarmesin analogs containing Aze or Pip at position 7. *J. Med. Chem.* **1993,** 36, 904-11.

123. Copeland, T. D.; Wondrak, E. M.; Tozser, J.; Roberts, M. M.; Oroszlan, S. Substitution of proline with pipecolic acid at the scissile bond converts a peptide substrate of HIV proteinase into a selective inhibitor. *Biochem. Biophys. Res. Commun.* **1990,** 169, 310-14.

124. Tsuda, Y.; Cygler, M.; Gibbs, B. F.; Pedyczak, A.; Fethiere, J.; Yue, S. Y.; Konishi, Y. Design of Potent Bivalent Thrombin Inhibitors Based on Hirudin Sequence: Incorporation of Nonsubstrate-Type Active Site Inhibitors. *Biochemistry* **1994,** 33, 14443-51.

125. Toniolo, C.; Bardi, R.; Piazzesi, A. M.; Crisma, M.; Balaram, P.; Sukumar, M.; Paul, P. K. C. Preferred conformations of pipecolic acid-containing peptides. *Pept., Proc. Eur. Pept. Symp., 20th* **1989,** 477-9.

126. Didierjean, C.; Aubry, A.; Wyckaert, F.; Boussard, G. Structural features of the Pip/AzPip couple in the crystalline state: influence of the relative AzPip location in an aza dipeptide sequence upon the induced chirality and conformational characteristics. *J. Pept. Res.* **2000,** 55, 308-317.

127. Jhon, J. S.; Kang, Y. K. Conformational Preferences of Proline Analogues with Different Ring Size. *J. Phys. Chem. B* **2007,** 111, 3496-3507.

128. Cowell, G. W.; Ledwith, A. Developments in the chemistry of diazo-alkanes. *Quart. Rev., Chem. Soc.* **1970,** 24, 119-67.

129. Gutsche, C. D. The reaction of diazomethane and its derivatives with aldehydes and ketones. *Org. React.* **1954,** 364-429.

130. Hashimoto, N.; Aoyama, T.; Shioiri, T. New methods and reagents in organic synthesis. 10. Trimethylsilyldiazomethane(TMSCHN2). A new, stable, and safe reagent for the homologation of ketones. *Tetrahedron Lett.* **1980,** 21, 4619-22.

131. Krow, G. R. One carbon ring expansions of bridged bicyclic ketones. *Tetrahedron* **1987,** 43, 3-38.

132. Maruoka, K.; Concepcion, A. B.; Yamamoto, H. Selective homologation of ketones and aldehydes with diazoalkanes promoted by organoaluminum reagents. *Synthesis* **1994,** 1283-90.

133. Maruoka, K.; Concepcion, A. B.; Yamamoto, H. Organoaluminum-Promoted Homologation of Ketones with Diazoalkanes. *J. Org. Chem.* **1994,** 59, 4725-6.

134. Bolin, D. R.; Sytwu, I. I.; Humiec, F.; Meienhofer, J. Preparation of oligomer-free Nalpha -Fmoc and Nalpha -urethane amino acids. *Int. J. Pept. Protein Res.* **1989,** 33, 353-9.

135. Patchett, A. A.; Witkop, B. Hydroxyproline. *J. Am. Chem. Soc.* **1957,** 79, 185-92.

136. Anderson, G. W.; Callahan, F. M. tert-Butyl esters of amino acids and peptides and their use in peptide synthesis. *J. Am. Chem. Soc.* **1960,** 82, 3359-63.

137. Pellicciari, R.; Natalini, B.; Luneia, R.; Marinozzi, M.; Roberti, M.; Rosato, G. C.; Sadeghpour, B. M.; Synyder, J. P.; Monahan, J. B.; Moroni, F. Enantioselective synthesis of naturally occurring trans-4-hydroxy-S-pipecolic acid-4-sulfate, a new potent and selective NMDA receptor agonist. *Med. Chem. Res.* **1992,** 2, 491-6.

138. Liu, H. J.; Ogino, T. New approach to the synthesis of hydrindanonecarboxylates. *Tetrahedron Lett.* **1973,** 4937-40.

139. Marchand, A. P.; Rajapaksa, D.; Reddy, S. P.; Watson, W. H.; Nagl, A. Tieffeneau-Demjanov ring homologations of two pentacyclo[5.4.0.02,6.03,10.05,9]undecane-8,11-diones. *J. Org. Chem.* **1989,** 54, 5086-9.

140. Tai, W. T.; Warnhoff, E. W. beta -Oxo esters from reaction of ethyl diazoacetate with ketones. *Can. J. Chem.* **1964,** 42, 1333-40.

141. Krapcho, A. P.; Glynn, G. A.; Grenon, B. J. The decarbethoxylation of geminal dicarbethoxy compounds. *Tetrahedron Lett.* **1967,** 8, 215-219.

142. Bucherer, H. T.; Fischbeck, H. Hexahydrodiphenylamine and its Derivatives. *J. Prakt. Chem.* **1934,** 140, 69-89.

143. Bucherer, H. T.; Steiner, W. Syntheses of Hydantoins. I. Reactions of α-Oxy and α-Amino Nitriles. *J. Prakt. Chem.* **1934,** 140, 129-50.

144. Ferguson, D. M.; Raber, D. J. A new approach to probing conformational space with molecular mechanics: random incremental pulse search. *J. Am. Chem. Soc.* **1989,** 111, 4371-8.

145. Cornell, W. D.; Cieplak, P.; Bayly, C. I.; Gould, I. R.; Merz, K. M., Jr.; Ferguson, D. M.; Spellmeyer, D. C.; Fox, T.; Caldwell, J. W.; Kollman, P. A. A Second Generation Force Field for the Simulation of Proteins, Nucleic Acids, and Organic Molecules. *J. Am. Chem. Soc.* **1995,** 117, 5179-97.

146. MOE. *2005.06 ed.; Chemical Computing Group, Inc.: Montreal, Canada* **2005**.

147. Kubik, S.; Meissner, R. S.; Rebek, J., Jr. Synthesis of alpha ,alpha -dialkylated amino acids with adenine or thymine residues. A new mild and facile hydrolysis of hydantoins. *Tetrahedron Lett.* **1994,** 35, 6635-8.

148. Rink, H. Solid-phase synthesis of protected peptide fragments using a trialkoxy-diphenyl-methyl ester resin. *Tetrahedron Lett.* **1987,** 28, 3787-90.

149. Carpino, L. A. 1-Hydroxy-7-azabenzotriazole. An efficient peptide coupling additive. *J. Am. Chem. Soc.* **1993,** 115, 4397-8.

150. Bernatowicz, M. S.; Daniels, S. B.; Koster, H. A comparison of acid-labile linkage agents for the synthesis of peptide C-terminal amides. *Tetrahedron Lett.* **1989,** 30, 4645-8.

151. Ciufolini, M. A.; Rivera-Fortin, M. A.; Zuzukin, V.; Whitmire, K. H. Origin of Regioselectivity in Paterno-Buechi Reactions of Benzoquinones with Alkylidenecycloalkanes. *J. Am. Chem. Soc.* **1994,** 116, 1272-7.

152. Bunnett, J. F.; Cartano, A. V. Differing Behavior of Pyrrolidine and Piperidine as Nucleophiles toward 2,4-Dinitrophenyl and 2,4-Dinitro-6-methylphenyl Ethers. *J. Am. Chem. Soc.* **1981,** 103, 4861-4865.

153. Zhang, F.; Peng, Y.; Liao, S.; Gong, Y. Pyrrolidine as an efficient organocatalyst for direct aldol reaction of trifluoroactealdehyde ethyl hemiacetal with ketones. *Tetrahedron* **2007,** 63, 4636-4641.

154. Carey, F. A.; Sundberg, R. J., *Advanced Organic Chemistry, Part-A: Structure and Mechanism*. 4th ed.; Kluwer Academics: New York, 2000; p 4636-4641.

155.   Ciufolini, M. A.; Xi, N. Synthesis, chemistry and conformational properties of piperazic acids. *Chem. Soc. Rev.* **1998,** 27, 437-445.

156.   Albericio, F.; Chinchilla, R.; Dodsworth, D. J.; Najera, C. New trends in peptide coupling reagents. *Org. Prep. Proced. Int.* **2001,** 33, 203-303.

157.   Elmore, D. T. Peptide synthesis. *Amino Acids, Pept., Proteins* **2002,** 33, 83-134.

158.   Knorr, R.; Trzeciak, A.; Bannwarth, W.; Gillessen, D. New coupling reagents in peptide chemistry. *Tetrahedron Lett.* **1989,** 30, 1927-30.

159.   Dourtoglou, V.; Ziegler, J. C.; Gross, B. O-Benzotriazolyl-N,N-tetramethyluronium hexafluorophosphate: a new and effective reagent for peptide coupling. *Tetrahedron Lett.* **1978,** 1269-72.

160.   Sheehan, J. C.; Hess, G. P. A new method of forming peptide bonds. *J. Am. Chem. Soc.* **1955,** 77, 1067-8.

161.   Izdebski, J.; Pachulska, M.; Orlowska, A. N-cyclohexyl-N'-isopropylcarbodiimide: a hybrid that combines the structural features of DCC and DIC. *Int J Pept Protein Res* **1994,** 44, 414-9.

162.   Olah, G. A.; Nojima, M.; Kerekes, I. Synthetic methods and reactions. IV. Fluorination of carboxylic acids with cyanuric fluoride. *Synthesis* **1973,** 487-8.

163.   Anderson, G. W.; Zimmerman, J. E.; Callahan, F. M. N-Hydroxysuccinimide esters in peptide synthesis. *J. Am. Chem. Soc.* **1963,** 85, 3039.

164.   Bodanszky, M. Synthesis of peptides by aminolysis of nitrophenyl esters. *Nature* **1955,** 175, 685.

165.   Dondoni, A.; Franco, S.; Junquera, F.; Merchan, F. L.; Merino, P.; Tejero, T. Applications of Sugar Nitrones in Synthesis: The Total Synthesis of (+)-Polyoxin J. *J. Org. Chem.* **1997,** 62, 5497-5507.

166.   Goddard, T. D.; Kneller, D. G. SPARKY 3 version 3.111. *University of California, San Fransisco:* **2004**.

167.   Sheehan, J. C.; Preston, J.; Cruickshank, P. A. A Rapid Synthesis of Oligopeptide Derivatives without Isolation of Intermediates. *J. Am. Chem. Soc.* **1965,** 87, 2492-2493.

168.   Falchi, A.; Giacomelli, G.; Porcheddu, A.; Taddei, M. 4-(4,6-Dimethoxy[1,3,5]triazin-2-yl)-4-methylmorpholinium chloride (DMTMM): a valuable alternative to PyBOP for solid-phase peptide synthesis. *Synlett* **2000,** 275-277.

169.   Fischer, P. M. Diketopiperazines in peptide and combinatorial chemistry. *J. Pept. Sci.* **2003,** 9, 9-35.

170. Dinsmore, C. J.; Beshore, D. C. Recent advances in the synthesis of diketopiperazines. *Tetrahedron* **2002,** 58, 3297-3312.

171. Gisin, B. F.; Merrifield, R. B. Carboxyl-catalyzed intramolecular aminolysis. Side reaction in solid-phase peptide synthesis. *J. Am. Chem. Soc.* **1972,** 94, 3102-6.

172. Gund, P.; Veber, D. F. Ease of base-catalyzed epimerization of N-methylated peptides and diketopiperazines. *J. Am. Chem. Soc.* **1979,** 101, 1885-7.

173. Fife, T. H.; DeMark, B. R. Intramolecular nucleophilic aminolysis of aliphatic esters. Cyclization of methyl 2-aminomethylbenzoate to phthalimidine. *J. Am. Chem. Soc.* **1976,** 98, 6978-82.

174. Fife, T. H.; Chauffe, L. General Base and General Acid Catalyzed Intramolecular Aminolysis of Esters. Cyclization of Esters of Esters of 2-Aminomethylbenzoic Acid to Phthalimidine. *J. Org. Chem.* **2000,** 65, 3579-3586.

175. Rony, P. R. Polyfunctional catalysis. III. Tautomeric catalysis. *J. Am. Chem. Soc.* **1969,** 91, 6090-6.

176. Nakamizo, N. Catalysis in peptide synthesis with active esters. I. Bifunctional catalysis in the aminolysis of benzyloxycarbonyl-L-phenylalanine p-nitrophenyl ester in dioxane. *Bull. Chem. Soc. Jap.* **1969,** 42, 1071-7.

177. Robins, M. J.; Sarker, S.; Xie, M.; Zhang, W.; Peterson, M. A. Nucleic acid related compounds. 90. Synthesis of 2',3'-fused (3.3.0) gamma -butyrolactone-nucleosides and coupling with amino-nucleosides to give amide-linked nucleotide-dimer analogs. *Tetrahedron Lett.* **1996,** 37, 3921-3924.

178. Openshaw, H. T.; Whittaker, N. The synthesis of emetine and related compounds. VII. The utility of Bi-functional catalysts in amine-ester interactions. *J Chem Soc [Perkin 1]* **1969,** 1, 89-91.

179. Cossy, J.; Thellend, A. A 4-dimethylaminopyridine-catalyzed aminolysis of beta -keto esters. Formation of beta -keto amides. *Synthesis* **1989,** 753-5.

180. Melander, C.; Horne, D. A. Kinetic Analysis of Ester Aminolysis Catalyzed by Nucleosides in a Nonpolar Medium. Evidence of Bifunctional Catalysis. *J. Org. Chem.* **1997,** 62, 9295-9297.

181. Hogberg, T.; Strom, P.; Ebner, M.; Ramsby, S. Cyanide as an Efficient and Mild Catalyst in the Aminolysis of Esters. *J. Org. Chem.* **1987,** 52, 2033-2036.

182. Ivanova, G.; Bratovanova, E.; Petkov, D. Catechol as a Nucleophilic Catalyst of Peptide Bond Formation. *Journal of Peptide Science* **2002,** 8, 8-12.

183. Wasserman, H. H.; Robinson, R. P.; Carter, C. G. Total synthesis of (+-)-chaenorhine. *J. Am. Chem. Soc.* **1983,** 105, 1697-8.

184.   Sakaitani, M.; Hori, K.; Ohfune, Y. One-pot conversion of the N-(benzyloxy)carbonyl group into an N-(tert-butoxycarbonyl) group. *Tetrahedron Lett.* **1988,** 29, 2983-4.

185.   Matsueda, G. R.; Stewart, J. M. A p-methylbenzhydrylamine resin for improved solid-phase synthesis of peptide amides. *Peptides* **1981,** 2, 45-50.

186.   Gallant, M.; Phan Viet Minh, T.; Wuest, J. D. Hydrogen-bonded dimers. Direct study of the interconversion of pyridone dimers and hydroxypyridine monomers by low-temperature nuclear magnetic resonance spectroscopy. *J. Am. Chem. Soc.* **1991,** 113, 721-3.

187.   Capasso, S.; Mazzarella, L. Activation of diketopiperazine formation by alkylammonium carboxylate salts and aprotic dipolar protophobic solvents. *Peptides* **1998,** 19, 389-391.

188.   Giralt, E.; Pedroso, E.; Eritja, R. Diketopiperazine formation in acetamido- and Nitrobenzamido bridged polymeric supports. *Tetrahedron Lett.* **1986,** 22, 3779-3782.

189.   Menger, F. M.; Smith, J. H. Mechanism of ester aminolyses in aprotic solvents. *J. Am. Chem. Soc.* **1972,** 94, 3824-9.

190.   Menger, F. M.; Vitale, A. C. Anion-catalyzed ester aminolyses in a hydrocarbon solvent. *J. Am. Chem. Soc.* **1973,** 95, 4931-4.

191.   Goldwasser, J. M.; Leznoff, C. C. The use of polymer supports in organic synthesis. Part XVI. The solid phase synthesis of monoester monoamides and monoester monoalcohols from symmetrical diacid chlorides. *Can. J. Chem.* **1978,** 56, 1562-8.

192.   Goodman, C. M.; Choi, S.; Shandler, S.; DeGrado, W. F. Foldamers as versatile frameworks for the design and evolution of function. *Nat. Chem. Biol.* **2007,** 3, 252-262.

193.   Karlsson, A. J.; Pomerantz, W. C.; Weisblum, B.; Gellman, S. H. Antifungal activity from 14-helical beta-peptides. *J. Am. Chem. Soc.* **2006,** 128, 12630-12631.

194.   Epand, R. M.; Raguse, T. L.; Gellman, S. H.; Epand, R. M. Antimicrobial 14-helical β-peptides: Potent bilayer disrupting agents. *Biochemistry* **2004,** 43, 9527-9535.

195.   Werder, M.; Hauser, H.; Abele, S.; Seebach, D. β-peptides as inhibitors of small intestinal cholestoral and fat absorption. *Helv. Chim. Acta* **1999,** 82, 1774-1783.

196.   Seurynck-Servoss, S. L.; Brown, N. J.; Dohm, M. T.; Wu, C. W.; Barron, A. E. Lipid composition greatly affects the *in vitro* surface activity of lung surfuctant protein mimics. *Colloids Surf. B: Biointerfaces* **2007,** 57, 37-55.

197.   Patch, J. A.; Barron, A. E. Helical Peptoid Mimics of Magainin-2 amide. *J. Am. Chem. Soc.* **2003,** 125, 12092-12093.

198.   Prince, R. B.; Barnes, S. A.; Moore, J. S. Foldamers Based Molecular Recognition. *J. Am. Chem. Soc.* **2000,** 122, 2758-2762.

199. Schafmeister, C. E.; Belasco, L. G.; Brown, P. H. Observation of Contraction and Expansion in a Bis(peptide)-Based Mechanical Molecular Actuator. *Chem. Eur. J.* **2008,** 14, 6406-6412.

200. Schafmeister, C. E.; Brown, Z. Z.; Gupta, S. Shape-Programmable Macromolecules. *Acc. Chem. Res.* **2008,** 41, 1387-1398.

201. Polgár, L. The catalytic triad of serine peptidases. *Cellular and Molecular Life Sciences* **2005,** 62, 2161.

202. Peris, G.; Jakobsche, C. E.; Miller, S. J. Aspartate-Catalyzed Asymmetric Epoxidation Reactions. *J. Am. Chem. Soc.* **2007,** 129, 8710-8711.

203. Jakobsche, C. E.; Peris, G.; Miller, S. J. Functional analysis of an aspartate-based epoxidation catalyst with amide-to-alkene peptidomimetic catalyst analogues. *Angew. Chem. Int. Ed.* **2008,** 47, 6707-6711.

204. Whitesell, J. K.; Whitesell, M. A. Alkylation of ketones and aldehydes via their nitrogen derivatives. *Synthesis* **1983,** 517.

205. Garst, M. E.; Bonfiglio, J. N.; Grudoski, D. A.; Marks, J. Specific Enolates from α-Amino ketones. *J. Org. Chem.* **1980,** 45, 2307-2315.

206. Sharma, R.; Lubell, W. D. Regioselective Enolization and Alkylation of 4-Oxo-N-(9-phenylfluoren-9-yl)proline: Synthesis of Enantiopure Proline-Valine and Hydroxyproline-Valine Chimeras. *J. Org. Chem.* **1996,** 61, 202-209.

207. Lubell, W. D.; Jamison, T. F.; Rapoport, H. N-(9-phenylfluoren-9-yl)-.alpha.-amino ketones and N-(9-phenylfluoren-9-yl)-.alpha.-amino aldehydes as chiral educts for the synthesis of optically pure 4-alkyl-3-hydroxy-2-amino acids. Synthesis of the C-9 amino acid MeBmt present in cyclosporin. *J. Org. Chem.* **1990,** 55, 3511-3522.

208. Lubell, W.; Rapoport, H. Surrogates for chiral aminomalondialdehyde. Synthesis of N-(9-phenylfluoren-9-yl)serinal and N-(9-phenylfluoren-9-yl)vinylglycinal. *J. Org. Chem.* **1989,** 54, 3824-3831.

209. Lubell, W. D.; Rapoport, H. .alpha.-Amino acids as chiral educts for asymmetric products. Alkylation of N-phenylfluorenyl .alpha.-amino ketones. Synthesis of optically pure .alpha.-alkyl carboxylic acids. *J. Am. Chem. Soc.* **1988,** 110, 7447-7455.

210. Lubell, W. D.; Rapoport, H. Configurational stability of N-protected .alpha.-amino aldehydes. *J. Am. Chem. Soc.* **1987,** 109, 236-239.

211. Webb, T. R.; Eigenbrot, C. Conformationally restricted arginine analogs. *J. Org. Chem.* **1991,** 56, 3009-3016.

212. Atfani, M.; Lubell, W. D. Synthesis of (S)-2-Amino-3-(3-tert-butyl-5-oxo-2H-isoxazol-4-yl)propionic Acid. *J. Org. Chem.* **1995,** 60, 3184-3188.

213. Mancuso, A. J.; Huang, S.-L.; Swern, D. Oxidation of long-chain and related alcohols to carbonyls by dimethyl sulfoxide "activated" by oxalyl chloride. *J. Org. Chem.* **1978,** 43, 2480-2482.

214. Poisson, J. F.; Orellana, A.; Greene, A. E. Stereocontrolled Synthesis of (-)-Kainic Acid from trans-4-Hydroxy-L-proline. *J. Org. Chem.* **2005,** 70, 10860-10863.

215. Blanco, M. J.; Paleo, M. R.; Penide, C.; Sardina, F. J. Stereoselective Reactions of N-(9-Phenylfluoren-9-yl)-4-oxoproline Enolates. An Expedient Route for the Preparation of Conformationally Restricted Amino Acid Analogues. *J. Org. Chem.* **1999,** 64, 8786-8793.

216. Corey, E. J.; Link, J. O. A general, catalytic, and enantioselective synthesis of .alpha.-amino acids. *J. Am. Chem. Soc.* **1992,** 114, 1906-1908.

217. Jocic, Z. Z. *Zh. Russ. Fiz. Khim. Ova.* **1897,** 29, 97.

218. Dominguez, C.; Ezquerra, J.; Baker, S. R.; Borrelly, S.; Prieto, L.; Espada, M.; Pedregal, C. Enantiospecific synthesis of (1S,2S,5R,6S)-2-aminobicyclo[3.1.0]hexane-2,6-dicarboxylic acid by a modified Corey-Link reaction *Tetrahedron Lett.* **1998,** 39, 9305.

219. Barlos, K.; Gatos, D.; Schäfer, W. Synthesis of Prothymosinα (ProTα)—a Protein Consisting of 109 Amino Acid Residues. *Angew. Chem., Int. Ed. Eng.* **1991,** 30, 590.

220. Brown, Z. Z.; Schafmeister, C. E. Exploiting an Inherent Neighboring Group Effect of α;-Amino Acids To Synthesize Extremely Hindered Dipeptides. *J. Am. Chem. Soc.* **2008,** 130, 14382-14383.

221. Spivey A. C., M. A. Asymmetric catalysis of acyl transfer by Lewis acids and nucleophiles. *Org. Prep. Proc. Int.* **2000,** 32, 331-365.

222. Copeland, G. T.; Miller, S. J. A Chemosensor based approach to catalyst discovery in solution and on solid support. *J. Am. Chem. Soc.* **1999,** 121, 4306-4307.

223. Copeland, G. T.; Miller, S. J. Selection of enantioselective acyl transfer catalysts from a pooled library through a fluorescence-based activity assay: an approach to kinetic resolution of secondary alcohols of broad structural scope. *J. Am. Chem. Soc.* **2001,** 123, 6496-6502.

224. Collman, J. P.; Zhong, M.; Costanzo, S.; Zhang, C. New Imidazole-Based Tripodal Ligands as CuB Site Mimics of Cytochrome c Oxidase. *J. Org. Chem.* **2001,** 66, 8252-8256.

225. Dener, J. M.; Zhang, L. H.; Rapoport, H. An effective chirospecific synthesis of (+)-pilocarpine from L-aspartic acid. *J. Org. Chem.* **1993,** 58, 1159-1166.